Best Available Copy 06-09-06

AF

PTO/SB/21 (09-04)
Approval for use through 07/31/2006. OMB 0651-0031
U.S. Patent and Trademark Office; U.S. DEPARTMENT OF COMMERCE
Under the Paperwork Reduction Act of 1995, no persons are required to respond to a collection of information unless it displays a valid OMB control number.

TRANSMITTAL FORM

(to be used for all correspondence after initial filing)

		Application Number	09/703,253
		Filing Date	Oct 31, 2000
		First Named Inventor	Harras, Marie
		Art Unit	1647
		Examiner Name	R. Landsman
Total Number of Pages in This Submission	28 + exhibits	Attorney Docket Number	LEX-0081-USA

ENCLOSURES *(Check all that apply)*

- [ ] Fee Transmittal Form
  - [ ] Fee Attached
- [ ] Amendment / Reply
  - [ ] After Final
  - [ ] Affidavits/declaration(s)
- [ ] Extension of Time Request
- [ ] Express Abandonment Request
- [ ] Information Disclosure Statement
- [ ] Certified Copy of Priority Document(s)
- [ ] Reply to Missing Parts/ Incomplete Application
  - [ ] Reply to Missing Parts under 37 CFR 1.52 or 1.53
- [ ] Drawing(s)
- [ ] Licensing-related Papers
- [ ] Petition
- [ ] Petition to Convert to a Provisional Application
- [ ] Power of Attorney, Revocation Change of Correspondence Address
- [ ] Terminal Disclaimer
- [ ] Request for Refund
- [ ] CD, Number of CD(s) _____
  - [ ] Landscape Table on CD
- [ ] After Allowance communication to (TC)
- [ ] Appeal Communication to Board of Appeals and Interferences
- [X] Appeal Communication to TC **(Appeal Notice, Brief, Reply Brief)**
- [ ] Proprietary Information
- [ ] Status Letter
- [X] Other Enclosure(s) (please identify below):

Return postcard
Submission of copy of lost appeal brief
EX A-E EX L-N

Remarks

Customer # 24231

SIGNATURE OF APPLICANT, ATTORNEY, OR AGENT

Firm Name	Lexicon Genetics Incorporated		
Signature	Ron C. Ishimoto by Peter G. Sefenaii 40,162		
Printed name	Lance K. Ishimoto		
Date	June 8, 2006	Reg. No.	41,866

CERTIFICATE OF TRANSMISSION/MAILING

I hereby certify that this correspondence is being facsimile transmitted to the USPTO or deposited with the United States Postal Service with sufficient postage as Express Mail (EV 766804930 US) I in an envelope addressed to: Commissioner for Patents, MS Appeal Brief, P.O. Box 1450, Alexandria, VA 22313-1450 on the date shown below.

Signature	Nancy Stacey		
Typed or printed name	Nancy Stacey	Date	June 8, 2006

This collection of information is required by 37 CFR 1.5. The information is required to obtain or retain a benefit by the public which is to file (and by the USPTO to process) an application. Confidentiality is governed by 35 U.S.C. 122 and 37 CFR 1.11 and 1.14. This collection is estimated to take 2 hours to complete, including gathering, preparing, and submitting the completed application form to the USPTO. Time will vary depending upon the individual case. Any comments on the amount of time you require to complete this form and/or suggestions for reducing this burden, should be sent to the Chief Information Officer, U.S. Patent and Trademark Office, U.S. Department of Commerce, P.O. Box 1450, Alexandria, VA 22313-1450. DO NOT SEND FEES OR COMPLETED FORMS TO THIS ADDRESS. **SEND TO: Commissioner for Patents. P.O. Box 1450, Alexandria, VA 22313-1450.**

If you need assistance in completing the form, call 1-800-PTO-9199 and select option 2.

IN THE UNITED STATES PATENT AND TRADEMARK OFFICE

Applicant(s):	Harras, *et al.*	Group Art Unit: 1647
Application No.:	09/703,253	Examiner: R. Landsman
Filed:	10/31/2000	
Title: Sequences Encoding Human ATP-binding Cassette Transporter Proteins		Atty. Docket No. LEX-0081-USA

SUBMISSION OF COPY OF LOST APPEAL BRIEF

Mail Stop Appeal Brief
Commissioner for Patents
Alexandria, VA 22313

Sir:

In response to the Examiners request, Applicants herein submit a copy of a previously filed Appeal Brief which has been lost. When this Appeal Brief was originally submitted (September 18, 2003) it was misfiled and this resulted in the erroneous issuance of a Notice of Abandonment (mailed on February 4, 2004). In response, Applicants filed a "Petition to Withdraw a Holding of Abandonment"under 37 C.F.R. § 1.181 on February 26, 2004, which was granted and at which time the Examiner said that the missing Brief had been located. On March 30, 2004 a Withdrawal of Abandonment was mailed that also confirmed that the missing Appeal Brief had been located. However, following several conversations with the Examiner, it is clear that the Brief has in fact not been entered into the system. Therefore, in response to the Examiners request, a copy of the Appeal Brief as filed on September 18, 2003 is provided herein **(as Exhibit 1)**.

Applicants note for the record that while the Appeal Brief filed on September 18, 2003 , does not comply with the recently enacted new rules concerning appellate procedure, as codified at 37 C.F.R. § 41 (in particular 37 C.F.R. § 41.37), the Appeal Brief is, however, fully compliant with 37 C.F.R. § 1.192, which was the rule that was in effect on September 18, 2003, when the Appeal

Brief was originally filed. Applicants believe that the provided Exhibits A-E and L-N are a true representation of the exhibits originally filed with the Appeal Brief on September 18, 2003 and lost by the Office. However, in light of repeated requests from the Office not to submit copies of issued U.S. Patents, Exhibits F-K and O-R from the Appeal Brief as originally filed on September 18, 2003, all of which are issued U.S. Patents, are not provided herein.

Applicants believe no fees are due in connection with this response. However, the Commissioner is authorized to charge any underpayment or credit any overpayment to Deposit Account No. 50-0892.

Respectfully submitted,

June 8, 2006
Date

Peter G. Seferian Reg. No. 40,162
Agent for Applicants

LEXICON GENETICS INCORPORATED
(281) 863-3399

Customer # 24231

IN THE UNITED STATES PATENT AND TRADEMARK OFFICE

Appellant(s):	Harras, *et al.*	Group Art Unit: 1647
Application No.:	09/703,253	Examiner: R. Landsman
Filed:	10/31/2000	
Title:	Sequences Encoding Human ATP-binding Cassette Transporter Proteins	Atty. Docket No. LEX-0081-USA

COPY

APPEAL BRIEF

Mail Stop Appeal Brief
Commissioner for Patents
Alexandria, VA 22313

TABLE OF CONTENTS

TABLE OF AUTHORITIES

CASES

STATUTES

APPEAL BRIEF

Sir:

Appellants hereby submit an original and two copies of this Appeal Brief to the Board of Patent Appeals and Interferences ("the Board") in response to the December 18, 2002 (Paper No. 17). The Notice of Appeal was timely submitted on March 13, 2003, and was received in the Patent and Trademark Office ("the Office") on March 18, 2003. This Appeal Brief is timely submitted in light of the concurrently filed Petition for an Extension of Time of four months to and including September 1, 2003 and authorization to deduct the fee as required under 37 C.F.R. § 1.17(a)(4) from Appellants' Representatives' deposit account. The Commissioner is also authorized to charge the fee for filing this Appeal Brief (**$160.00**), as required under 37 C.F.R. § 1.17(c), to Lexicon Genetics Incorporated Deposit Account No. 50-0892.

Appellants believe no fees in addition to the fee for filing the Appeal Brief and the fee for the extension of time are due in connection with this Appeal Brief. However, should any additional fees under 37 C.F.R. §§ 1.16 to 1.21 be required for any reason related to this communication, the Commissioner is authorized to charge any underpayment or credit any overpayment to Lexicon Genetics Incorporated Deposit Account No. 50-0892.

I. REAL PARTY IN INTEREST

The real party in interest is the Assignee, Lexicon Genetics Incorporated, 8800 Technology Forest Place, The Woodlands, Texas, 77381.

II. RELATED APPEALS AND INTERFERENCES

Appellants know of no related appeals or interferences.

III. STATUS OF THE CLAIMS

The present application was filed on October 31, 2000, claiming the benefit of U.S. Provisional

Application Number 60/163,018, which was filed on November 2, 1999, and included original claims 1-4.

The Examiner issued a Restriction and Election Requirement separating the original claims into three separate and distinct inventions, and in a telephone conversation Appellants elected of Group I (claims 1-2), with traverse, for prosecution on the merits.

A First Official Action, was issued on December 19, 2001 ("the First Action" Paper No: 11), Claims 1-2 were rejected under 35 U.S.C. § 101, due to the alleged lack of patentable utility, claims 1-2 were also rejected under 35 U.S.C. § 112, first paragraph, as allegedly unusable by the skilled artisan due to the alleged lack of patentable utility, claim 2 was rejected under 35 U.S.C. § 112, second paragraph, as allegedly indefinite, claim 1 is rejected under 35 U.S.C. § 102(b) as allegedly being anticipated and claims 3-4 were withdrawn from further consideration by examiner as being drawn to a non-elected invention.

In a response to the First Official Action, submitted to the Office on April 19, 2002 ("response to the First Action"), Appellants acknowledged the Restriction and Election Response and amended claim 2 to further improve its clarity.

A Second Official Action, was issued on July 9, 2002 ("the Second Action": Paper No 14), claims 1-2 were maintained under 35 U.S.C. § 101, due to the alleged lack of patentable utility, rejection of claims 1-2 was also maintained under 35 U.S.C. § 112, first paragraph, as allegedly unusable by the skilled artisan due to the alleged lack of patentable utility, rejection of claim 2 was maintained under 35 U.S.C. § 112, second paragraph, as allegedly indefinite, the rejection to Claim 1 was withdrawn under 35 U.S.C. § 102(b), but claim 1 was rejected under 35 U.S.C. § 102(a) as allegedly being anticipated.

In a response to the Second Official Action, submitted to the Office on November 11, 2002 ("response to the Second Action"), Appellants amended Claim 1 and new claims 5-7 were added to further improve its clarity and Claim 2 was canceled without prejudice and without disclaimer.

A third and Final Official Action, was issued on December 18, 2002 (the "Final Action" : Paper No. 17), in which rejection of claims 1 and 5-7 was maintained under 35 U.S.C. § 101 and

35 U.S.C. § 112, first paragraph and in view of Appellants amendments to the claim, the rejection of Claim 1 was withdrawn under 35 U.S.C. § 102(a).

In a response to the Final Action, submitted on April 18, 2003 ("response to the Final Action") Appellants again addressed the outstanding rejections of claims 1 and 5-7.

An Advisory Action ("the Advisory Action") was mailed on May 5, 2003, maintaining the rejection of claims 1 and 5-7 were maintained under 35 U.S.C. § 101 as allegedly lacking a patentable utility and under 35 U.S.C. § 112, first paragraph, as one skilled in the art clearly would not know how to use the skilled invention. A copy of the appealed claims is included below in the Appendix (Section IX).

IV. STATUS OF THE AMENDMENTS

For the purposes of Appeal Appellants believe that no outstanding amendments exist.

V. SUMMARY OF THE INVENTION

The present invention relates to Appellants' discovery and identification of novel human sequences that encodes a novel isoform of an ATP-binding cassette transporter protein, a class of proteins that are well known to be involved in mammalian multi-drug resistance(Page 2, lines 7-8). The specification details a number of uses for the presently claimed polynucleotide sequences, including the detection and diagnosis of human disease (page 12) as well as to therapeutically augment the efficacy of chemotherapeutic agents used in the treatment of breast or prostate cancer (page 14, lines 4-6) . The sequences of the present invention are noted to be expressed in prostate (page 3, line 10). Additional uses include assessing temporal and tissue specific gene expression patterns (specification at page 5, line 15-18), particularly using a high throughput "chip" format (specification at page 5, line 19-22), mapping the sequences to a specific region of a human chromosome and identifying protein encoding regions and determining the genomic structure (specification at page 8, lines 11-16). As a still further example of utility is the use of the present sequences in such diagnostic assays (at least at page 14, line 1) as those associated with identification of paternity and forensic analysis, among others. The

sequences of the present invention have particular utility as the application as filed identified several polymorphisms (page 13, lines 16-25).

VI. ISSUES ON APPEAL

1. Do claims 1, and 5-7 lack a patentable utility?
2. Are claims 1 and 5-7 unusable by a skilled artisan due to a lack of patentable utility?

VII. GROUPING OF THE CLAIMS

For the purposes of the outstanding rejections under 35 U.S.C. § 101 and 35 U.S.C. § 112, first paragraph, the claims will stand or fall together.

VIII. ARGUMENT

A. Do Claims 1 and 5- 7 Lack a Patentable Utility?

The Final Action first rejects claims 1 and 5 - 7 under 35 U.S.C. § 101, as allegedly lacking a patentable utility due to not being supported by either a specific and substantial utility or a well-established utility, this rejection is maintained in the Advisory Action.

Appellants strongly disagree, as the specification details a number of specific and substantial utilities for the presently claimed polynucleotide sequences which encode a novel isoform of an ATP-binding cassette transporter protein, a class of proteins that are well known to be involved in mammalian multi-drug resistance(Page 2, lines 7-8). The specification details a number of uses for the presently claimed polynucleotide sequences, including the detection and diagnosis of human disease (page 12) as well as to therapeutically augment the efficacy of chemotherapeutic agents used in the treatment of breast or prostate cancer (page 14, lines 4-6) . The sequences of the present invention are noted to be expressed in prostate (page 3, line 10). Additional uses include assessing temporal and tissue specific gene expression patterns (specification at page 5, line 15-18), particularly using a high throughput "chip" format (specification at page 5, line 19-22), mapping the sequences to a specific region of a human chromosome and identifying protein encoding regions and determining the genomic

structure (specification at page 8, lines 11-16). As a still further example of utility is the use of the present sequences in such diagnostic assays (at least at page 14, line 1) as those associated with identification of paternity and forensic analysis, among others. The sequences of the present invention have particular utility as the application as filed identified several polymorphisms (page 13, lines 16-25).

Appellants would like to invite the Board's attention to the fact that a sequence sharing 94% identity at the nucleic acid level with the sequences of the present invention is present in the leading scientific repository for biological sequence data (GenBank), and has been annotated by third party scientists *wholly unaffiliated with Appellants* as ATP-binding cassette, sub-family C, member 11 isoform a; multi-resistance protein 8 (GenBank accession number NP_115972; **abstrac**t, alignment and GenBank report provided in **Exhibit A**) and as ATP-binding cassette, sub-family C, member 11 isoform b; multi-resistance protein 8 (GenBank accession number NP_660187; **abstrac**t, alignment and GenBank report provided in **Exhibit B**) . The legal test for utility simply involves an assessment of whether those skilled in the art would find any of the utilities described for the invention to be credible or believable. Given this GenBank annotation, there can be little question that those skilled in the art would clearly believe that Appellants' sequence is a novel human isoform of the ATP-binding cassette, sub-family C, member 11; multi-resistance protein 8. Thus, the present claims clearly meet the requirements of 35 U.S.C. § 101.

The Advisory Action (at page 2, lines 6-7), states that "post filing references can only be used to support an asserted utility in the specification. Appellants have only disclosed that in their specification that the protein of the present invention was believed to be an MDR protein." and that Appellants did not know the identity of the protein encoded by the sequences of the of present invention "thereby supporting the Examiner's position that utility was not known at the time of filing." However, Appellants respectfully submit that the issue with regards to 35U.S.C, section 101 is one of utility, not identity or nomenclature and that the legal test for utility simply involves an assessment of whether those skilled in the art would find any of the utilities described for the invention to be credible or believable. The application as filed clearly describes the current invention as a novel human transporter protein (*inter alia,* title, page 1) and the function of transporter proteins as integral

membrane proteins that mediate or facilitate the passage of materials across the lipid bilayer (page 1, lines 26-28) and identifies their role as a mechanism of drug resistance wherein diseased cells using cellular transporter systems to export chemotherapeutic agents from the cell (page 1, line 30-33) and later in the specification asserts a utility in augmenting the efficacy of chemotherapeutic agents used in the treatment of breast or prostate cancer (specification at page 14, lines 8-10).

Appellants have asserted that the present invention is a human transporter protein, and provided evidence that the sequences of the present invention indeed encode a transporter protein, in particular, a variant that encodes and isoform of the ATP-binding cassette, sub-family C, member 11; multi-resistance protein 8. In light of the well-established fact that ATP-binding cassette transporters are known to the art to be frequently associated with multiple drug resistance by cancer cells and that mutations in these genes can cause accelerated removal of chemotherapeutic agents, it is clear the present invention has utility. Appellants have further asserted that similar MDR encoding sequences, uses, and applications that are germane to the proteins encoded by the sequences of the present invention, were described in issued U.S. Patents Nos. 5,198,344 and 5,866,699 which were incorporated by reference in their entirety into the present application.

The well-established utility of the class of transporter proteins encoded by the sequences of the present invention is further evidenced by the NCBI LocusLink summary for ABCC11 genetic locus.

> "The protein encoded by this gene is a member of the superfamily of ATP-binding cassette (ABC) transporters. ABC proteins transport various molecules across extra- and intra-cellular membranes."

> "This ABC full transporter is a member of the **MRP subfamily which is involved in multi-drug resistance. It is expressed at low levels** in all tissues, except kidney, spleen, and colon. This gene and family member ABCC12 are determined to be derived by duplication and are both localized to chromosome 16q12.1. Their chromosomal localization, potential function, and expression patterns identify them as candidates for paroxysmal kinesigenic choreoathetosis, a disorder characterized by attacks of involuntary movements and postures,

chorea, and dystonia. Multiple alternatively spliced transcript variants have been described for this gene."

(http://www.ncbi.nlm.nih.gov/LocusLink/LocRpt.cgi?l=85320)

Clearly the utility of ABCC 11 transporter proteins, and thus logically the sequences of the present invention which encode an ABCC11 transporter protein isoform, have a very well established utility that is readily recognized by those of skill in the art.

In the Second Official Action (Paper No.14) references, Tammur *et al.* **(Exhibit C)** and Yabuuchi *et al.* **(Exhibit D)** are used to attempt to discredit Appellants' assertion of utility. However these publications support rather than dispute Appellants assertion that the present invention has utility and is a splice variant of ABCC11. For example, Tammur *et al*, in the final paragraph of the introduction (page 90, 4th paragraph), state that they had undertaken a long-term project of cloning new human ABC transporters and linking them to various disease phenotypes and have identified ABCC11 and ABCC12 as two such members. Thus, clearly, Tammur et al., recognize the value and utility of ABCC11 and ABCC12 and their association with human diseases. In addition, with regard to function, Tammur *et al.*, state on page 93, lines 8-10 that "it would be reasonable to suggest that ABC11 and ABCC12 could share functional similarities with ABCC4 and ABCC5." Said function being recognized by the art as the transport of organic anions, nucleotide analogs and cyclic nucleotides. Thus rather than contradicting the utility of the present invention the conclusions of Tammur *et al.* support the position that those of skill in the art would recognize Appellants' asserted utility of the present invention as credible.

Yabuuchi *et al.* clearly supports Appellants' assertion that the present invention is a splice variant of ABCC11, for there appear to be many such variants. And although these authors speculate that "splice variants may represent diverse biological functions" (emphasis added), this speculation is not supported by any data or based on any fact or reference and thus appears to be pure speculation , "Therefore, it is of interest to know whether some of these splice variants...represent biological

functions" (pg 937, lines 17-19). However, Yabuuchi *et al.* also recognize in their concluding remarks the utility of ABCC11 with regard to human disease and therefore also indicate that Appellants' utility assertions as credible. Further recognition of the utility of ABCC11 sequences is provided by other scientific publications, such as that of Turriziani, *et al.*, (Impaired 2',3'-dideoxy-3'-thiacytidine accumulation in T-lymphoblastoid cells as a mechanism of acquired resistance independent of multidrug resistant protein 4 with a possible role for ATP-binding cassette C11, Biochem. J. 368, 325-332 ,2002: **Exhibit E**). Turriziani, *et al.*, describe the finding that increased expression of ATP-binding cassette C11 (ABCC11) was observed in the CEM 3TC cells and that the decreased 3TC accumulation in the CEM 3TC might be due to the upregulation of ABCC11.

Clearly evidence supports Appellants' assertions that the sequences of the present invention which encode a novel human transporter protein,(an isoform of the ATP-binding cassette, sub-family C, member 11; multi-resistance protein 8) have well established utility that is recognized by those of skill in the art.

Furthermore, this situation parallels Example 10 of the PTO's Revised Interim Utility Guidelines Training Materials (pages 53-55), which establishes that a rejection under 35 U.S.C. § 101 as allegedly lacking a patentable utility and under 35 U.S.C. § 112, first paragraph as allegedly unusable by the skilled artisan due to the alleged lack of patentable utility, is not proper when there is no reason to doubt the asserted utility of a full length sequence (such as the presently claimed sequence) that has a similarity to a protein having a known function. In the Analysis portion of Example 10 it states that "Based on applicant's disclosure and the results of the PTO search, there is no reason to doubt the assertion that SEQ ID NO:2 encodes a DNA ligase . Further DNA ligases have a well-established use in the molecular biology art based on this class of proteins ability to ligate DNA. .....Note that if there is a well-established utility already associated with the claimed invention, the utility need not be asserted in the specification as filed..... Thus the conclusion reached from this analysis is that a 35 U.S.C. § 101 and a 35 U.S.C. § 112 first paragraph, utility rejection should not be made."

The present case is similar to that presented in Example 10 of the Revised Interim Utility Guidelines Training Materials (pages 53-55). In the present case it is clear that the sequences of the present invention encode an ATP-binding cassette (ABC) transporter. ATP-binding cassette (ABC) transporters have a well-established utility. "Note that if there is a well-established utility already associated with the claimed invention, the utility need not be asserted in the specification as filed...Thus the conclusion reached from this analysis is that a 35 U.S.C. § 101 and a 35 U.S.C. § 112 first paragraph, utility rejection should not be made." Thus the rejection of the presently claimed invention under a 35 U.S.C. § 101 and a 35 U.S.C. § 112 first paragraph utility rejection should be overruled.

The Advisory action also discounts Appellants' assertion regarding the use of the presently claimed polynucleotides on DNA gene chips, based on the position that such a use would allegedly be generic. Further, these Actions seem to be requiring Appellants to identify the biological role of the nucleic acid or function of the protein encoded by the presently claimed polynucleotides before the present sequences can be used in gene chip applications that meet the requirements of § 101. Appellants respectfully point out that knowledge of the exact function or role of the presently claimed sequence is not required to track expression patterns using a DNA chip. As set forth in at least Appellants Response to Final, given the widespread utility of such "gene chip" methods using *public domain* gene sequence information, there can be little doubt that the use of the presently described *novel* sequences would have great utility in such DNA chip applications.

Clearly, the claimed sequences provide a specific marker of the gene encoding an ABC transporter protein and provide a unique identifier of the corresponding gene in the human genome. Such specific markers are targets for discovering drugs that are associated with human kidney disease, such as congenital nephrotic syndrome. Thus, those skilled in the art would instantly recognize that the present nucleotide sequence would be an ideal, novel candidate for assessing gene expression using, for example, DNA chips, as the specification details at least on page 5, line 19-22. Such "DNA chips" clearly have utility, as evidenced by hundreds of issued U.S. Patents, exemplified by U.S. Patent Nos. 5,445,934 (**Exhibit F**), 5,556,752 (**Exhibit G**), 5,744,305 (**Exhibit H**), as well as more recently issued U.S. Patent Nos. 5,837,832 (**Exhibit I**), 6,156,501 (**Exhibit J**) and 6,261,776 (**Exhibit K**).

The Board is further requested to consider that, given the huge expense of the drug discovery process, even negative information has great "real world" practical utility. Knowing that a given gene is not expressed in medically relevant tissue provides an informative finding of great value to industry by allowing for the more efficient deployment of expensive drug discovery resources. Such practical considerations are equally applicable to the scientific community in general, in that time and resources are not wasted chasing what are essentially scientific dead-ends (from the perspective of medical relevance). Clearly, compositions that enhance the utility of such DNA gene chips, such as the presently claimed sequences encoding ATP-binding cassette (ABC) transporters, must in themselves be useful. Moreover, the presently described ABC transporter provides uniquely specific sequence resources for identifying and quantifying full length transcripts that were encoded by the corresponding human genomic locus. Accordingly, there can be no question that the described sequences provide an exquisitely specific utility for analyzing gene expression.

Additionally, only a small percentage of the genome (2-4%) actually encodes exons, which in turn encode amino acid sequences. Thus, not all human genomic DNA sequences are useful in such gene chip applications. This further discounts the Examiner's position that such uses are "generic". The present claims clearly meet the requirements of 35 U.S.C. § 101. It has been clearly established that a statement of utility in a specification must be accepted absent reasons why one skilled in the art would have reason to doubt the objective truth of such statement. *In re Langer*, 503 F.2d 1380, 1391, 183 USPQ 288, 297 (CCPA, 1974); *In re Marzocchi*, 439 F.2d 220, 224, 169 USPQ 367, 370 (CCPA, 1971).

Evidence of the "real world" substantial utility of the present invention is further provided by the fact that there is an entire industry based on the use of gene sequences or fragments thereof in a gene chip format. Perhaps the most notable gene chip company is Affymetrix. However, there are many companies which have, at one time or another, concentrated on the use of gene sequences or fragments, in gene chip and non-gene chip formats, for example: Gene Logic, ABI-Perkin-Elmer, HySeq and Incyte. In addition, one such company, Rosetta Inpharmatics, was viewed to have such "real world" value that it was acquired by large pharmaceutical company, Merck & Co., for substantial

sums of money (net equity value of the transaction was $620 million). The "real world" substantial industrial utility of gene sequences or fragments would, therefore, appear to be widespread and well established. Clearly, persons of skill in the art, as well as venture capitalists and investors, readily recognize the utility, both scientific and commercial, of genomic data in general, and specifically human genomic data. Billions of dollars have been invested in the human genome project, resulting in useful genomic data (see, *e.g.*, Venter *et al.*, 2001, Science *291*:1304; **Exhibit L**). The results have been a stunning success as the utility of human genomic data has been widely recognized as a great gift to humanity (see, *e.g.*, Jasny and Kennedy, 2001, Science *291*:1153; **Exhibit M**). Clearly, the usefulness of human genomic data, such as the presently claimed nucleic acid molecules, is substantial and credible (worthy of billions of dollars and the creation of numerous companies focused on such information) and well-established (the utility of human genomic information has been clearly understood for many years).

As a still further example of utility is the use of the present sequences in such diagnostic assays (at least at page 14, line 1) as those associated with identification of paternity and forensic analysis, among others. The sequences of the present invention have particular utility as the application as filed identified several polymorphisms (page 13, lines16-25). This is also not a case of a potential utility. Appellants respectfully submit that even in the worst case scenario, the described polymorphisms are each useful to distinguish 50% of the population (in other words, the marker being present in half of the population) and that the ability of a polymorphic marker to distinguish at least 50% of the population is an inherent feature of any polymorphic marker, and this feature is well understood by those of skill in the art. Appellants note that as a matter of law, it is well settled that a patent need not disclose what is well known in the art. *In re Wands*, 8 USPQ 2d 1400 (Fed. Cir. 1988). Appellants support for Appellants' assertion of utility is provided by the fact that the skilled artisan would readily recognize and easily believe that the presently described polymorphic markers could be useful in forensic analysis. The fact that forensic biologists use polymorphic markers such as those described by Appellants every day provides more that ample support for the assertion that forensic biologists would also be able to use the specific polymorphic markers described by Appellants in the same fashion. Therefore, again it is clear that the sequences of the present invention have utility.

Given the physiologic activity and importance of ABC transporters known to those of skill in the art, those of skill in the art would readily appreciate the importance of tracking the expression of the genes encoding the described proteins, particularly due to well established role of ABC transporters in drug resistance in cancer cells. In the present case this apparent utility is further bolstered by the expression of the sequences of the present invention in the prostate, a tissue which when involved in cancer often under goes multiple drug resistance. The use of the claimed polypeptide in an array for screening purposes Appellants respectfully point out that nucleic acid sequences have the greatest specific utility in gene chip applications once the role of the sequence has been identified, as have tissues of interest, as in the present case. Once the role of the particular nucleic acid is known, the level of gene expression has and even greater significance. By identifying the physiological activity role of the claimed sequence, the claimed sequence has a far greater utility in gene chip applications that just any random piece of DNA. Appellants respectfully submit that **specific** utility, which is the proper standard for utility under 35 U.S.C. § 101, is distinct from the requirement for a **unique** utility, which is clearly an improper standard. As clearly stated by the Federal Circuit in *Carl Zeiss Stiftung v. Renishaw PLC*, 20 USPQ2d 1101 (Fed. Cir. 1991; "*Carl Zeiss*"):

> An invention need not be the best or only way to accomplish a certain result, and it need only be useful to some extent and in certain applications: "[T]he fact that an invention has only limited utility and is only operable in certain applications is not grounds for finding a lack of utility." *Envirotech Corp. v. Al George, Inc.*, 221 USPQ 473, 480 (Fed. Cir. 1984)

Therefore, just because other nucleic acid sequences find utility in gene chip applications does not mean that the use of Appellants' sequence in gene chip applications is not a specific utility. Furthermore, the requirement for a unique utility is clearly not the standard adopted by the Patent and Trademark Office. If every invention were required to have a unique utility, the Patent and Trademark Office would no longer be issuing patents on batteries, automobile tires, golf balls, golf clubs, and treatments for a variety of human diseases, such as cancer and bacterial or viral infections, just to name a few particular examples, because examples of each of these have already been described and patented. All batteries have the exact same utility - specifically, to provide power. All automobile tires have the exact same

utility - specifically, for use on automobiles. All golf balls and golf clubs have the exact same utility - specifically, use in the game of golf. All cancer treatments have the exact same utility - specifically, to treat cancer. All anti-infectious agents have the exact same broader utility - specifically, to treat infections. However, only the briefest perusal of virtually any issue of the Official Gazette provides numerous examples of patents being granted on each of the above compositions every week. Furthermore, if a composition needed to be unique to be patented, the entire class and subclass system would be an effort in futility, as the class and subclass system serves solely to group such common inventions, which would not be required if each invention needed to have a unique utility. Thus, the present sequence clearly meets the requirements of 35 U.S.C. § 101.

Further evidence of utility of the presently claimed polynucleotide, although only one is needed to meet the requirements of 35 U.S.C. § 101 (*Raytheon v. Roper*, 220 USPQ 592 (Fed. Cir. 1983); *In re Gottlieb*, 140 USPQ 665 (CCPA 1964); *In re Malachowski*, 189 USPQ 432 (CCPA 1976); *Hoffman v. Klaus*, 9 USPQ2d 1657 (Bd. Pat. App. & Inter. 1988)), is the specific utility the present nucleotide sequence has in determining the genomic structure of the corresponding human chromosome (specification at page 14, lines 9-10), for example mapping the protein encoding regions as described in the specification (page 3, line 26-29) and evidenced below. Clearly, the present polynucleotide provides exquisite specificity in localizing the specific region of the human chromosome containing the gene encoding the given polynucleotide, a utility not shared by virtually any other nucleic acid sequence. In fact, it is this specificity that makes this particular sequence so useful. Early gene mapping techniques relied on methods such as Giemsa staining to identify regions of chromosomes. However, such techniques produced genetic maps with a resolution of only 5 to 10 megabases, far too low to be of much help in identifying specific genes involved in disease. The skilled artisan readily appreciates the significant benefit afforded by markers that map a specific locus of the human genome, such as the present nucleic acid sequence.

Only a minor percentage of the genome actually encodes exons, which in turn encode amino acid sequences. The presently claimed polynucleotide sequence provides biologically validated empirical data (*e.g.*, showing which sequences are transcribed, spliced, and polyadenylated) that

specifically defines that portion of the corresponding genomic locus that actually encodes exon sequence. Equally significant is that the claimed polynucleotide sequence defines how the encoded exons are actually spliced together to produce an active transcript (*i.e.*, the described sequences are useful for functionally defining exon splice-junctions). The Appellants respectfully submit that the practical scientific value of expressed, spliced, and polyadenylated mRNA sequences is readily apparent to those skilled in the relevant biological and biochemical arts. For further evidence supporting the Appellants' position, the Board is requested to review, for example, section 3 of Venter *et al.* (*supra at* pp. 1317-1321, including Fig. 11 at pp.1324-1325), which demonstrates the significance of expressed sequence information in the structural analysis of genomic data. The presently claimed polynucleotide sequence defines a biologically validated sequence that provides a unique and specific resource for mapping the genome essentially as described in the Venter *et al.* article.

As still further evidence supporting Appellants' assertions of the specific utility of the sequences of the present invention in localizing the specific region of the human chromosome and identification of functionally active intron/exon splice junctions is the information provided in **Exhibit N**. This is the result of a blast analysis using SEQ ID NO:23 of the present invention when compared to the identified human genomic sequence. This result indicates that the sequence of the present invention is encoded by 25 exons spread non-contiguously along a region of human chromosome 16, which is contained within represented by clone, AC0076005. Thus clearly one would not simply be able to identify the 25 protein encoding exons that make up the sequence of the present intention from within the large genomic sequence. Nor, would one be able to map the protein encoding regions identified specifically by the sequences of the present invention without knowing exactly what those specific sequences were.

Rather, the question of utility is a straightforward one. As set forth by the Federal Circuit, "(t)he threshold of utility is not high: An invention is 'useful' under section 101 if it is capable of providing some identifiable benefit." *Juicy Whip Inc. v. Orange Bang Inc.*, 51 USPQ2d 1700 (Fed. Cir. 1999) (citing *Brenner v. Manson*, 383 U.S. 519, 534 (1966)). Additionally, the Federal Circuit has stated that "(t)o violate § 101 the claimed device must be totally incapable of achieving a useful result." *Brooktree Corp. v. Advanced Micro Devices, Inc.*, 977 F.2d 1555, 1571 (Fed. Cir. 1992),

emphasis added. *Cross v. Iizuka* (224 USPQ 739 (Fed. Cir. 1985); "*Cross*") states "any utility of the claimed compounds is sufficient to satisfy 35 U.S.C. § 101". *Cross* at 748, emphasis added. Indeed, the Federal Circuit recently emphatically confirmed that "anything under the sun that is made by man" is patentable *(State Street Bank & Trust Co. v. Signature Financial Group Inc.*, 47 USPQ2d 1596, 1600 (Fed. Cir. 1998), citing the U.S. Supreme Court's decision in *Diamond vs. Chakrabarty*, 206 USPQ 193 (S.Ct. 1980)).

The legal test for utility simply involves an assessment of whether those skilled in the art would find any of the utilities described for the invention to be credible or believable. According to the Examination Guidelines for the Utility Requirement, if the applicant has asserted that the claimed invention is useful for any particular purpose (i.e., it has a "specific and substantial utility") and the assertion would be considered credible by a person of ordinary skill in the art, the Examiner should not impose a rejection based on lack of utility (66 Federal Register 1098, January 5, 2001).

In *In re Brana,* (34 USPQ2d 1436 (Fed. Cir. 1995), "*Brana*"), the Federal Circuit admonished the P.T.O. for confusing "the requirements under the law for obtaining a patent with the requirements for obtaining government approval to market a particular drug for human consumption". *Brana* at 1442. The Federal Circuit went on to state:

> At issue in this case is an important question of the legal constraints on patent office examination practice and policy. The question is, with regard to pharmaceutical inventions, what must the applicant provide regarding the practical utility or usefulness of the invention for which patent protection is sought. This is not a new issue; it is one which we would have thought had been settled by case law years ago.

Brana at 1439, emphasis added. The choice of the phrase "utility or usefulness" in the foregoing quotation is highly pertinent. The Federal Circuit is evidently using "utility" to refer to rejections under 35 U.S.C. § 101, and is using "usefulness" to refer to rejections under 35 U.S.C. § 112, first paragraph. This is made evident in the continuing text in *Brana*, which explains the correlation between 35 U.S.C. §§ 101 and 112, first paragraph. The Federal Circuit concluded:

> FDA approval, however, is not a prerequisite for finding a compound useful within the meaning of the patent laws. Usefulness in patent law, and in particular in the context of

> pharmaceutical inventions, necessarily includes the expectation of further research and development. The stage at which an invention in this field becomes useful is well before it is ready to be administered to humans. Were we to require Phase II testing in order to prove utility, the associated costs would prevent many companies from obtaining patent protection on promising new inventions, thereby eliminating an incentive to pursue, through research and development, potential cures in many crucial areas such as the treatment of cancer.

Brana at 1442-1443, citations omitted. In assessing the question of whether undue experimentation would be required in order to practice the claimed invention, the key term is "undue", not "experimentation". *In re Angstadt and Griffin*, 190 USPQ 214 (C.C.P.A. 1976). The need for some experimentation does not render the claimed invention unpatentable. Indeed, a considerable amount of experimentation may be permissible if such experimentation is routinely practiced in the art. *In re Angstadt and Griffin, supra*; *Amgen, Inc. v. Chugai Pharmaceutical Co., Ltd.*, 18 USPQ2d 1016 (Fed. Cir. 1991). As a matter of law, it is well settled that a patent need not disclose what is well known in the art. *In re Wands*, 8 USPQ 2d 1400 (Fed. Cir. 1988).

Finally, with regards to the issue of due process, while Appellants are well aware of the new Utility Guidelines set forth by the USPTO, Appellants respectfully point out that the current rules and regulations regarding the examination of patent applications is and always has been the patent laws as set forth in 35 U.S.C. and the patent rules as set forth in 37 C.F.R., not the Manual of Patent Examination Procedure or particular guidelines for patent examination set forth by the USPTO. Furthermore, it is the job of the judiciary, not the USPTO, to interpret these laws and rules. Appellants are unaware of any significant recent changes in either 35 U.S.C. § 101, or in the interpretation of 35 U.S.C. § 101 by the Supreme Court or the Federal Circuit that is in keeping with the new Utility Guidelines set forth by the USPTO. This is underscored by numerous patents that have been issued over the years that claim nucleic acid fragments that do not comply with the new Utility Guidelines. As examples of such issued U.S. Patents, the Board is invited to review U.S. Patent Nos. 5,817,479 (**Exhibit O**), 5,654,173 (**Exhibit P**), and 5,552,281 (**Exhibit Q**; each of which claims short polynucleotides), and recently issued U.S. Patent No. 6,340,583 (**Exhibit R**; which includes no working examples), none of which contain examples of the "real-world" utilities that the Examiner

seems to be requiring. As issued U.S. Patents are presumed to meet all of the requirements for patentability, including 35 U.S.C. §§ 101 and 112, first paragraph (see Section VIII(B), below), Appellants submit that the present polynucleotides must also meet the requirements of 35 U.S.C. § 101. While Appellants agree that each application is examined on its own merits, Appellants are unaware of any changes to 35 U.S.C. § 101, or in the interpretation of 35 U.S.C. § 101 by the Supreme Court or the Federal Circuit, since the issuance of these patents that render the subject matter claimed in these patents, which is similar to the subject matter in question in the present application, as suddenly non-statutory or failing to meet the requirements of 35 U.S.C. § 101. Given the rapid pace of development in the biotechnology arts, it is difficult for the Appellants to understand how an invention fully disclosed and free of prior art at the time the present application was filed, could somehow retain *less* utility and be *less* enabled than inventions in the cited issued U.S. patents (which were filed during a time when the level of skill in the art was clearly lower). Simply put, Appellants invention is *more* enabled and retains *at least as much* utility as the inventions described in the claims of the U.S. patents of record. Thus, holding Appellants to a different standard of utility would be arbitrary and capricious, and, like other clear violations of due process, cannot stand.

For each of the foregoing reasons, Appellants submit that the rejection of claims 1 and 5-7 under 35 U.S.C. § 101 must be overruled.

B. Are Claims 1 and 5-7 Unusable Due to a Lack of Patentable Utility?

The Final Action and Advisory Action maintain the rejection of claims 1 and 5-7 under 35 U.S.C. § 112, first paragraph, since allegedly one skilled in the art would not know how to use the invention, as the invention allegedly is not supported by either a clear asserted utility or a well-established utility.

The arguments detailed above in **Section VIII(A)** concerning the utility of the presently claimed sequences are incorporated herein by reference. As the Federal Circuit and its predecessor have determined that the utility requirement of Section 101 and the how to use requirement of Section 112, first paragraph, have the same basis, specifically the disclosure of a credible utility (*In re Brana, supra*;

In re Jolles, 628 F.2d 1322, 1326 n.11, 206 USPQ 885, 889 n.11 (CCPA 1980); *In re Fouche*, 439 F.2d 1237, 1243, 169 USPQ 429, 434 (CCPA 1971)), Appellants submit that as claims 1 and 5-7 have been shown to have "a specific, substantial, and credible utility", as detailed in **Section VIII(A)** above, the present rejection of claims 1 and 5-7 under 35 U.S.C. § 112, first paragraph, cannot stand.

Appellants therefore submit that the rejection of claims 1 and 5-7 under 35 U.S.C. § 112, first paragraph, must be overruled.

IX. APPENDIX

The claims involved in this appeal are as follows:

1. An isolated nucleic acid molecule comprising the nucleotide sequence of SEQ ID NO:23.

5. An isolated nucleic acid molecule comprising a nucleotide sequence that encodes the amino acid sequence of SEQ ID NO:24.

6. An expression vector comprising a nucleic acid sequence encoding the amino acid sequence of SEQ ID NO: 24.

7. A cell comprising the expression vector of Claim 6.

X. CONCLUSION

Appellants respectfully submit that, in light of the foregoing arguments, the Final Action's conclusion that claims 1 and 5-7 lack a patentable utility and are unusable by the skilled artisan due to a lack of patentable utility is unwarranted. It is therefore requested that the Board overturn the Final Action's rejections.

Respectfully submitted,

September 18, 2003
Date

Peter G. Sefevinn
Reg No 41016

Lance K. Ishimoto Reg. No. 41,866
Agent For Appellants

LEXICON GENETICS INCORPORATED
(281) 863-3399

Customer # 24231

EXHIBIT A

1: Gene 2001 Jul 25;273 (1):89-96

Related Articles, Nucleotide, Protein, NEW Books, LinkOut

ELSEVIER SCIENCE FULL-TEXT ARTICLE

Two new genes from the human ATP-binding cassette transporter superfamily, ABCC11 and ABCC12, tandemly duplicated on chromosome 16q12.

Tammur J, Prades C, Arnould I, Rzhetsky A, Hutchinson A, Adachi M, Schuetz JD, Swoboda KJ, Ptacek LJ, Rosier M, Dean M, Allikmets R.

Department of Biotechnology, Institute of Molecular and Cell Biology, Tartu University, Tartu, Estonia.

Several years ago, we initiated a long-term project of cloning new human ATP-binding cassette (ABC) transporters and linking them to various disease phenotypes. As one of the results of this project, we present two new members of the human ABCC subfamily, ABCC11 and ABCC12. These two new human ABC transporters were fully characterized and mapped to the human chromosome 16q12. With the addition of these two genes, the complete human ABCC subfamily has 12 identified members (ABCC1-12), nine from the multidrug resistance-like subgroup, two from the sulfonylurea receptor subgroup, and the CFTR gene. Phylogenetic analysis determined that ABCC11 and ABCC12 are derived by duplication, and are most closely related to the ABCC5 gene. Genetic variation in some ABCC subfamily members is associated with human inherited diseases, including cystic fibrosis (CFTR/ABCC7), Dubin-Johnson syndrome (ABCC2), pseudoxanthoma elasticum (ABCC6) and familial persistent hyperinsulinemic hypoglycemia of infancy (ABCC8). Since ABCC11 and ABCC12 were mapped to a region harboring gene(s) for paroxysmal kinesigenic choreoathetosis, the two genes represent positional candidates for this disorder.

PMID: 11483364 [PubMed - indexed for MEDLINE]

```
FASTA searches a protein or DNA sequence data bank
 version 3.3t05 March 30, 2000
 Please cite:
 W.R. Pearson & D.J. Lipman PNAS (1988) 85:2444-2448

/tmp/fastaCAACZaWfX: 1219 aa
 >SEQ ID NO 23 human transporter
 vs  /tmp/fastaDAADZaWfX library
searching /tmp/fastaDAADZaWfX library

   1382 residues in 1 sequences

FASTA (3.34 January 2000) function [optimized, BL50 matrix (15:-5)] ktup: 2
 join: 40, opt: 28, gap-pen: -12/ -2, width:  16
 Scan time:  0.050
The best scores are: opt
gi|21729873|ref|NP_115972.2| ATP-binding cassette  (1382) 4838

>>gi|21729873|ref|NP_115972.2| ATP-binding cassette, sub  (1382 aa)
 initn: 7928 init1: 4838 opt: 4838
Smith-Waterman score: 7606; 88.061% identity in 1382 aa overlap (1-1219:1-
1382)

               10        20        30        40        50        60
SEQ    MTRKRTYWVPNSSGGLVNRGIDIGDDMVSGLIYKTYTLQDGPWSQQERNPEAPGRAAVPP
       ::::::::::::::::::::::::::::::::::::::::::::::::::::::::::::
gi|217 MTRKRTYWVPNSSGGLVNRGIDIGDDMVSGLIYKTYTLQDGPWSQQERNPEAPGRAAVPP
               10        20        30        40        50        60

               70        80        90       100       110       120
SEQ    WGKYDAALRTMIPFRPKPRFPAPQPLDNAGLFSYLTVSWLTPLMIQSLRSRLDENTIPPL
       ::::::::::::::::::::::::::::::::::::::::::::::::::::::::::::
gi|217 WGKYDAALRTMIPFRPKPRFPAPQPLDNAGLFSYLTVSWLTPLMIQSLRSRLDENTIPPL
               70        80        90       100       110       120

              130       140       150       160       170       180
SEQ    SVHDASDKNVQRLHRLWEEEVSRRGIEKASVLLVMLRFQRTRLIFDALLGICFCIASVLG
       ::::::::::::::::::::::::::::::::::::::::::::::::::::::::::::
gi|217 SVHDASDKNVQRLHRLWEEEVSRRGIEKASVLLVMLRFQRTRLIFDALLGICFCIASVLG
              130       140       150       160       170       180

              190       200       210       220       230       240
SEQ    PILIIPKILEYSEEQLGNVVHGVGLCFALFLSECVKSLSFSSSWIINQRTAIRFQAAVSS
       ::::::::::::::::::::::::::::::::::::::::::::::::::::::::.:::::
gi|217 PILIIPKILEYSEEQLGNVVHGVGLCFALFLSECVKSLSFSSSWIINQRTAIRFRAAVSS
              190       200       210       220       230       240

              250       260       270       280       290       300
SEQ    FAFEKLIQFKSVIHITSGEAISFFTGDVNYLFEGVCYGPLVLITCASLVICSISSYFIIG
       ::::::::::::::::::::::::::::::::::::::::::::::::::::::::::::
gi|217 FAFEKLIQFKSVIHITSGEAISFFTGDVNYLFEGVCYGPLVLITCASLVICSISSYFIIG
              250       260       270       280       290       300

              310       320       330       340       350       360
SEQ    YTAFIAILCYLLVFPLEVFMTRMAVKAQHHTSEVSDQRIRVTSEVLTCIKLIKMYTWEKP
       :::::::::::::::: ::::::::::::::::::::::::::::::::::::::::::::
gi|217 YTAFIAILCYLLVFPLAVFMTRMAVKAQHHTSEVSDQRIRVTSEVLTCIKLIKMYTWEKP
              310       320       330       340       350       360

              370       380       390       400       410       420
SEQ    FAKIIEDLRRKERKLLEKCGLVQSLTSITLFIIPTVATAVWVLIHTSLKLKLTASMAFSM
       ::::::::::::::::::::::::::::::::::::::::::::::::::::::::::::
gi|217 FAKIIEDLRRKERKLLEKCGLVQSLTSITLFIIPTVATAVWVLIHTSLKLKLTASMAFSM
              370       380       390       400       410       420
```

```
                430       440       450       460       470       480
SEQ     LASLNLLRLSVFFVPIAVKGLTNSKSAVMRFKKFFLQESPVFYVQTLQDPSKALVFEEAT
        :::::::::::::::::::::::::::::::::::::::::::::::::::::::::::::
gi|217 LASLNLLRLSVFFVPIAVKGLTNSKSAVMRFKKFFLQESPVFYVQTLQDPSKALVFEEAT
                430       440       450       460       470       480

                490       500       510       520       530       540
SEQ     LSWQQTCPGIVNGALELERNGHASEGMTRPRDALGPEEEGNSLGPELHKINLVVSKGMML
        ::::::::::::::::::::::::::::::::::::::::::::::::::::::::::::::
gi|217 LSWQQTCPGIVNGALELERNGHASEGMTRPRDALGPEEEGNSLGPELHKINLVVSKGMML
                490       500       510       520       530       540

                550       560       570       580       590       600
SEQ     GVCGNTGSGKSSLLSAILEEMHLLEGSVGVQGSLAYVPQQAWIVSGNIRENILMGGAYDK
        ::::::::::::::::::::::::::::::::::::::::::::::::::::::::::::::
gi|217 GVCGNTGSGKSSLLSAILEEMHLLEGSVGVQGSLAYVPQQAWIVSGNIRENILMGGAYDK
                550       560       570       580       590       600

                610       620       630       640       650       660
SEQ     ARYLQVLHCCSLNRDLELLPFGDMTEIGERGLNLSGGQKQRISLARAVYSDRQIYLLDDP
        ::::::::::::::::::::::::::::::::::::::::::::::::::::::::::::::
gi|217 ARYLQVLHCCSLNRDLELLPFGDMTEIGERGLNLSGGQKQRISLARAVYSDRQIYLLDDP
                610       620       630       640       650       660

                670       680       690       700       710       720
SEQ     LSAVDAHVGKHIFEECIKKTLRGKTVVLVTHQLQYLEFCGQIILLENGKICENGTHSELM
        ::::::::::::::::::::::::::::::::::::::::::::::::::::::::::::::
gi|217 LSAVDAHVGKHIFEECIKKTLRGKTVVLVTHQLQYLEFCGQIILLENGKICENGTHSELM
                670       680       690       700       710       720

                730
SEQ     QKKGKYAQLIQKMHKEATS----------------------------------------
        ::::::::::::::::::
gi|217 QKKGKYAQLIQKMHKEATSDMLQDTAKIAEKPKVESQALATSLEESLNGNAVPEHQLTQE
                730       740       750       760       770       780

SEQ     ----------------------------------------------------------

gi|217 EEMEEGSLSWRVYHHYIQAAGGYMVSCIIFFFVVLIVFLTIFSFWWLSYWLEQGSGTNSS
                790       800       810       820       830       840

SEQ     ----------------------------------------------------------

gi|217 RESNGTMADLGNIADNPQLSFYQLVYGLNALLLICVGVCSSGIFTKVTRKASTALHNKLF
                850       860       870       880       890       900

        740       750       760       770       780       790
SEQ     --VFRCPMSFFDTIPIGRLLNCFAGDLEQLDQLLPIFSEQFLVLSLMVIAVLLIVSVLSP
        ~::::::::::::::::::::::::::::::::::::::::::::::::::::::::::::
gi|217 NKVFRCPMSFFDTIPIGRLLNCFAGDLEQLDQLLPIFSEQFLVLSLMVIAVLLIVSVLSP
                910       920       930       940       950       960

        800       810       820       830       840       850
SEQ     YILLMGAIIMVICFIYYMMFKKAIGVFKRLENYSRSPLFSHILNSLQGLSSIHVYGKTED
        ::::::::::::::::::::::::::::::::::::::::::::::::::::::::::::::
gi|217 YILLMGAIIMVICFIYYMMFKKAIGVFKRLENYSRSPLFSHILNSLQGLSSIHVYGKTED
                970       980       990      1000      1010      1020
```

```
        860       870       880       890       900       910
SEQ     FISQFKRLTDAQNNYLLLFLSSTRWMALRLEIMTNLVTLAVALFVAFGISSTPYSFKVMA
        ::::::::::::::::::::::::::::::::::::::::::::::::::::::::::::
gi|217 FISQFKRLTDAQNNYLLLFLSSTRWMALRLEIMTNLVTLAVALFVAFGISSTPYSFKVMA
              1030      1040      1050      1060      1070      1080

        920       930       940       950       960       970
SEQ     VNIVLQLASSFQATARIGLETEAQFTAVERILQYMKMCVSEAPLHMEGTSCPQGWPQHGE
        ::::::::::::::::::::::::::::::::::::::::::::::::::::::::::::
gi|217 VNIVLQLASSFQATARIGLETEAQFTAVERILQYMKMCVSEAPLHMEGTSCPQGWPQHGE
              1090      1100      1110      1120      1130      1140

        980       990      1000      1010      1020      1030
SEQ     IIFQDYHMKYRDNTPTVLHGINLTIRGHEVVGIVGRTGSGKSSLGMALFRLVEPMAGRIL
        ::::::::::::::::::::::::::::::::::::::::::::::::::::::::::::
gi|217 IIFQDYHMKYRDNTPTVLHGINLTIRGHEVVGIVGRTGSGKSSLGMALFRLVEPMAGRIL
              1150      1160      1170      1180      1190      1200

      1040      1050      1060      1070      1080      1090
SEQ     IDGVDICSIGLEDLRSKLSVIPQDPVLLSGTIRFNLDPFDRHTDQQIWDALERTFLTKAI
        ::::::::::::::::::::::::::::::::::::::::::::::::::::::::::::
gi|217 IDGVDICSIGLEDLRSKLSVIPQDPVLLSGTIRFNLDPFDRHTDQQIWDALERTFLTKAI
              1210      1220      1230      1240      1250      1260

      1100      1110      1120      1130      1140      1150
SEQ     SKFPKKLHTDVVENGGNFSVGERQLLCIARAVLRNSKIILIDEATASIDMETDTLIQRTI
        ::::::::::::::::::::::::::::::::::::::::::::::::::::::::::::
gi|217 SKFPKKLHTDVVENGGNFSVGERQLLCIARAVLRNSKIILIDEATASIDMETDTLIQRTI
              1270      1280      1290      1300      1310      1320

      1160      1170      1180      1190      1200      1210
SEQ     REAFQGCTVLVIAHRVTTVLNCDHILVMGNGKVVEFDRPEVLRKKPGSLFAALMATATSS
        ::::::::::::::::::::::::::::::::::::::::::::::::::::::::::::
gi|217 REAFQGCTVLVIAHRVTTVLNCDHILVMGNGKVVEFDRPEVLRKKPGSLFAALMATATSS
              1330      1340      1350      1360      1370      1380


SEQ     LR
        ::
gi|217 LR
```

1219 residues in 1 query sequences
1382 residues in 1 library sequences
Scomplib [version 3.3t05 March 30, 2000]
start: Mon Nov 11 10:23:05 2002 done: Mon Nov 11 10:23:06 2002
Scan time: 0.050 Display time: 2.400

Function used was FASTA

1: NP_115972. ATP-binding casse...[gi:21729873]

Links

LOCUS ABCC11 1382 aa linear PRI 05-NOV-2002
DEFINITION ATP-binding cassette, sub-family C, member 11 isoform a; multi-resistance protein 8; ATP-binding cassette transporter MRP8; ATP-binding cassette protein C11 [Homo sapiens].
ACCESSION NP_115972
VERSION NP_115972.2 GI:21729873
DBSOURCE REFSEQ: accession NM_032583.2
KEYWORDS .
SOURCE Homo sapiens (human)
ORGANISM Homo sapiens
Eukaryota; Metazoa; Chordata; Craniata; Vertebrata; Euteleostomi; Mammalia; Eutheria; Primates; Catarrhini; Hominidae; Homo.
REFERENCE 1 (residues 1 to 1382)
AUTHORS Dean,M., Rzhetsky,A. and Allikmets,R.
TITLE The human ATP-binding cassette (ABC) transporter superfamily
JOURNAL Genome Res. 11 (7), 1156-1166 (2001)
MEDLINE 21329047
PUBMED 11435397
REFERENCE 2 (residues 1 to 1382)
AUTHORS Tammur,J., Prades,C., Arnould,I., Rzhetsky,A., Hutchinson,A., Adachi,M., Schuetz,J.D., Swoboda,K.J., Ptacek,L.J., Rosier,M., Dean,M. and Allikmets,R.
TITLE Two new genes from the human ATP-binding cassette transporter superfamily, ABCC11 and ABCC12, tandemly duplicated on chromosome 16q12
JOURNAL Gene 273 (1), 89-96 (2001)
MEDLINE 21376129
PUBMED 11483364
REFERENCE 3 (residues 1 to 1382)
AUTHORS Bera,T.K., Lee,S., Salvatore,G., Lee,B. and Pastan,I.
TITLE MRP8, a new member of ABC transporter superfamily, identified by EST database mining and gene prediction program, is highly expressed in breast cancer
JOURNAL Mol. Med. 7 (8), 509-516 (2001)
MEDLINE 21475973
PUBMED 11591886
REFERENCE 4 (residues 1 to 1382)
AUTHORS Yabuuchi,H., Shimizu,H., Takayanagi,S. and Ishikawa,T.
TITLE Multiple splicing variants of two new human ATP-binding cassette transporters, ABCC11 and ABCC12
JOURNAL Biochem. Biophys. Res. Commun. 288 (4), 933-939 (2001)
MEDLINE 21547789
PUBMED 11688999
COMMENT REVIEWED REFSEQ: This record has been curated by NCBI staff. The reference sequence was derived from AF367202.1.
On Jul 11, 2002 this sequence version replaced gi:14211905.
Summary: The protein encoded by this gene is a member of the

superfamily of ATP-binding cassette (ABC) transporters. ABC proteins transport various molecules across extra- and intra-cellular membranes. ABC genes are divided into seven distinct subfamilies (ABC1, MDR/TAP, MRP, ALD, OABP, GCN20, White). This ABC full transporter is a member of the MRP subfamily which is involved in multi-drug resistance. It is expressed at low levels in all tissues, except kidney, spleen, and colon. This gene and family member ABCC12 are determined to be derived by duplication and are both localized to chromosome 16q12.1. Their chromosomal localization, potential function, and expression patterns identify them as candidates for paroxysmal kinesigenic choreoathetosis, a disorder characterized by attacks of involuntary movements and postures, chorea, and dystonia. Multiple alternatively spliced transcript variants have been described for this gene. Transcript Variant: This variant (1), as well as variant 2, encodes the predominant isoform (a).

FEATURES Location/Qualifiers

source 1..1382
/organism="Homo sapiens"
/db_xref="taxon:9606"
/chromosome="16"
/map="16q12.1"

Protein 1..1382
/product="ATP-binding cassette, sub-family C, member 11 isoform a"
/note="multi-resistance protein 8; ATP-binding cassette transporter MRP8; ATP-binding cassette protein C11"

Region 163..427
/region_name="ABC transporter transmembrane region. This family represents a unit of six transmembrane helices. Many members of the ABC transporter family (pfam00005) have two such regions"
/note="ABC_membrane"
/db_xref="CDD:pfam00664"

Region 536..691
/region_name="ATPases associated with a variety of cellular activities"
/note="AAA"
/db_xref="CDD:smart00382"

Region 537..708
/region_name="ABC transporter. ABC transporters for a large family of proteins responsible for translocation of a variety of compounds across biological membranes. ABC transporters are the largest family of proteins in many completely sequenced bacteria. ABC transporters are composed of two copies of this domain and two copies of a transmembrane domain pfam00664. These four domains may belong to a single polypeptide or belong in different polypeptide chains"
/note="ABC_tran"
/db_xref="CDD:pfam00005"

Region 849..1094
/region_name="ABC transporter transmembrane region. This family represents a unit of six transmembrane helices. Many members of the ABC transporter family (pfam00005) have two such regions"
/note="ABC_membrane"
/db_xref="CDD:pfam00664"

Region 1168..1360
/region_name="ATPases associated with a variety of

```
                     cellular activities"
                     /note="AAA"
                     /db_xref="CDD:smart00382"
     Region          1169..1351
                     /region_name="ABC transporter. ABC transporters for a
                     large family of proteins responsible for translocation of
                     a variety of compounds across biological membranes. ABC
                     transporters are the largest family of proteins in many
                     completely sequenced bacteria. ABC transporters are
                     composed of two copies of this domain and two copies of a
                     transmembrane domain pfam00664. These four domains may
                     belong to a single polypeptide or belong in different
                     polypeptide chains"
                     /note="ABC_tran"
                     /db_xref="CDD:pfam00005"
     CDS             1..1382
                     /gene="ABCC11"
                     /coded_by="NM_032583.2:79..4227"
                     /note="transporter"
                     /db_xref="LocusID:85320"
                     /db_xref="MIM:607040"
ORIGIN
        1 mtrkrtywvp nssgglvnrg idigddmvsg liyktytlqd gpwsqqernp eapgraavpp
       61 wgkydaalrt mipfrpkprf papqpldnag lfsyltvswl tplmiqslrs rldentippl
      121 svhdasdknv qrlhrlweee vsrrgiekas vllvmlrfqr trlifdallg icfciasvlg
      181 piliipkile yseeqlgnvv hgvglcfalf lsecvkslsf ssswiinqrt airfraavss
      241 fafekliqfk svihitsgea isfftgdvny lfegvcygpl vlitcaslvi csissyfiig
      301 ytafiailcy llvfplavfm trmavkaqhh tsevsdqrir vtsevltcik likmytwekp
      361 fakiiedlrr kerkllekcg lvqsltsitl fiiptvatav wvlihtslkl kltasmafsm
      421 laslnllrls vffvpiavkg ltnsksavmr fkkfflqesp vfyvqtlqdp skalvfeeat
      481 lswqqtcpgi vngalelern ghasegmtrp rdalgpeeeg nslgpelhki nlvvskgmml
      541 gvcgntgsgk ssllsailee mhllegsvgv qgslayvpqq awivsgnire nilmggaydk
      601 arylqvlhcc slnrdlellp fgdmteiger glnlsggqkq rislaravys drqiyllddp
      661 lsavdahvgk hifeecikkt lrgktvvlvt hqlqylefcg qiillengki cengthselm
      721 qkkgkyaqli qkmhkeatsd mlqdtakiae kpkvesqala tsleeslngn avpehqltqe
      781 eemeegslsw rvyhhyiqaa ggymvsciif ffvvlivflt ifsfwwlsyw leqgsgtnss
      841 resngtmadl gniadnpqls fyqlvyglna lllicvgvcs sgiftkvtrk astalhnklf
      901 nkvfrcpmsf fdtipigrll ncfagdleql dqllpifseq flvlslmvia vllivsvlsp
      961 yillmgaiim vicfiyymmf kkaigvfkrl enysrsplfs hilnslqgls sihvygkted
     1021 fisqfkrltd aqnnylllfl sstrwmalrl eimtnlvtla valfvafgis stpysfkvma
     1081 vnivlqlass fqatarigle teaqftaver ilqymkmcvs eaplhmegts cpqgwpqhge
     1141 iifqdyhmky rdntptvlhg inltirghev vgivgrtgsg ksslgmalfr lvepmagril
     1201 idgvdicsig ledlrsklsv ipqdpvllsg tirfnldpfd rhtdqqiwda lertfltkai
     1261 skfpkklhtd vvenggnfsv gerqllciar avlrnskiil ideatasidm etdtliqrti
     1321 reafqgctvl viahrvttvl ncdhilvmgn gkvvefdrpe vlrkkpgslf aalmatatss
     1381 lr
//
```

Revised: July 5, 2002.

EXHIBIT B

1: Biochem J. 2002 Nov 15;368(Pt 1):325-32. Related Articles, Links

Impaired 2',3'-dideoxy-3'-thiacytidine accumulation in T-lymphoblastoid cells as a mechanism of acquired resistance independent of multidrug resistant protein 4 with a possible role for ATP-binding cassette C11.

Turriziani O, Schuetz JD, Focher F, Scagnolari C, Sampath J, Adachi M, Bambacioni F, Riva E, Antonelli G.

Department of Experimental Medicine and Pathology, University "La Sapienza", 00185 Rome, Italy.

Cellular factors may contribute to the decreased efficacy of chemotherapy in HIV infection. Indeed, prolonged treatment with nucleoside analogues, such as azidothymidine (AZT), 2',3'-deoxycytidine or 9-(2-phosphonylmethoxyethyl)adenine, induces cellular resistance. We have developed a human T lymphoblastoid cell line (CEM 3TC) that is selectively resistant to the antiproliferative effect of 2',3'-dideoxy-3'-thiacytidine (3TC) because the CEM 3TC cells were equally sensitive to AZT, as well as the antimitotic agent, vinblastine. The anti-retroviral activity of 3TC against HIV-1 was also severely impaired in the CEM 3TC cells. Despite similar deoxycytidine kinase activity and unchanged uptake of nucleosides such as AZT and 2'-deoxycytidine, CEM 3TC had profoundly impaired 3TC accumulation. Further studies indicated that CEM 3TC retained much less 3TC. However, despite a small overexpression of multidrug resistance protein (MRP) 4, additional studies with cells specifically engineered to overexpress MRP4 demonstrated there was no impact on either 3TC accumulation or efflux. Finally, an increased expression of the MRP5 homologue, ATP-binding cassette C11 (ABCC11) was observed in the CEM 3TC cells. We speculate that the decreased 3TC accumulation in the CEM 3TC might be due to the upregulation of ABCC11.

PMID: 12133003 [PubMed - indexed for MEDLINE]

1: NP_660187. Reports ATP-binding casse...[gi:21729876]

Comment Features Sequence BLink, Conserved Domains, Links

```
LOCUS       NP_660187                 1344 aa            linear   PRI 06-APR-2003
DEFINITION  ATP-binding cassette, sub-family C, member 11 isoform b;
            multi-resistance protein 8; ATP-binding cassette transporter MRP8;
            ATP-binding cassette protein C11 [Homo sapiens].
ACCESSION   NP_660187
VERSION     NP_660187.1  GI:21729876
DBSOURCE    REFSEQ: accession NM_145186.1
KEYWORDS    .
SOURCE      Homo sapiens (human)
  ORGANISM  Homo sapiens
            Eukaryota; Metazoa; Chordata; Craniata; Vertebrata; Euteleostomi;
            Mammalia; Eutheria; Primates; Catarrhini; Hominidae; Homo.
REFERENCE   1  (residues 1 to 1344)
  AUTHORS   Turriziani,O., Schuetz,J.D., Focher,F., Scagnolari,C., Sampath,J.,
            Adachi,M., Bambacioni,F., Riva,E. and Antonelli,G.
  TITLE     Impaired 2',3'-dideoxy-3'-thiacytidine accumulation in
            T-lymphoblastoid cells as a mechanism of acquired resistance
            independent of multidrug resistant protein 4 with a possible role
            for ATP-binding cassette C11
  JOURNAL   Biochem. J. 368 (Pt 1), 325-332 (2002)
  PUBMED    12133003
  REMARK    GeneRIF: Impaired 2',3'-dideoxy-3'-thiacytidine accumulation in
            T-lymphoblastoid cells as a mechanism of acquired resistance
            independent of multidrug resistant protein 4 with a possible role
            for ATP-binding cassette C11.
REFERENCE   2  (residues 1 to 1344)
  AUTHORS   Yabuuchi,H., Shimizu,H., Takayanagi,S. and Ishikawa,T.
  TITLE     Multiple splicing variants of two new human ATP-binding cassette
            transporters, ABCC11 and ABCC12
  JOURNAL   Biochem. Biophys. Res. Commun. 288 (4), 933-939 (2001)
  PUBMED    11688999
  REMARK    GeneRIF: alternative splice variants and gene expression
REFERENCE   3  (residues 1 to 1344)
  AUTHORS   Bera,T.K., Lee,S., Salvatore,G., Lee,B. and Pastan,I.
  TITLE     MRP8, a new member of ABC transporter superfamily, identified by
            EST database mining and gene prediction program, is highly
            expressed in breast cancer
  JOURNAL   Mol. Med. 7 (8), 509-516 (2001)
  PUBMED    11591886
REFERENCE   4  (residues 1 to 1344)
  AUTHORS   Tammur,J., Prades,C., Arnould,I., Rzhetsky,A., Hutchinson,A.,
            Adachi,M., Schuetz,J.D., Swoboda,K.J., Ptacek,L.J., Rosier,M.,
```

Dean,M. and Allikmets,R.
TITLE Two new genes from the human ATP-binding cassette transporter superfamily, ABCC11 and ABCC12, tandemly duplicated on chromosome 16q12
JOURNAL Gene 273 (1), 89-96 (2001)
PUBMED 11483364
REFERENCE 5 (residues 1 to 1344)
AUTHORS Dean,M., Rzhetsky,A. and Allikmets,R.
TITLE The human ATP-binding cassette (ABC) transporter superfamily
JOURNAL Genome Res. 11 (7), 1156-1166 (2001)
PUBMED 11435397
COMMENT REVIEWED REFSEQ: This record has been curated by NCBI staff. The reference sequence was derived from AF411579.1.

Summary: The protein encoded by this gene is a member of the superfamily of ATP-binding cassette (ABC) transporters. ABC proteins transport various molecules across extra- and intra-cellular membranes. ABC genes are divided into seven distinct subfamilies (ABC1, MDR/TAP, MRP, ALD, OABP, GCN20, White). This ABC full transporter is a member of the MRP subfamily which is involved in multi-drug resistance. It is expressed at low levels in all tissues, except kidney, spleen, and colon. This gene and family member ABCC12 are determined to be derived by duplication and are both localized to chromosome 16q12.1. Their chromosomal localization, potential function, and expression patterns identify them as candidates for paroxysmal kinesigenic choreoathetosis, a disorder characterized by attacks of involuntary movements and postures, chorea, and dystonia. Multiple alternatively spliced transcript variants have been described for this gene.

Transcript Variant: This variant (3) lacks an alternate in-frame exon compared to variant 1, resulting in a shorter protein (isoform b), compared to isoform a.

FEATURES Location/Qualifiers
source 1..1344
/organism="Homo sapiens"
/db_xref="taxon:9606"
/chromosome="16"
/map="16q12.1"
Protein 1..1344
/product="ATP-binding cassette, sub-family C, member 11 isoform b"
/note="multi-resistance protein 8; ATP-binding cassette transporter MRP8; ATP-binding cassette protein C11"
/calculated_mol_wt=149963
Region 150..732
/region_name="ABC-type multidrug transport system, ATPase and permease components [Defense mechanisms]"
/note="MdlB"
/db_xref="CDD:COG1132"
Region 163..>431
/region_name="ABC transporter transmembrane region"
/note="ABC_membrane"
/db_xref="CDD:40747"
Region 517..>709
/region_name="Domain 1 of the ABC subfamily C"
/note="ABC_subfamilyC_domain1"
/db_xref="CDD:48283"
Region 849..>1094
/region_name="ABC transporter transmembrane region"

```
                     /note="ABC_membrane"
                     /db_xref="CDD:40747"
     Region          853..1338
                     /region_name="ABC-type multidrug transport system, ATPase
                     and permease components [Defense mechanisms]"
                     /note="MdlB"
                     /db_xref="CDD:COG1132"
     Region          1141..>1314
                     /region_name="Domain 1 of the ABC subfamily C"
                     /note="ABC_subfamilyC_domain1"
                     /db_xref="CDD:48283"
     CDS             1..1344
                     /gene="ABCC11"
                     /coded_by="NM_145186.1:79..4113"
                     /db_xref="GeneID:85320"
                     /db_xref="MIM:607040"
ORIGIN
        1 mtrkrtywvp nssgglvnrg idigddmvsg liyktytlqd gpwsqqernp eapgraavpp
       61 wgkydaalrt mipfrpkprf papqpldnag lfsyltvswl tplmiqslrs rldentippl
      121 svhdasdknv qrlhrlweee vsrrgiekas vllvmlrfqr trlifdallg icfciasvlg
      181 piliipkile yseeqlgnvv hgvglcfalf lsecvkslsf ssswiinqrt airfraavss
      241 fafekliqfk svihitsgea isfftgdvny lfegvcygpl vlitcaslvi csissyfiig
      301 ytafiailcy llvfplavfm trmavkaqhh tsevsdqrir vtsevltcik likmytwekp
      361 fakiiedlrr kerkllekcg lvqsltsitl fiiptvatav wvlihtslkl kltasmafsm
      421 laslnllrls vffvpiavkg ltnsksavmr fkkfflqesp vfyvqtlqdp skalvfeeat
      481 lswqqtcpgi vngalelern ghasegmtrp rdalgpeeeg nslgpelhki nlvvskgmml
      541 gvcgntgsgk ssllsailee mhllegsvgv qgslayvpqq awivsgnire nilmggaydk
      601 arylqvlhcc slnrdlellp fgdmteiger glnlsgggkq rislaravys drqiyllddp
      661 lsavdahvgk hifeecikkt lrgktvvlvt hqlqylefcg qiillengki cengthselm
      721 qkkgkyaqli qkmhkeatsd mlqdtakiae kpkvesqala tsleeslngn avpehqltqe
      781 eemeegslsw rvyhhyiqaa ggymvsciif ffvvlivflt ifsfwwlsyw leqgsgtnss
      841 resngtmadl gniadnpqls fyqlvyglna lllicvgvcs sgiftkvtrk astalhnklf
      901 nkvfrcpmsf fdtipigrll ncfagdleql dqllpifseq flvlslmvia vllivsvlsp
      961 yillmgaiim vicfiyymmf kkaigvfkrl enysrsplfs hilnslqgls sihvygkted
     1021 fisqfkrltd aqnnylllfl sstrwmalrl eimtnlvtla valfvafgis stpysfkvma
     1081 vnivlqlass fqatarigle teaqftaver ilqymkmcvs eaplhmegts cpqgwpqhge
     1141 iifqdyhmky rdntptvlhg inltirghev vgivgrtgsg ksslgmalfr lvepmagril
     1201 idgvdicsig ledlrsklsv ipqdpvllsg tirfnldpfd rhtdqqiwda lertfltkai
     1261 ilideatasi dmetdtliqr tireafqgct vlviahrvtt vlncdhilvm gngkvvefdr
     1321 pevlrkkpgs lfaalmatat sslr
//
```

Comparison of the Amino Acid Sequences of SEQ ID NO:24 and NP_660187

```
FASTA searches a protein or DNA sequence data bank
 version 3.3t05 March 30, 2000
Please cite:
 W.R. Pearson & D.J. Lipman PNAS (1988) 85:2444-2448

/tmp/fastaGAABJayWj: 1219 aa
 >seqid24
 vs  /tmp/fastaHAACJayWj library
searching /tmp/fastaHAACJayWj library

   1344 residues in     1 sequences

FASTA (3.34 January 2000) function [optimized, BL50 matrix (15:-5)] ktup: 2
 join: 40, opt: 28, gap-pen: -12/ -2, width:  16
 Scan time:  0.034
The best scores are:                                                opt
NP_660187 ACCESSION:NP_660187 NID: gi 21729876 re  (1344) 4838

>>NP_660187 ACCESSION:NP_660187 NID: gi 21729876 ref NP_  (1344 aa)
 initn: 7156 init1: 4838 opt: 4838
Smith-Waterman score: 7274;  85.311% identity in 1382 aa overlap (1-1219:1-
1344)

               10        20        30        40        50        60
seqid2 MTRKRTYWVPNSSGGLVNRGIDIGDDMVSGLIYKTYTLQDGPWSQQERNPEAPGRAAVPP
       ::::::::::::::::::::::::::::::::::::::::::::::::::::::::::::
NP_660 MTRKRTYWVPNSSGGLVNRGIDIGDDMVSGLIYKTYTLQDGPWSQQERNPEAPGRAAVPP
               10        20        30        40        50        60

               70        80        90       100       110       120
seqid2 WGKYDAALRTMIPFRPKPRFPAPQPLDNAGLFSYLTVSWLTPLMIQSLRSRLDENTIPPL
       ::::::::::::::::::::::::::::::::::::::::::::::::::::::::::::
NP_660 WGKYDAALRTMIPFRPKPRFPAPQPLDNAGLFSYLTVSWLTPLMIQSLRSRLDENTIPPL
               70        80        90       100       110       120

              130       140       150       160       170       180
seqid2 SVHDASDKNVQRLHRLWEEEVSRRGIEKASVLLVMLRFQRTRLIFDALLGICFCIASVLG
       ::::::::::::::::::::::::::::::::::::::::::::::::::::::::::::
NP_660 SVHDASDKNVQRLHRLWEEEVSRRGIEKASVLLVMLRFQRTRLIFDALLGICFCIASVLG
              130       140       150       160       170       180

              190       200       210       220       230       240
seqid2 PILIIPKILEYSEEQLGNVVHGVGLCFALFLSECVKSLSFSSSWIINQRTAIRFQAAVSS
       ::::::::::::::::::::::::::::::::::::::::::::::::::::::::::.::::
NP_660 PILIIPKILEYSEEQLGNVVHGVGLCFALFLSECVKSLSFSSSWIINQRTAIRFRAAVSS
              190       200       210       220       230       240

              250       260       270       280       290       300
seqid2 FAFEKLIQFKSVIHITSGEAISFFTGDVNYLFEGVCYGPLVLITCASLVICSISSYFIIG
       ::::::::::::::::::::::::::::::::::::::::::::::::::::::::::::
NP_660 FAFEKLIQFKSVIHITSGEAISFFTGDVNYLFEGVCYGPLVLITCASLVICSISSYFIIG
              250       260       270       280       290       300

              310       320       330       340       350       360
seqid2 YTAFIAILCYLLVFPLEVFMTRMAVKAQHHTSEVSDQRIRVTSEVLTCIKLIKMYTWEKP
```

```
                 :::::::::::::::: ::::::::::::::::::::::::::::::::::::::::::::
NP_660 YTAFIAILCYLLVFPLAVFMTRMAVKAQHHTSEVSDQRIRVTSEVLTCIKLIKMYTWEKP
                310       320       330       340       350       360

                370       380       390       400       410       420
seqid2 FAKIIEDLRRKERKLLEKCGLVQSLTSITLFIIPTVATAVWVLIHTSLKLKLTASMAFSM
               ::::::::::::::::::::::::::::::::::::::::::::::::::::::::::::::
NP_660 FAKIIEDLRRKERKLLEKCGLVQSLTSITLFIIPTVATAVWVLIHTSLKLKLTASMAFSM
                370       380       390       400       410       420

                430       440       450       460       470       480
seqid2 LASLNLLRLSVFFVPIAVKGLTNSKSAVMRFKKFFLQESPVFYVQTLQDPSKALVFEEAT
               ::::::::::::::::::::::::::::::::::::::::::::::::::::::::::::::
NP_660 LASLNLLRLSVFFVPIAVKGLTNSKSAVMRFKKFFLQESPVFYVQTLQDPSKALVFEEAT
                430       440       450       460       470       480

                490       500       510       520       530       540
seqid2 LSWQQTCPGIVNGALELERNGHASEGMTRPRDALGPEEEGNSLGPELHKINLVVSKGMML
               ::::::::::::::::::::::::::::::::::::::::::::::::::::::::::::::
NP_660 LSWQQTCPGIVNGALELERNGHASEGMTRPRDALGPEEEGNSLGPELHKINLVVSKGMML
                490       500       510       520       530       540

                550       560       570       580       590       600
seqid2 GVCGNTGSGKSSLLSAILEEMHLLEGSVGVQGSLAYVPQQAWIVSGNIRENILMGGAYDK
               ::::::::::::::::::::::::::::::::::::::::::::::::::::::::::::::
NP_660 GVCGNTGSGKSSLLSAILEEMHLLEGSVGVQGSLAYVPQQAWIVSGNIRENILMGGAYDK
                550       560       570       580       590       600

                610       620       630       640       650       660
seqid2 ARYLQVLHCCSLNRDLELLPFGDMTEIGERGLNLSGGQKQRISLARAVYSDRQIYLLDDP
               ::::::::::::::::::::::::::::::::::::::::::::::::::::::::::::::
NP_660 ARYLQVLHCCSLNRDLELLPFGDMTEIGERGLNLSGGQKQRISLARAVYSDRQIYLLDDP
                610       620       630       640       650       660

                670       680       690       700       710       720
seqid2 LSAVDAHVGKHIFEECIKKTLRGKTVVLVTHQLQYLEFCGQIILLENGKICENGTHSELM
               ::::::::::::::::::::::::::::::::::::::::::::::::::::::::::::::
NP_660 LSAVDAHVGKHIFEECIKKTLRGKTVVLVTHQLQYLEFCGQIILLENGKICENGTHSELM
                670       680       690       700       710       720

                730
seqid2 QKKGKYAQLIQKMHKEATS----------------------------------------
               ::::::::::::::::::
NP_660 QKKGKYAQLIQKMHKEATSDMLQDTAKIAEKPKVESQALATSLEESLNGNAVPEHQLTQE
                730       740       750       760       770       780


seqid2 ------------------------------------------------------------

NP_660 EEMEEGSLSWRVYHHYIQAAGGYMVSCIIFFFVVLIVFLTIFSFWWLSYWLEQGSGTNSS
                790       800       810       820       830       840


seqid2 ------------------------------------------------------------

NP_660 RESNGTMADLGNIADNPQLSFYQLVYGLNALLLICVGVCSSGIFTKVTRKASTALHNKLF
                850       860       870       880       890       900

       740       750       760       770       780       790
seqid2 --VFRCPMSFFDTIPIGRLLNCFAGDLEQLDQLLPIFSEQFLVLSLMVIAVLLIVSVLSP
         ::::::::::::::::::::::::::::::::::::::::::::::::::::::::::::::
```

```
NP_660 NKVFRCPMSFFDTIPIGRLLNCFAGDLEQLDQLLPIFSEQFLVLSLMVIAVLLIVSVLSP
              910       920       930       940       950       960

       800       810       820       830       840       850
seqid2 YILLMGAIIMVICFIYYMMFKKAIGVFKRLENYSRSPLFSHILNSLQGLSSIHVYGKTED
       ::::::::::::::::::::::::::::::::::::::::::::::::::::::::::::
NP_660 YILLMGAIIMVICFIYYMMFKKAIGVFKRLENYSRSPLFSHILNSLQGLSSIHVYGKTED
              970       980       990      1000      1010      1020

       860       870       880       890       900       910
seqid2 FISQFKRLTDAQNNYLLLFLSSTRWMALRLEIMTNLVTLAVALFVAFGISSTPYSFKVMA
       ::::::::::::::::::::::::::::::::::::::::::::::::::::::::::::
NP_660 FISQFKRLTDAQNNYLLLFLSSTRWMALRLEIMTNLVTLAVALFVAFGISSTPYSFKVMA
             1030      1040      1050      1060      1070      1080

       920       930       940       950       960       970
seqid2 VNIVLQLASSFQATARIGLETEAQFTAVERILQYMKMCVSEAPLHMEGTSCPQGWPQHGE
       ::::::::::::::::::::::::::::::::::::::::::::::::::::::::::::
NP_660 VNIVLQLASSFQATARIGLETEAQFTAVERILQYMKMCVSEAPLHMEGTSCPQGWPQHGE
             1090      1100      1110      1120      1130      1140

       980       990      1000      1010      1020      1030
seqid2 IIFQDYHMKYRDNTPTVLHGINLTIRGHEVVGIVGRTGSGKSSLGMALFRLVEPMAGRIL
       ::::::::::::::::::::::::::::::::::::::::::::::::::::::::::::
NP_660 IIFQDYHMKYRDNTPTVLHGINLTIRGHEVVGIVGRTGSGKSSLGMALFRLVEPMAGRIL
             1150      1160      1170      1180      1190      1200

      1040      1050      1060      1070      1080      1090
seqid2 IDGVDICSIGLEDLRSKLSVIPQDPVLLSGTIRFNLDPFDRHTDQQIWDALERTFLTKAI
       ::::::::::::::::::::::::::::::::::::::::::::::::::::::::::::
NP_660 IDGVDICSIGLEDLRSKLSVIPQDPVLLSGTIRFNLDPFDRHTDQQIWDALERTFLTKAI
             1210      1220      1230      1240      1250      1260

      1100      1110      1120      1130      1140      1150
seqid2 SKFPKKLHTDVVENGGNFSVGERQLLCIARAVLRNSKIILIDEATASIDMETDTLIQRTI
                                           ::::::::::::::::::::::
NP_660 -----------------------------------ILIDEATASIDMETDTLIQRTI
                                                  1270      1280

      1160      1170      1180      1190      1200      1210
seqid2 REAFQGCTVLVIAHRVTTVLNCDHILVMGNGKVVEFDRPEVLRKKPGSLFAALMATATSS
       ::::::::::::::::::::::::::::::::::::::::::::::::::::::::::::
NP_660 REAFQGCTVLVIAHRVTTVLNCDHILVMGNGKVVEFDRPEVLRKKPGSLFAALMATATSS
           1290      1300      1310      1320      1330      1340


seqid2 LR
       ::
NP_660 LR
```

EXHIBIT C

ELSEVIER

Gene 273 (2001) 89–96

GENE
AN INTERNATIONAL JOURNAL ON GENES AND GENOMES

www.elsevier.com/locate/gene

Two new genes from the human ATP-binding cassette transporter superfamily, *ABCC11* and *ABCC12*, tandemly duplicated on chromosome 16q12

Jaana Tammur[a,b], Catherine Prades[c], Isabelle Arnould[c], Andrey Rzhetsky[d], Amy Hutchinson[b], Masashi Adachi[e], John D. Schuetz[e], Kathryn J. Swoboda[f,g,h], Louis J. Ptácek[f,h,i], Marie Rosier[c], Michael Dean[j], Rando Allikmets[b,k,*]

[a]*Department of Biotechnology, Institute of Molecular and Cell Biology, Tartu University, Tartu, Estonia*
[b]*Department of Ophthalmology, Columbia University, New York, NY, USA*
[c]*Functional Genomics Department, Aventis Pharma, Paris, France*
[d]*Columbia Genome Center, Columbia University, New York, NY, USA*
[e]*Department of Pharmacological Sciences, St. Jude Children's Research Hospital, Memphis, TN, USA*
[f]*Department of Neurology, University of Utah School of Medicine, Salt Lake City, UT, USA*
[g]*Department of Pediatrics, University of Utah School of Medicine, Salt Lake City, UT, USA*
[h]*Department of Human Genetics, University of Utah School of Medicine, Salt Lake City, UT, USA*
[i]*Howard Hughes Medical Institute, University of Utah School of Medicine, Salt Lake City, UT, USA*
[j]*Laboratory of Genomic Diversity, NCI-FCRDC, Frederick, MD, USA*
[k]*Department of Pathology, Columbia University, New York, NY, USA*

Received 7 March 2001; received in revised form 18 May 2001; accepted 14 June 2001
Received by M. D'Urso

Abstract

Several years ago, we initiated a long-term project of cloning new human ATP-binding cassette (ABC) transporters and linking them to various disease phenotypes. As one of the results of this project, we present two new members of the human ABCC subfamily, *ABCC11* and *ABCC12*. These two new human ABC transporters were fully characterized and mapped to the human chromosome 16q12. With the addition of these two genes, the complete human ABCC subfamily has 12 identified members (ABCC1–12), nine from the multidrug resistance-like subgroup, two from the sulfonylurea receptor subgroup, and the *CFTR* gene. Phylogenetic analysis determined that *ABCC11* and *ABCC12* are derived by duplication, and are most closely related to the *ABCC5* gene. Genetic variation in some ABCC subfamily members is associated with human inherited diseases, including cystic fibrosis (*CFTR/ABCC7*), Dubin–Johnson syndrome (*ABCC2*), pseudoxanthoma elasticum (*ABCC6*) and familial persistent hyperinsulinemic hypoglycemia of infancy (*ABCC8*). Since *ABCC11* and *ABCC12* were mapped to a region harboring gene(s) for paroxysmal kinesigenic choreoathetosis, the two genes represent positional candidates for this disorder.

Keywords: ATP-binding cassette transporters; Mapping; Paroxysmal kinesigenic choreoathetosis

1. Introduction

The ATP-binding cassette (ABC) transporter superfamily is one of the largest gene families and encodes a functionally diverse group of membrane proteins involved in energy-dependent transport of a wide variety of substrates across membranes (Dean and Allikmets, 1995). Phylogenetic analysis further divides human ABC transporters into seven subfamilies: ABCA (ABC1 subfamily), ABCB (MDR/TAP subfamily), ABCC (CFTR/MRP subfamily), ABCD (ALD subfamily), ABCE (OABP subfamily), ABCF (GCN20 subfamily), and ABCG (white subfamily)

Abbreviations: ABC, ATP-binding cassette; BAC, bacterial artificial chromosome; bp, base pair(s); CEM, a human T-lymphoid cell line; CEM-r1, a PMEA-resistant variant of CEMss; CEMss, a human T-lymphoid cell line sensitive to PMEA; EST, expressed sequence tag; GSH, glutathione; ICCA, infantile convulsions with paroxysmal choreoathetosis; MRP, multidrug resistance protein; MTX, methotrexate; PCR, polymerase chain reaction; PKC, paroxysmal kinesigenic choreoathetosis; PMEA, 9-(2-phosphonylmethoxyethyl) adenine; 3TC, 2′,3′-dideoxy-3′-thiacytidine; UTR, untranslated region

* Corresponding author. Department of Ophthalmology, Columbia University, Eye Research Addition, Room 715, 630 West 168th Street, New York, NY 10032, USA. Tel.: +1-212-305-8989; fax: +1-212-305-7014.

E-mail address: rla22@columbia.edu (R. Allikmets).

0378-1119/01/$ - see front matter
PII: S0378-1119(01)00572-8

(Allikmets et al., 1996; http://www.gene.ucl.ac.uk/users/hester/abc.html). Most ABC proteins from eukaryotes encode so-called 'full transporters', each consisting of two ATP-binding domains and two transmembrane domains (Hyde et al., 1990).

The human ABCC subfamily currently has ten identified members (ABCC1–10), seven from the multidrug resistance-like (MRP) subgroup, two from the sulfonylurea receptor (SUR) subgroup, and the *CFTR* gene. MRP-like proteins are organic anion transporters, i.e. they transport anionic drugs, exemplified by methotrexate (MTX), as well as neutral drugs conjugated to acidic ligands, such as glutathione (GSH), glucuronate, or sulfate, and play a role in resistance to nucleoside analogs (Cui et al., 1999; Kool et al., 1999; Schuetz et al., 1999; Wijnholds et al., 2000). Genetic variation in some ABCC subfamily members is associated with human inherited diseases, including cystic fibrosis (*CFTR/ABCC7*) (Riordan et al., 1989), Dubin–Johnson syndrome (*ABCC2*) (Wada et al., 1998), pseudoxanthoma elasticum (*ABCC6*) (Bergen et al., 2000; Le Saux et al., 2000) and familial persistent hyperinsulinemic hypoglycemia of infancy (*ABCC8*) (Thomas et al., 1995).

Paroxysmal kinesigenic choreoathetosis (PKC; MIM# 128200), the most frequent type of paroxysmal dyskinesia, is a disorder characterized by recurrent, frequent attacks of involuntary movements and postures, including chorea and dystonia, induced by sudden voluntary movements, stress, or excitement (for a detailed description of clinical and genetic features, see Swoboda et al., 2000). In most families it is inherited as an autosomal dominant trait with incomplete penetrance. The gene locus has been mapped to human chromosome 16q11-q12 (Tomita et al., 1999; Bennett et al., 2000).

We initiated a long-term project of cloning new human ABC transporters and linking them to various disease phenotypes (Allikmets et al., 1996, 1997, 1999). As one of the results of this project, we present here two new members of the human ABCC subfamily, *ABCC11* and *ABCC12*.

2. Materials and methods

2.1. Sequence analysis

Searches of the GenBank HTGS database were performed with the TBLASTN and TBLASTP programs on the NCBI file server (http://www.ncbi.nlm.nih.gov) with the known ABC transporter nucleotide and protein sequences as queries. Potential transmembrane spanning segments were predicted with the TMAP program (http://bioweb.pasteur.fr/seqanal/interfaces/tmap.html). Amino acid alignments were generated with the PILEUP program included in the Genetics Computer Group (GCG) Package. The GRAIL and GeneScan programs on Genome Analysis Pipeline I (http://compbio.ornl.gov/GP/) were utilized to predict genomic structures of the new genes.

2.2. cDNA cloning and determining the genomic structure

Primers were designed from expressed sequence tag (EST) clone sequences and from predicted cDNA sequences from 5′ and 3′ regions of genes. cDNA sequences of *ABCC11* and *ABCC12* were confirmed by PCR amplification of testis or liver cDNA (Clontech). Sequencing was performed on the ABI 377 sequencer according to the manufacturer's protocols (Perkin Elmer). Positions of introns were determined by comparison between genomic (BAC AC007600) and cDNA sequences. The sequence of the *ABCC11* and *ABCC12* cDNA was deposited with the GenBank Database under the accession numbers AY040219 and AY040220, respectively.

2.3. Physical mapping

The chromosomal localization of the human *ABCC11* and *ABCC12* genes was determined by mapping on the GeneBridge4 radiation hybrid panel (Research Genetics), according to the manufacturer's protocol.

2.4. Expression analysis

Expression profiles of the human *ABCC11* and *ABCC12* genes were determined by PCR on human Multiple Tissue cDNA (MTC™, Clontech) Panels I and II according to the manufacturer's instructions. Each MTC panel contains normalized, first-strand cDNA from eight human tissues/cells: (I) heart, whole brain, placenta, lung, liver skeletal muscle, kidney and pancreas; (II) spleen, thymus, prostate, testis, ovary, small intestine, colon and peripheral blood leukocyte. The following primer pairs amplified specific gene products: ABCC11: forward 5′-AGA ATG GCT GTG AAG GCT CAG CAT C-3′, reverse 5′-GTT CCT CTC CAG CTC CAG TGC-3′; ABCC12: forward 5′-GGT GAC AGA CAA GCG AGT TCA GAC AAT G-3′, reverse 5′-CTT TGC TCC TCT GGG CCA GTG-3′.

2.5. Cell lines

The human erythroleukemia K562 cells were obtained form the American Tissue Culture Collection (Rockville, MD) and were cultured in RPMI-1640 medium supplemented with 10% fetal calf serum and 2 mM L-glutamine. The 9-(2-phosphonylmethoxyethyl)adenine (PMEA) resistant cells, K562/PMEA, were derived as described earlier (Hatse et al., 1996), and were kindly provided by Dr Jan Balzarini (Rega Institute for Medical Research, Katholieke Universiteit, Leuven, Belgium). The T-lymphoblast cell lines CEM and (−)2′,3′-dideoxy-3′-thiacytidine (3TC)-resistant CEM-3TC cells were provided by Dr Guido Antonelli (Department of Experimental Medicine and Pathology Virology Section, University "La Sapienza", Rome, Italy). The selection of the 3TC-resistant cell line and its pheno-

Table 1
Splice site sequences and exon sizes for *ABCC11* and *ABCC12*[a]

Exon	ABCC11			ABCC12		
	Size (bp)	Splice acceptor	Splice donor	Size (bp)	Splice acceptor	Splice donor
1	5′ UTR + 99	Not determined	ACTTATTTATgtaagtagat	5′ UTR + 119	Not determined	CCTGTGCAAGgtaagtcaga
2	137	cttttccaagAAAACCTATA	CCAAGCCGAGgtgagtcctg	156	ttgtctgcagGTTAGCACCC	ATGCCAAAAGgtaccaggat
3	159	cctctactagGTTTCCTGCC	ATGTCCAAAGgtgaagctgc	152	ttcatcacagATTTCGAGTC	GGGCCGGTGAgtgcggcagc
4	148	tcttttcaagGCTTCACCGC	ACTCGGGCCAgtaagtggca	230	ttacagacagTTCTCATTCA	TGTTGGCGAGgtaagctggc
5	234	ttccttgtagATATTGATTA	CTCAGGAGAGgtaagcagct	164	ttctttccagGTGCTCAATA	ACCCGTCCAGgtaacggcat
6	174	tgtcttgcagGCCATCAGCT	CCCACTGGCGgtaatgtctt	148	ttgatttcagATGTTTATGG	ACTATCCAAGgtaggacaag
7	148	ctgactccagGTATTCATGA	ATCATTGAAGgtatggaaag	149	tattttgcagATATAAGAAG	CGCACCCGTGgtaagagctg
8	149	tatttcccagACCTAAGAAG	AGCGTCAATGgtaagggttt	108	tgttcttcagGCATTTAGTG	GAGAATGAAGgtataactaa
9	108	tcttatccagGCCTTCAGCA	GAGGTTCAAGgtaggtcatc	279	ttaatcttagAAAATTCTCA	GGTGAGAAAGgtgggtgtgt
10	252	gtctttacagAAGTTTTTCC	GGTGTCCAAGgtagccttgt	72	tctctggcagGGGAAGATCT	CCTAGGACAGgtaagctgtg
11	72	tggcttgcagGGGATGATGT	CCTGGAGGAGgtaagtgatc	125	gttgttccagATGCAGCTGC	ATCACCAAAGgtaatattaa
12	125	tctgccgcagATGCACTTGC	ACAAGGCCCGgtaagctcct	73	gcaccaacagGTATCAGCAC	CCTGACTGAGgtgagcgggg
13	73	tccttcacagATACCTCCAG	CATGACAGAGgtgagaggga	204	ctgtccacagATTGGGGAGC	CCAGCTACAGgtgatgggac
14	204	ctgtctgcagATTGGAGAGC	CCAGCTGCAGgttagcaccc	135	acttctgcagTTCTTAGAGT	GCAGTTCAAGgtaactcaca
15	135	gactgtccagTACTTAGAAT	AGCCACTTCGgtgagtcctg	85	ttgtctccagGATCCTGAAC	GGTATAATCGgttagaatcc
16	97	ctctccccagGACATGTTGC	GGAAATGCTGgtaatggtgt	73	ctcaccctagTTTTGGCTCC	GACACAAAAGgtatttacca
17	90	cctgacccagTGCCGGAGCA	GCAGCTGGAGgtacggtccc	90	gtctccacagTTCCTGAGCA	GCTTCTGGAGgttcagtata
18	104	tccctcccagGTTACATGGT	GGGCTCGGGGgtgagtgcca	104	cctcttgcagGGTACCTCCT	GGGCTCACGGgtgagtttcc
19	198	tttcttgaagACCAATAGCA	CTTCAACAAGgtatgggcct	198	ttctccaaagATGACCTGTG	GTTTGATAAGgtagggccac
20	227	gtccctgcagGTTTTCCGCT	TTTATTATATgtgagtaggt	227	ttctccacagATCTTAAAGA	TTCTGTTACGgtaggcccat
21	138	gtccatgcagGATGTTCAAG	TCATCAGCCAgtgagtcctt	138	tttcttccagCATTTTCCAC	GCATCACCTAgtgagtccca
22	187	tccttctcagCCAGTTTAAG	CGTGCTGCAGgtgaggggt	187	aaaactccagTCACCTCCTC	CATCATCCAGgtaatgcctg
23	90	ttccttctagCTGGCGTCCA	GTACATGAAGgtggggttca	90	ttttcaacagCTGAGCGGAC	ATACATTTCGgtaagaaatt
24	190	caaaaacaagATGTGTGTCT	ACGGGCTCTGgtgagctgag	190	tcctttacagACCTGTGTTC	ACAGGTTCCGgtgaggacaa
25	160	tgccccacagGGAAGTCCTC	GAACCATCAGgtgagtgccg	160	tggttcccagGAAAGTCATC	GTACAGTAAGgtagctgttt
26	79	catatggtagATTCAACCTA	GACCAAGGCCgtaagtagct	79	ttcattgcagGTACAACTTG	GAGAGACACAgtaggtctct
27	114	catatcgcagATCTCAAAGT	CAACTCCAAGgtgaggccac	114	tgttttgtagATAATGAAAC	TAATTCAAAGgtaagaaaac
28	165	tattcatcagATCATCCTTA	CAATGGGAAGgtgaaggctg	165	tcctccacagATCATTCTCC	AAATGGGAAGgtataggaag
29	93 + 3′ UTR	taccctccagGTGGTAGAAT	Not determined	87 + 3′ UTR	tgactttcagGTGATTGAGT	Not determined

[a] Exon and intron sequences are shown in uppercase and lowercase, respectively.

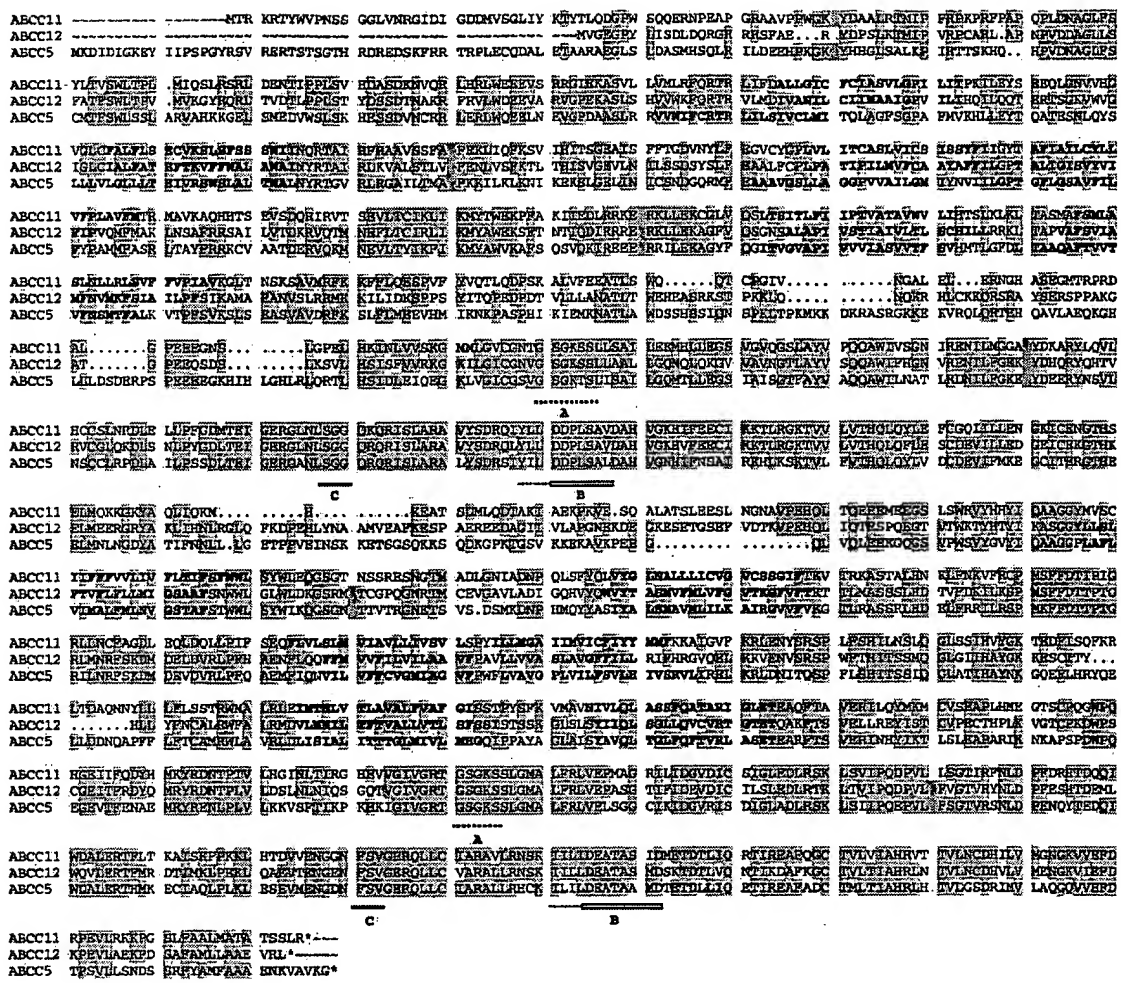

Fig. 1. Amino acid alignment of ABCC11, ABCC12, and ABCC5 proteins. Identical amino acids are shaded and gaps are indicated by periods. Walker A and B motifs and the ABC transporter family signature sequence C are underlined and labeled with respective letters. Potential transmembrane spanning segments are given in bold type.

typic properties will be described in detail in an upcoming publication. Another previously described pair of cell lines, CEMss and CEM-r1, were acquired from Dr Arnold Fridland (Robbins et al., 1995). CEM-r1 is highly resistant to PMEA due to an overexpression of *ABCC4* (Schuetz et al., 1999). Total RNA from these six cell lines (three pairs of wild-type and resistant cell lines) was isolated with TRIZOL (GIBCO BRL), and RT-PCR was performed at varying cycle numbers with primers described in Section 2.4. The PCR products were subcloned into the pCR 2.1 vector and verified by direct sequencing.

2.6. Phylogenetic analysis

Complete protein sequences were aligned with the CLUSTALW program (Thompson et al., 1994). The result-

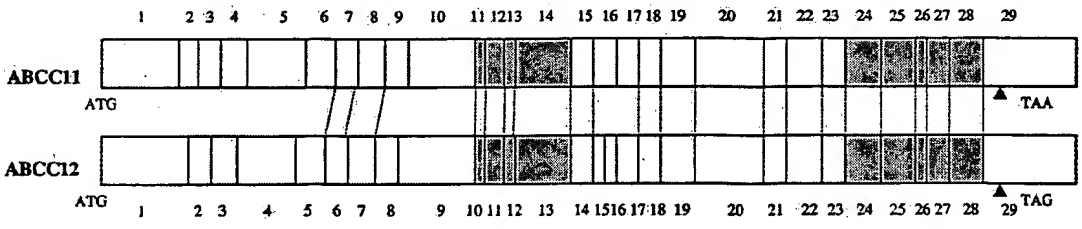

Fig. 2. Splicing pattern comparison of the *ABCC11* and *ABCC12* genes. Clear boxes represent exons and vertical lines define splice sites. Exon numbers for each gene are shown both above and below the drawing. Filled boxes indicate the exons encoding ABC domains. Regions in which the two genes show identical splicing patterns are indicated by dashed lines.

ing multiple alignment was analyzed with program NJBOOT by N. Takezaki (pers. commun.) implementing the neighbor-joining tree-making algorithm (Saitou and Nei, 1987). The Poisson correction for multiple hits (Zuckerkandl and Pauling, 1965) was used as the distance measure between sequences for generating a phylogenetic tree.

3. Results and discussion

3.1. Cloning and genomic structure of ABCC11 and ABCC12

Two new human ABC transporter gene sequences were detected on the bacterial artificial chromosome (BAC) clone #AC007600 from the GenBank HTGS database. cDNA sequencing, genomic structure prediction programs, and computer searches determined the sequence and genomic structure of both new genes belonging to the ABCC (MRP) subfamily. Only the combination of all these methods allowed for the correct assembly of these genes which are closely related and highly conserved in evolution.

The human *ABCC11* and *ABCC12* genes consists of 29 exons. Exon sizes range from 72 to 252 bp for *ABCC11* and from 73 to 279 bp for *ABCC12*. All exons were flanked by GT and AG dinucleotides consistent with the consensus sequences for splice junctions in eukaryotic genes (Table 1). Of the 28 introns in *ABCC11*, 18 are class 0 (where the splice occurs between codons), four are class 1 (where the codon is interrupted between the first and the second nucleotide), and six are class 2 (where the splice occurs between the second and the third nucleotide of the codon). For the *ABCC12* gene these numbers are 16, six and six, respectively. The *ABCC11* gene encodes a protein of 1382 amino acids, and *ABCC12* a protein of 1359 amino acids (Fig. 1). Topology predictions based on hydropathy profiles and comparison with other known ABC transporters suggest that both encoded proteins are full ABC transporters containing two ATP-binding domains (including Walker A and B domains, and signature motifs) and two transmembrane domains (Fig. 1). The amino acid sequence of ABCC11 is 40% identical to the human ABCC5 protein, 33% identical to human ABCC4 and 32% identical to ABCC2 and ABCC3 proteins. The ABCC12 protein is even more closely related to ABCC5 (42% identity on protein level; Fig. 1).

The splicing pattern of the two new genes is very similar, especially towards the 3′ end (Fig. 2), suggesting a close evolutionary relationship between these ABC transporters. The ABCC11 and ABCC12 proteins, as well as ABCC4 and ABCC5, are smaller than another well-known member of the subgroup, ABCC1 (MRP1), appearing to lack the extra N-terminal domain (Fig. 1) (Borst et al., 2000). It has been shown, however, that the extra N-terminal part of ABCC1 is not required for the transport function (Bakos et al., 1998). The ABCC4 and ABCC5 proteins confer resistance to nucleotide analogs, including PMEA and purine base analogs (Schuetz et al., 1999; Wijnholds et al., 2000). ABCC1, ABCC2 and ABCC3 transport drugs conjugated to GSH, glucuronate, sulfate and other organic anions, such as MTX (Cui et al., 1999; Kool et al., 1999; Wijnholds et al., 2000). Since structurally related ABC proteins often transport similar substrates across cell membranes, it would be reasonable to suggest that ABCC11 and ABCC12 could share functional similarities with ABCC4 and/or ABCC5.

3.2. Expression of ABCC11 and ABCC12 in human tissues and nucleoside-resistant cell lines

The expression patterns for the *ABCC11* and *ABCC12* genes were examined by PCR on MTC panels (Clontech) with gene-specific primers resulting in about 500 bp PCR fragments (Fig. 3B). *ABCC11* was expressed in all tissues except kidney, spleen, and colon. The *ABCC12* transcript was detected, at much lower levels, only in testes, ovary, and prostate. The size for both transcripts was determined at approximately 5000 bp on MTN blots (Clontech, data not shown). The primers used in expression studies amplified the *ABCC11* cDNA from exon 7 to exon 10, resulting in a 527 bp PCR fragment (Fig. 3B). In the case of lung, and occasionally some other tissues (data not shown), a smaller (419 bp) fragment was detected (Fig. 3B). Direct sequen-

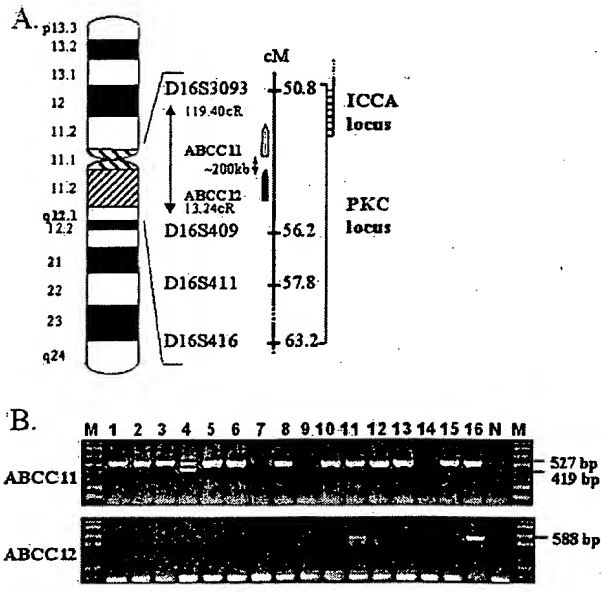

Fig. 3. Chromosomal localization and expression analysis of the *ABCC11* and *ABCC12* genes. (A) Human *ABCC11* and *ABCC12* genes, flanked by markers D16S3093 and D16S409, are separated by ~200 kb, and organized in a head-to-tail fashion, with their 5′ ends facing the centromere. Loci for ICCA, PKC, and their overlap, are defined by brackets. (B) Expression analysis of the human *ABCC11* and *ABCC12* genes by PCR on MTC panels. Lanes 1–16 represent cDNA from heart, brain, placenta, lung, liver, muscle, kidney, pancreas, spleen, thymus, testis, ovary, intestine, colon, leukocyte, and prostate, respectively. N, negative control; M, marker lane (1 kb Plus DNA Ladder).

cing of the PCR product determined that the shorter PCR product lacked exon 9 of the *ABCC11* gene. Since these results were confirmed in repeated experiments, frequent skipping of *ABCC11* exon 9 may occur *in vivo*. Exon skipping and alternative splicing events have been well-documented for several ABC genes (Rickers et al., 1994; Bellincampi et al., 2001).

Systematic analysis of the tissue source of the *ABCC12* ESTs from the public dbEST and the proprietary Incyte LifeSeq Gold databases indicates that 11/18 of the matching sequences are derived from various CNS origins, and the rest are from testis (three clones) and immune system (four clones). Similar analysis for the *ABCC11* gene resulted in 29 ESTs, with the majority being derived from breast tumor tissue (17). The others were from prostate (five clones), testis (three), CNS (two), and colon (two). Certain discrepancies between the two expression profiling methods are often observed for low abundance transcripts, which have high tissue distribution selectivity.

Since the new genes show extensive structural similarity to ABCC5 (and to a certain extent, ABCC4), we checked their expression in three pairs of cell lines, K562 and K562-PMEA, CEMss and CEM-r1, and CEM and CEM-3TC. The K562-PMEA and CEM-r1 lines have been selected for resistance to PMEA, and the CEM-3TC for resistance to the cytidine nucleoside analog, 3TC. No difference was observed in expression levels of *ABCC11* between the parental and PMEA-resistant cell lines. In contrast, the CEM-3TC cell line revealed a reproducible two- to three-fold increase in the expression of *ABCC11*, when compared to the parental line CEM (data not shown). This is a potentially interesting finding when one considers the close evolutionary relationship of ABCC11 and ABCC5 (Figs. 1 and 4), and that a recent study by Borst and colleagues (Wijnholds et al., 2000) has demonstrated selective nucleotide analog transport by ABCC5. In addition, since the efflux-resistant phenotype of CEM-3TC can be explained only in part by *ABCC4* overexpression (J.D.S., unpublished data), the higher expression of *ABCC11* in these cells warrants further investigation.

3.3. Radiation hybrid mapping

Radiation hybrid mapping placed *ABCC11* and *ABCC12* to the centromeric region of human chromosome 16, flanked by markers D16S3093 and D16S409 (Fig. 3A). The region encompasses 5.4 cM, or 132.5 cR, and could not be narrowed down further due to lack of recombination and/or mapped polymorphic markers in this region. Both genes are most likely localized on chromosome 16q12.1, since

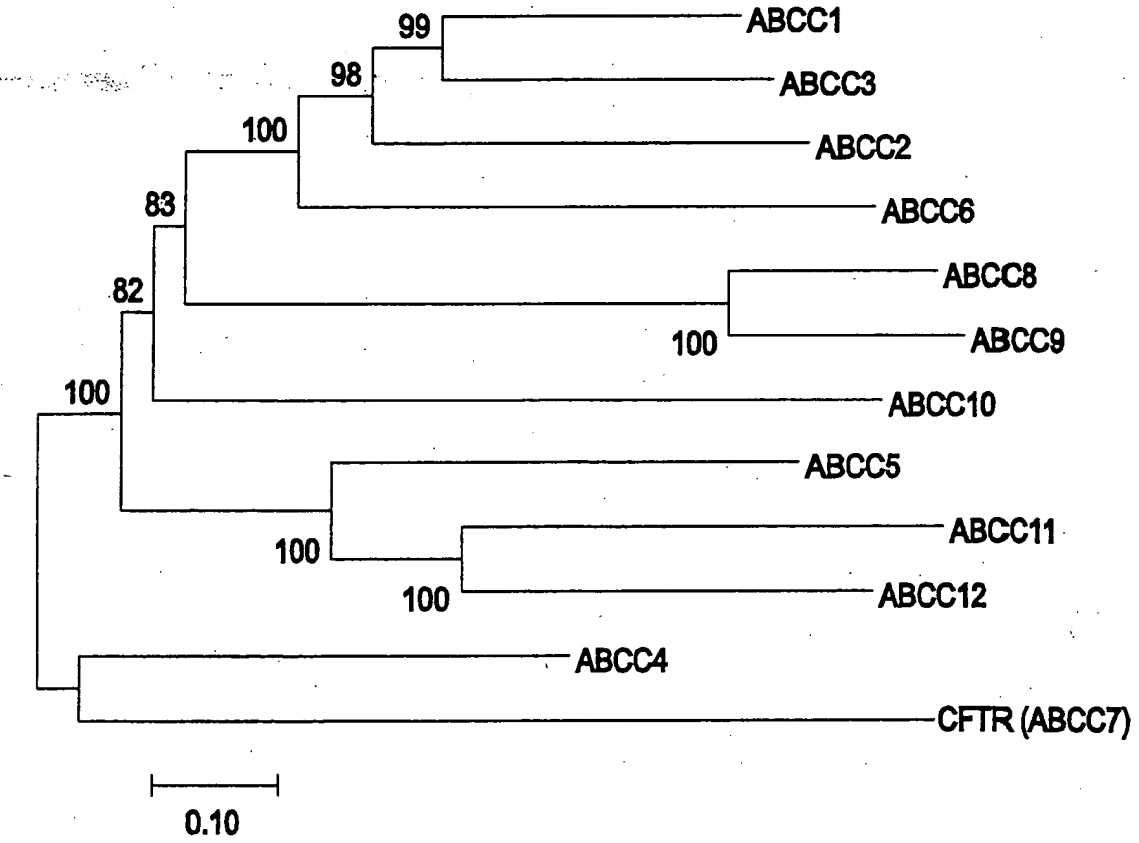

Fig. 4. Phylogenetic relationship of genes in the ABCC subfamily. Complete protein sequences of all members of the ABCC subfamily were aligned with the CLUSTALW program. The distance measure is given in substitutions per amino acid.

they map much closer to the 16q marker D16S409 (13.24 cR) than the 16p marker D16S3093 (119.40 cR) (Fig. 3A). The location of the new genes was confirmed also by LANL BAC mapping data, where the BAC clone #AC007600 was mapped to 16q12.1 by the STS marker s9B1 (http://www.jgi.doe.gov/JGI_home.html). *ABCC11* and *ABCC12* are located tandemly, separated by about 200 kb, with their 5′ ends facing towards the centromere (Fig. 3). Two more ABCC subfamily genes, *ABCC1* and *ABCC6*, have been mapped to the short arm of the same chromosome, at 16p13.1 (Cole et al., 1992; Allikmets et al., 1996). The 3′ ends of *ABCC1* and *ABCC6* are only about 9 kb apart from each other so the genes face opposite directions (Cai et al., 2000).

3.4. Phylogenetic analyses

Phylogenetic analyses of the ABCC subfamily proteins clearly demonstrate a relatively recent duplication of the *ABCC11* and *ABCC12* genes (Fig. 4). The resulting neighbor-joining tree shows with maximum confidence (100-level of bootstrap support) a close evolutionary relationship of the *ABCC11/ABCC12* cluster with the *ABCC5* gene (Fig. 4). In addition, the analysis of the tree suggests a recent duplication of the *ABCC8* and *ABCC9* genes, while *ABCC10* seems to be one of the first genes to separate from the common ancestor. *ABCC1*, *ABCC2*, *ABCC3*, and *ABCC6* genes constitute a well-defined sub-cluster, while the *ABCC4* and *CFTR* (*ABCC7*) genes form another reliable subset despite apparent early divergence.

3.5. ABCC11 and ABCC12 as candidate genes for PKC

The locus for PKC has been assigned to 16p11.2-q12.1, between markers D16S3093 and D16S416 (Tomita et al., 1999; Bennett et al., 2000) (Fig. 3A). An overlapping locus has been predicted to contain the gene for infantile convulsions with paroxysmal choreoathetosis (ICCA; Lee et al., 1998). Expression analysis by PCR and by EST database mining suggests that the two genes are expressed in tissues (CNS, muscle) potentially involved in the etiology of PKC. In summary, chromosomal localization, potential function, and expression profiles make both genes promising candidates for PKC/ICCA. Preliminary analysis of the *ABCC11* gene has identified several single nucleotide polymorphisms, including an amino acid-changing variant (56G > A, R19H) in the first exon. Complete screening of the *ABCC11* and *ABCC12* genes for genetic variation in families segregating PKC is currently under way.

Acknowledgements

We wish to thank Laurent Naudin, Catherine Devaud and Carole Lafargue for their skilled scientific contribution to this collaborative work. The assistance of Delphine Debono, Karine Nadal and Gilles Haussy in the sequencing group is also acknowledged.

References

Allikmets, R., Gerrard, B., Hutchinson, A., Dean, M., 1996. Characterization of the human ABC superfamily: isolation and mapping of 21 new genes using the expressed sequence tags database. Hum. Mol. Genet. 5, 1649–1655.

Allikmets, R., Singh, N., Sun, H., Shroyer, N.F., Hutchinson, A., Chidambaram, A., Gerrard, B., Baird, L., Stauffer, D., Peiffer, A., Rattner, A., Smallwood, P., Li, Y., Anderson, K.L., Lewis, R.A., Nathans, J., Leppert, M., Dean, M., Lupski, J.R., 1997. A photoreceptor cell-specific ATP-binding transporter gene (ABCR) is mutated in recessive Stargardt macular dystrophy. Nat. Genet. 15, 236–246.

Allikmets, R., Raskind, W.H., Hutchinson, A., Schueck, N.D., Dean, M., Koeller, D.M., 1999. Mutation of a putative mitochondrial iron transporter gene (ABC7) in X-linked sideroblastic anemia and ataxia (XLSA/A). Hum. Mol. Genet. 8, 743–749.

Bakos, E., Evers, R., Szakacs, G., Tusnady, G.E., Welker, E., Szabo, K., de Haas, M., van Deemter, L., Borst, P., Varadi, A., Sarkadi, B., 1998. Functional multidrug resistance protein (MRP1) lacking the N-terminal transmembrane domain. J. Biol. Chem. 273, 32167–32175.

Bellincampi, L., Simone, M.L., Motti, C., Cortese, C., Bernardini, S., Bertolini, S., Calandra, S., 2001. Identification of an alternative transcript of ABCA1 gene in different human cell types. Biochem. Biophys. Res. Commun. 283, 590–597.

Bennett, L.B., Roach, E.S., Bowcock, A.M., 2000. A locus for paroxysmal kinesigenic dyskinesia maps to human chromosome 16. Neurology 54, 125–130.

Bergen, A.A., Plomp, A.S., Schuurman, E.J., Terry, S., Breuning, M., Dauwerse, H., Swart, J., Kool, M., van Soest, S., Baas, F., ten Brink, J.B., de Jong, P.T., 2000. Mutations in ABCC6 cause pseudoxanthoma elasticum. Nat. Genet. 25, 228–231.

Borst, P., Evers, R., Kool, M., Wijnholds, J., 2000. A family of drug transporters: the multidrug resistance-associated proteins. J. Natl. Cancer Inst. 92, 1295–1302.

Cai, L., et al., 2000. A 500-kb region on chromosome 16p13.1 contains the pseudoxanthoma elasticum locus: high-resolution mapping and genomic structure. J. Mol. Med. 78, 36–46.

Cole, S.P., Bhardwaj, G., Gerlach, J.H., Mackie, J.E., Grant, C.E., Almquist, K.C., Stewart, A.J., Kurz, E.U., Duncan, A.M., Deeley, R.G., 1992. Overexpression of a transporter gene in a multidrug-resistant human lung cancer cell line. Science 258, 1650–1654.

Cui, Y., Konig, J., Buchholz, J.K., Spring, H., Leier, I., Keppler, D., 1999. Drug resistance and ATP-dependent conjugate transport mediated by the apical multidrug resistance protein, MRP2, permanently expressed in human and canine cells. Mol. Pharmacol. 55, 929–937.

Dean, M., Allikmets, R., 1995. Evolution of ATP-binding cassette transporter genes. Curr. Opin. Genet. Dev. 5, 779–785.

Hatse, S., De Clercq, E., Balzarini, J., 1996. Evidence for distinction of the differentiation-inducing activities and cytostatic properties of 9-(2-phosphonylmethoxyethyl)adenine and a variety of differentiation-inducing agents in human erythroleukemia K562 cells. Mol. Pharmacol. 50, 1231–1242.

Hyde, S.C., Emsley, P., Hartshorn, M.J., Mimmack, M.M., Gileadi, U., Pearce, S.R., Gallagher, M.P., Gill, D.R., Hubbard, R.E., Higgins, C.F., 1990. Structural model of ATP-binding proteins associated with cystic fibrosis, multidrug resistance and bacterial transport. Nature 346, 362–365.

Kool, M., van der Linden, M., de Haas, M., Scheffer, G.L., de Vree, J.M., Smith, A.J., Jansen, G., Peters, G.J., Ponne, N., Scheper, R.J., Elferink, R.P., Baas, F., Borst, P., 1999. MRP3, an organic anion transporter able to transport anti-cancer drugs. Proc. Natl. Acad. Sci. USA 96, 6914–6919.

Lee, W.L., Tay, A., Ong, H.T., Goh, L.M., Monaco, A.P., Szepetowski, P., 1998. Association of infantile convulsions with paroxysmal dyskinesias (ICCA syndrome): confirmation of linkage to human chromosome 16p12-q12 in a Chinese family. Hum. Genet. 103, 608–612.

Le Saux, O., Urban, Z., Tschuch, C., Csiszar, K., Bacchelli, B., Quaglino, D., Pasquali-Ronchetti, I., Pope, F.M., Richards, A., Terry, S., Bercovitch, L., de Paepe, A., Boyd, C.D., 2000. Mutations in a gene encoding an ABC transporter cause pseudoxanthoma elasticum. Nat. Genet. 25, 223–227.

Rickers, A., Rininsland, F., Osborne, L., Reiss, J., 1994. Skipping of multiple CFTR exons is not a result of single exon omissions. Hum. Genet. 94, 311–313.

Riordan, J.R., Rommens, J.M., Kerem, B., Alon, N., Rozmahel, R., Grzelczak, Z., Zielenski, J., Lok, S., Plavsic, N., Chou, J.L., et al., 1989. Identification of the cystic fibrosis gene: cloning and characterization of complementary DNA (published erratum appears in Science 1989, 245(4925), 1437). Science 245, 1066–1073.

Robbins, B.L., Connelly, M.C., Marshall, D.R., Srinivas, R.V., Fridland, A., 1995. A human T lymphoid cell variant resistant to the acyclic nucleoside phosphonate 9-(2-phosphonylmethoxyethyl)adenine shows a unique combination of a phosphorylation defect and increased efflux of the agent. Mol. Pharmacol. 47, 391–397.

Saitou, N., Nei, M., 1987. The neighbor-joining method: a new method for reconstructing phylogenetic trees. Mol. Biol. Evol. 4, 406–425.

Schuetz, J.D., Connelly, M.C., Sun, D., Paibir, S.G., Flynn, P.M., Srinivas, R.V., Kumar, A., Fridland, A., 1999. MRP4: a previously unidentified factor in resistance to nucleoside-based antiviral drugs. Nat. Med. 5, 1048–1051.

Swoboda, K.J., Soong, B., McKenna, C., Brunt, E.R., Litt, M., Bale, J.F., Ashizawa, T., Bennett, L.B., Bowcock, A.M., Roach, E.S., Gerson, D., Matsuura, T., Heydemann, P.T., Nespeca, M.P., Jankovic, J., Leppert, M., Ptácek, L.J., 2000. Paroxysmal kinesigenic dyskinesia and infantile convulsions: clinical and linkage studies. Neurology 55, 224–230.

Thomas, P.M., Cote, G.J., Wohllk, N., Haddad, B., Mathew, P.M., Rabl, W., Aguilar-Bryan, L., Gagel, R.F., Bryan, J., 1995. Mutations in the sulfonylurea receptor gene in familial persistent hyperinsulinemic hypoglycemia of infancy. Science 268, 426–429.

Thompson, J.D., Higgins, D.G., Gibson, T.J., 1994. CLUSTAL W: improving the sensitivity of progressive multiple sequence alignment through sequence weighting, position-specific gap penalties and weight matrix choice. Nucleic Acids Res. 22, 4673–4680.

Tomita, H., et al., 1999. Paroxysmal kinesigenic choreoathetosis locus maps to chromosome 16p11.2-q12.1. Am. J. Hum. Genet. 65, 1688–1697.

Wada, M., Toh, S., Taniguchi, K., Nakamura, T., Uchiumi, T., Kohno, K., Yoshida, I., Kimura, A., Sakisaka, S., Adachi, Y., Kuwano, M., 1998. Mutations in the canalicular multispecific organic anion transporter (cMOAT) gene, a novel ABC transporter, in patients with hyperbilirubinemia II/Dubin-Johnson syndrome. Hum. Mol. Genet. 7, 203–207.

Wijnholds, J., Mol, C.A., van Deemter, L., de Haas, M., Scheffer, G.L., Baas, F., Beijnen, J.H., Scheper, R.J., Hatse, S., De Clercq, E., Balzarini, J., Borst, P., 2000. Multidrug-resistance protein 5 is a multispecific organic anion transporter able to transport nucleotide analogs. Proc. Natl. Acad. Sci. USA 97, 7476–7481.

Zuckerkandl, F Pauling, L., 1965. Molecules as documents of evolutionary history. J. Theor. Biol. 8, 357–366.

EXHIBIT D

Biochemical and Biophysical Research Communications 288, 933–939 (2001)
doi:10.1006/bbrc.2001.5865, available online at http://www.idealibrary.com on IDEAL®

Multiple Splicing Variants of Two New Human ATP-Binding Cassette Transporters, ABCC11 and ABCC12

Hikaru Yabuuchi, Hidetada Shimizu, Shin-ichiro Takayanagi, and Toshihisa Ishikawa[1]
Department of Biomolecular Engineering, Graduate School of Bioscience and Biotechnology, Tokyo Institute of Technology, 4259 Nagatsuta, Midori-ku, Yokohama 226-8501, Japan

Received October 5, 2001

Two new human ABC transporters, ABCC11 and ABCC12, were cloned from a cDNA library of human adult liver. ABCC11 and ABCC12 genes consist of 30 and 29 exons, respectively, and they are tandemly located in a tail-to-head orientation on human chromosome 16q12.1. The predicted amino acid sequences of both gene products show a high similarity with ABCC5. The transcripts of ABCC11 and ABCC12 genes were detected by PCR in various adult human tissues, including liver, lung, and kidney, and also in several fetal tissues. By searching cDNA libraries from various human tissues, we have identified alternative splicing variants of ABCC11 and ABCC12 genes at significantly high frequencies. One splice variant lacking the exon 28 corresponded to about 25% of total ABCC11 gene transcripts. Furthermore, four splicing variants encoding putatively short peptides were predominant in ABCC12 gene transcripts. Those splicing variants may represent diverse biological functions of these ABC transporter genes. © 2001 Academic Press

Key Words: **ABC transporter; ABCC11; ABCC12; genetic polymorphism; alternative splicing; human chromosome 16.**

The ATP-binding cassette (ABC) transporters form one of the largest protein families and play a biologically important role as membrane transporters or ion channel modulators (1, 2). Until now more than 48 human ABC-transporter genes have been identified and sequenced (3, 4). Based on the arrangement of molecular structure components, i.e., the nucleotide binding domain and the topology of transmembrane domains, human ABC transporters are classified into seven different gene families (A to G) (2–4). Mutations of human ABC transporter genes have been reported to cause of certain genetic diseases, such as Tangier disease (5–7), cystic fibrosis (8), Dubin–Johnson syndrome (9), Stargardt disease (10), and sitosterolemia (11).

The ABCC gene family (according to the new nomenclature of human ABC transporter genes) comprises the members of multidrug resistance-associated proteins (MRP) (12), sulfonylurea receptors (SUR) (13), and cystic fibrosis transmembrane conductance regulator (CFTR) (8). MRP1 (ABCC1 according to new nomenclature for human ABC transporter genes) was first identified by molecular cloning from human multidrug-resistant lung cancer cells (14). MRP1 encodes one of the previously characterized GS-X pumps (15) that transport leukotriene C_4 (16) and drugs either conjugated with glutathione (GSH), glucuronide or sulfate (17). In addition, MRP1 reportedly transports some anticancer drugs in an unmodified form together with GSH (18, 19). After the discovery of the MRP1 gene, six MRP1 homologues have been identified. At present, the human MRP subfamily consists of at least seven members (MRP1, MRP2/cMOAT, MRP3, MRP4, MRP5, MRP6, and MRP7) (2, 3, 12, 20, 21) and exhibits a wide spectrum of biological functions. Accumulating evidence shows that ABC transporters of the MRP subfamily are involved in transport of drugs as well as endogenous substances (12, 16–19, 22, 23).

The draft sequence of the human genome has recently published (24, 25), and more than 50 of human ABC transporter genes have been anticipated to exist in the human genome (4). However, at present, because of the difficulty in the precise prediction of exon–intron boundaries using currently available software programs, actual cloning and sequencing of cDNA is still a critical step for our understanding of the molecular

The cDNA sequences of ABCC11 and its transcript variant A as well as ABCC12 variants A, B, C and D have been registered in GenBank under the Accession Nos. AF367202, AF411579, AF395908, AF395909, AF411577, and AF411578, respectively.

Abbreviations used: ABC, ATP-binding cassette; MRP, multidrug resistance-associated protein; PCR, polymerase chain reaction; GS-X pump, ATP-dependent glutathione S-conjugate export pump.

[1] To whom correspondence and reprint requests should be addressed. Fax: +81-45-924-5838. E-mail: tishikaw@bio.titech.ac.jp.

0006-291X/01 $35.00

structure and function of novel ABC transporters. We have recently discovered two novel ABC transporters, i.e., human ABCC11 and ABCC12 that belong to the ABCC gene family and are located on the chromosome 16q12.1. In the present study, we have analyzed multiple splicing variants transcribed from ABCC11 and ABCC12 genes and herein demonstrate the gene features and expression profiles of these two ABC transporter genes in human organs.

MATERIALS AND METHODS

Cloning of cDNA encoding human ABCC11 and ABCC12 and their splicing variants. The draft sequence of the human chromosome 16 (GenBank Accession No. AC007600) was analyzed using the GENSCAN program (http://genes.mit.edu/GENSCAN.html) to predict exons. EST clones were extracted from the currently available EST database to find partial sequences of ABCC11 and ABCC12.

To clone full length and splicing variant of ABCC11 cDNA, the following three sets of PCR primers were designed: the 5′-part (C11-1 forward primer: 5′-ATGGCTTCGCGCTGCTCTCT-3′ and C11-1 backward primer: 5′-CCTCAGATGTGTGATGCCGAGCCTT-3′), the middle part (C11-2 forward primer: 5′-GGTATTCATGACAAGAATGG-3′, and C11-2 backward primer: 5′-GACGATCAGCACCACGAAGA-3′), and the 3′-part (C11-3 forward primer: 5′-CCTTGA-GTTGGAGGGTCTAC-3′, C11-3 backward primer: 5′-AAGTAGCCTATTCCAGGGTTT-3′). PCR was performed using human adult liver cDNA (Clontech, Palo Alto, CA) and the Ex Taq polymerase (Takara, Japan), where the PCR consisted of 30 cycles of 94°C for 30 s, 60°C for 30 s, and 72°C for 2 min. In addition, the 3′-portion of noncoding region was cloned by 3′-rapid amplification of cDNA ends (3′RACE) using human liver Marathon-Ready cDNA (Clontech) and two primers (first primer: 5′-GCCAGGG-CTGTGCTTCGCAAC-3′ and nested primer: 5′-CAGGGCTGCAC-CGTGCTCGT-3′) under the PCR conditions of 30 cycles of 94°C for 1 min and 68°C for 2 min.

To clone four splicing variants of ABCC12 cDNA in a similar manner, six sets of PCR primers were designed: the 5′-parts (C12-1 forward primer: 5′-ATCAGGATGGTGGGTGAAGG-3′, C12-1 backward primer: 5′-CTGGCTTCATGCTCCCATGTC–3′ and C12-2 forward primer: 5′-GGTGGGTGAAGGACCCTA–3′, C12-2 backward primer 5′-CAGAACCGATTTGAG GCTGTCACT-3′), the middle parts (C12-3 forward primer: 5′-TGAAGCCAGC-AGGAAAGTACC-3′, C12-3 backward primer: 5′-CTGCAGAAA GTTCTCTGCGT–3′ and C12-4 forward primer 5′-CTCCTCTCTGCATGACACGG–3′, C12-4 backward primer 5′-CACACA-AAGCAGCTGACGTTC-3′), the 3′-parts (C12-5 forward primer: 5′-GTAAGGTACAACTT-GGATCCCT-3′, C12-5 backward primer: 5′-TGCTGCTAGTAACATCGCAA-3′ and C12-6 forward primer: 5′-CACCGCCTCTATG GACTCCAAGACTG-3′, C12-6 backward primer: 5′-CGCTACAAATCTGTGTCATTACCAC-3′). PCR was performed using the human adult liver, pancreas and testis cDNA (Clontech). The PCR consisted of 35 cycles of 94°C for 30 s, 60°C for 30 s, and 72°C for 2 min.

The sequences of PCR products were analyzed by automated DNA sequencing (TOYOBO Gene Analysis, Japan). The whole cDNA sequences of ABCC11 and ABCC12 as well as their splicing variants were determined by assembling the partial sequences thus obtained. The cDNA sequences of ABCC11 and its splicing variant A as well as ABCC12 splicing variants A, B, C, and D have been deposited to GenBank under Accession Nos. AF367202, AF411579, AF395908, AF395909, AF411577, and AF411578, respectively.

Detection of ABCC11 and ABCC12 transcripts in human normal tissues and cancer cell lines. Transcripts of ABCC11 and ABCC12 genes were detected by means of PCR, where human cDNA of normal tissues and cancer cell lines were purchased from Clontech. The PCR primers to detect ABCC11 and ABCC12 were as follows: C11 forward primer: 5′-TCTGCGA-CCTTCTTGTTTGG-3′, C11 backward primer: 5′-TCAGTACAGCATTTGCAACACTT-3′ and C12 forward primer: 5′-CACCGCCTCTATGGACTCCAAGACTG-3′, C12 backward primer: 5′-TCAATCTCAGGCACTGGGGTGGT-3′. The PCR consisted of 38 cycles of 95°C for 30 s, 58°C for 30 s, and 72°C for 2 min and was followed by reaction at 72°C for 2 min.

RESULTS AND DISCUSSION

ABCC11 and ABCC12 Genes Located on Human Chromosome 16q12

Two new ABCC transporters, named ABCC11 and ABCC12, were identified by database search on human chromosome 16 working draft (GenBank Accession No. AC007600) using the BLASTN program. In the present study, we have cloned cDNAs of these two new ABC transporters and their splicing variants to analyze the genetic polymorphism and expression profiles.

ABCC11 and ABCC12 genes are tandemly located on human chromosome 16q12.1 in a tail-to-head orientation with a separation distance of about 20 kb (Fig. 1). The ABCC11 gene is encoded by a ~68 kb gene consisting of 30 exons, whereas the ABCC12 gene spans a ~63 kb size and consists of 29 exons. The cDNAs of both ABCC11 and ABCC12 had a Kozak consensus initiation sequence for translation (26) around the first ATG region, namely, 5′-CTG**A**AA ATG **A**-3′ for ABCC11 and 5′-ATC**A**GG-ATG **G**-3′ for ABCC12. The amino acid sequence deduced from the cDNA sequence with the GENSCAN program revealed that ABCC11 and ABCC12 cDNAs contain single open reading frames encoding proteins consisting of 1383 and 1359 amino acid residues, respectively. ABCC11 and ABCC12 proteins have two sets of Walker A and Walker B motifs as well as two ABC signature sequences, so-called "C motifs," within the deduced protein. In terms of the amino acid sequence, the identity of ABCC11 with human ABCC1, 2, 3, 4, 5, 6, 7, 8, 9, and 10 was 30.7, 30.8, 30.9, 32.9, 40.1, 29.9, 26.0, 27.8, 27.9, and 29.3%, respectively. Likewise, the identity of ABCC12 with human ABCC1, 2, 3, 4, 5, 6, 7, 8, 9, and 10 was 31.1, 30.4, 30.0, 32.8, 43.6, 28.8, 26.9, 27.9, 27.8, and 29.0%, respectively. The identity between ABCC11 and ABCC12 was 47.4%. Based on the phylogenetic relationship, ABCC11 and ABCC12 are suggested to comprise a new subgroup with a close relation to ABCC5 that reportedly transports several organic anions, including nucleotide analogues and cyclic nucleotides (23, 27, 28).

Splicing Variants of Human ABCC11 and ABCC12

Figure 2 shows splicing variants of ABCC11 and ABCC12 cloned in this study. The cDNA of ABCC11 variant A consists of 4476 nucleotides with 29 exons; however, the exon 28 is entirely deleted. This intron splicing follows the conventional GT-AG rule. The cDNA of this variant encodes a protein consisting of

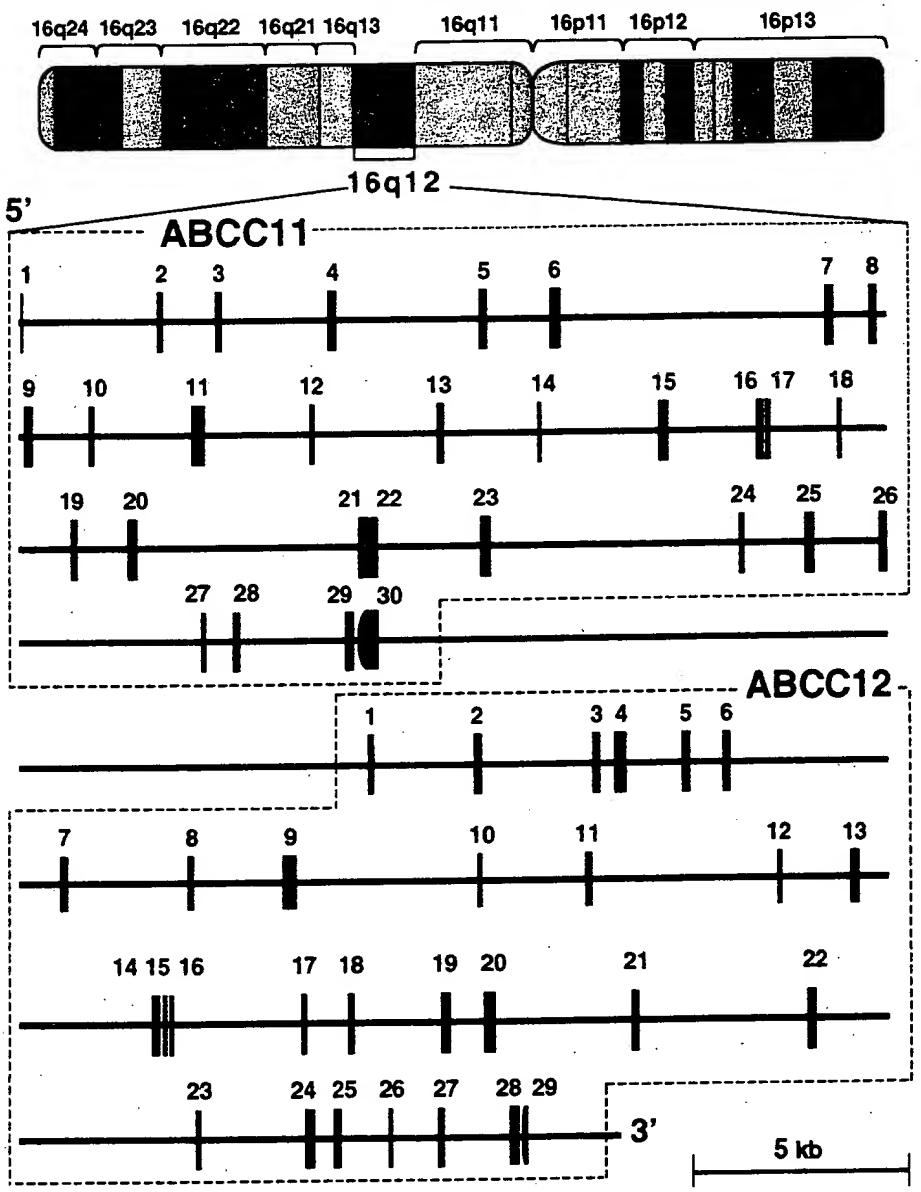

FIG. 1. The genomic structures of ABCC11 and ABCC12 genes on the human chromosome 16. The cytogenetic location of the ABCC11 and ABCC12 genes as well as the structures of exons and introns were analyzed by BLAST search on the Human Genome Project Working Draft (http://genome.cse.ucsc.edu/).

1344 amino acid residues. Based on hydropathy analysis, it is suggested that the variant A has 12 membrane-spanning domains like ABCC11 (Fig. 3, left). However, due to the deletion of the exon 28, the variant A protein lacks 38 amino acid residues in the second ATP-binding cassette.

In addition to ABCC12, there are four splicing variants of ABCC12, namely variants A, B, C, and D consisting of 4034, 3886, 4127 and 4048 nucleotides, respectively. These splicing variants were identified in cDNA libraries from various tissues, such as adult liver, pancreas, testis, and fetal thymus. Figure 2A shows the exon alignments of the splicing variants. The 5′-half (exons 1 to 19) of cDNAs of these variants is identical to that of the ABCC12 cDNA. However, in the 3′-half, variants A and D lack the exon 26, whereas the variant B lacks the exon 20. Furthermore, both variants A and B lack 14 bp (GTAGGTACAGTAAG) in the exon 25, as indicated by 25Δ in Figs. 2A and 2B. The alternative splicing causing the 14-bp deletion may be related to the repeated GTAG sequence at the boundary between the exon 25 and the following intron (Fig. 2B). Importantly, all of these variants have an extra 30 bp sequence at the 5′-end of the exon 22 (Fig. 2A), where a putative stop codon for translation, i.e., TAG or TAA, was incorporated in their cDNAs (Fig. 2B).

Figure 3 shows the putative protein structures of these splicing variants. Variants A, B and D cDNA

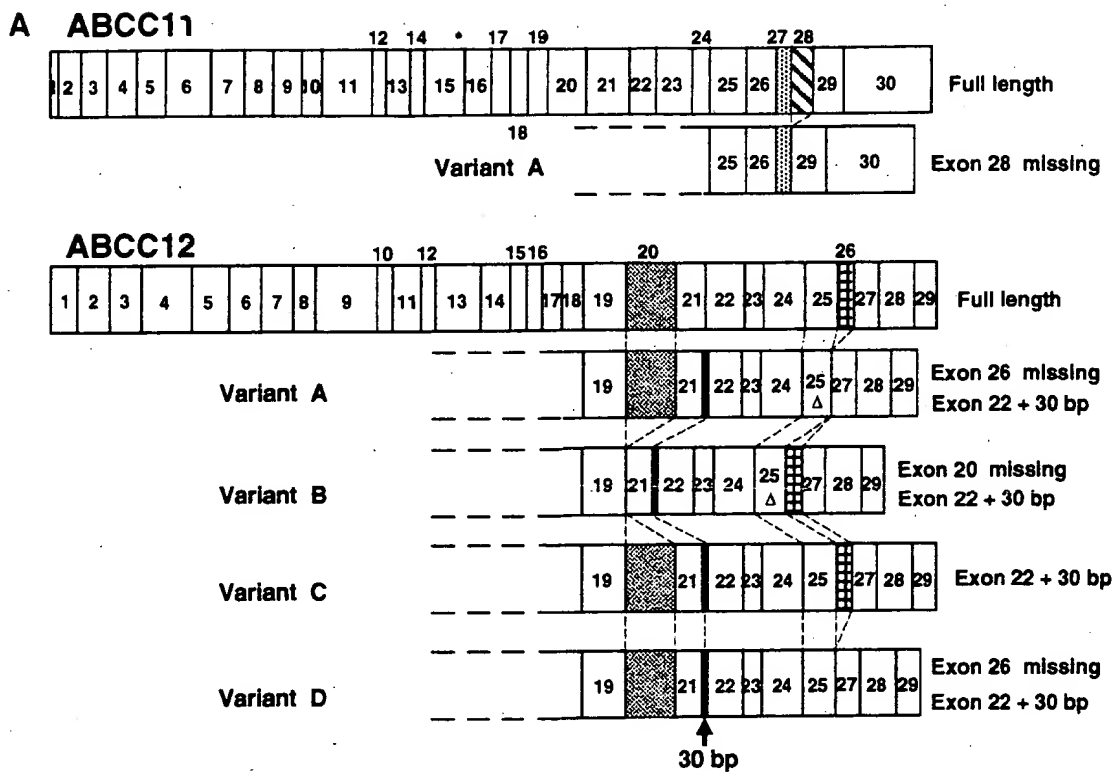

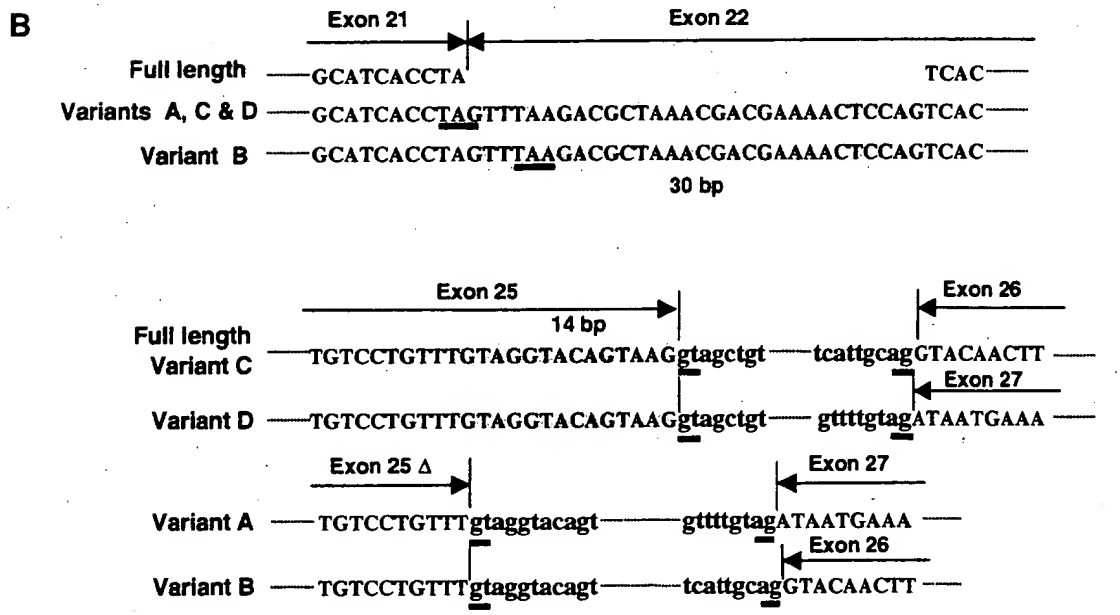

FIG. 2. (A) Schematic illustration of the cDNA structures of ABCC11, ABCC12 and their splicing variants. Based on our cDNA sequence data, exon structures were analyzed using the BLASTN program (http://www.ncbi.nlm.nih.gov/BLAST/) and human genome database. The number of 25Δ indicates the exon that is 14 bp shorter than the exon 25. (B) Comparison of exon 21 and 22 structures among cDNAs of ABCC12 and its splicing variants (upper column). Putative stop codons, i.e., TAG and TAA, in the cDNA of ABCC12 splicing variants are indicated by an underline. The sequence difference between the exons 25 and 25Δ of ABCC12 cDNA (lower column). The sequences of exon and intron are written in capital and small letters, respectively.

contain a single open-reading frame encoding 1009, 935, and 1009 amino acid residue proteins, respectively. Because of the above-mentioned stop codon, these variants may have only eight to nine transmembrane domains and lack the C-terminal domain with the second ATP-binding cassette (Fig. 3, right). Inter-

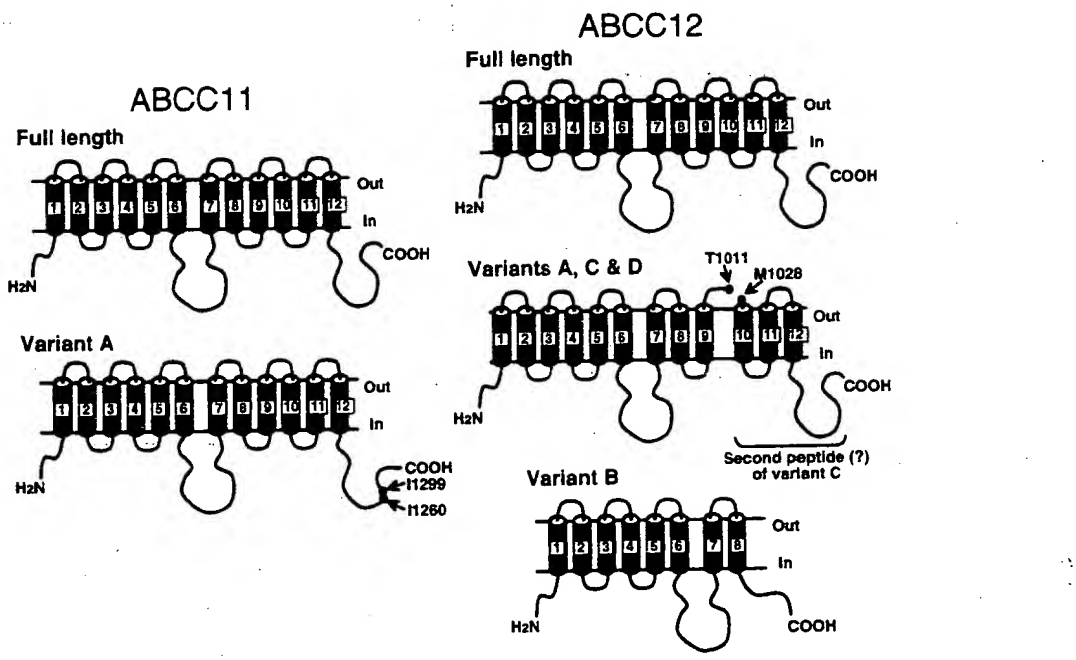

FIG. 3. Schematic illustration of the putative protein topologies of ABCC11 and ABCC12 as well as their splicing variants. Transmembrane domains were predicted using the SOSUI program (http://sosui.proteome.bio.tuat.ac.jp/sosuimenu0.html) and are numerically indicated in the illustration.

estingly, the cDNA of the variant C is suggested to have two open reading frames encoding peptides consisting of 1009 and 331 amino acid residues, since the Kozak consensus sequence resides around the first ATG regions of these two peptide-coding sequences, i.e., 5′-ATCAGG ATG G-3′ for the first peptide; 5′-CTGAGA ATG G-3′ for the second peptide. Hydropathy analysis suggests that, if translated, the first and the second peptides may have nine and three putative transmembrane domains, respectively (Fig. 3). In the case of ABCC8 (SUR1), coexpression of two parts of the protein divided at Pro1042 between transmembrane domains reportedly restored glibenclamide-binding activity (29). Furthermore, it was also reported that small carboxyl-terminal deletions of up to 23 amino acids left the functional activity of ABCB1 (MDR1/P-glycoprotein) (30). Therefore, it is of interest to know whether some of these splicing variants of ABCC12 represent biological functions. Expression of those splicing variants and their function remain to be elucidated.

Detection of ABCC11 and ABCC12 Transcripts in Human Normal Tissues and Cancer Cell Lines

The transcripts of ABCC11 and ABCC12 genes were widely detected by PCR in various adult human tissues, including liver, lung, and kidney, as well as in several fetal tissues (Fig. 4). In addition, the transcripts of ABCC11 and ABCC12 genes were observed in cell lines of carcinoma and adenocarcinoma originated from breast, lung, colon and prostate. It should be noted, however, that the PCR products relatively reflected the amount of the transcripts of both full-length forms and splicing variants.

To clarify this ambiguity, we therefore cloned 30 ABCC11 cDNAs from human adult liver. The splicing variant A lacking the exon 28 (Fig. 2A) was observed at a frequency rate of about 25% in our cDNA clones of the ABCC11 gene (data not shown). Likewise, we have cloned a total of fifty cDNAs of the ABCC12 gene from adult human liver, testis, and pancreas, as well as from fetal liver and thymus. Interestingly, cDNAs of splicing variants A, B, C, and D (Fig. 2) were predominant, exceeding full-length one. Indeed, the total of those four splicing variants was more than 95% of the cloned cDNAs (data not shown).

CONCLUDING REMARKS

The present study provides evidence that ABCC11 and ABCC12 genes are transcribed in multiple splicing variant forms. Detailed profiling and functional analysis of these splicing variants needs further studies. During this study, Tammur *et al.* have most recently reported the cloning of ABCC11 and ABCC12 (31), however splicing variants of these genes were not addressed in their report. On the other hand, recent studies have suggested a relationship between paroxysmal kinesigenic choreoathetosis and a certain gene(s) located in the region of 16p11.2-q12.1 (32, 33).

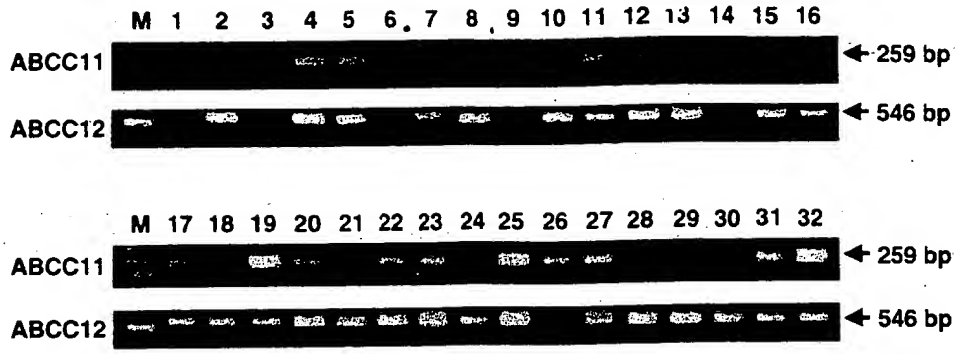

FIG. 4. Detection of the transcripts of ABCC11 and ABCC12 genes in human normal tissues and cancer cells by PCR. M, marker lane (100 bp DNA ladder). Normal tissues: Lanes—1, heart; 2, brain; 3, placenta; 4, lung; 5, liver; 6, skeletal muscle; 7, kidney; 8, pancreas; 9, spleen; 10, thymus; 11, prostate; 12, testis; 13, ovary; 14, small intestine; 15, colon; 16, leukocyte; 17, fetal brain; 18, fetal lung; 19, fetal liver; 20, fetal kidney; 21, fetal heart; 22, fetal spleen; 23, fetal thymus; 24, fetal skeletal muscle. Human cancer cell lines: Lanes—25, breast carcinoma (GI-101); 26, lung carcinoma (LX-1); 27, colon adenocarcinoma (CX-1); 28, lung carcinoma (GI-117); 29, prostatic adenocarcinoma (PC3); 30, colon adenocarcinoma (GI-112); 31, ovarian carcinoma (GI-102); 32, pancreas adenocarcinoma (GI-103).

Since ABCC11 and ABCC12 genes are encoded at 16q12.1, it is tempting to study the biological function of ABCC11 and ABCC12 as well as to examine a potential link between the genetic polymorphism of these ABC transporters, including multiple splicing variants, and the pathogenesis of paroxysmal kinesigenic choreoathetosis.

ACKNOWLEDGMENTS

This study was supported by a research grant (H12-Genome-026) entitled "Studies on the genetic polymorphism and function of pharmacokinetics-related proteins in Japanese population" from the Japanese Ministry of Health and Welfare as well as, in part, by research grants of a NEDO project "Development of the hepatocyte-chip for drug toxicity evaluation" and Grant-in-Aid for Creative Scientific Research (No. 13NP0401) of Japan Society for the Promotion of Science.

REFERENCES

1. Higgins, C. F. (1992) ABC transporters: From microorganisms to man. *Annu. Rev. Cell Biol.* **8,** 67–113.
2. Klein, I., Sarkadi, B., and Varadi, A. (1999) An inventory of the human ABC proteins. *Biochim. Biophys. Acta* **1461,** 237–262.
3. Dean, M., Rzhetsky, A., and Allikmets, R. (2001) The human ATP-binding cassette (ABC transporter superfamily. *Genome Res.* **11,** 1156–1166.
4. http://gene.ucl.ac.uk/nomenclature/genefamily/abc.html.
5. Brooks-Wison, A., Marcil, M., Clee, S. M., Zhang, L.-H., Roomp, K., van Dam, M., Yu, L., Brewer, C., Collins, J. A., Molhuizen, H. O. F., Loubser, O., Ouelette, B. F. F., Fichter, K., Ashbourne-Excoffon, K. J. D., Sensen, C. W., Scherer, S., Mott, S., Denis, M., Martindale, D., Frohlich, J., Morgan, K., Koop, B., Pistone, S., Kastelein, J. J. P., Genest, J., and Hayden, M. R. (1999) Mutations in ABC1 in Tangier disease and familial high-density lipoprotein deficiency. *Nat. Genet.* **22,** 336–345.
6. Bodzioch, M., Orso, E., Klucken, J., Langmann, T., Böttcher, A., Diederich, W., Drobnik, W., Barlage, S., Büchler, C., Porsch-Özcümetz, M., Kaminski, W. E., Hahmann, H. W., Oette, K., Rothe, G., Aslanidis, C., Lackner, K. J., and Schmitz, G. (1999) The gene encoding ATP-binding cassette transporter 1 is mutated in Tangier disease. *Nat. Genet.* **22,** 347–351.
7. Rust, S., Rosier, M., Funke, H., Real, J., Amoura, Z., Piette, J.-C., Deleuze, J.-F., Brewer, H. B., Duverger, N., Denefle, P., and Assmann, G. (1999) Tangier disease is caused by mutations in the gene encoding ATP-binding cassette transporter 1. *Nat. Genet.* **22,** 352–355.
8. Rommens, J. M., Iannuzzi, M. C., Kerem, B., Drumm, M. L., Melmer, G., Dean, M., Rozmahel, R., Cole, J. L., Kennedy, D., Hidaka, N., *et al.* (1989) Identification of the cystic fibrosis gene: Chromosome walking and jumping. *Science* **245,** 1059–1065.
9. Wada, M., Toh, S., Taniguchi, K., Nakamura, T., Uchiumi, T., Kohno, K., Yoshida, I., Kimura, A., Sakisaka, S., Adachi, Y., and Kuwano, M. (1998) Mutations in the canilicular multispecific organic anion transporter (cMOAT) gene, a novel ABC transporter, in patients with hyperbilirubinemia II/Dubin–Johnson syndrome. *Hum. Mol. Genet.* **7,** 203–207.
10. Allikmets, R., Shroyer, N. F., Singh, N., Seddon, J. M., Lewis, R. A., Bernstein, P. S., Peiffer, A., Zabriskie, N. A., Li, Y., Hutchinson, A., Dean, M., Lupski, J. R., and Leppert, M. (1997) Mutation of the Stargardt disease gene (ABCR) in age-related macular degeneration. *Science* **277,** 1805–1807.
11. Berge, K. E., Tian, H., Graf, G. A., Yu, L., Grishin, N. V., Schultz, J., Kwiterovich, P., Shan, B., Barnes, R., and Hobbs, H. H. (2000) Accumulation of dietary cholesterol in sitosterolemia caused by mutations in adjacent ABC transporters. *Science* **290,** 1771–1775.
12. Borst, P., Evers, R., Kool, M., and Wijnholds, J. (1999) The multidrug resistance protein family. *Biochim. Biophys. Acta* **1461,** 347–357.
13. Bryan, J., and Aguilar-Bryan, L. (1997) The ABCs of ATP-sensitive potassium channels: More pieces of the puzzle. *Curr. Opin. Cell. Biol.* **9,** 553–559.
14. Cole, S. P., Bhardwaj, G., Gerlach, J. H., Mackie, J. E., Grant, C. E., Almquist, K. C., Stewart, A. J., Kurz, E. U., Duncan, A. M., and Deeley, R. G. (1992) Overexpression of a transporter gene in a multidrug-resistant human lung cancer cell line. *Science* **258,** 1650–1654.
15. Ishikawa, T. (1992) The ATP-dependent glutathione S-conjugate export pump. *Trends Biochem. Sci.* **17,** 463–468.
16. Müller, M., Meijer, C., Zaman, G. J., Borst, P., Scheper, R. J., Mulder, N. H., de Vries, E. G. E., and Jansen, P. L. M. (1994) Overexpression of the gene encoding the multidrug resistance-

associated protein results in increased ATP-dependent glutathione S-conjugate transport. *Proc. Natl. Acad. Sci. USA* **91,** 13033–13037.

17. Jedlitschky, G., Leier, I., Buchholz, U., Barnouin, K., Kurz, G., and Keppler, D. (1995) Transport of glutathione, glucuronate, and sulfate conjugates by the MRP gene-encoded conjugate export pump. *Cancer Res.* **56,** 988–994.
18. Zaman, G. J. R., Lankelma, J., van Tellingen, O., Beijnen, J., Dekker, H., Paulusma, C., Oude Elferink, R. P. J., Baas, F., and Borst, P. (1995) Role of glutathione in the export of compounds from cells by the multidrug-resistance-associated protein. *Proc. Natl. Acad. Sci. USA* **92,** 7690–7694.
19. Loe, D. W., Almquist, K. C., Deeley, R. G., and Cole, S. P. C. (1996) Multidrug resistance protein (MRP)-mediated transport of leukotriene C_4 and chemotherapeutic agents in membrane vesicles. Demonstration of glutathione-dependent vincristine transport. *J. Biol. Chem.* **271,** 9675–9682.
20. Kool, M., van der Linden, M., de Haas, M., Baas, F., and Borst, P. (1999) Expression of human MRP6, a homologue of the multidrug resistance protein gene MRP1, in tissues and cancer cells. *Cancer Res.* **59,** 175–182.
21. Hopper, E., Belinsky, M. G., Zeng, H., Tosolini, A., Testa, J. R., and Kruh, G. D. (2001) Analysis of the structure and expression pattern of MRP7 (ABCC10), a new member of the MRP subfamily. *Cancer Lett.* **162,** 181–191.
22. Schuetz, J., Connelly, M. C., Sun, D., Paibir, S., Flynn, P. M., Srinivas, R. V., and Kumar, A., and Fridland, A. (1999) MRP4: A previously unidentified factor in resistance to nucleoside-based antiviral drugs. *Nat. Med.* **5,** 1048–1051.
23. Jedlitschky, G., Burchell, B., and Keppler D. (2000) The multidrug resistance protein 5 functions as an ATP-dependent export pump for cyclic nucleotides. *J. Biol. Chem.* **275,** 30069–30074.
24. International Human Genome Sequence Consortium (2001) Initial sequencing and analysis of the human genome. *Nature* 409, 860–921.
25. Venter, C., Adams, M. D., Meyers, E. W., *et al.* (2001) The sequence of the human genome. *Science* 291, 1305–1351.
26. Kozak, M. (1991) An analysis of vertebrate mRNA sequences: Intimations of translational control. *J. Cell Biol.* **115,** 887–903.
27. McAleer, M. A., Breen, M. A., White, N. L., and Matthews, N. (1999) pABC11 (also known as MOAT-C and MRP5), a member of the ABC family of proteins, has anion transporter activity but does not confer multidrug resistance when overexpressed in human embryonic kidney 293 cells. *J. Biol. Chem.* **274,** 23541–23548.
28. Wijnholds, J., Mol, C. A., van Deemter, L., de Haas, M., Scheffer, G. L., Baas, F., Beijnen, J. H., Scheper, R. J., Hatse, S., De Clercq, E., Balzarini, J., and Borst, P. (2000) Multidrug-resistance protein 5 is a multispecific organic anion transporter able to transport nucleotide analogs. *Proc. Natl. Acad. Sci. USA* **97,** 7476–7481.
29. Mikhailov, M. V., Mikhailova, E. A., and Aschcroft, S. J. H. (2000) Investigation of the molecular assembly of β-cell K_{ATP} channels. *FEBS Lett.* 482, 59–64.
30. Currier, S. J., Ueda, K., Willingham, M. C., Pastan, I., and Gottesman, M. M. (1989) Deletion and insertion mutants of the multidrug transporter. *J. Biol. Chem.* **264,** 14376–14381.
31. Tammur, J., Prades, C., Arnould, I., Rzhetsky, A., Hutchinson, A., Adachi, M., Shuetz, J. D., Swoboda, K. J., Ptacek, L. J., Rosier, M., Dean, M., and Allikmets, R. (2001) Two new genes from the human ATP-binding cassette transporter superfamily, ABCC11 and ABCC12, tandemly duplicated on chromosome 16q12. *Gene* **273,** 89–96.
32. Lee, W.-L., Tay, A., Ong, H.-T., Goh, L.-M., Monaco, A. P., and Szepetowski, P. (1998) Association of infantile convulsions with paroxysmal dyskinesias (ICCA syndrome): Confirmation of linkage to human chromosome 16p12-q12 in a Chinese family. *Hum. Genet.* **103,** 608–612.
33. Tomita, H., Nagamitsu, S., Wakui, K., Fukushima, Y., Yamada, K., *et al.* (1999) Paroxysmal kinesigenic choreoathetosis locus maps to chromosome 16p11.2-p12.1. *Am. J. Hum. Genet.* **65,** 1688–1697.

Biochem. J. (2002) 368, 325–332 (Printed in Great Britain)

Impaired 2′,3′-dideoxy-3′-thiacytidine accumulation in T-lymphoblastoid cells as a mechanism of acquired resistance independent of multidrug resistant protein 4 with a possible role for ATP-binding cassette C11

O. TURRIZIANI*, J. D. SCHUETZ†[1], F. FOCHER‡, C. SCAGNOLARI*, J. SAMPATH†, M. ADACHI†, F. BAMBACIONI*, E. RIVA§ and G. ANTONELLI*

*Department of Experimental Medicine and Pathology, University "La Sapienza", 00185 Rome, Italy, †Department of Pharmaceutical Sciences, St. Jude Children's Research Hospital, Memphis, TN 38105, U.S.A., ‡Institute of Molecular Genetics, CNR, 27100 Pavia, Italy, and §Libera Università "Campus Biomedico", 00155 Rome, Italy

Cellular factors may contribute to the decreased efficacy of chemotherapy in HIV infection. Indeed, prolonged treatment with nucleoside analogues, such as azidothymidine (AZT), 2′,3′-deoxycytidine or 9-(2-phosphonylmethoxyethyl)adenine, induces cellular resistance. We have developed a human T lymphoblastoid cell line (CEM_{3TC}) that is selectively resistant to the anti-proliferative effect of 2′,3′-dideoxy-3′-thiacytidine (3TC) because the CEM_{3TC} cells were equally sensitive to AZT, as well as the antimitotic agent, vinblastine. The anti-retroviral activity of 3TC against HIV-1 was also severely impaired in the CEM_{3TC} cells. Despite similar deoxycytidine kinase activity and unchanged uptake of nucleosides such as AZT and 2′-deoxycytidine, CEM_{3TC} had profoundly impaired 3TC accumulation. Further studies indicated that CEM_{3TC} retained much less 3TC. However, despite a small overexpression of multidrug resistance protein (MRP) 4, additional studies with cells specifically engineered to overexpress MRP4 demonstrated there was no impact on either 3TC accumulation or efflux. Finally, an increased expression of the MRP5 homologue, ATP-binding cassette C11 (ABCC11) was observed in the CEM_{3TC} cells. We speculate that the decreased 3TC accumulation in the CEM_{3TC} might be due to the upregulation of ABCC11.

Key words: ABC transporter, HIV, retrovirus, nucleoside analogues.

INTRODUCTION

Long-term anti-retroviral therapy is the main strategy in clinical treatment of HIV-1 infected patients. It is known that the best results in the efficacy of HIV therapy are obtained when various combinations of drugs are administered. Generally, combination anti-retroviral therapies consist of one or more nucleoside reverse transcriptase inhibitors (NRTIs), protease inhibitors, and or non-nucleoside reverse transcriptase inhibitors [1–3]. In fact, the combination of two nucleoside-based reverse transcriptase inhibitors and a protease inhibitor, referred to as 'highly active anti-retroviral therapy' (HAART), dramatically suppresses plasma HIV-RNA levels to < 50 copies/ml [4–6]. Despite the efficacy of such therapeutic regimens, long-term treatment with HAART leads to the emergence of drug-resistant HIV strains, and genetic mutations in the reverse transcriptase gene have been isolated in many patients treated with HAART [7–9].

The presence of HIV mutations has been associated with virological failure; however, individuals also display signs of drug resistance in the absence of drug-resistant virus [10,11]. This observation is consistent with the concept that 'cellular' factors contribute to the failure of anti-retroviral therapy [12–15]. Indeed, most anti-HIV agents, specifically dideoxynucleosides, are phosphorylated by cellular kinases to compounds that inhibit HIV replication. Consequently, decreasing the cellular levels of these compounds could lead to an inability to suppress viral replication and contribute to the failure of anti-retroviral therapy. In this regard, it has been shown that long-term treatment of cell lines with NRTIs [such as 3′-azido-3′-deoxythymidine (AZT) and 2′-3′-dideoxycytidine (ddC)] results in diminished amounts of the phosphorylated forms of NRTIs. In these cases, decreased activity of the cellular kinases leads to antiviral resistance because of an impaired ability to accumulate phosphorylated metabolites [16–18].

Another cellular mechanism has previously been described to explain decreased drug accumulation and resistance to retroviral inhibitors: the increased efflux of phosphorylated drug [19]. Subsequently, we demonstrated that overexpression of a functionally uncharacterized ATP-binding cassette (ABC) drug-transporter [multidrug resistance protein (MRP) 4] was genetically linked to the decreased drug accumulation and resistance to some, but not all NRTIs [20] (for an overview of the ABC-family members and nomenclature see http://nutrigene.4t.com/humanabc.htm). The ABC transporters are mostly plasma membrane localized and show ATP-dependent transport of a broad range of compounds. Most MRP substrates are organic

Abbreviations used: ABC, ATP-binding cassette; AZT, 3′-azido-3′-deoxythymidine; CNT, concentrative nucleoside carrier; dCK, deoxycytidine kinase; dCyd, deoxycytidine; ddC, 2′-3′-dideoxycytidine; ENT, equilibrative nucleoside carrier; GFP, green fluorescence protein; HAART, highly active anti-retroviral therapy; [^{3}H]Cyd, [5-^{3}H]cytidine; ID_{50}, 50% inhibitory dose; MDR, multidrug resistance; [^{3}H]AZT, [*Me*-^{3}H]AZT; MRP, multidrug resistant protein; MTT, 3-(4,5-dimethylthiazol-2-yl)-2,5-diphenyl-2*H*-tetrazolium bromide; NRTI, nucleoside reverse transcriptase inhibitor; Pgp, P-glycoprotein; PMEA, 9-(2-phosphonylmethoxyethyl)adenine; RT, reverse transcriptiase; 3TC, 2′-3′-dideoxy-3′-thiacytidine (also called lamivudine); [^{3}H]3TC, [*Me*-^{3}H]3TC.

[1] To whom correspondence should be addressed (e-mail John.schuetz@stjude.org).

anions and they are often conjugated to glutathione, glucuronide or sulphate. Notably, two members of the MRP family (MRP4 and 5) efflux nucleotide analogues such as the nucleotide analogue, 9-(2-phosphonylmethoxyethyl)adenine (PMEA), azidothymidine-monophosphate, and thioguanine-monophosphate [21,22]. Further, the cells that overexpressed MRP4 had decreased antiviral efficacy for 2′,3′-dideoxy-3′-thiacytidine (3TC), a finding strongly implicating MRP4 as a contributor to 3TC cellular resistance. In order to evaluate whether the prolonged treatment with 3TC was able to induce cellular resistance by this mechanism, we cultured a T-lymphoblastoid cell line in the presence of increasing concentrations of this nucleoside analogue. Our findings indicate that these cells acquire stable resistance to 3TC by a mechanism whereby 3TC accumulation is substantially decreased. Furthermore, the cells harbor no defect in the enzyme activating 3TC to a nucleotide, nor is there a general impairment in nucleoside uptake. However, despite a small overexpression of MRP4 in these cells, it is clear that another mechanism is responsible because MCF-7 cells engineered to overexpress MRP4 do not show impaired 3TC accumulation or increased 3TC efflux.

MATERIALS AND METHODS

Chemicals

The 3TC, kindly provided by Glaxo Wellcome (Stevenage, Herts., U.K.), was dissolved in PBS and kept at −20 °C. AZT, [*Me*-^{3}H]AZT ([^{3}H]AZT, 3 Ci/mmol), ddC and [5-^{3}H]cytidine ([^{3}H]Cyd, 17.4 Ci/mmol) were purchased from Sigma Chemical Co (Milan, Italy). [*Me*-^{3}H]3TC ([^{3}H]3TC, 17.5 Ci/mmol) was purchased from Moravek Biochemicals (Brea, CA, U.S.A.). Commercial reagents and solvents were of analytical grade, unless otherwise stated. [^{3}H]2′-deoxycytidine ([^{3}H]dCyd, 18–30 Ci/mmol) was from Amersham (Milan, Italy).

Selection of 3TC-resistant cell lines

3TC-resistant cells were obtained by exposure of CEM cells, the parental cell line, to increasing concentrations of 3TC. CEM cells were initially propagated in the presence of 10 μM 3TC. Doubling concentrations of 3TC were added to the culture medium and the cells were allowed to grow until they reached a cell density of 10^6 cells/ml. After approx. 4 months, a stably resistant 3TC CEM line grew in the presence of 1 mM 3TC, with a doubling time similar to non-drug selected CEM cells. These cells were called CEM_{3TC}.

Assay to determine the anti-growth activity of drugs in CEM and CEM_{3TC}

The 3-(4,5-dimethylthiazol-2-yl)-2,5-diphenyl-2*H*-tetrazolium bromide (MTT) assay was used to evaluate the anti-growth activity of drugs in CEM and CEM_{3TC} [23]. Briefly, CEM and CEM_{3TC} were seeded in 96-well microtitre plates at a concentration of 50000 cells/well. Different concentrations of drugs were added to triplicate cultures. Four days later, 20 μl of MTT solution was added to each well and the cultures were incubated at 37 °C. The viability of cells was examined spectrophotometrically and the values were used to calculate the 50% toxic concentration (TC_{50}) of the various test compounds.

Assay of drug sensitivity

CEM and CEM_{3TC} cells (3×10^5) were incubated with the HIV-PNL43 strain at a multiplicity of infection ('MOI') of 1 $TCID_{50}$ (50% tissue culture infectious dose)/cell. After 1 h at 0 °C, the cultures were washed three times with medium, resuspended in medium containing 3TC (or AZT or ddC) at the appropriate concentrations, and incubated at 37 °C. After 5 days the amount of viral antigens produced by infected cells was determined by ELISA (Abbott Laboratories, Abbott Park, IL, U.S.A.). The values for the 50% inhibitory dose (ID_{50}) were calculated from plots of the percentage reduction of viral antigens.

Determination of intracellular accumulation of 3TC or other nucleosides

CEM and CEM_{3TC} cells were treated with [^{3}H]3TC (0.1 μM; 2 μCi/ml) at different times (as indicated in the Figures) and then rapidly washed with ice-cold buffer and, after lysis, the amount of radioactivity was determined. The intracellular uptake of 3TC was also determined using a range of drug concentrations (from 0.02 μM to 0.2 μM). To study the intracellular accumulation of AZT and dCyd, CEM and CEM_{3TC} cells were exposed to [^{3}H]AZT (0.6 μM; 2 μCi/ml) and [^{3}H]dCyd (0.1 μM; 2 μCi/ml). At the indicated time, cells were washed, lysed and the radioactivity was determined.

3TC retention

CEM and CEM_{3TC} were preincubated with [^{3}H]3TC (2 μCi/ml) for 2 h, washed with ice-cold PBS by centrifugation, resuspended in drug-free medium, and maintained at 37 °C. After 1 h, the intracellular radioactivity and radiolabelled drug released into the medium was assessed by scintillation counting.

Reverse transcription (RT) and PCR

RNA from 5×10^6 CEM or CEM_{3TC} was isolated using Trizol reagents (Gibco BRL, NY, U.S.A.). The RT-PCR analysis of the RNA sample was performed as follows. RNA (10 μg) was incubated with 2 μl of random primers (150 μg/ml) at 72 °C for 10 min, then combined with a mixture containing 4 μl of 5% reaction buffer [250 mM Tris (pH 8.3), 375 mM KCl, 15 mM $MgCl_2$; Roche Molecular Biochemicals, Milan, Italy], 25 units of human placental ribonuclease inhibitor, 1 μl of 10 mM dNTP (Roche Molecular Biochemicals), 8 units of Moloney murine leukaemia virus RT (Roche Molecular Biochemicals). After 90 min at 42 °C, 5 μl of cDNA was subjected to the PCR-mediated amplification for P-glycoprotein (Pgp) according to conditions described previously [24].

Cell extracts

CEM and CEM_{3TC} cell pellets, prepared as described above, were resuspended in 5 vols of 20 mM Bis-Tris, pH 6.5, containing 1 mM dithiothreitol (DTT) and 0.5 mM PMSF, and sonicated for 5 s on ice at 50 W. Sonication was repeated five times at intervals of 10 s. Cell extracts were centrifuged at 4 °C at 5000 *g* in a benchtop centrifuge for 15 min. Supernatants were collected and assayed for protein concentration using the spectrophotometric-based Bio-Rad Protein Assay.

2′-Deoxycytidine kinase assay

Deoxcytidine kinase (dCK) activity present in cell extracts was assayed with a radiochemical method which measures the formation of [^{3}H]dCMP from [^{3}H]dCyd. The cell extracts were incubated at 37 °C in 25 μl of a mixture containing 30 mM Hepes-K^+ (pH 7.5), 5 mM $MgCl_2$, 5 mM ATP, 0.5 mM DTT and 2.4 μM [^{3}H]dCyd (2200 c.p.m./pmole) or [^{3}H]3TC

(1500 c.p.m./pmole). The reaction, after 20 min incubation, was terminated by spotting 20 μl of the incubation mixture onto a 25 mm DEAE paper disk (DE-81 paper; Whatman Biosystems Ltd., Maidstone, Kent, U.K.). The disks were washed three times in an excess of 1 mM ammonium formate, pH 3.6, in order to remove unconverted nucleoside, followed by a final wash in ethanol. The filters were dried and radioactive dCMP was estimated by scintillation counting in 1 ml of Betamax scintillating fluid (ICN Pharmaceuticals, Milan, Italy). One unit is defined as the amount of enzyme catalysing the formation of 1 nmol of dCMP in 1 h at 37 °C.

Immunoblot analysis

Crude membranes were prepared from cells as described previously [20]. Proteins were estimated using the Bio-Rad Protein Assay (Bio-Rad, Milan, Italy) and BSA was used as the standard. The crude membrane proteins (200 μg) were resuspended in standard Laemmli sample preparation buffer and loaded onto a 7.5 % denaturing polyacrylamide gel and transferred to nitrocellulose filters. The filters were blocked in 1 × PBS containing 0.1 % Tween 20 and 10 % non-fat dry milk, immunoreacted with polyclonal rabbit anti-(MRP4) IgG followed by peroxidase conjugated anti-(rabbit IgG), and then developed with the Amersham ECL® detection system (Amersham, Airlington Heights, IL, U.S.A.). The immunoblots were stripped with glycine and reprobed with a monoclonal antibody to MRP1 (mPr1; Signet Laboratories, MA, U.S.A.).

Pgp detection

Pgp was also detected by FACS analysis. CEM, CEM_{3TC} and CEMVBL100 (a T-cell line expressing a high level of Pgp) cells were incubated with a Pgp-specific monoclonal antibody that recognizes an external epitope of Pgp (mMRK16, Alexis Italia, Florence, Italy). After incubation (30 min at 18–25 °C) the cells were washed with PBS and incubated with FITC-labelled goat anti-mouse immunoglobulin (Bioline Diagnostics, Turin, Italy) for an additional 30 min. After washing with PBS, the cells were resuspended in PBS and analysed by flow cytometry. This was performed using a FACScan (DAKO-Galaxy, Milan, Italy) flow cytometer. Forward and side light scatter were collected in linear mode and served to exclude unwanted events (i.e. debris, dead cells and aggregates). The fluorescence signal was collected in the log mode.

Generation of MRP4 stable cell lines

The human MRP4 cDNA was cloned into the MSCV-IRES-GFP [25] vector (kindly provided by Dr Robert Hawley, Holland Laboratory, American Red Cross, Rockville, MD, U.S.A.) using the *EcoR*I site. 293T cells were cotransfected with 10 μg each of MSCV-MRP4-IRES-GFP, the helper plasmid pSRa-G, and pEQPAM3-e (kindly supplied by P. Kelly and E. F. Vanin, Department of Hematology/Oncology St Jude Children's Research Hospital, Memphis, TN, U.S.A.) by standard calcium phosphate precipitation [26]. The supernatant was collected 48 h after transfection, filtred, titred and frozen at −80 °C. To confirm transfection, the 293T cells were analysed for green fluorescence protein (GFP) expression. Subsequently, the cells were transduced with MRP4. Briefly, the cells were plated at 5×10^4 cells/60 mm tissue culture dish and then the medium was replaced by the retroviral supernatant supplemented with 6 μg/ml polybrene and placed overnight in an incubator at 37 °C in a 5 % CO_2 humidified atmosphere. The transduction was repeated again twice for a total of three times. The transduced cells were expanded and the GFP-positive cells were selected after FACS [26]. Subsequently, a total lysate was prepared and loaded on a denaturing polyacrylamide gel for MRP4 and MRP1 detection by immunoblot [20].

Semi-quantitative RT-PCR analysis of MRP5 and ABCC11

RNA was isolated from CEM and CEM_{3TC} cells using Trizol. First-strand cDNA was made from 2.5 μg of RNA using the cDNA synthesis kit for PCR (Boehringer Mannheim, Indianapolis, IN, U.S.A.) in a final volume of 20 μl. MRP5 and ABCC11 (also called MRP8) were amplified with 125 ng of cDNA in a final volume of 50 μl containing 200 μM each of dATP, dCTP, dGTP, and dTTP, and 300 nM each of forward and reverse primers using the Expand High Fidelity PCR System (Boehringer Mannheim). Samples were denatured for 5 min at 94 °C, followed by cycles of 94 °C for 30 s, 60 °C for 30 s, 68 °C for 2 min, and a final incubation at 68 °C for 2 min. The number of cycles for MRP5 was 26 and the number of cycles for ABCC11 was 30. Primers were as follows: MRP5, forward primer, 5′-TCCTGCCTTCTGTCCTGGTGT-3′ and reverse primer, 5′-CTGTGCGACGACTGCGGTGAG-3′; ABCC11 forward primer, 5′-AGAATGGCTGTGAAGGCTCAGC-3′ and reverse primer, 5′ GTTCCTCTCCAGCTCCAGTGC 3′. The predicted sizes for the MRP5 and ABCC11 products were 390 bp and 550 bp respectively. Aliquots (10 μl) of the PCR reactions were loaded onto a 1 % agarose gel containing ethidium bromide.

RESULTS

Selection of 3TC-resistant CEM cells

Cellular factors, such as altered drug activation and/or decreased accumulation may cause failure of anti-retroviral drugs [13–15]. To determine if these cellular factors account for the variable response to the anti-retroviral drug 3TC, we cultured the CEM T-cell line in increasing concentrations of 3TC. After approx. 4 months of culture in the presence of 1 mM 3TC, CEM cells were obtained that were refractory to the growth inhibitory properties of 3TC. These cells are referred to as CEM_{3TC} and their resistance to 3TC was stable for 4 months in the absence of 3TC. Furthermore, the resistance to the cytotoxic effects of 3TC was selective because CEM_{3TC} were equally sensitive to AZT and vinblastine (Table 1).

CEM_{3TC} are impaired for antiviral efficacy

To evaluate whether the CEM_{3TC} cells had an impaired ability to inhibit HIV replication, CEM and CEM_{3TC} cells were infected with HIV (see Materials and methods section) and then treated

Table 1 Sensitivity of CEM and CEM_{3TC} to antiviral and antigrowth activities of 3TC, AZT, ddC and vinblastine

TC_{50} is the concentration producing 50% cytotoxicity and ID_{50} is the dose producing 50% inhibition of HIV replication.

	TC_{50}			ID_{50}		
Cells	3TC (mM)	AZT (mM)	VBL (ng/ml)	3TC (nM)	AZT (nM)	ddC (nM)
CEM	4.00 ± 2	0.30 ± 0.10	0.08 ± 0.06	6 ± 3	7 ± 4	8 ± 3
CEM_{3TC}	> 10†	0.40 ± 0.15	0.10 ± 0.09	60 ± 10*	9 ± 5	10 ± 4

† Owing to 3TC insolubility, concentrations greater than 10 mM were not evaluated.
* CEM versus CEM_{3TC}, $P < 0.05$.

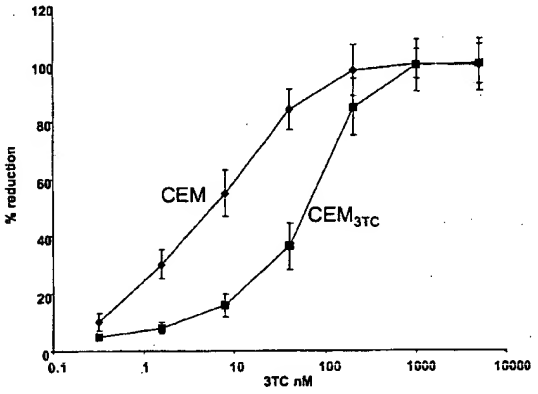

Figure 1 Antiviral activity is reduced in 3TC resistant cells

Antiviral activity of 3TC in CEM (diamonds) and CEM_{3TC} (squares). Cells were infected with HIV-PNL43 and cultured in the presence of different concentrations of 3TC. After 5 days the amount of viral antigen produced by infected cells was measured as described in the Material and methods section. Each point represents the mean and the bars $\pm$ one standard deviation from the mean.

with various concentrations of 3TC (Figure 1). The viral yield was determined 5 days later by measuring the viral antigen released into the culture supernatant. We found that CEM_{3TC} were markedly resistant to the antiviral activity of 3TC, with the 3TC ID_{50} value for HIV-1 being approx. 10-fold higher in CEM_{3TC} (ID_{50} = 60 nM) compared with the CEM cell line (ID_{50} = 6.0 nM) (Figure 1). Again, the resistance to the antiviral activity of 3TC was selective because CEM_{3TC} were equally sensitive to the antiviral activity of ddC and AZT (Table 1).

Deoxycytidine kinase activity is not decreased in CEM_{3TC}

After cellular uptake by nucleoside uptake carriers, 3TC is phosphorylated by deoxycytidine kinase [27]. Deoxycytidine kinase effectively phosphorylates both enantiomers of dCyd [28] and dCyd analogues, such as 3TC [29]. Therefore, we evaluated the enzymic activity of dCK in CEM and CEM_{3TC} cells using both 3TC and dCyd as the substrate. The results indicated that the enzymic activity of dCK from CEM_{3TC} was not decreased compared with the parental CEM cells. In fact, using 3TC as substrate, the dCK activity was 0.12 ± 0.01 units/mg of protein in CEM and 0.16 ± 0.02 units/mg in CEM_{3TC}. Similarly, when dCyd was used as substrate the dCK activity was 0.8 ± 0.08 units/mg in CEM and 1.24 ± 0.12 units/mg in CEM_{3TC}. These results indicate, using either dCyd or 3TC, that the 3TC-resistance of CEM_{3TC} cannot simply be ascribed to a reduction in dCK activity.

Decreased 3TC accumulation in CEM_{3TC} without a general decrease in nucleoside uptake

Resistance to 3TC could be due to the reduced intracellular accumulation of drug, secondary to either transport changes or alterations in enzymic activation. Uptake of radiolabelled 3TC was used to assess variations in 3TC transport. Figure 2(A) shows there was no significant difference between the two cell lines in their initial uptake of 3TC (< 50 min). However, when the cells were incubated for longer intervals (> 1 h) dramatic differences in accumulation emerged. The CEM cells continued to accumulate radiolabelled 3TC, whereas at 8 h, the CEM_{3TC} achieved a steady-state level of drug that was as much as 3-fold

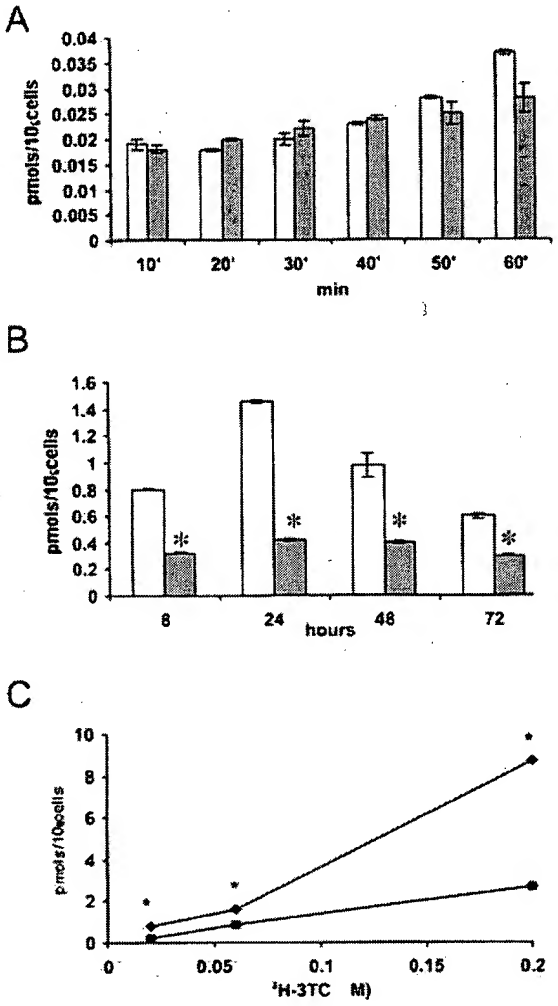

Figure 2 3TC Accumulation is impaired in 3TC resistant cells

(**A**) Intracellular uptake of [^{3}H]3TC in CEM (open bars) and CEM_{3TC} (closed bars). Cell cultures were incubated with 0.1 μM [^{3}H]3TC, and at the indicated times cells were extensively washed with ice-cold PBS, lysed and the radioactivity determined by scintillation counting. The results are the mean ($\pm$SD) from three independent experiments (*$P < 0.05$). (**B**) Long-term 3TC accumulation. Either CEM (open bars) or CEM_{3TC} (closed bars) were incubated with 0.1 μM [^{3}H]3TC for the indicated intervals (*$P < 0.05$). (**C**) Uptake of different concentrations of [^{3}H]3TC. CEM (diamonds) and CEM_{3TC} (squares) were incubated with different concentrations of [^{3}H]3TC. After 8 h, intracellular radioactivity was evaluated by scintillation counting. The points represent the mean of two independent experiments performed in triplicate, with the error bars indicating $\pm$ one standard deviation (*$P < 0.05$).

lower than the maximum attained in the CEM cells. It is interesting to note that despite the continued presence of extracellular drug, the 3TC accumulation decreased in the CEM cells after 72 h of 3TC incubation. This suggests that the transporter effluxing 3TC is induced, a phenomenon previously reported for AZT [30] (Figure 2B). Finally, the CEM_{3TC} cells acccumulated much less drug than the CEM cells at multiple concentrations of 3TC (Figure 2C). It is notable that the 5-fold lower 3TC accumulation roughly corresponds with the greater 3TC concentration required to inhibit HIV replication (Figure 1 and Table 1) and supports the idea that impaired 3TC accumulation is responsible for the enhanced survival of these cells in 3TC, as well as the requirement for more 3TC to inhibit HIV replication.

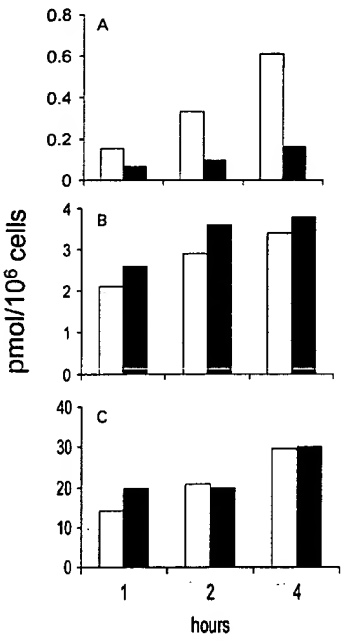

Figure 3 3TC resistant cells have a selective defect in 3TC accumulation

Intracellular accumulation of 3TC, AZT and dCyd in CEM (open bars) and CEM_{3TC} (solid bars). Cells were incubated with (**A**) 0.1 μM [^{3}H]3TC, (**B**) 0.6 μM [^{3}H]AZT or (**C**) 0.1 μM [^{3}H]dCyd. At the indicated times, cells were washed with ice-cold PBS, lysed and the radioactivity determined by scintillation counting. The results are the average of two independent experiments done in triplicate.

Table 2 3TC drug accumulation and retention in 3TC resistant cells

The values are the means of two independent experiments, each done in duplicate. For both intracellular radioactivity and radioactivity released into the supernatant, values were significantly different, $P < 0.05$ in each case.

	Percentage of total [^{3}H]3TC	
Cells	Intracellular	Supernatant
CEM	82.4 ± 1.8	17.6 ± 1.8
CEM_{3TC}	65.7 ± 0.8	34.3 ± 0.8

To determine if the impaired accumulation of 3TC was specific for 3TC, and to rule out a general defect in nucleoside uptake carriers, accumulation of [^{3}H]3TC, [^{3}H]AZT and [^{3}H]dCyd was determined (Figure 3). It is known that AZT is a substrate for both the concentrative nucleoside carrier (CNT) and equilibrative nucleoside carrier (ENT2) [31], while deoxycytidine is a known substrate for CNT [32]. The intracellular radioactivity was then measured as described in the Material and methods section. The studies reveal that CEM_{3TC} cells are not impaired for the accumulation [^{3}H]AZT and [^{3}H]dCyd, which indicates that the nucleoside-uptake carriers transporting these nucleosides are not impaired in the CEM_{3TC} cells.

CEM_{3TC} have decreased retention of 3TC, with no change in Pgp and a small increase in MRP4 expression

To explore whether the defect in cellular 3TC accumulation could be associated with a decreased capability of the resistant cell line to retain 3TC, we evaluated 3TC retention. The cells were pre-loaded with [^{3}H]3TC followed by resuspension in drug-free media. Subsequently, the amount of radioactivity in the cells and media was determined. The results, shown in Table 2, indicate that the CEM_{3TC} cells retained much less intracellular radioactivity than the CEM cells. Furthermore, a correspondingly higher percentage of radioactivity was released into the medium from CEM_{3TC} compared with CEM cells. This indicates that CEM_{3TC} have a decreased ability to retain 3TC, and this correlates with the selective impaired accumulation of 3TC (Figure 2).

Next, we evaluated whether the decreased 3TC accumulation could be due to an increased expression of Pgp using FACS analysis with an antibody that detects a surface Pgp epitope (see Materials and methods section). We found that both CEM and CEM_{3TC} have undetectable Pgp, unlike the positive control, $CEMVBL_{100}$, that expresses high amounts of Pgp (results not shown). Furthermore, we demonstrated that neither the CEM nor CEM_{3TC} cells had detectable levels of MDR1 transcript when used amplified to the same extent as the MDR1-positive cell, $CEMVBL_{100}$.

Expression of MRP4 in CEM_{3TC} and transport of 3TC in cells ectopically expressing MRP4

Recent studies indicated that the ABC transporter, MRP4, plays a role in the cellular resistance to anti-retroviral nucleoside drugs, including 3TC [20]. To evaluate MRP4 expression, we performed immunoblot analysis on crude membranes from the CEM_{3TC} cells (Figure 4). We found that the level of immunoreactive MRP4 increased approximately 2-fold in the CEM_{3TC} cells. In contrast, MRP1 was not different in the two cell lines. It is interesting to note that MRP4, which is only a 1325-amino-acid-residue protein, runs at an estimated size of 220 kDa, whereas MRP1, a 1531-amino-acid-residue protein, runs at an estimated size of 190 kDa. This is probably due to the fact that MRP4 is extensively glycosylated with at least seven predicted N-linked asparagine glycosylation sites [25].

To determine whether MRP4 played a role in transport of 3TC, we developed cell lines that ectopically overexpressed MRP4 (Figure 4B). We confirmed the phenotype of these cells by evaluating the uptake of PMEA, a known MRP4 substrate [20] (Figure 4C). These cells were then assessed for the uptake of 3TC (Figure 4D). We evaluated 3TC uptake after a 24 h incubation in concentrations of 3TC from 0.5 to 10 μM. The total accumulation of 3TC radioactivity was the same in the MRP4 cells as in the vector-only transfected cells (Figure 4D). Since longer incubations (48 h) produced slightly lower 3TC accumulation, we assessed whether efflux was faster in the MRP4 cells. The cells were loaded with 3TC, resuspened in drug-free media, and then assessed for both 3TC intracellular-associated radioactivity and the radioactivity released into the media (Figure 4E). For both cells lines, the time to decrease the intracellular radioactivity to one-half the initial level was approx. 20 min and, notably, a corresponding efflux of radioactivity into the media occurred. These studies directly demonstrate in MCF-7 cells overexpressing MRP4 that 3TC efflux is not enhanced by MRP4 overexpression.

Expression of MRP4, MRP5 and ABCC11 in CEM_{3TC}

The efflux of nucleotide analogues in mammalian cells has been confirmed for MRP4 and MRP5 [21]. Although we have demonstrated that cells specifically overexpressing MRP4 do not have

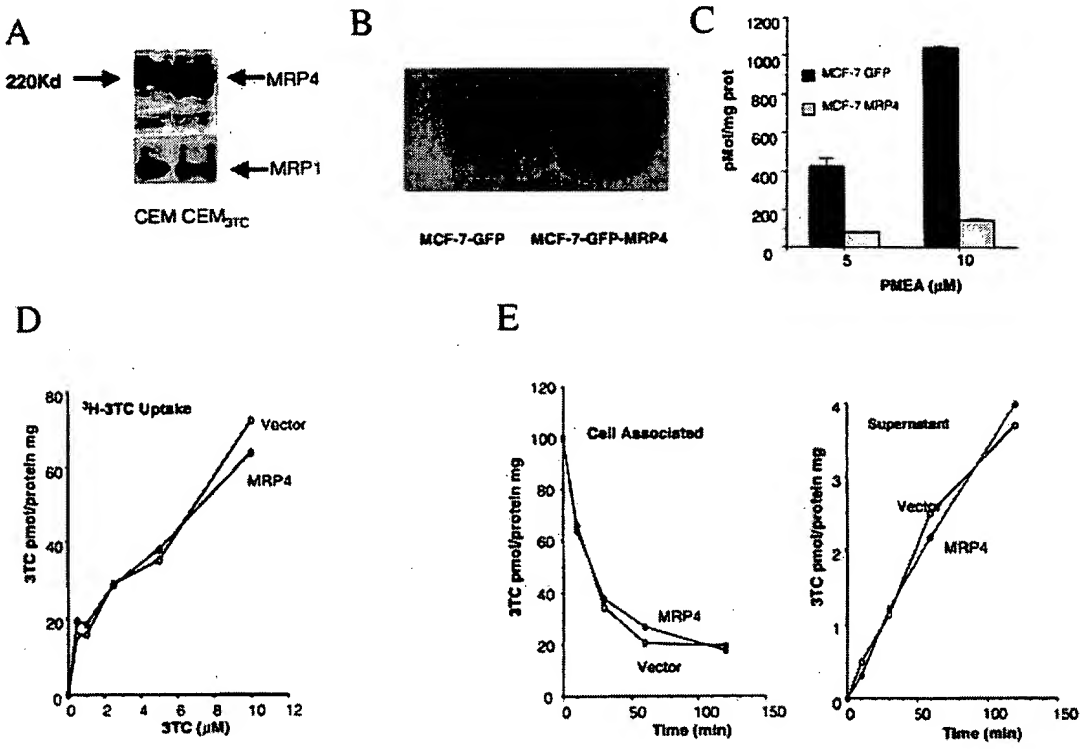

Figure 4 Analysis of MRP1 and MRP4 in CEM_{3TC} and the impact of MRP4 upon 3TC transport

(**A**) Lysates of CEM and CEM_{3TC} cells were analysed on an immunoblot with antiserum against MRP4, and then with antiserum against MRP1. (**B**) Immunoblot analysis of MRP4 expression in cells engineered to overexpress MRP4. (**C**) Functional analysis of MRP4 using PMEA accumulation, as described in the Materials and methods section. (**D**) MCF-7 cells ectopically expressing MRP4 (●) or the control vector (○) were incubated with [^{3}H]3TC (0.5–10 μM). After 24 h, the accumulation of 3TC radioactivity was determined. (**E**) 3TC efflux in cells ectopically expressing MRP4. Control vector (○) and MRP4 expressing cells (●) were loaded with [^{3}H]3TC followed by resuspension in drug-free media. Both intracellular-associated 3TC radioactivity (Cell Associated) and 3TC radioactivity released into the media (Supernatant) were assessed.

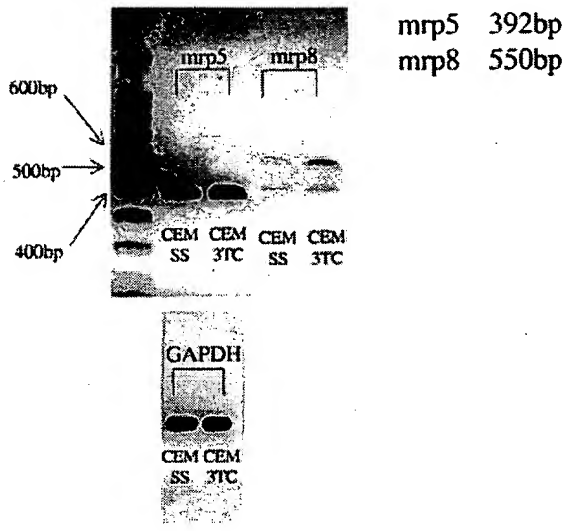

Figure 5 Analysis of MRP5 and ABCC11 (MRP8) expression in CEM_{3TC} cells

Total RNA was isolated from both CEM and CEM_{3TC} cells, followed by RT-PCR. The lower band in MRP8 (ABCC11) was sequenced and found to be a non-specific band. The primers and conditions are described in the Materials and methods section.

decreased accumulation or increased efflux of 3TC, it remains possible that another ABC transporter effluxes 3TC metabolites. Our recent investigations and others studies [33,34] indicate that MRP5 has two closely related homologues on chromosome 16. We evaluated the expression of ABCC11 mRNA levels in CEM and CEM_{3TC} cells by RT-PCR (ABCC12 was not detected). In addition, we assessed the level of MRP5 mRNA (Figure 5). We found that the level of MRP5 was unchanged in the CEM_{3TC} cells. In contrast, semi-quantitative RT-PCR revealed that ABCC11 was increased 6-fold. The magnitude of this increase in ABCC11 mRNA is comparable with the impairment in 3TC antiviral efficacy in these cells. The lack of a direct correspondence may be due to the possibility that the protein is expressed at a much higher level than the mRNA; however, at this time, it is impossible to determine whether ABCC11 protein levels are increased due to the unavailability of a specific antibody.

DISCUSSION

Recent findings have recognized that anti-retroviral drug treatment causes a phenotype described as cellular resistance [12–15]. This phenomenon is consistent with the knowledge that different cell lines require a broad range in the concentration of anti-retroviral drug to inhibit HIV replication [35]. Two main mechanisms contribute to cellular resistance: altered metabolism of nucleoside analogues due to impaired nucleoside phosphoryl-

ation and increased efflux of the compounds by membrane transport mechanisms [20,21].

Our results demonstrate that prolonged treatment with 3TC selects for cells with an acquired, stable resistance to 3TC. Compared with the CEM cells, CEM_{3TC} required about 10-fold more 3TC to inhibit HIV. Moreover, these cells showed increased resistance to the cytotoxic effects of 3TC. However, the CEM_{3TC} were as sensitive to AZT, ddC and vinblastine as the CEM cells, demonstrating that this resistance is specific for 3TC. Notably, 3TC resistance was not due to decreased dCK activity, the principal enzyme required for activation of 3TC [27]. Furthermore, uptake of the natural nucleosides dCyd and azidothymidine was unaltered in CEM_{3TC}. Thus, these findings rule out the possibility of a general defect in nucleoside uptake because such alterations would have undoubtedly have impacted upon AZT and dCyd accumulation, considering that AZT is transported by both ENT2 and CNT, and that dCyd is transported by CNT [32,36]. In contrast, 3TC accumulation was substantially reduced in CEM_{3TC} cells and was associated with decreased intracellular retention. Consequently, we postulated that an efflux transporter was responsible for preventing 3TC accumulation in the resistant cells. In fact, drug efflux pumps are an important part of the cellular defence against cytotoxic compounds. Specifically, cells overexpressing drug-transporting proteins become resistant to a wide range of drugs with different structures and/or cellular targets. This phenomenon is known as multidrug resistance (MDR). The most well characterized of these drug transporters is Pgp [37]. The overexpression of Pgp has been described for many cancer cells with acquired resistance to chemotherapuetics [38]. Several studies have reported that Pgp-expressing cells are also resistant to the anti-growth and antiviral activity of some NRTIs [39–41]. On the basis of these findings, we evaluated Pgp expression in CEM_{3TC}. However, as anticipated, based upon 3TC structure, the CEM_{3TC} cells had no detectable Pgp overexpression.

Recently, it has been reported that one member of the MRP family, MRP4, is overexpressed in cells that acquire resistance to the cytotoxic effects of the modified nucleotide analogue, PMEA [20]. Notably, overexpression of MRP4 impairs the antiviral efficacy of PMEA and other nucleoside analogues, such as 3TC and AZT. In our 3TC resistant cells, we found a small increase in MRP4 (< 2-fold), suggesting that 3TC metabolites could be MRP4 substrates. However, an analysis of MCF-7 cells ectopically expressing MRP4 showed that MRP4 does not affect either the accumulation or the efflux of 3TC. This result contrasts with the previously reported findings; however, it should be noted that only PMEA and AZT-monophosphate were effluxed to a greater extent in the MRP4 overexpressing cells, and it was not directly demonstrated that 3TC metabolites were more readily effluxed in those cells [20]. Thus, based on the current studies, it seems unlikely that MRP4-mediated efflux is directly involved in cellular 3TC resistance and that the impaired 3TC accumulation and decreased retention is due to an additional 3TC transporter in the CEM_{3TC} cells. Since MRP5 has been demonstrated to transport similar substrates as MRP4 [21], we evaluated its mRNA expression, but found no difference in MRP5 expression in the CEM_{3TC} cells. However, recent studies [33] have determined that MRP4 and MRP5 homologues are found on chromosome 16q12. These homologous genes also lack an N-terminal domain that is found in the prototypical ABCC1 (i.e. MRP1). In the CEM_{3TC} cells, we found increases in ABCC11 mRNA expression (6-fold). However, in the absence of an antibody we are unable, at this time, to confirm if ABC11 protein is overexpressed. Nevertheless, it is possible that this transporter contributes to the efflux-mediated resistance to 3TC.

In conclusion, our reuslts are most consistent with the concept that 3TC resistance is mediated by an inability to adequately accumulate 3TC. This is not due to impaired 3TC phosphorylation or initial uptake. It is possible that increased ABCC11 expression decreases 3TC accumulation and increases cellular 3TC resistance. However, at the present time, we cannot directly confirm this possibility. The current studies support the idea that 3TC resistance may be due to ABC11 overexpression. However, we can not exclude the likelihood that a combination of increased MRP4 and ABCC11 underlie the 3TC resistance and impaired accumulation in these cells. This might be analogous to the overexpression and potential role of MRP1, MRP2 and ABCG2 in cells in resistance to the camptothecin class of cancer chemotherapeutic drugs [42]. Future studies will address the possibility of such interactions among ABCC11 and MRP4.

Supported by a grant from Ministero della Sanità-ISS (AIDS Project, grant no. 30C.5 to G.A.) and by a grant from National Institutes of Health GM 60904 (J.S.), P30 CA21765, and American Lebanese Syrian Associated Charities, ALSAC (J.S.).

REFERENCES

1 Gulick, R. M., Mellors, J. W., Havlir, D., Eron, J. J., Gonzalez, C., McMahon, D., Richman, D. D., Valentine, F. T., Jonas, L., Meibohm, A. et al. (1997) Treatment with indinavir, zidovudine, and lamivudine in adults with human immunodeficiency virus infection and prior antiretroviral therapy. N. Engl. J. Med. **337**, 734–739

2 Gulick, R. M., Mellors, J. W., Havlir, D., Eron, J. J., Gonzalez, C., McMahon, D., Jonas, L., Meibohm, A., Holder, D., Schleif, W. A. et al. (1998) Simultaneous vs sequential initiation of therapy with indinavir, zidovudine, and lamivudine for HIV-1 infection: 100-week follow-up. J. Am. Med. Assoc. JAMA **280**, 35–41

3 Cameron, D. W., Japour, A. J., Xu, Y., Hsu, A., Mellors, J., Farthing, C., Cohen, C., Poretz, D., Markowitz, M., Follansbee, S. et al. (1999) Ritonavir and saquinavir combination therapy for the treatment of HIV infection. AIDS (London) **13**, 213–224

4 Wong, J. K., Hezareh, M., Gunthard, H. F., Havlir, D. V., Ignacio, C. C., Spina, C. A. and Richman, D. D. (1997) Recovery of replication-competent HIV despite prolonged suppression of plasma viremia. Science **278**, 1291–1295

5 Finzi, D., Hermankova, M., Pierson, T., Carruth, L. M., Buck, C., Chaisson, R. E., Quinn, T. C., Chadwick, K., Margolick, J., Brookmeyer, R. et al. (1997) Identification of a reservoir for HIV-1 in patients on highly active antiretroviral therapy. Science **278**, 1295–1300

6 Zhang, L., Ramratnam, B., Tenner-Racz, K., He, Y., Vesanen, M., Lewin, S., Talal, A., Racz, P., Perelson, A. S., Korber, B. T. et al. (1999) Quantifying residual HIV-1 replication in patients receiving combination antiretroviral therapy. N. Engl. J. Med. **340**, 1605–1613

7 Gunthard, H. F., Wong, J. K., Ignacio, C. C., Guatelli, J. C., Riggs, N. L., Havlir, D. V. and Richman, D. D. (1998) Human immunodeficiency virus replication and genotypic resistance in blood and lymph nodes after a year of potent antiretroviral therapy. J. Virol. **72**, 2422–2428

8 O'Brien, W. A. (2000) Resistance against reverse transcriptase inhibitors. Clin. Infect. Dis. **30**, S185–S192

9 Martinez-Picado, J., De Pasquale, M. P., Kartsonis, N., Hanna, G. J., Wong, J., Finzi, D., Rosenberg, E., Gunthard, H. F., Sutton, L., Savara, A. et al. (2000) Antiretroviral resistance during successful therapy of HIV type 1 infection. Proc. Natl. Acad. Sci. U.S.A. **97**, 10948–10953

10 Di Gregorio, P., Iacobelli, S., Perrin, L. and Telenti, A. (1998) HIV treatment failure: testing for HIV resistance in clinical practice. Science **280**, 1871–1872

11 Durant, J., Clevenbergh, P., Halfon, P., Delgiudive, P., Porsin, S., Simonet, P., Montagne, N., Boucher, C. A., Schapiro, J. M. and Dellamonica, P. (1999) Drug-resistance genotyping in HIV-1 therapy: the VIRADAPT randomized controlled trial. Lancet **353**, 2195–2199

12 Dianzani, F., Antonelli, G., Turriziani, O., Riva, E., Simeoni, E., Signoretti, C., Strosselli, S. and Cianfriglia, M. (1994) Zidovudine induces the expression of cellular resistance affecting its antiviral activities. AIDS Res. Hum. Retroviruses **10**, 1471–1478

13 Groschel, B., Cinatl, J. and Cinatl, J. Jr (1997) Viral and cellular factors for resistance against antiretroviral agents. Intervirology **14**, 400–407

14 Fridland, A., Connelly, M. C. and Robbins, B. L. (2000) Cellular factors for resistance against antiretroviral agents. Antiviral Ther. **5**, 181–185

15 Turriziani, O., Antonelli, G. and Dianzani, F. (2000) Cellular factors involved in the induction of resistance of HIV to antiretroviral agents. Int. J. Antimicrob. Agents **16**, 353–356

16 Avramis, V. I., Kwock, R., Solorzano, M. M. and Gomperts, E. (1993) Evidence of *in vitro* development of drug resistance to azidothymidine in T-lymphotropic leukemia cell line (Jurkat E6–1/AZT-100) and in pediatric patients with HIV infection. J Acquired Immune Defic. Syndr. **6**, 1287–1296
17 Magnani, M., Brandi, G., Casabianca, A., Fraternale, A., Schiavano, F., Rossi, L. and Chiarantini, L. (1995) 2′,2′-Dideoxycytidine metabolism in a new drug-resistant cell line. Biochem. J. **312**, 115–123
18 Antonelli, G., Turriziani, O., Verri, A., Narciso, P., Ferri, F., D'Offizi, G. and Dianzani, F. (1996) Long-term exposure to zidovudine affects *in vitro* and *in vivo* the efficiency of phosphorylation of thymidine kinase. AIDS Res. Hum. Retroviruses **12**, 223–228
19 Robbins, B. L., Connelly, M. C., Marshall, D. R., Srinivas, R. V. and Friedland, A. (1995) A human T lymphoid cells variant resistant to the acyclic nucleoside phosphonate 9-(2-phosphonylmethoxyethyl)adenine shows a unique combination of a phosphorylation defect and increased efflux of the agent. Mol. Pharmacol. **47**, 391–397
20 Schuetz, J. D., Connelly, M. C., Sun, D., Paibir, S. G., Flynn, P. M., Srinivas, R. V., Kumar, A. and Fridland, A. (1999) MRP4: a previously unidentified factor in resistance to nucleoside-based antiviral drugs. Nat. Med. (N.Y.) **5**, 1048–1051
21 Wijnholds, J., Mol, C. A., van Deemter, L., de Haas, M., Scheffer, G. L., Baas, F., Beijen, J. H., Scheper, R. J., Hatse, S., De Clercq, E., Balzarini, J. and Borst, P. (2000) Multidrug-resistance protein 5 is a multispecific organic anion transporter able to transport nucleotide analogs. Proc. Natl. Acad. Sci. U.S.A. **97**, 7476–7481
22 Borst, P., Evers, R., Kool, M. and Wijnholds, J. (2000) A family of drug transporters: the multidrug resistance-associated proteins. J. Nat. Cancer Inst. **92**, 1295–1302
23 Denizot, F. and Lang, R. (1986) Rapid colorimetric assay for cell growth and survival. J. Immunol. Methods. **89**, 271–277
24 El-Osta, A., Kantharidis, P. and Zalcberg, J. (1999) Absolute quantitation of MDR1 transcripts using heterologous DNA standards-validation of the competitive RT-PCR (CRT-PCR) approach. BioTechniques **26**, 1114–1124
25 Adachi, M., Sampath, J., Lan, L. B., Sun, D., Hargrove, P., Flatley, R. M., Tatum, A., Ziegelmeier, M. Z., Wezeman, M., Matherly, L. H. et al. (2002) Expression of MRP4 confers resistance to ganciclovir and compromises bystander killing J. Biol. Chem., in the press
26 Lecureur, V., Sun, D., Hargrove, P., Schuetz, E. G., Kim, R. B., Lan, L. B. and Schuetz, J. D. (2000) Cloning and expression of murine sister of P-glycoprotein reveals a more discriminating transporter than MDR1/P-glycoprotein. Mol. Pharmacol. **57**, 24–35
27 Chang, C. N., Skalski, V., Zhou, J. H. and Cheng, Y. (1992) Biochemical Pharmacology of (+)- and (−)-2′,3′-dideoxy-3′-thiacytidine as anti-hepatitis B virus agents. J. Biol. Chem. **267**, 22414–22420
28 Verri, A., Focher, F., Priori, G., Gosselin, G., Imbach, J. L., Capobianco, M., Garbesi, A. and Spadari, S. (1997) Lack of enantiospecificity of human 2′-deoxycytidine kinase: relevance for the activation of beta-L-deoxycytidine analogs as antineoplastic and antiviral agents. Mol. Pharmacol. **51**, 132–138
29 Spadari, S., Maga, G., Verri, A. and Focher, F. (1998) Molecular basis for the antiviral and anticancer activities of unnatural L-β-nucleosides. Exp. Opin. Invest. Drugs **7**, 1285–1300
30 Fridland, A., Connelly, M. C. and Ashmun, R. (1990) Relationship of deoxynucleotide changes to inhibition of DNA synthesis induced by the antiretroviral agent 3′-azido-3′′-deoxythymidine and release of its monophosphate by human lymphoid cells (CCRF-CEM). Mol. Pharmacol. **37**, 665–670
31 Yao, S. Y., Ng, A. M., Sundaram, M., Cass, C. E., Baldwin, S. A. and Young, J. D. (2001) Transport of antiviral 3′-deoxy-nucleoside drugs by recombinant human and rat equilibrative, nitrobenzylthioinosine (NBMPR)-insensitive (ENT2) nucleoside transporter proteins produced in Xenopus oocytes. Mol. Membr. Biol. **18**, 161–167
32 Lostao, M. P., Mata, J. F., Larrayoz, I. M., Inzillo, S. M., Casado, F. J. and Pastor-Anglada, M. (2000) Electrogenic uptake of nucleosides and nucleoside-derived drugs by the human nucleoside transporter 1 (hCNT1) expressed in Xenopus laevis oocytes. FEBS Lett. **481**, 137–140
33 Tammur, J., Prades, C., Arnould, I., Rzhetsky, A., Hutchinson, A., Adachi, M., Schuetz, J. D., Swoboda, K. J., Ptacek, L. J., Rosier, M. et al. (2001) Two new genes from the human ATP-binding cassette transporter superfamily, ABCC11 and ABCC12, tandemly duplicated on chromosome 16q12. Gene **273**, 89–96
34 Yabuuchi, H., Shimizu, H., Takayanagi, S. and Ishikawa, T. (2001) Multiple splicing variants of two new human ATP-binding cassette transporters, ABCC11 and ABCC12. Biochem. Biophys. Res. Commun. **288**, 933–939
35 Srinivas, R. V., Connely, M. and Fridland, A. (1997) (S)-1-(3-hydroxy-2-phosphonylmethoxypropyl)cytosine (HPMPC) inhibits HIV-1replication in epithelial cells, but not T-lymphocytes. Antiviral Res. **35**, 23–27
36 Cass, C. E., Young, J. D., Baldwin, S. A., Cabrita, M. A., Graham, K. A., Griffiths, M., Jennings, L. L., Mackey, J. R., Ng, A. M., Ritzel, M. W. et al. (1999) Nucleoside transporters of mammalian cells. Pharm. Biotechnol. **12**, 313–352
37 Bradley, G., Juranka, P. F and Ling, V. (1998) Mechanism of multidrug resistance. Biochem. Biophys. Acta **948**, 87–128
38 Gottesman, M. M., Fojo, T. and Bates, S. E. (2002) Multidrug resistance in cancer: role of ATP-dependent transporters. Nat. Rev. Cancer **2**, 48–58
39 Gollapudi, S. and Gupta, S. (1990) Human immunodeficiency virus 1-induced expression of P-glycoprotein. Biochem. Biophys. Res. Commun. **171**, 1002–1007
40 Yusa, K., Oh Hara, T., Yamazaki, A., Tsukara, S., Satoh, W. and Tsuruo, T. (1990) Cross-resistance to anti-HIV nucleoside analogues in multidrug-resistance human cells. Biochem. Biophys. Res. Commun. **169**, 986–990
41 Antonelli, G., Turriziani, O., Cianfriglia, M., Riva, E., Dong, G., Fattorossi, A. and Dianzani, F. (1992) Resistance of HIV-1 to AZT might also involve the cellular expression of multidrug resistance P-glycoprotein. AIDS Res. Hum. Retroviruses **8**, 1839–1844
42 Litman, T., Brangi, M., Hudson, E., Fetsch, P., Abati, A., Ross, D. D., Miyake, K., Reseau, J. H. and Bates, S. E. (2000) The multidrug-resistant phenotype associated with overexpression of the new ABC half-transporter, MXR(ABCG2). J. Cell Sci. **113**, 2011–2021

Received 28 March 2002/26 June 2002; accepted 19 July 2002
Published as BJ Immediate Publication 19 July 2002, DOI 10.1042/BJ20020494

The Sequence of the Human Genome

J. Craig Venter,[1]* Mark D. Adams,[1] Eugene W. Myers,[1] Peter W. Li,[1] Richard J. Mural,[1] Granger G. Sutton,[1] Hamilton O. Smith,[1] Mark Yandell,[1] Cheryl A. Evans,[1] Robert A. Holt,[1] Jeannine D. Gocayne,[1] Peter Amanatides,[1] Richard M. Ballew,[1] Daniel H. Huson,[1] Jennifer Russo Wortman,[1] Qing Zhang,[1] Chinnappa D. Kodira,[1] Xiangqun H. Zheng,[1] Lin Chen,[1] Marian Skupski,[1] Gangadharan Subramanian,[1] Paul D. Thomas,[1] Jinghui Zhang,[1] George L. Gabor Miklos,[2] Catherine Nelson,[3] Samuel Broder,[1] Andrew G. Clark,[4] Joe Nadeau,[5] Victor A. McKusick,[6] Norton Zinder,[7] Arnold J. Levine,[7] Richard J. Roberts,[8] Mel Simon,[9] Carolyn Slayman,[10] Michael Hunkapiller,[11] Randall Bolanos,[1] Arthur Delcher,[1] Ian Dew,[1] Daniel Fasulo,[1] Michael Flanigan,[1] Liliana Florea,[1] Aaron Halpern,[1] Sridhar Hannenhalli,[1] Saul Kravitz,[1] Samuel Levy,[1] Clark Mobarry,[1] Knut Reinert,[1] Karin Remington,[1] Jane Abu-Threideh,[1] Ellen Beasley,[1] Kendra Biddick,[1] Vivien Bonazzi,[1] Rhonda Brandon,[1] Michele Cargill,[1] Ishwar Chandramouliswaran,[1] Rosane Charlab,[1] Kabir Chaturvedi,[1] Zuoming Deng,[1] Valentina Di Francesco,[1] Patrick Dunn,[1] Karen Eilbeck,[1] Carlos Evangelista,[1] Andrei E. Gabrielian,[1] Weiniu Gan,[1] Wangmao Ge,[1] Fangcheng Gong,[1] Zhiping Gu,[1] Ping Guan,[1] Thomas J. Heiman,[1] Maureen E. Higgins,[1] Rui-Ru Ji,[1] Zhaoxi Ke,[1] Karen A. Ketchum,[1] Zhongwu Lai,[1] Yiding Lei,[1] Zhenya Li,[1] Jiayin Li,[1] Yong Liang,[1] Xiaoying Lin,[1] Fu Lu,[1] Gennady V. Merkulov,[1] Natalia Milshina,[1] Helen M. Moore,[1] Ashwinikumar K Naik,[1] Vaibhav A. Narayan,[1] Beena Neelam,[1] Deborah Nusskern,[1] Douglas B. Rusch,[1] Steven Salzberg,[12] Wei Shao,[1] Bixiong Shue,[1] Jingtao Sun,[1] Zhen Yuan Wang,[1] Aihui Wang,[1] Xin Wang,[1] Jian Wang,[1] Ming-Hui Wei,[1] Ron Wides,[13] Chunlin Xiao,[1] Chunhua Yan,[1] Alison Yao,[1] Jane Ye,[1] Ming Zhan,[1] Weiqing Zhang,[1] Hongyu Zhang,[1] Qi Zhao,[1] Liansheng Zheng,[1] Fei Zhong,[1] Wenyan Zhong,[1] Shiaoping C. Zhu,[1] Shaying Zhao,[12] Dennis Gilbert,[1] Suzanna Baumhueter,[1] Gene Spier,[1] Christine Carter,[1] Anibal Cravchik,[1] Trevor Woodage,[1] Feroze Ali,[1] Huijin An,[1] Aderonke Awe,[1] Danita Baldwin,[1] Holly Baden,[1] Mary Barnstead,[1] Ian Barrow,[1] Karen Beeson,[1] Dana Busam,[1] Amy Carver,[1] Angela Center,[1] Ming Lai Cheng,[1] Liz Curry,[1] Steve Danaher,[1] Lionel Davenport,[1] Raymond Desilets,[1] Susanne Dietz,[1] Kristina Dodson,[1] Lisa Doup,[1] Steven Ferriera,[1] Neha Garg,[1] Andres Gluecksmann,[1] Brit Hart,[1] Jason Haynes,[1] Charles Haynes,[1] Cheryl Heiner,[1] Suzanne Hladun,[1] Damon Hostin,[1] Jarrett Houck,[1] Timothy Howland,[1] Chinyere Ibegwam,[1] Jeffery Johnson,[1] Francis Kalush,[1] Lesley Kline,[1] Shashi Koduru,[1] Amy Love,[1] Felecia Mann,[1] David May,[1] Steven McCawley,[1] Tina McIntosh,[1] Ivy McMullen,[1] Mee Moy,[1] Linda Moy,[1] Brian Murphy,[1] Keith Nelson,[1] Cynthia Pfannkoch,[1] Eric Pratts,[1] Vinita Puri,[1] Hina Qureshi,[1] Matthew Reardon,[1] Robert Rodriguez,[1] Yu-Hui Rogers,[1] Deanna Romblad,[1] Bob Ruhfel,[1] Richard Scott,[1] Cynthia Sitter,[1] Michelle Smallwood,[1] Erin Stewart,[1] Renee Strong,[1] Ellen Suh,[1] Reginald Thomas,[1] Ni Ni Tint,[1] Sukyee Tse,[1] Claire Vech,[1] Gary Wang,[1] Jeremy Wetter,[1] Sherita Williams,[1] Monica Williams,[1] Sandra Windsor,[1] Emily Winn-Deen,[1] Keriellen Wolfe,[1] Jayshree Zaveri,[1] Karena Zaveri,[1] Josep F. Abril,[14] Roderic Guigó,[14] Michael J. Campbell,[1] Kimmen V. Sjolander,[1] Brian Karlak,[1] Anish Kejariwal,[1] Huaiyu Mi,[1] Betty Lazareva,[1] Thomas Hatton,[1] Apurva Narechania,[1] Karen Diemer,[1] Anushya Muruganujan,[1] Nan Guo,[1] Shinji Sato,[1] Vineet Bafna,[1] Sorin Istrail,[1] Ross Lippert,[1] Russell Schwartz,[1] Brian Walenz,[1] Shibu Yooseph,[1] David Allen,[1] Anand Basu,[1] James Baxendale,[1] Louis Blick,[1] Marcelo Caminha,[1] John Carnes-Stine,[1] Parris Caulk,[1] Yen-Hui Chiang,[1] My Coyne,[1] Carl Dahlke,[1] Anne Deslattes Mays,[1] Maria Dombroski,[1] Michael Donnelly,[1] Dale Ely,[1] Shiva Esparham,[1] Carl Fosler,[1] Harold Gire,[1] Stephen Glanowski,[1] Kenneth Glasser,[1] Anna Glodek,[1] Mark Gorokhov,[1] Ken Graham,[1] Barry Gropman,[1] Michael Harris,[1] Jeremy Heil,[1] Scott Henderson,[1] Jeffrey Hoover,[1] Donald Jennings,[1] Catherine Jordan,[1] James Jordan,[1] John Kasha,[1] Leonid Kagan,[1] Cheryl Kraft,[1] Alexander Levitsky,[1] Mark Lewis,[1] Xiangjun Liu,[1] John Lopez,[1] Daniel Ma,[1] William Majoros,[1] Joe McDaniel,[1] Sean Murphy,[1] Matthew Newman,[1] Trung Nguyen,[1] Ngoc Nguyen,[1] Marc Nodell,[1] Sue Pan,[1] Jim Peck,[1] Marshall Peterson,[1] William Rowe,[1] Robert Sanders,[1] John Scott,[1] Michael Simpson,[1] Thomas Smith,[1] Arlan Sprague,[1] Timothy Stockwell,[1] Russell Turner,[1] Eli Venter,[1] Mei Wang,[1] Meiyuan Wen,[1] David Wu,[1] Mitchell Wu,[1] Ashley Xia,[1] Ali Zandieh,[1] Xiaohong Zhu[1]

A 2.91-billion base pair (bp) consensus sequence of the euchromatic portion of the human genome was generated by the whole-genome shotgun sequencing method. The 14.8-billion bp DNA sequence was generated over 9 months from 27,271,853 high-quality sequence reads (5.11-fold coverage of the genome) from both ends of plasmid clones made from the DNA of five individuals. Two assembly strategies—a whole-genome assembly and a regional chromosome assembly—were used, each combining sequence data from Celera and the publicly funded genome effort. The public data were shredded into 550-bp segments to create a 2.9-fold coverage of those genome regions that had been sequenced, without including biases inherent in the cloning and assembly procedure used by the publicly funded group. This brought the effective coverage in the assemblies to eightfold, reducing the number and size of gaps in the final assembly over what would be obtained with 5.11-fold coverage. The two assembly strategies yielded very similar results that largely agree with independent mapping data. The assemblies effectively cover the euchromatic regions of the human chromosomes. More than 90% of the genome is in scaffold assemblies of 100,000 bp or more, and 25% of the genome is in scaffolds of 10 million bp or larger. Analysis of the genome sequence revealed 26,588 protein-encoding transcripts for which there was strong corroborating evidence and an additional ~12,000 computationally derived genes with mouse matches or other weak supporting evidence. Although gene-dense clusters are obvious, almost half the genes are dispersed in low G+C sequence separated by large tracts of apparently noncoding sequence. Only 1.1% of the genome is spanned by exons, whereas 24% is in introns, with 75% of the genome being intergenic DNA. Duplications of segmental blocks, ranging in size up to chromosomal lengths, are abundant throughout the genome and reveal a complex evolutionary history. Comparative genomic analysis indicates vertebrate expansions of genes associated with neuronal function, with tissue-specific developmental regulation, and with the hemostasis and immune systems. DNA sequence comparisons between the consensus sequence and publicly funded genome data provided locations of 2.1 million single-nucleotide polymorphisms (SNPs). A random pair of human haploid genomes differed at a rate of 1 bp per 1250 on average, but there was marked heterogeneity in the level of polymorphism across the genome. Less than 1% of all SNPs resulted in variation in proteins, but the task of determining which SNPs have functional consequences remains an open challenge.

Decoding of the DNA that constitutes the human genome has been widely anticipated for the contribution it will make toward understanding human evolution, the causation of disease, and the interplay between the environment and heredity in defining the human condition. A project with the goal of determining the complete nucleotide sequence of the human genome was first formally proposed in 1985 (*1*). In subsequent years, the idea met with mixed reactions in the scientific community (*2*). However, in 1990, the Human Genome Project (HGP) was officially initiated in the United States under the direction of the National Institutes of Health and the U.S. Department of Energy with a 15-year, $3 billion plan for completing the genome sequence. In 1998 we announced our intention to build a unique genome-sequencing facility, to determine the sequence of the human genome over a 3-year period. Here we report the penultimate milestone along the path toward that goal, a nearly complete sequence of the euchromatic portion of the human genome. The sequencing was performed by a whole-genome random shotgun method with subsequent assembly of the sequenced segments.

The modern history of DNA sequencing began in 1977, when Sanger reported his method for determining the order of nucleotides of DNA using chain-terminating nucleotide analogs (*3*). In the same year, the first human gene was isolated and sequenced (*4*). In 1986, Hood and co-workers (*5*) described an improvement in the Sanger sequencing method that included attaching fluorescent dyes to the nucleotides, which permitted them to be sequentially read by a computer. The first automated DNA sequencer, developed by Applied Biosystems in California in 1987, was shown to be successful when the sequences of two genes were obtained with this new technology (*6*). From early sequencing of human genomic regions (*7*), it became clear that cDNA sequences (which are reverse-transcribed from RNA) would be essential to annotate and validate gene predictions in the human genome. These studies were the basis in part for the development of the expressed sequence tag (EST) method of gene identification (*8*), which is a random selection, very high throughput sequencing approach to characterize cDNA libraries. The EST method led to the rapid discovery and mapping of human genes (*9*). The increasing numbers of human EST sequences necessitated the development of new computer algorithms to analyze large amounts of sequence data, and in 1993 at The Institute for Genomic Research (TIGR), an algorithm was developed that permitted assembly and analysis of hundreds of thousands of ESTs. This algorithm permitted characterization and annotation of human genes on the basis of 30,000 EST assemblies (*10*).

The complete 49-kbp bacteriophage lambda genome sequence was determined by a shotgun restriction digest method in 1982 (*11*). When considering methods for sequencing the smallpox virus genome in 1991 (*12*), a whole-genome shotgun sequencing method was discussed and subsequently rejected owing to the lack of appropriate software tools for genome assembly. However, in 1994, when a microbial genome-sequencing project was contemplated at TIGR, a whole-genome shotgun sequencing approach was considered possible with the TIGR EST assembly algorithm. In 1995, the 1.8-Mbp *Haemophilus influenzae* genome was completed by a whole-genome shotgun sequencing method (*13*). The experience with several subsequent genome-sequencing efforts established the broad applicability of this approach (*14*, *15*).

A key feature of the sequencing approach used for these megabase-size and larger genomes was the use of paired-end sequences (also called mate pairs), derived from subclone libraries with distinct insert sizes and cloning characteristics. Paired-end sequences are sequences 500 to 600 bp in length from both ends of double-stranded DNA clones of prescribed lengths. The success of using end sequences from long segments (18 to 20 kbp) of DNA cloned into bacteriophage lambda in assembly of the microbial genomes led to the suggestion (*16*) of an approach to simulta-

[1]Celera Genomics, 45 West Gude Drive, Rockville, MD 20850, USA. [2]GenetixXpress, 78 Pacific Road, Palm Beach, Sydney 2108, Australia. [3]Berkeley *Drosophila* Genome Project; University of California, Berkeley, CA 94720, USA. [4]Department of Biology, Penn State University, 208 Mueller Lab, University Park, PA 16802, USA. [5]Department of Genetics, Case Western Reserve University School of Medicine, BRB-630, 10900 Euclid Avenue, Cleveland, OH 44106, USA. [6]Johns Hopkins University School of Medicine, Johns Hopkins Hospital, 600 North Wolfe Street, Blalock 1007, Baltimore, MD 21287–4922, USA. [7]Rockefeller University, 1230 York Avenue, New York, NY 10021–6399, USA. [8]New England BioLabs, 32 Tozer Road, Beverly, MA 01915, USA. [9]Division of Biology, 147-75, California Institute of Technology, 1200 East California Boulevard, Pasadena, CA 91125, USA. [10]Yale University School of Medicine, 333 Cedar Street, P.O. Box 208000, New Haven, CT 06520–8000, USA. [11]Applied Biosystems, 850 Lincoln Centre Drive, Foster City, CA 94404, USA. [12]The Institute for Genomic Research, 9712 Medical Center Drive, Rockville, MD 20850, USA. [13]Faculty of Life Sciences, Bar-Ilan University, Ramat-Gan, 52900 Israel. [14]Grup de Recerca en Informàtica Mèdica, Institut Municipal d'Investigació Mèdica, Universitat Pompeu Fabra, 08003-Barcelona, Catalonia, Spain.

*To whom correspondence should be addressed. E-mail: humangenome@celera.com

neously map and sequence the human genome by means of end sequences from 150-kbp bacterial artificial chromosomes (BACs) (*17*, *18*). The end sequences spanned by known distances provide long-range continuity across the genome. A modification of the BAC end-sequencing (BES) method was applied successfully to complete chromosome 2 from the *Arabidopsis thaliana* genome (*19*).

In 1997, Weber and Myers (*20*) proposed whole-genome shotgun sequencing of the human genome. Their proposal was not well received (*21*). However, by early 1998, as less than 5% of the genome had been sequenced, it was clear that the rate of progress in human genome sequencing worldwide was very slow (*22*), and the prospects for finishing the genome by the 2005 goal were uncertain.

In early 1998, PE Biosystems (now Applied Biosystems) developed an automated, high-throughput capillary DNA sequencer, subsequently called the ABI PRISM 3700 DNA Analyzer. Discussions between PE Biosystems and TIGR scientists resulted in a plan to undertake the sequencing of the human genome with the 3700 DNA Analyzer and the whole-genome shotgun sequencing techniques developed at TIGR (*23*). Many of the principles of operation of a genome-sequencing facility were established in the TIGR facility (*24*). However, the facility envisioned for Celera would have a capacity roughly 50 times that of TIGR, and thus new developments were required for sample preparation and tracking and for whole-genome assembly. Some argued that the required 150-fold scale-up from the *H. influenzae* genome to the human genome with its complex repeat sequences was not feasible (*25*). The *Drosophila melanogaster* genome was thus chosen as a test case for whole-genome assembly on a large and complex eukaryotic genome. In collaboration with Gerald Rubin and the Berkeley *Drosophila* Genome Project, the nucleotide sequence of the 120-Mbp euchromatic portion of the *Drosophila* genome was determined over a 1-year period (*26*–*28*). The *Drosophila* genome-sequencing effort resulted in two key findings: (i) that the assembly algorithms could generate chromosome assemblies with highly accurate order and orientation with substantially less than 10-fold coverage, and (ii) that undertaking multiple interim assemblies in place of one comprehensive final assembly was not of value.

These findings, together with the dramatic changes in the public genome effort subsequent to the formation of Celera (*29*), led to a modified whole-genome shotgun sequencing approach to the human genome. We initially proposed to do 10-fold sequence coverage of the genome over a 3-year period and to make interim assembled sequence data available quarterly. The modifications included a plan to perform random shotgun sequencing to ~5-fold coverage and to use the unordered and unoriented BAC sequence fragments and subassemblies published in GenBank by the publicly funded genome effort (*30*) to accelerate the project. We also abandoned the quarterly announcements in the absence of interim assemblies to report.

Although this strategy provided a reasonable result very early that was consistent with a whole-genome shotgun assembly with eight-fold coverage, the human genome sequence is not as finished as the *Drosophila* genome was with an effective 13-fold coverage. However, it became clear that even with this reduced coverage strategy, Celera could generate an accurately ordered and oriented scaffold sequence of the human genome in less than 1 year. Human genome sequencing was initiated 8 September 1999 and completed 17 June 2000. The first assembly was completed 25 June 2000, and the assembly reported here was completed 1 October 2000. Here we describe the whole-genome random shotgun sequencing effort applied to the human genome. We developed two different assembly approaches for assembling the ~3 billion bp that make up the 23 pairs of chromosomes of the *Homo sapiens* genome. Any GenBank-derived data were shredded to remove potential bias to the final sequence from chimeric clones, foreign DNA contamination, or misassembled contigs. Insofar as a correctly and accurately assembled genome sequence with faithful order and orientation of contigs is essential for an accurate analysis of the human genetic code, we have devoted a considerable portion of this manuscript to the documentation of the quality of our reconstruction of the genome. We also describe our preliminary analysis of the human genetic code on the basis of computational methods. Figure 1 (see fold-out chart associated with this issue; files for each chromosome can be found in Web fig. 1 on *Science* Online at www.sciencemag.org/cgi/content/full/291/5507/1304/DC1) provides a graphical overview of the genome and the features encoded in it. The detailed manual curation and interpretation of the genome are just beginning.

To aid the reader in locating specific analytical sections, we have divided the paper into seven broad sections. A summary of the major results appears at the beginning of each section.

1 Sources of DNA and Sequencing Methods

Summary. This section discusses the rationale and ethical rules governing donor selection to ensure ethnic and gender diversity along with the methodologies for DNA extraction and library construction. The plasmid library construction is the first critical step in shotgun sequencing. If the DNA libraries are not uniform in size, nonchimeric, and do not randomly represent the genome, then the subsequent steps cannot accurately reconstruct the genome sequence. We used automated high-throughput DNA sequencing and the computational infrastructure to enable efficient tracking of enormous amounts of sequence information (27.3 million sequence reads; 14.9 billion bp of sequence). Sequencing and tracking from both ends of plasmid clones from 2-, 10-, and 50-kbp libraries were essential to the computational reconstruction of the genome. Our evidence indicates that the accurate pairing rate of end sequences was greater than 98%.

Various policies of the United States and the World Medical Association, specifically the Declaration of Helsinki, offer recommendations for conducting experiments with human subjects. We convened an Institutional Review Board (IRB) (*31*) that helped us establish the protocol for obtaining and using human DNA and the informed consent process used to enroll research volunteers for the DNA-sequencing studies reported here. We adopted several steps and procedures to protect the privacy rights and confidentiality of the research subjects (donors). These included a two-stage consent process, a secure random alphanumeric coding system for specimens and records, circumscribed contact with the subjects by researchers, and options for off-site contact of donors. In addition, Celera applied for and received a Certificate of Confidentiality from the Department of Health and Human Services. This Certificate authorized Celera to protect the privacy of the individuals who volunteered to be donors as provided in Section 301(d) of the Public Health Service Act 42 U.S.C. 241(d).

Celera and the IRB believed that the initial version of a completed human genome should be a composite derived from multiple donors of diverse ethnic backgrounds Prospective donors were asked, on a voluntary basis, to self-designate an ethnogeographic category (e.g., African-American, Chinese, Hispanic, Caucasian, etc.). We enrolled 21 donors (*32*).

Three basic items of information from each donor were recorded and linked by confidential code to the donated sample: age, sex, and self-designated ethnogeographic group. From females, ~130 ml of whole, heparinized blood was collected. From males, ~130 ml of whole, heparinized blood was

collected, as well as five specimens of semen, collected over a 6-week period. Permanent lymphoblastoid cell lines were created by Epstein-Barr virus immortalization. DNA from five subjects was selected for genomic DNA sequencing: two males and three females—one African-American, one Asian-Chinese, one Hispanic-Mexican, and two Caucasians (see Web fig. 2 on *Science* Online at www.sciencemag.org/cgi/content/291/5507/1304/DC1). The decision of whose DNA to sequence was based on a complex mix of factors, including the goal of achieving diversity as well as technical issues such as the quality of the DNA libraries and availability of immortalized cell lines.

1.1 Library construction and sequencing

Central to the whole-genome shotgun sequencing process is preparation of high-quality plasmid libraries in a variety of insert sizes so that pairs of sequence reads (mates) are obtained, one read from both ends of each plasmid insert. High-quality libraries have an equal representation of all parts of the genome, a small number of clones without inserts, and no contamination from such sources as the mitochondrial genome and *Escherichia coli* genomic DNA. DNA from each donor was used to construct plasmid libraries in one or more of three size classes: 2 kbp, 10 kbp, and 50 kbp (Table 1) (*33*).

In designing the DNA-sequencing process, we focused on developing a simple system that could be implemented in a robust and reproducible manner and monitored effectively (Fig. 2) (*34*).

Current sequencing protocols are based on the dideoxy sequencing method (*35*), which typically yields only 500 to 750 bp of sequence per reaction. This limitation on read length has made monumental gains in throughput a prerequisite for the analysis of large eukaryotic genomes. We accomplished this at the Celera facility, which occupies about 30,000 square feet of laboratory space and produces sequence data continuously at a rate of 175,000 total reads per day. The DNA-sequencing facility is supported by a high-performance computational facility (*36*).

The process for DNA sequencing was modular by design and automated. Intermodule sample backlogs allowed four principal modules to operate independently: (i) library transformation, plating, and colony picking; (ii) DNA template preparation; (iii) dideoxy sequencing reaction set-up and purification; and (iv) sequence determination with the ABI PRISM 3700 DNA Analyzer. Because the inputs and outputs of each module have been carefully matched and sample backlogs are continuously managed, sequencing has proceeded without a single day's interruption since the initiation of the *Drosophila* project in May 1999. The ABI 3700 is a fully automated capillary array sequencer and as such can be operated with a minimal amount of hands-on time, currently estimated at about 15 min per day. The capillary system also facilitates correct associations of sequencing traces with samples through the elimination of manual sample loading and lane-tracking errors associated with slab gels. About 65 production staff were hired and trained, and were rotated on a regular basis through the four production modules. A central laboratory information management system (LIMS) tracked all sample plates by unique bar code identifiers. The facility was supported by a quality control team that performed raw material and in-process testing and a quality assurance group with responsibilities including document control, validation, and auditing of the facility. Critical to the success of the scale-up was the validation of all software and instrumentation before implementation, and production-scale testing of any process changes.

1.2 Trace processing

An automated trace-processing pipeline has been developed to process each sequence file (*37*). After quality and vector trimming, the average trimmed sequence length was 543 bp, and the sequencing accuracy was exponentially distributed with a mean of 99.5% and with less than 1 in 1000 reads being less than 98% accurate (*26*). Each trimmed sequence was screened for matches to contaminants including sequences of vector alone, *E. coli* genomic DNA, and human mitochondrial DNA. The entire read for any sequence with a significant match to a contaminant was discarded. A total of 713 reads matched *E. coli* genomic DNA and 2114 reads matched the human mitochondrial genome.

1.3 Quality assessment and control

The importance of the base-pair level accuracy of the sequence data increases as the size and repetitive nature of the genome to be sequenced increases. Each sequence read must be placed uniquely in the ge-

Table 1. Celera-generated data input into assembly.

	Individual	Number of reads for different insert libraries				Total number of base pairs
		2 kbp	10 kbp	50 kbp	Total	
No. of sequencing reads	A	0	0	2,767,357	2,767,357	1,502,674,851
	B	11,736,757	7,467,755	66,930	19,271,442	10,464,393,006
	C	853,819	881,290	0	1,735,109	942,164,187
	D	952,523	1,046,815	0	1,999,338	1,085,640,534
	F	0	1,498,607	0	1,498,607	813,743,601
	Total	13,543,099	10,894,467	2,834,287	27,271,853	14,808,616,179
Fold sequence coverage (2.9-Gb genome)	A	0	0	0.52	0.52	
	B	2.20	1.40	0.01	3.61	
	C	0.16	1.17	0	0.32	
	D	0.18	0.20	0	0.37	
	F	0	0.28	0	0.28	
	Total	2.54	2.04	0.53	5.11	
Fold clone coverage	A	0	0	18.39	18.39	
	B	2.96	11.26	0.44	14.67	
	C	0.22	1.33	0	1.54	
	D	0.24	1.58	0	1.82	
	F	0	2.26	0	2.26	
	Total	3.42	16.43	18.84	38.68	
Insert size* (mean)	Average	1,951 bp	10,800 bp	50,715 bp		
Insert size* (SD)	Average	6.10%	8.10%	14.90%		
% Mates†	Average	74.50	80.80	75.60		

*Insert size and SD are calculated from assembly of mates on contigs. †% Mates is based on laboratory tracking of sequencing runs.

nome, and even a modest error rate can reduce the effectiveness of assembly. In addition, maintaining the validity of mate-pair information is absolutely critical for the algorithms described below. Procedural controls were established for maintaining the validity of sequence mate-pairs as sequencing reactions proceeded through the process, including strict rules built into the LIMS. The accuracy of sequence data produced by the Celera process was validated in the course of the *Drosophila* genome project (*26*). By collecting data for the entire human genome in a single facility, we were able to ensure uniform quality standards and the cost advantages associated with automation, an economy of scale, and process consistency.

2 Genome Assembly Strategy and Characterization

Summary. We describe in this section the two approaches that we used to assemble the genome. One method involves the computational combination of all sequence reads with shredded data from GenBank to generate an independent, nonbiased view of the genome. The second approach involves clustering all of the fragments to a region or chromosome on the basis of mapping information. The clustered data were then shredded and subjected to computational assembly. Both approaches provided essentially the same reconstruction of assembled DNA sequence with proper order and orientation. The second method provided slightly greater sequence coverage (fewer gaps) and was the principal sequence used for the analysis phase. In addition, we document the completeness and correctness of this assembly process

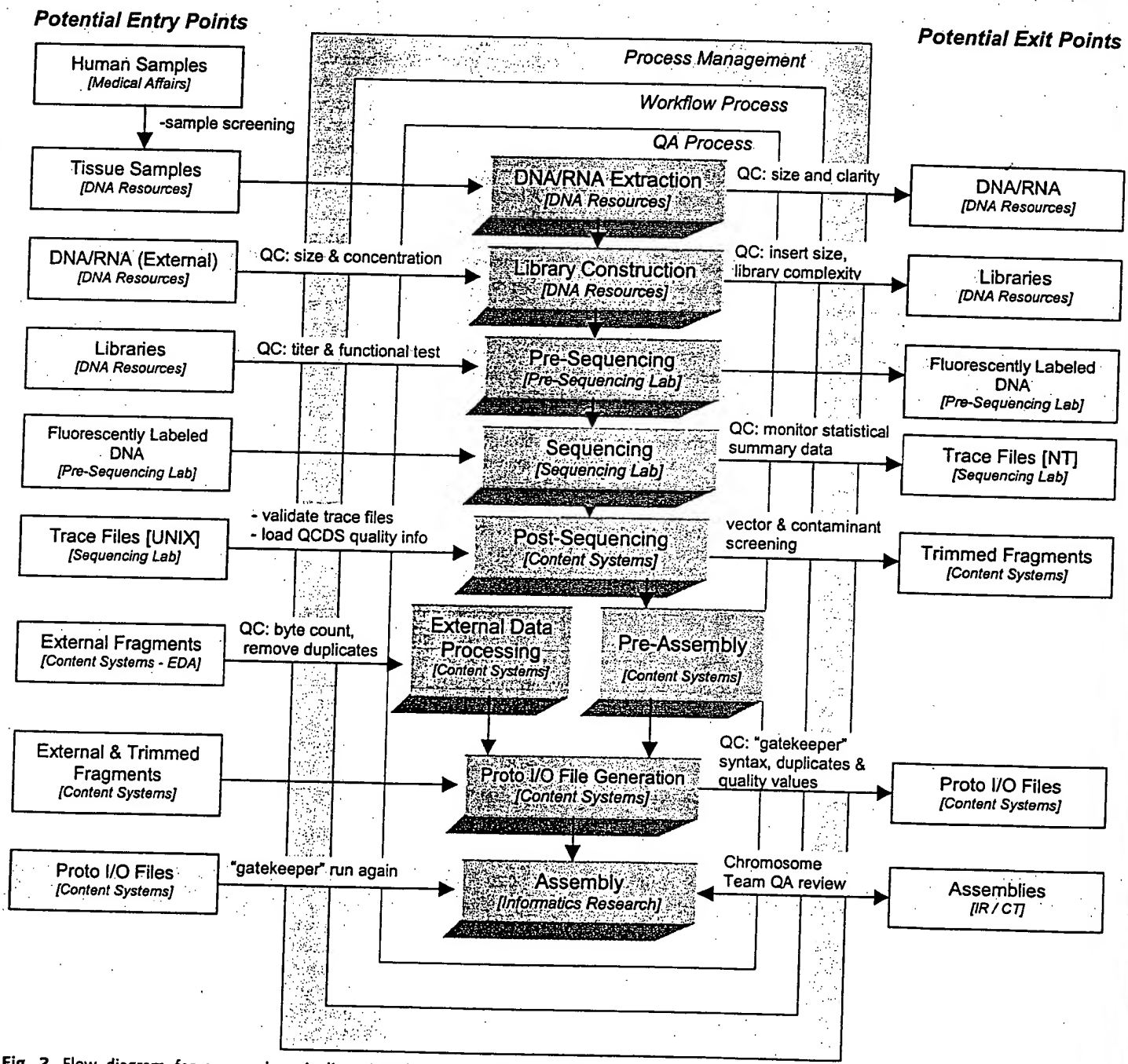

Fig. 2. Flow diagram for sequencing pipeline. Samples are received, selected, and processed in compliance with standard operating procedures, with a focus on quality within and across departments. Each process has defined inputs and outputs with the capability to exchange samples and data with both internal and external entities according to defined quality guidelines. Manufacturing pipeline processes, products, quality control measures, and responsible parties are indicated and are described further in the text.

and provide a comparison to the public genome sequence, which was reconstructed largely by an independent BAC-by-BAC approach. Our assemblies effectively covered the euchromatic regions of the human chromosomes. More than 90% of the genome was in scaffold assemblies of 100,000 bp or greater, and 25% of the genome was in scaffolds of 10 million bp or larger.

Shotgun sequence assembly is a classic example of an inverse problem: given a set of reads randomly sampled from a target sequence, reconstruct the order and the position of those reads in the target. Genome assembly algorithms developed for *Drosophila* have now been extended to assemble the ~25-fold larger human genome. Celera assemblies consist of a set of contigs that are ordered and oriented into scaffolds that are then mapped to chromosomal locations by using known markers. The contigs consist of a collection of overlapping sequence reads that provide a consensus reconstruction for a contiguous interval of the genome. Mate pairs are a central component of the assembly strategy. They are used to produce scaffolds in which the size of gaps between consecutive contigs is known with reasonable precision. This is accomplished by observing that a pair of reads, one of which is in one contig, and the other of which is in another, implies an orientation and distance between the two contigs (Fig. 3). Finally, our assemblies did not incorporate all reads into the final set of reported scaffolds. This set of unincorporated reads is termed "chaff," and typically consisted of reads from within highly repetitive regions, data from other organisms introduced through various routes as found in many genome projects, and data of poor quality or with untrimmed vector.

2.1 Assembly data sets

We used two independent sets of data for our assemblies. The first was a random shotgun data set of 27.27 million reads of average length 543 bp produced at Celera. This consisted largely of mate-pair reads from 16 libraries constructed from DNA samples taken from five different donors. Libraries with insert sizes of 2, 10, and 50 kbp were used. By looking at how mate pairs from a library were positioned in known sequenced stretches of the genome, we were able to characterize the range of insert sizes in each library and determine a mean and standard deviation. Table 1 details the number of reads, sequencing coverage, and clone coverage achieved by the data set. The clone coverage is the coverage of the genome in cloned DNA, considering the entire insert of each clone that has sequence from both ends. The clone coverage provides a measure of the amount of physical DNA coverage of the genome. Assuming a genome size of 2.9 Gbp, the Celera trimmed sequences gave a 5.1× coverage of the genome, and clone coverage was 3.42×, 16.40×, and 18.84× for the 2-, 10-, and 50-kbp libraries, respectively, for a total of 38.7× clone coverage.

The second data set was from the publicly funded Human Genome Project (PFP) and is primarily derived from BAC clones (*30*). The BAC data input to the assemblies came from a download of GenBank on 1 September 2000 (Table 2) totaling 4443.3 Mbp of sequence. The data for each BAC is deposited at one of four levels of completion. Phase 0 data are a set of generally unassembled sequencing reads from a very light shotgun of the BAC, typically less than 1×. Phase 1 data are unordered assemblies of contigs, which we call BAC contigs or bactigs. Phase 2 data are ordered assemblies of bactigs. Phase 3 data are complete BAC sequences. In the past 2 years the PFP has focused on a product of lower quality and completeness, but on a faster time-course, by concentrating on the production of Phase 1 data from a 3× to 4× light-shotgun of each BAC clone.

We screened the bactig sequences for contaminants by using the BLAST algorithm against three data sets: (i) vector sequences in Univec core (*38*), filtered for a 25-bp match at 98% sequence identity at the ends of the sequence and a 30-bp match internal to the sequence; (ii) the nonhuman portion of the High Throughput Genomic (HTG) Seqences division of GenBank (*39*), filtered at 200 bp at 98%; and (iii) the nonredundant nucleotide sequences from GenBank without primate and human virus entries, filtered at 200 bp at 98%. Whenever 25 bp or more of vector was found within 50 bp of the end of a contig, the tip up to the matching vector was excised. Under these criteria we removed 2.6 Mbp of possible contaminant and vector from the Phase 3 data, 61.0 Mbp from the Phase 1 and 2 data, and 16.1 Mbp from the Phase 0 data (Table 2). This left us with a total of 4363.7 Mbp of PFP sequence data 20% finished, 75% rough-draft (Phase 1 and 2), and 5% single sequencing reads (Phase 0). An additional 104,018 BAC end-sequence mate pairs were also downloaded and included in the data sets for both assembly processes (*18*).

2.2 Assembly strategies

Two different approaches to assembly were pursued. The first was a whole-genome assembly process that used Celera data and the PFP data in the form of additional synthetic shotgun data, and the second was a compartmentalized assembly process that first partitioned the Celera and PFP data into sets localized to large chromosomal segments and then performed ab initio shotgun assembly on each set. Figure 4 gives a schematic of the overall process flow.

For the whole-genome assembly, the PFP data was first disassembled or "shredded" into a synthetic shotgun data set of 550-bp reads that form a perfect 2× covering of the bactigs. This resulted in 16.05 million "faux" reads that were sufficient to cover the genome 2.96× because of redundancy in the BAC data set, without incorporating the biases inherent in the PFP assembly process. The combined data set of 43.32 million reads (8×), and all associated mate-pair information, were then subjected to our whole-genome assembly algorithm to produce a reconstruction of the genome. Neither the location of a BAC in the genome nor its assembly of bactigs was used in this process. Bactigs were shredded into reads because we found strong evidence that 2.13% of them were misassembled (*40*). Furthermore, BAC location

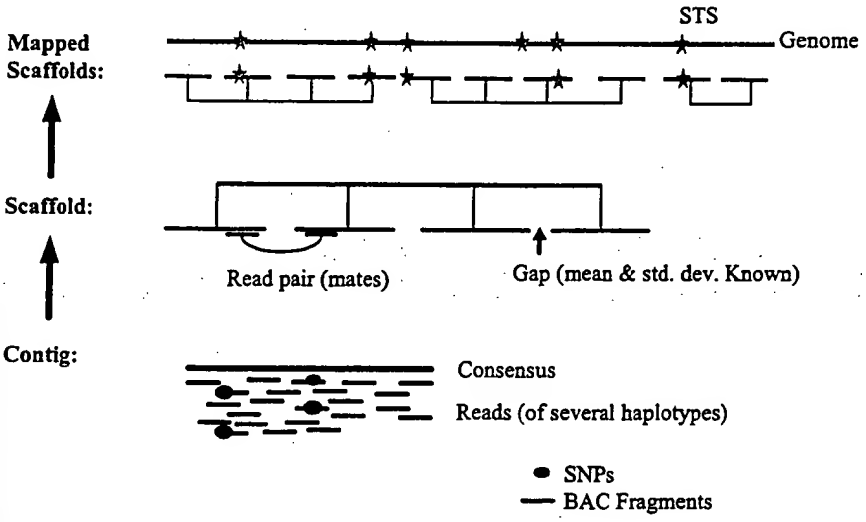

Fig. 3. Anatomy of whole-genome assembly. Overlapping shredded bactig fragments (red lines) and internally derived reads from five different individuals (black lines) are combined to produce a contig and a consensus sequence (green line). Contigs are connected into scaffolds (red) by using mate pair information. Scaffolds are then mapped to the genome (gray line) with STS (blue star) physical map information.

information was ignored because some BACs were not correctly placed on the PFP physical map and because we found strong evidence that at least 2.2% of the BACs contained sequence data that were not part of the given BAC (*41*), possibly as a result of sample-tracking errors (see below). In short, we performed a true, ab initio whole-genome assembly in which we took the expedient of deriving additional sequence coverage, but not mate pairs, assembled bactigs, or genome locality, from some externally generated data.

Table 2. GenBank data input into assembly.

Center	Statistics	Completion phase sequence		
		0	1 and 2	3
Whitehead Institute/ MIT Center for Genome Research, USA	Number of accession records	2,825	6,533	363
	Number of contigs	243,786	138,023	363
	Total base pairs	194,490,158	1,083,848,245	48,829,358
	Total vector masked (bp)	1,553,597	875,618	2,202
	Total contaminant masked (bp)	13,654,482	4,417,055	98,028
	Average contig length (bp)	798	7,853	134,516
Washington University, USA	Number of accession records	19	3,232	1,300
	Number of contigs	2,127	61,812	1,300
	Total base pairs	1,195,732	561,171,788	164,214,395
	Total vector masked (bp)	21,604	270,942	8,287
	Total contaminant masked (bp)	22,469	1,476,141	469,487
	Average contig length (bp)	562	9,079	126,319
Baylor College of Medicine, USA	Number of accession records	0	1,626	363
	Number of contigs	0	44,861	363
	Total base pairs	0	265,547,066	49,017,104
	Total vector masked (bp)	0	218,769	4,960
	Total contaminant masked (bp)	0	1,784,700	485,137
	Average contig length (bp)	0	5,919	135,033
Production Sequencing Facility, DOE Joint Genome Institute, USA	Number of accession records	135	2,043	754
	Number of contigs	7,052	34,938	754
	Total base pairs	8,680,214	294,249,631	60,975,328
	Total vector masked (bp)	22,644	162,651	7,274
	Total contaminant masked (bp)	665,818	4,642,372	118,387
	Average contig length (bp)	1,231	8,422	80,867
The Institute of Physical and Chemical Research (RIKEN), Japan	Number of accession records	0	1,149	300
	Number of contigs	0	25,772	300
	Total base pairs	0	182,812,275	20,093,926
	Total vector masked (bp)	0	203,792	2,371
	Total contaminant masked (bp)	0	308,426	27,781
	Average contig length (bp)	0	7,093	66,978
Sanger Centre, UK	Number of accession records	0	4,538	2,599
	Number of contigs	0	74,324	2,599
	Total base pairs	0	689,059,692	246,118,000
	Total vector masked (bp)	0	427,326	25,054
	Total contaminant masked (bp)	0	2,066,305	374,561
	Average contig length (bp)	0	9,271	94,697
Others*	Number of accession records	42	1,894	3,458
	Number of contigs	5,978	29,898	3,458
	Total base pairs	5,564,879	283,358,877	246,474,157
	Total vector masked (bp)	57,448	279,477	32,136
	Total contaminant masked (bp)	575,366	1,616,665	1,791,849
	Average contig length (bp)	931	9,478	71,277
All centers combined†	Number of accession records	3,021	21,015	9,137
	Number of contigs	258,943	409,628	9,137
	Total base pairs	209,930,983	3,360,047,574	835,722,268
	Total vector masked (bp)	1,655,293	2,438,575	82,284
	Total contaminant masked (bp)	14,918,135	16,311,664	3,365,230
	Average contig length (bp)	811	8,203	91,466

*Other centers contributing at least 0.1% of the sequence include: Chinese National Human Genome Center; Genomanalyse Gesellschaft fuer Biotechnologische Forschung mbH; Genome Therapeutics Corporation; GENOSCOPE; Chinese Academy of Sciences; Institute of Molecular Biotechnology; Keio University School of Medicine; Lawrence Livermore National Laboratory; Cold Spring Harbor Laboratory; Los Alamos National Laboratory; Max-Planck Institut fuer Molekulare, Genetik; Japan Science and Technology Corporation; Stanford University; The Institute for Genomic Research; The Institute of Physical and Chemical Research, Gene Bank; The University of Oklahoma; University of Texas Southwestern Medical Center, University of Washington. †The 4,405,700,825 bases contributed by all centers were shredded into faux reads resulting in 2.96× coverage of the genome.

In the compartmentalized shotgun assembly (CSA), Celera and PFP data were partitioned into the largest possible chromosomal segments or "components" that could be determined with confidence, and then shotgun assembly was applied to each partitioned subset wherein the bactig data were again shredded into faux reads to ensure an independent ab initio assembly of the component. By subsetting the data in this way, the overall computational effort was reduced and the effect of interchromosomal duplications was ameliorated. This also resulted in a reconstruction of the genome that was relatively independent of the whole-genome assembly results so that the two assemblies could be compared for consistency. The quality of the partitioning into components was crucial so that different genome regions were not mixed together. We constructed components from (i) the longest scaffolds of the sequence from each BAC and (ii) assembled scaffolds of data unique to Celera's data set. The BAC assemblies were obtained by a combining assembler that used the bactigs and the 5× Celera data mapped to those bactigs as input. This effort was undertaken as an interim step solely because the more accurate and complete the scaffold for a given sequence stretch, the more accurately one can tile these scaffolds into contiguous components on the basis of sequence overlap and mate-pair information. We further visually inspected and curated the scaffold tiling of the components to further increase its accuracy. For the final CSA assembly, all but the partitioning was ignored, and an independent, ab initio reconstruction of the sequence in each component was obtained by applying our whole-genome assembly algorithm to the partitioned, relevant Celera data and the shredded, faux reads of the partitioned, relevant bactig data.

2.3 Whole-genome assembly

The algorithms used for whole-genome assembly (WGA) of the human genome were enhancements to those used to produce the sequence of the *Drosophila* genome reported in detail in (*28*).

The WGA assembler consists of a pipeline composed of five principal stages: Screener, Overlapper, Unitigger, Scaffolder, and Repeat Resolver, respectively. The Screener finds and marks all microsatellite repeats with less than a 6-bp element, and screens out all known interspersed repeat elements, including Alu, Line, and ribosomal DNA. Marked regions get searched for overlaps, whereas screened regions do not get searched, but can be part of an overlap that involves unscreened matching segments.

The Overlapper compares every read against every other read in search of complete end-to-end overlaps of at least 40 bp and with no more than 6% differences in the match. Because all data are scrupulously vector-trimmed, the Overlapper can insist on complete overlap matches. Computing the set of all overlaps took roughly 10,000 CPU hours with a suite of four-processor Alpha SMPs with 4 gigabytes of RAM. This took 4 to 5 days in elapsed time with 40 such machines operating in parallel.

Every overlap computed above is statistically a 1-in-10^{17} event and thus not a coincidental event. What makes assembly combinatorially difficult is that while many overlaps are actually sampled from overlapping regions of the genome, and thus imply that the sequence reads should be assembled together, even more overlaps are actually from two distinct copies of a low-copy repeated element not screened above, thus constituting an error if put together. We call the former "true overlaps" and the latter "repeat-induced overlaps." The assembler must avoid choosing repeat-induced overlaps, especially early in the process.

We achieve this objective in the Unitigger. We first find all assemblies of reads that appear to be uncontested with respect to all other reads. We call the contigs formed from these subassemblies unitigs (for uniquely assembled contigs). Formally, these unitigs are the uncontested interval subgraphs of the graph of all overlaps (*42*). Unfortunately, although empirically many of these assemblies are correct (and thus involve only true overlaps), some are in fact collections of reads from several copies of a repetitive element that have been overcollapsed into a single subassembly. However, the overcollapsed unitigs are easily identified because their average coverage depth is too high to be consistent with the overall level of sequence coverage. We developed a simple statistical discriminator that gives the logarithm of the odds ratio that a unitig is composed of unique DNA or of a repeat consisting of two or more copies. The discriminator, set to a sufficiently stringent threshold, identifies a subset of the unitigs that we are certain are correct. In addition, a second, less stringent threshold identifies a subset of remaining unitigs very likely to be correctly assembled, of which we select those that will consistently scaffold (see below), and thus are again almost certain to be correct. We call the union of these two sets U-unitigs. Empirically, we found from a 6× simulated shotgun of human chromosome 22 that we get U-unitigs covering 98% of the stretches of unique DNA that are >2 kbp long. We are further able to identify the boundary of the start of a repetitive element at the ends of a U-unitig and leverage this so that U-unitigs span more than 93% of all singly interspersed Alu, elements and other 100-to 400-bp repetitive segments.

The result of running the Unitigger was thus a set of correctly assembled subcontigs covering an estimated 73.6% of the human genome. The Scaffolder then proceeded to use mate-pair information to link these together into scaffolds. When there are two or more mate pairs that imply that a given pair of U-unitigs are at a certain distance and orientation with respect to each other, the probability of this being wrong is again roughly 1 in 10^{10}, assuming that mate pairs are false less than 2% of the time. Thus, one can with high confidence link together all U-unitigs that are linked by at least two 2- or 10-kbp mate pairs producing intermediate-sized scaffolds that are then recursively linked together by confirming 50-kbp mate pairs and BAC end sequences. This process yielded scaffolds that are on the order of megabase pairs in size with gaps between their contigs that generally correspond to repetitive elements and occasionally to small sequencing gaps. These scaffolds reconstruct the majority of the unique sequence within a genome.

For the *Drosophila* assembly, we engaged in a three-stage repeat resolution strategy where each stage was progressively more aggressive and thus more likely to make a mistake. For the human assembly, we continued to use the first "Rocks" substage where all unitigs with a good, but not definitive, discriminator score are placed in a scaffold gap. This was done with the condition that two or more mate pairs with one of their reads already in the scaffold unambiguously place the unitig in the given gap. We estimate the probability of inserting a unitig into an incorrect gap with this strategy to be less than 10^{-7} based on a probabilistic analysis.

We revised the ensuing "Stones" substage of the human assembly, making it more like the mechanism suggested in our earlier work (*43*). For each gap, every read R that is placed in the gap by virtue of its mated pair M being in a contig of the scaffold and implying R's placement is collected. Celera's mate-pairing information is correct more than 99% of the time. Thus, almost every, but not all, of the reads in the set belong in the gap, and when a read does not belong it rarely agrees with the remainder of the reads. Therefore, we simply assemble this set of reads within the gap, eliminating any reads that conflict with the assembly. This operation proved much more reliable than the one it replaced for the *Drosophila* assembly; in the assembly of a simulated shotgun data set of human chromo-

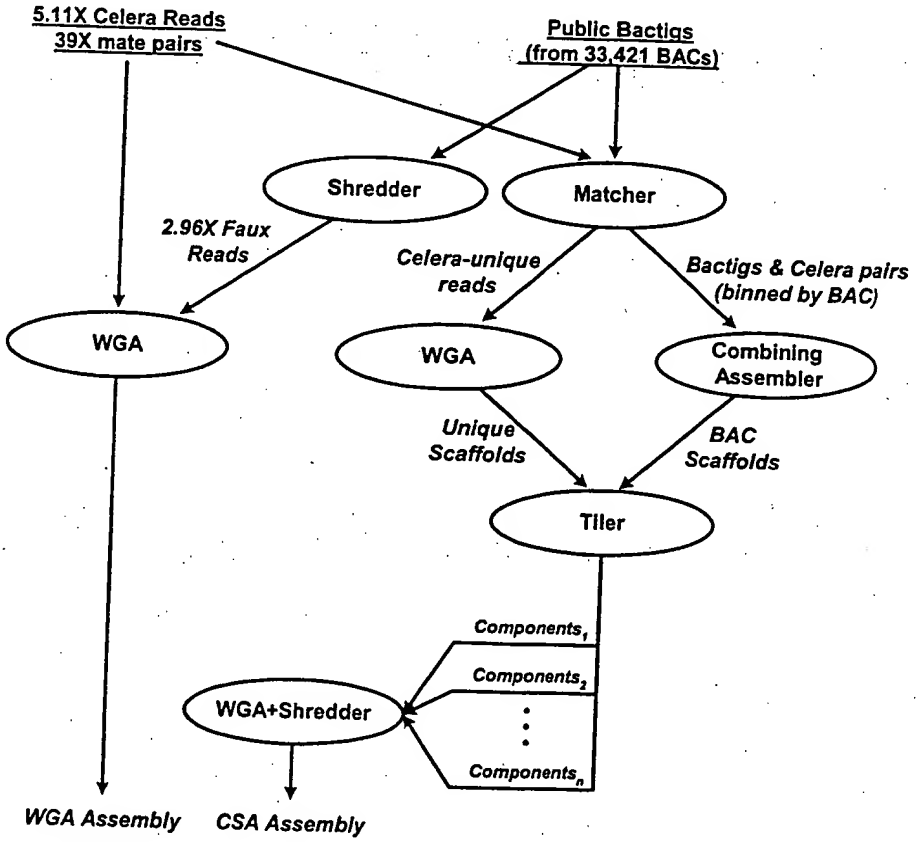

Fig. 4. Architecture of Celera's two-pronged assembly strategy. Each oval denotes a computation process performing the function indicated by its label, with the labels on arcs between ovals describing the nature of the objects produced and/or consumed by a process. This figure summarizes the discussion in the text that defines the terms and phrases used.

some 22, all stones were placed correctly.

The final method of resolving gaps is to fill them with assembled BAC data that cover the gap. We call this external gap "walking." We did not include the very aggressive "Pebbles" substage described in our *Drosophila* work, which made enough mistakes so as to produce repeat reconstructions for long interspersed elements whose quality was only 99.62% correct. We decided that for the human genome it was philosophically better not to introduce a step that was certain to produce less than 99.99% accuracy. The cost was a somewhat larger number of gaps of somewhat larger size.

At the final stage of the assembly process, and also at several intermediate points, a consensus sequence of every contig is produced. Our algorithm is driven by the principle of maximum parsimony, with quality-value–weighted measures for evaluating each base. The net effect is a Bayesian estimate of the correct base to report at each position. Consensus generation uses Celera data whenever it is present. In the event that no Celera data cover a given region, the BAC data sequence is used.

A key element of achieving a WGA of the human genome was to parallelize the Overlapper and the central consensus sequence–constructing subroutines. In addition, memory was a real issue—a straightforward application of the software we had built for *Drosophila* would have required a computer with a 600-gigabyte RAM. By making the Overlapper and Unitigger incremental, we were able to achieve the same computation with a maximum of instantaneous usage of 28 gigabytes of RAM. Moreover, the incremental nature of the first three stages allowed us to continually update the state of this part of the computation as data were delivered and then perform a 7-day run to complete Scaffolding and Repeat Resolution whenever desired. For our assembly operations, the total compute infrastructure consists of 10 four-processor SMPs with 4 gigabytes of memory per cluster (Compaq's ES40, Regatta) and a 16-processor NUMA machine with 64 gigabytes of memory (Compaq's GS160, Wildfire). The total compute for a run of the assembler was roughly 20,000 CPU hours.

The assembly of Celera's data, together with the shredded bactig data, produced a set of scaffolds totaling 2.848 Gbp in span and consisting of 2.586 Gbp of sequence. The chaff, or set of reads not incorporated in the assembly, numbered 11.27 million (26%), which is consistent with our experience for *Drosophila*. More than 84% of the genome was covered by scaffolds >100 kbp long, and these averaged 91% sequence and 9% gaps with a total of 2.297 Gbp of sequence. There were a total of 93,857 gaps among the 1637 scaffolds >100 kbp. The average scaffold size was 1.5 Mbp, the average contig size was 24.06 kbp, and the average gap size was 2.43 kbp, where the distribution of each was essentially exponential. More than 50% of all gaps were less than 50 bp long, >62% of all gaps were less than 1 kbp long, and no gap was >100 kbp long. Similarly, more than 65% of the sequence is in contigs >30 kbp, more than 31% is in contigs >100 kbp, and the largest contig was 1.22 Mbp long. Table 3 gives detailed summary statistics for the structure of this assembly with a direct comparison to the compartmentalized shotgun assembly.

2.4 Compartmentalized shotgun assembly

In addition to the WGA approach, we pursued a localized assembly approach that was intended to subdivide the genome into segments, each of which could be shotgun assembled individually. We expected that this would help in resolution of large interchromosomal duplications and improve the statistics for calculating U-unitigs. The compartmentalized assembly process involved clustering Celera reads and bactigs into large, multiple megabase regions of the genome, and then running the WGA assembler on the Celera data and shredded, faux reads obtained from the bactig data.

The first phase of the CSA strategy was to separate Celera reads into those that matched the BAC contigs for a particular PFP BAC entry, and those that did not match any public data. Such matches must be guaranteed to

Table 3. Scaffold statistics for whole-genome and compartmentalized shotgun assemblies.

	Scaffold size				
	All	>30 kbp	>100 kbp	>500 kbp	>1000 kbp
	Compartmentalized shotgun assembly				
No. of bp in scaffolds (including intrascaffold gaps)	2,905,568,203	2,748,892,430	2,700,489,906	2,489,357,260	2,248,689,128
No. of bp in contigs	2,653,979,733	2,524,251,302	2,491,538,372	2,320,648,201	2,106,521,902
No. of scaffolds	53,591	2,845	1,935	1,060	721
No. of contigs	170,033	112,207	107,199	93,138	82,009
No. of gaps	116,442	109,362	105,264	92,078	81,288
No. of gaps ≤1 kbp	72,091	69,175	67,289	59,915	53,354
Average scaffold size (bp)	54,217	966,219	1,395,602	2,348,450	3,118,848
Average contig size (bp)	15,609	22,496	23,242	24,916	25,686
Average intrascaffold gap size (bp)	2,161	2,054	1,985	1,832	1,749
Largest contig (bp)	1,988,321	1,988,321	1,988,321	1,988,321	1,988,321
% of total contigs	100	95	94	87	79
	Whole-genome assembly				
No. of bp in scaffolds (including intrascaffold gaps)	2,847,890,390	2,574,792,618	2,525,334,447	2,328,535,466	2,140,943,032
No. of bp in contigs	2,586,634,108	2,334,343,339	2,297,678,935	2,143,002,184	1,983,305,432
No. of scaffolds	118,968	2,507	1,637	818	554
No. of contigs	221,036	99,189	95,494	84,641	76,285
No. of gaps	102,068	96,682	93,857	83,823	75,731
No. of gaps ≤1 kbp	62,356	60,343	59,156	54,079	49,592
Average scaffold size (bp)	23,938	1,027,041	1,542,660	2,846,620	3,864,518
Average contig size (bp)	11,702	23,534	24,061	25,319	25,999
Average intrascaffold gap size (bp)	2,560	2,487	2,426	2,213	2,082
Largest contig (bp)	1,224,073	1,224,073	1,224,073	1,224,073	1,224,073
% of total contigs	100	90	89	83	77

properly place a Celera read, so all reads were first masked against a library of common repetitive elements, and only matches of at least 40 bp to unmasked portions of the read constituted a hit. Of Celera's 27.27 million reads, 20.76 million matched a bactig and another 0.62 million reads, which did not have any matches, were nonetheless identified as belonging in the region of the bactig's BAC because their mate matched the bactig. Of the remaining reads, 2.92 million were completely screened out and so could not be matched, but the other 2.97 million reads had unmasked sequence totaling 1.189 Gbp that were not found in the GenBank data set. Because the Celera data are 5.11× redundant, we estimate that 240 Mbp of unique Celera sequence is not in the GenBank data set.

In the next step of the CSA process, a combining assembler took the relevant 5× Celera reads and bactigs for a BAC entry, and produced an assembly of the combined data for that locale. These high-quality sequence reconstructions were a transient result whose utility was simply to provide more reliable information for the purposes of their tiling into sets of overlapping and adjacent scaffold sequences in the next step. In outline, the combining assembler first examines the set of matching Celera reads to determine if there are excessive pileups indicative of unscreened repetitive elements. Wherever these occur, reads in the repeat region whose mates have not been mapped to consistent positions are removed. Then all sets of mate pairs that consistently imply the same relative position of two bactigs are bundled into a link and weighted according to the number of mates in the bundle. A "greedy" strategy then attempts to order the bactigs by selecting bundles of mate-pairs in order of their weight. A selected mate-pair bundle can tie together two formative scaffolds. It is incorporated to form a single scaffold only if it is consistent with the majority of links between contigs of the scaffold. Once scaffolding is complete, gaps are filled by the "Stones" strategy described above for the WGA assembler.

The GenBank data for the Phase 1 and 2 BACs consisted of an average of 19.8 bactigs per BAC of average size 8099 bp. Application of the combining assembler resulted in individual Celera BAC assemblies being put together into an average of 1.83 scaffolds (median of 1 scaffold) consisting of an average of 8.57 contigs of average size 18,973 bp. In addition to defining order and orientation of the sequence fragments, there were 57% fewer gaps in the combined result. For Phase 0 data, the average GenBank entry consisted of 91.52 reads of average length 784 bp. Application of the combining assembler resulted in an average of 54.8 scaffolds consisting of an average of 58.1 contigs of average size 873 bp. Basically, some small amount of assembly took place, but not enough Celera data were matched to truly assemble the 0.5× to 1× data set represented by the typical Phase 0 BACs. The combining assembler was also applied to the Phase 3 BACs for SNP identification, confirmation of assembly, and localization of the Celera reads. The phase 0 data suggest that a combined whole-genome shotgun data set and 1× light-shotgun of BACs will not yield good assembly of BAC regions; at least 3× light-shotgun of each BAC is needed.

The 5.89 million Celera fragments not matching the GenBank data were assembled with our whole-genome assembler. The assembly resulted in a set of scaffolds totaling 442 Mbp in span and consisting of 326 Mbp of sequence. More than 20% of the scaffolds were >5 kbp long, and these averaged 63% sequence and 27% gaps with a total of 302 Mbp of sequence. All scaffolds >5 kbp were forwarded along with all scaffolds produced by the combining assembler to the subsequent tiling phase.

At this stage, we typically had one or two scaffolds for every BAC region constituting at least 95% of the relevant sequence, and a collection of disjoint Celera-unique scaffolds. The next step in developing the genome components was to determine the order and overlap tiling of these BAC and Celera-unique scaffolds across the genome. For this, we used Celera's 50-kbp mate-pairs information, and BAC-end pairs (*18*) and sequence tagged site (STS) markers (*44*) to provide long-range guidance and chromosome separation. Given the relatively manageable number of scaffolds, we chose not to produce this tiling in a fully automated manner, but to compute an initial tiling with a good heuristic and then use human curators to resolve discrepancies or missed join opportunities. To this end, we developed a graphical user interface that displayed the graph of tiling overlaps and the evidence for each. A human curator could then explore the implication of mapped STS data, dot-plots of sequence overlap, and a visual display of the mate-pair evidence supporting a given choice. The result of this process was a collection of "components," where each component was a tiled set of BAC and Celera-unique scaffolds that had been curator-approved. The process resulted in 3845 components with an estimated span of 2.922 Gbp.

In order to generate the final CSA, we assembled each component with the WGA algorithm. As was done in the WGA process, the bactig data were shredded into a synthetic 2× shotgun data set in order to give the assembler the freedom to independently assemble the data. By using faux reads rather than bactigs, the assembly algorithm could correct errors in the assembly of bactigs and remove chimeric content in a PFP data entry. Chimeric or contaminating sequence (from another part of the genome) would not be incorporated into the reassembly of the component because it did not belong there. In effect, the previous steps in the CSA process served only to bring together Celera fragments and PFP data relevant to a large contiguous segment of the genome, wherein we applied the assembler used for WGA to produce an ab initio assembly of the region.

WGA assembly of the components resulted in a set of scaffolds totaling 2.906 Gbp in span and consisting of 2.654 Gbp of sequence. The chaff, or set of reads not incorporated into the assembly, numbered 6.17 million, or 22%. More than 90.0% of the genome was covered by scaffolds spanning >100 kbp long, and these averaged 92.2% sequence and 7.8% gaps with a total of 2.492 Gbp of sequence. There were a total of 105,264 gaps among the 107,199 contigs that belong to the 1940 scaffolds spanning >100 kbp. The average scaffold size was 1.4 Mbp, the average contig size was 23.24 kbp, and the average gap size was 2.0 kbp where each distribution of sizes was exponential. As such, averages tend to be underrepresentative of the majority of the data. Figure 5 shows a histogram of the bases in scaffolds of various size ranges. Consider also that more than 49% of all gaps were <500 bp long, more than 62% of all gaps were <1 kbp, and all gaps are <100 kbp long. Similarly, more than 73% of the sequence is in contigs > 30 kbp, more than 49% is in contigs >100 kbp, and the largest contig was 1.99 Mbp long. Table 3 provides summary statistics for the structure of this assembly with a direct comparison to the WGA assembly.

2.5 Comparison of the WGA and CSA scaffolds

Having obtained two assemblies of the human genome via independent computational processes (WGA and CSA), we compared scaffolds from the two assemblies as another means of investigating their completeness, consistency, and contiguity. From each assembly, a set of reference scaffolds containing at least 1000 fragments (Celera sequencing reads or bactig shreds) was obtained; this amounted to 2218 WGA scaffolds and 1717 CSA scaffolds, for a total of 2.087 Gbp and 2.474 Gbp. The sequence of each reference scaffold was compared to the sequence of all scaffolds from the other assembly with which it shared at least 20 fragments or at least 20% of the fragments of the smaller scaffold. For each such comparison, all matches of at least 200 bp with at most 2% mismatch were tabulated.

From this tabulation, we estimated the amount of unique sequence in each assembly in two ways. The first was to determine the number of bases of each assembly that were

not covered by a matching segment in the other assembly. Some 82.5 Mbp of the WGA (3.95%) was not covered by the CSA, whereas 204.5 Mbp (8.26%) of the CSA was not covered by the WGA. This estimate did not require any consistency of the assemblies or any uniqueness of the matching segments. Thus, another analysis was conducted in which matches of less than 1 kbp between a pair of scaffolds were excluded unless they were confirmed by other matches having a consistent order and orientation. This gives some measure of consistent coverage: 1.982 Gbp (95.00%) of the WGA is covered by the CSA, and 2.169 Gbp (87.69%) of the CSA is covered by the WGA by this more stringent measure.

The comparison of WGA to CSA also permitted evaluation of scaffolds for structural inconsistencies. We looked for instances in which a large section of a scaffold from one assembly matched only one scaffold from the other assembly, but failed to match over the full length of the overlap implied by the matching segments. An initial set of candidates was identified automatically, and then each candidate was inspected by hand. From this process, we identified 31 instances in which the assemblies appear to disagree in a nonlocal fashion. These cases are being further evaluated to determine which assembly is in error and why.

In addition, we evaluated local inconsistencies of order or orientation. The following results exclude cases in which one contig in one assembly corresponds to more than one overlapping contig in the other assembly (as long as the order and orientation of the latter agrees with the positions they match in the former). Most of these small rearrangements involved segments on the order of hundreds of base pairs and rarely >1 kbp. We found a total of 295 kbp (0.012%) in the CSA assemblies that were locally inconsistent with the WGA assemblies, whereas 2.108 Mbp (0.11%) in the WGA assembly were inconsistent with the CSA assembly.

The CSA assembly was a few percentage points better in terms of coverage and slightly more consistent than the WGA, because it was in effect performing a few thousand shotgun assemblies of megabase-sized problems, whereas the WGA is performing a shotgun assembly of a gigabase-sized problem. When one considers the increase of two-and-a-half orders of magnitude in problem size, the information loss between the two is remarkably small. Because CSA was logistically easier to deliver and the better of the two results available at the time when downstream analyses needed to be begun, all subsequent analysis was performed on this assembly.

2.6 Mapping scaffolds to the genome

The final step in assembling the genome was to order and orient the scaffolds on the chromosomes. We first grouped scaffolds together on the basis of their order in the components from CSA. These grouped scaffolds were reordered by examining residual mate-pairing data between the scaffolds. We next mapped the scaffold groups onto the chromosome using physical mapping data. This step depends on having reliable high-resolution map information such that each scaffold will overlap multiple markers. There are two genome-wide types of map information available: high-density STS maps and fingerprint maps of BAC clones developed at Washington University (*45*). Among the genome-wide STS maps, GeneMap99 (GM99) has the most markers and therefore was most useful for mapping scaffolds. The two different mapping approaches are complementary to one another. The fingerprint maps should have better local order because they were built by comparison of overlapping BAC clones. On the other hand, GM99 should have a more reliable long-range order, because the framework markers were derived from well-validated genetic maps. Both types of maps were used as a reference for human curation of the components that were the input to the regional assembly, but they did not determine the order of sequences produced by the assembler.

In order to determine the effectiveness of the fingerprint maps and GM99 for mapping scaffolds, we first examined the reliability of these maps by comparison with large scaffolds. Only 1% of the STS markers on the 10 largest scaffolds (those >9 Mbp) were mapped on a different chromosome on GM99. Two percent of the STS markers disagreed in position by more than five framework bins. However, for the fingerprint maps, a 2% chromosome discrepancy was observed, and on average 23.8% of BAC locations in the scaffold sequence disagreed with fingerprint map placement by more than five BACs. When further examining the source of discrepancy, it was found that most of the discrepancy came from 4 of the 10 scaffolds, indicating this there is variation in the quality of either the map or the scaffolds. All four scaffolds were assembled, as well as the other six, as judged by clone coverage analysis, and showed the same low discrepancy rate to GM99, and thus we concluded that the fingerprint map global order in these cases was not reliable. Smaller scaffolds had a higher discordance rate with GM99 (4.21% of STSs were discordant by more than five framework bins), but a lower discordance rate with the fingerprint maps (11% of BACs disagreed with fingerprint maps by more than five BACs). This observation agrees with the clone coverage analysis (*46*) that Celera scaffold construction was better supported by long-range mate pairs in larger scaffolds than in small scaffolds.

We created two orderings of Celera scaffolds on the basis of the markers (BAC or STS) on these maps. Where the order of scaffolds agreed between GM99 and the WashU BAC map, we had a high degree of confidence that that order was correct; these scaffolds were termed "anchor scaffolds." Only scaffolds with a low overall discrepancy rate with both maps were considered anchor scaffolds. Scaffolds in GM99 bins were allowed to permute in their order to match WashU ordering, provided they did not violate their framework orders. Orientation of individual scaffolds was determined by the presence of multiple mapped markers with consistent order. Scaffolds with only one marker have insufficient information to assign orientation. We found 70.1% of the genome in anchored scaffolds, more than 99% of which are also oriented (Table 4). Because GM99 is of lower resolution than the WashU map, a number of scaffolds without STS matches could be ordered relative to the anchored scaffolds because they included sequence from the same or adjacent BACs on the WashU map. On the other hand, because of occasional WashU global ordering discrepancies, a number of scaffolds determined to be "unmappable" on the WashU map could be ordered relative to the anchored scaffolds

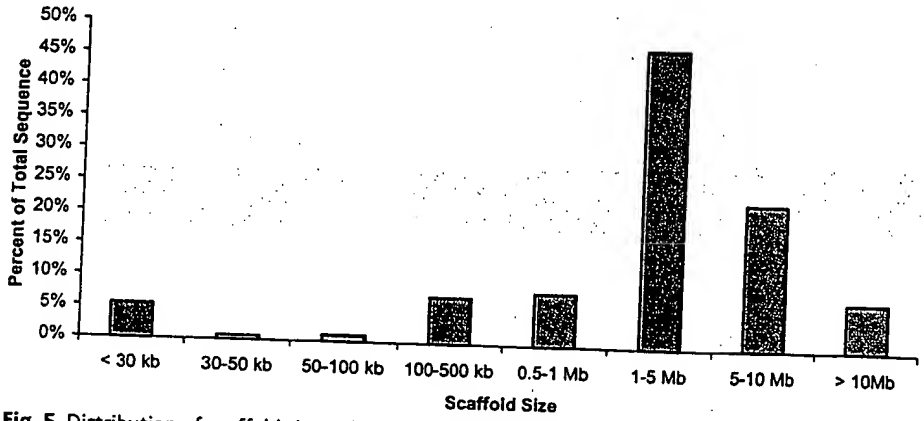

Fig. 5. Distribution of scaffold sizes of the CSA. For each range of scaffold sizes, the percent of total sequence is indicated.

with GM99. These scaffolds were termed "ordered scaffolds." We found that 13.9% of the assembly could be ordered by these additional methods, and thus 84.0% of the genome was ordered unambiguously.

Next, all scaffolds that could be placed, but not ordered, between anchors were assigned to the interval between the anchored scaffolds and were deemed to be "bounded" between them. For example, small scaffolds having STS hits from the same GeneMap bin or hitting the same BAC cannot be ordered relative to each other, but can be assigned a placement boundary relative to other anchored or ordered scaffolds. The remaining scaffolds either had no localization information, conflicting information, or could only be assigned to a generic chromosome location. Using the above approaches, ~98% of the genome was anchored, ordered, or bounded.

Finally, we assigned a location for each scaffold placed on the chromosome by spreading out the scaffolds per chromosome. We assumed that the remaining unmapped scaffolds, constituting 2% of the genome, were distributed evenly across the genome. By dividing the sum of unmapped scaffold lengths with the sum of the number of mapped scaffolds, we arrived at an estimate of interscaffold gap of 1483 bp. This gap was used to separate all the scaffolds on each chromosome and to assign an offset in the chromosome.

During the scaffold-mapping effort, we encountered many problems that resulted in additional quality assessment and validation analysis. At least 978 (3% of 33,173) BACs were believed to have sequence data from more than one location in the genome (*47*). This is consistent with the bactig chimerism analysis reported above in the Assembly Strategies section. These BACs could not be assigned to unique positions within the CSA assembly and thus could not be used for ordering scaffolds. Likewise, it was not always possible to assign STSs to unique locations in the assembly because of genome duplications, repetitive elements, and pseudogenes.

Because of the time required for an exhaustive search for a perfect overlap, CSA generated 21,607 intrascaffold gaps where the mate-pair data suggested that the contigs should overlap, but no overlap was found. These gaps were defined as a fixed 50 bp in length and make up 18.6% of the total 116,442 gaps in the CSA assembly.

We chose not to use the order of exons implied in cDNA or EST data as a way of ordering scaffolds. The rationale for not using this data was that doing so would have biased certain regions of the assembly by rearranging scaffolds to fit the transcript data and made validation of both the assembly and gene definition processes more difficult.

2.7 Assembly and validation analysis

We analyzed the assembly of the genome from the perspectives of completeness (amount of coverage of the genome) and correctness (the structural accuracy of the order and orientation and the consensus sequence of the assembly).

Completeness. Completeness is defined as the percentage of the euchromatic sequence represented in the assembly. This cannot be known with absolute certainty until the euchromatin sequence has been completed. However, it is possible to estimate completeness on the basis of (i) the estimated sizes of intrascaffold gaps; (ii) coverage of the two published chromosomes, 21 and 22 (*48*, *49*); and (iii) analysis of the percentage of an independent set of random sequences (STS markers) contained in the assembly. The whole-genome libraries contain heterochromatic sequence and, although no attempt has been made to assemble it, there may be instances of unique sequence embedded in regions of heterochromatin as were observed in *Drosophila* (*50*, *51*).

The sequences of human chromosomes 21 and 22 have been completed to high quality and published (*48*, *49*). Although this sequence served as input to the assembler, the finished sequence was shredded into a shotgun data set so that the assembler had the opportunity to assemble it differently from the original sequence in the case of structural polymorphisms or assembly errors in the BAC data. In particular, the assembler must be able to resolve repetitive elements at the scale of components (generally multimegabase in size), and so this comparison reveals the level to which the assembler resolves repeats. In certain areas, the assembly structure differs from the published versions of chromosomes 21 and 22 (see below). The consequence of the flexibility to assemble "finished" sequence differently on the basis of Celera data resulted in an assembly with more segments than the chromosome 21 and 22 sequences. We examined the reasons why there are more gaps in the Celera sequence than in chromosomes 21 and 22 and expect that they may be typical of gaps in other regions of the genome. In the Celera assembly, there are 25 scaffolds, each containing at least 10 kb of sequence, that collectively span 94.3% of chromosome 21. Sixty-two scaffolds span 95.7% of chromosome 22. The total length of the gaps remaining in the Celera assembly for these two chromosomes is 3.4 Mbp. These gap sequences were analyzed by RepeatMasker and by searching against the entire genome assembly (*52*). About 50% of the gap sequence consisted of common repetitive elements identified by RepeatMasker; more than half of the remainder was lower copy number repeat elements.

A more global way of assessing completeness is to measure the content of an independent set of sequence data in the assembly. We compared 48,938 STS markers from Genemap99 (*51*) to the scaffolds. Because these markers were not used in the assembly processes, they provided a truly independent measure of completeness. ePCR (*53*) and BLAST (*54*) were used to locate STSs on the assembled genome. We found 44,524 (91%) of the STSs in the mapped genome. An additional 2648 markers (5.4%) were found by searching the unassembled data or "chaff." We identified 1283 STS markers (2.6%) not found in either Celera sequence or BAC data as of September 2000, raising the possibility that these markers may not be of human origin. If that were the case, the Celera assembled sequence would represent 93.4% of the human genome and the unassembled data 5.5%, for a total of 98.9% coverage. Similarly, we compared CSA against 36,678 TNG radiation hybrid markers (*55a*) using the same method. We found that 32,371 markers (88%) were located in the mapped CSA scaffolds, with 2055 markers (5.6%) found in the remainder. This gave a 94% coverage of the genome through another genome-wide survey.

Correctness. Correctness is defined as the structural and sequence accuracy of the assembly. Because the source sequences for the Celera data and the GenBank data are from different individuals, we could not directly compare the consensus sequence of the as-

Table 4. Summary of scaffold mapping. Scaffolds were mapped to the genome with different levels of confidence (anchored scaffolds have the highest confidence; unmapped scaffolds have the lowest). Anchored scaffolds were consistently ordered by the WashU BAC map and GM99. Ordered scaffolds were consistently ordered by at least one of the following: the WashU BAC map, GM99, or component tiling path. Bounded scaffolds had order conflicts between at least two of the external maps, but their placements were adjacent to a neighboring anchored or ordered scaffold. Unmapped scaffolds had, at most, a chromosome assignment. The scaffold subcategories are given below each category.

Mapped scaffold category	Number	Length (bp)	% Total length
Anchored	1,526	1,860,676,676	70
Oriented	1,246	1,852,088,645	70
Unoriented	280	8,588,031	0.3
Ordered	2,001	369,235,857	14
Oriented	839	329,633,166	12
Unoriented	1,162	39,602,691	2
Bounded	38,241	368,753,463	14
Oriented	7,453	274,536,424	10
Unoriented	30,788	94,217,039	4
Unmapped	11,823	55,313,737	2
Known chromosome	281	2,505,844	0.1
Unknown chromosome	11,542	52,807,893	2

sembly against other finished sequence for determining sequencing accuracy at the nucleotide level, although this has been done for identifying polymorphisms as described in Section 6. The accuracy of the consensus sequence is at least 99.96% on the basis of a statistical estimate derived from the quality values of the underlying reads.

The structural consistency of the assembly can be measured by mate-pair analysis. In a correct assembly, every mated pair of sequencing reads should be located on the consensus sequence with the correct separation and orientation between the pairs. A pair is termed "valid" when the reads are in the correct orientation and the distance between them is within the mean ± 3 standard deviations of the distribution of insert sizes of the library from which the pair was sampled. A pair is termed "misoriented" when the reads are not correctly oriented, and is termed "misseparated" when the distance between the reads is not in the correct range but the reads are correctly oriented. The mean ± the standard deviation of each library used by the assembler was determined as described above. To validate these, we examined all reads mapped to the finished sequence of chromosome 21 (*48*) and determined how many incorrect mate pairs there were as a result of laboratory tracking errors and chimerism (two different segments of the genome cloned into the same plasmid), and how tight the distribution of insert sizes was for those that were correct (Table 5). The standard deviations for all Celera libraries were quite small, less than 15% of the insert length, with the exception of a few 50-kbp libraries. The 2- and 10-kbp libraries contained less than 2% invalid mate pairs, whereas the 50-kbp libraries were somewhat higher (~10%). Thus, although the mate-pair information was not perfect, its accuracy was such that measuring valid, misoriented, and misseparated pairs with respect to a given assembly was deemed to be a reliable instrument for validation purposes, especially when several mate pairs confirm or deny an ordering.

The clone coverage of the genome was 39×, meaning that any given base pair was, on average, contained in 39 clones or, equivalently, spanned by 39 mate-paired reads. Areas of low clone coverage or areas with a high proportion of invalid mate pairs would indicate potential assembly problems. We computed the coverage of each base in the assembly by valid mate pairs (Table 6). In summary, for scaffolds >30 kbp in length, less than 1% of the Celera assembly was in regions of less than 3× clone coverage. Thus, more than 99% of the assembly, including order and orientation, is strongly supported by this measure alone.

We examined the locations and number of all misoriented and misseparated mates. In addition to doing this analysis on the CSA assembly (as of 1 October 2000), we also performed a study of the PFP assembly as of 5 September 2000 (*30*, *55b*). In this latter case, Celera mate pairs had to be mapped to the PFP assembly. To avoid mapping errors due to high-fidelity repeats, the only pairs mapped were those for which both reads matched at only one location with less than 6% differences. A threshold was set such that sets of five or more simultaneously invalid mate pairs indicated a potential breakpoint, where the construction of the two assemblies differed. The graphic comparison of the CSA chromosome 21 assembly with the published sequence (Fig. 6A) serves as a validation of this methodology. Blue tick marks in the panels indicate breakpoints. There were a similar (small) number of breakpoints on both chromosome sequences. The exception was 12 sets of scaffolds in the Celera assembly (a total of 3% of the chromosome length in 212 single-contig scaffolds) that were mapped to the wrong positions because they were too small to be mapped reliably. Figures 6 and 7 and Table 6 illustrate the mate-pair differences and breakpoints between the two assemblies. There was a higher percentage of misoriented and misseparated mate pairs in the large-insert libraries (50 kbp and BAC ends) than in the small-insert libraries in both assemblies (Table 6). The large-insert libraries are more likely to identify discrepancies simply because they span a larger segment of the genome. The graphic comparison between the two assemblies for chromosome 8 (Fig. 6, B and C) shows that there are many

Table 5. Mate-pair validation. Celera fragment sequences were mapped to the published sequence of chromosome 21. Each mate pair uniquely mapped was evaluated for correct orientation and placement (number of mate pairs tested). If the two mates had incorrect relative orientation or placement, they were considered invalid (number of invalid mate pairs).

Library type	Library no.	Chromosome 21						Genome		
		Mean insert size (bp)	SD (bp)	SD/ mean (%)	No. of mate pairs tested	No. of invalid mate pairs	% invalid	Mean insert size (bp)	SD (bp)	SD/ mean (%)
2 kbp	1	2,081	106	5.1	3,642	38	1.0	2,082	90	4.3
	2	1,913	152	7.9	28,029	413	1.5	1,923	118	6.1
	3	2,166	175	8.1	4,405	57	1.3	2,162	158	7.3
10 kbp	4	11,385	851	7.5	4,319	80	1.9	11,370	696	6.1
	5	14,523	1,875	12.9	7,355	156	2.1	14,142	1,402	9.9
	6	9,635	1,035	10.7	5,573	109	2.0	9,606	934	9.7
	7	10,223	928	9.1	34,079	399	1.2	10,190	777	7.6
50 kbp	8	64,888	2,747	4.2	16	1	6.3	65,500	5,504	8.4
	9	53,410	5,834	10.9	914	170	18.6	53,311	5,546	10.4
	10	52,034	7,312	14.1	5,871	569	9.7	51,498	6,588	12.8
	11	52,282	7,454	14.3	2,629	213	8.1	52,282	7,454	14.3
	12	46,616	7,378	15.8	2,153	215	10.0	45,418	9,068	20.0
	13	55,788	10,099	18.1	2,244	249	11.1	53,062	10,893	20.5
	14	39,894	5,019	12.6	199	7	3.5	36,838	9,988	27.1
BES	15	48,931	9,813	20.1	144	10	6.9	47,845	4,774	10.0
	16	48,130	4,232	8.8	195	14	7.2	47,924	4,581	9.6
	17	106,027	27,778	26.2	330	16	4.8	152,000	26,600	17.5
	18	160,575	54,973	34.2	155	8	5.2	161,750	27,000	16.7
	19	164,155	19,453	11.9	642	44	6.9	176,500	19,500	11.05
Sum					102,894	2,768 (mean = 2.7)	2.7			

more breakpoints for the PFP assembly than for the Celera assembly. Figure 7 shows the breakpoint map (blue tick marks) for both assemblies of each chromosome in a side-by-side fashion. The order and orientation of Celera's assembly shows substantially fewer breakpoints except on the two finished chromosomes. Figure 7 also depicts large gaps (>10 kbp) in both assemblies as red tick marks. In the CSA assembly, the size of all gaps have been estimated on the basis of the mate-pair data. Breakpoints can be caused by structural polymorphisms, because the two assemblies were derived from different human genomes. They also reflect the unfinished nature of both genome assemblies.

3 Gene Prediction and Annotation

Summary. To enumerate the gene inventory, we developed an integrated, evidence-based approach named Otto. The evidence used to increase the likelihood of identifying genes includes regions conserved between the mouse and human genomes, similarity to ESTs or other mRNA-derived data, or similarity to other proteins. A comparison of Otto (combined Otto-RefSeq and Otto homology) with Genscan, a standard gene-prediction algorithm, showed greater sensitivity (0.78 versus 0.50) and specificity (0.93 versus 0.63) of Otto in the ability to define gene structure. Otto-predicted genes were complemented with a set of genes from three gene-prediction programs that exhibited weaker, but still significant, evidence that they may be expressed. Conservative criteria, requiring at least two lines of evidence, were used to define a set of 26,383 genes with good confidence that were used for more detailed analysis presented in the subsequent sections. Extensive manual curation to establish precise characterization of gene structure will be necessary to improve the results from this initial computational approach.

3.1 Automated gene annotation

A gene is a locus of cotranscribed exons. A single gene may give rise to multiple transcripts, and thus multiple distinct proteins with multiple functions, by means of alternative splicing and alternative transcription initiation and termination sites. Our cells are able to discern within the billions of base pairs of the genomic DNA the signals for initiating transcription and for splicing together exons separated by a few or hundreds of thousands of base pairs. The first step in characterizing the genome is to define the structure of each gene and each transcription unit.

The number of protein-coding genes in mammals has been controversial from the outset. Initial estimates based on reassociation data placed it between 30,000 to 40,000, whereas later estimates from the brain were >100,000 (*56*). More recent data from both the corporate and public sectors, based on extrapolations from EST, CpG island, and transcript density–based extrapolations, have not reduced this variance. The highest recent number of 142,634 genes emanates from a report from Incyte Pharmaceuticals, and is based on a combination of EST data and the association of ESTs with CpG islands (*57*). In stark contrast are three quite different, and much lower estimates: one of ~35,000 genes derived with genome-wide EST data and sampling procedures in conjunction with chromosome 22 data (*58*); another of 28,000 to 34,000 genes derived with a comparative methodology involving sequence conservation between humans and the puffer fish *Tetraodon nigroviridis* (*59*); and a figure of 35,000 genes, which was derived simply by extrapolating from the density of 770 known and predicted genes in the 67 Mbp of chromosomes 21 and 22, to the approximately 3-Gbp euchromatic genome.

The problem of computational identification of transcriptional units in genomic DNA sequence can be divided into two phases. The first is to partition the sequence into segments that are likely to correspond to individual genes. This is not trivial and is a weakness of most de novo gene-finding algorithms. It is also critical to determining the number of genes in the human gene inventory. The second challenge is to construct a gene model that reflects the probable structure of the transcript(s) encoded in the region. This can be done with reasonable accuracy when a full-length cDNA has been sequenced or a highly homologous protein sequence is known. De novo gene prediction, although less accurate, is the only way to find genes that are not represented by homologous proteins or ESTs. The following section describes the methods we have developed to address these problems for the prediction of protein-coding genes.

We have developed a rule-based expert system, called Otto, to identify and characterize genes in the human genome (*60*). Otto attempts to simulate in software the process that a human annotator uses to identify a gene and refine its structure. In the process of annotating a region of the genome, a human curator examines the evidence provided by the computational pipeline (described below) and examines how various types of evidence relate to one another. A curator puts different levels of confidence in different types of evidence and looks for certain patterns of evidence to support gene annotation. For example, a curator may examine homology to a number of ESTs and evaluate whether or not they can be connected into a longer, virtual mRNA. The curator would also evaluate the strength of the similarity and the contiguity of the match, in essence asking whether any ESTs cross splice-junctions and whether the edges of putative exons have consensus splice sites. This kind of manual annotation process was used to annotate the *Drosophila* genome.

The Otto system can promote observed evidence to a gene annotation in one of two ways. First, if the evidence includes a high-quality match to the sequence of a known gene [here defined as a human gene represented in a curated subset of the RefSeq database (*61*)], then Otto can promote this to a gene annotation. In the second method, Otto evaluates a broad spectrum of evidence and determines if this evidence is adequate to support promotion to a gene annotation. These processes are described below.

Initially, gene boundaries are predicted on the basis of examination of sets of overlapping protein and EST matches generated by a computational pipeline (*62*). This pipeline searches the scaffold sequences against protein, EST, and genome-sequence databases to define regions of sequence similarity and runs three de novo gene-prediction programs.

To identify likely gene boundaries, regions of the genome were partitioned by Otto on the basis of sequence matches identified by BLAST. Each of the database sequences matched in the region under analysis was compared by an algorithm that takes into account both coordinates of the matching sequence, as well as the sequence type (e.g., protein, EST, and so forth). The results were used to group the matches into bins of related sequences that may define a gene and identify

Table 6. Genome-wide mate pair analysis of compartmentalized shotgun (CSA) and PFP assemblies.*

Genome library	CSA			PFP		
	% valid	% mis-oriented	% mis-separated†	% valid	% mis-oriented	% mis-separated†
2 kbp	98.5	0.6	1.0	95.7	2.0	2.3
10 kbp	96.7	1.0	2.3	81.9	9.6	8.6
50 kbp	93.9	4.5	1.5	64.2	22.3	13.5
BES	94.1	2.1	3.8	62.0	19.3	18.8
Mean	97.4	1.0	1.6	87.3	6.8	5.9

*Data for individual chromosomes can be found in Web fig. 3 on *Science* Online at www.sciencemag.org/cgi/content/full/291/5507/1304/DC1. †Mates are misseparated if their distance is >3 SD from the mean library size.

gene boundaries. During this process, multiple hits to the same region were collapsed to a coherent set of data by tracking the coverage of a region. For example, if a group of bases was represented by multiple overlapping ESTs, the union of these regions matched by the set of ESTs on the scaffold was marked as being supported by EST evidence. This resulted in a series of "gene bins," each of which was believed to contain a single gene. One weakness of this initial implementation of the algorithm was in predicting gene boundaries in regions of tandemly duplicated genes. Gene clusters frequently resulted in homologous neighboring genes being joined together, resulting in an annotation that artificially concatenated these gene models.

Next, known genes (those with exact matches of a full-length cDNA sequence to the genome) were identified, and the region corresponding to the cDNA was annotated as a predicted transcript. A subset of the curated human gene set RefSeq from the National Center for Biotechnology Information (NCBI) was included as a data set searched in the computational pipeline. If a RefSeq transcript matched the genome assembly for at least 50% of its length at >92% identity, then the SIM4 (*63*) alignment of the RefSeq transcript to the region of the genome under analysis was promoted to the status of an Otto annotation. Because the genome sequence has gaps and sequence errors such as frameshifts, it was not always possible to predict a transcript that agrees precisely with the experimentally determined cDNA sequence. A total of 6538 genes in our inventory were identified and transcripts predicted in this way.

Regions that have a substantial amount of sequence similarity, but do not match known genes, were analyzed by that part of the Otto system that uses the sequence similarity information to predict a transcript. Here, Otto

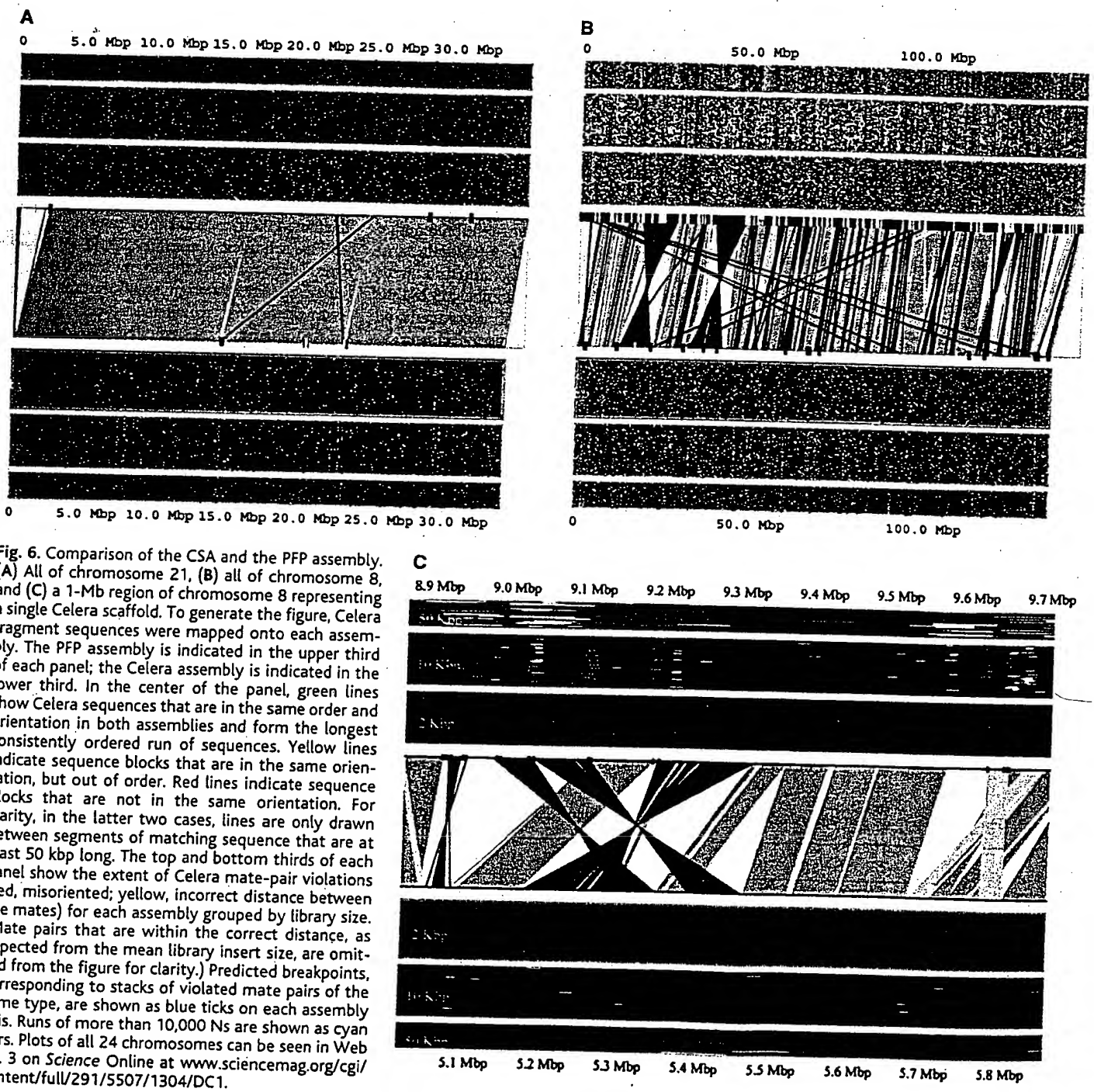

Fig. 6. Comparison of the CSA and the PFP assembly. (**A**) All of chromosome 21, (**B**) all of chromosome 8, and (**C**) a 1-Mb region of chromosome 8 representing a single Celera scaffold. To generate the figure, Celera fragment sequences were mapped onto each assembly. The PFP assembly is indicated in the upper third of each panel; the Celera assembly is indicated in the lower third. In the center of the panel, green lines show Celera sequences that are in the same order and orientation in both assemblies and form the longest consistently ordered run of sequences. Yellow lines indicate sequence blocks that are in the same orientation, but out of order. Red lines indicate sequence blocks that are not in the same orientation. For clarity, in the latter two cases, lines are only drawn between segments of matching sequence that are at least 50 kbp long. The top and bottom thirds of each panel show the extent of Celera mate-pair violations (red, misoriented; yellow, incorrect distance between the mates) for each assembly grouped by library size. (Mate pairs that are within the correct distance, as expected from the mean library insert size, are omitted from the figure for clarity.) Predicted breakpoints, corresponding to stacks of violated mate pairs of the same type, are shown as blue ticks on each assembly axis. Runs of more than 10,000 Ns are shown as cyan bars. Plots of all 24 chromosomes can be seen in Web fig. 3 on *Science* Online at www.sciencemag.org/cgi/content/full/291/5507/1304/DC1.

evaluates evidence generated by the computational pipeline, corresponding to conservation between mouse and human genomic DNA, similarity to human transcripts (ESTs and cDNAs), similarity to rodent transcripts (ESTs and cDNAs), and similarity of the translation of human genomic DNA to known proteins to predict potential genes in the human genome. The sequence from the region of genomic DNA contained in a gene bin was extracted, and the subsequences supported by any homology evidence were marked (plus 100

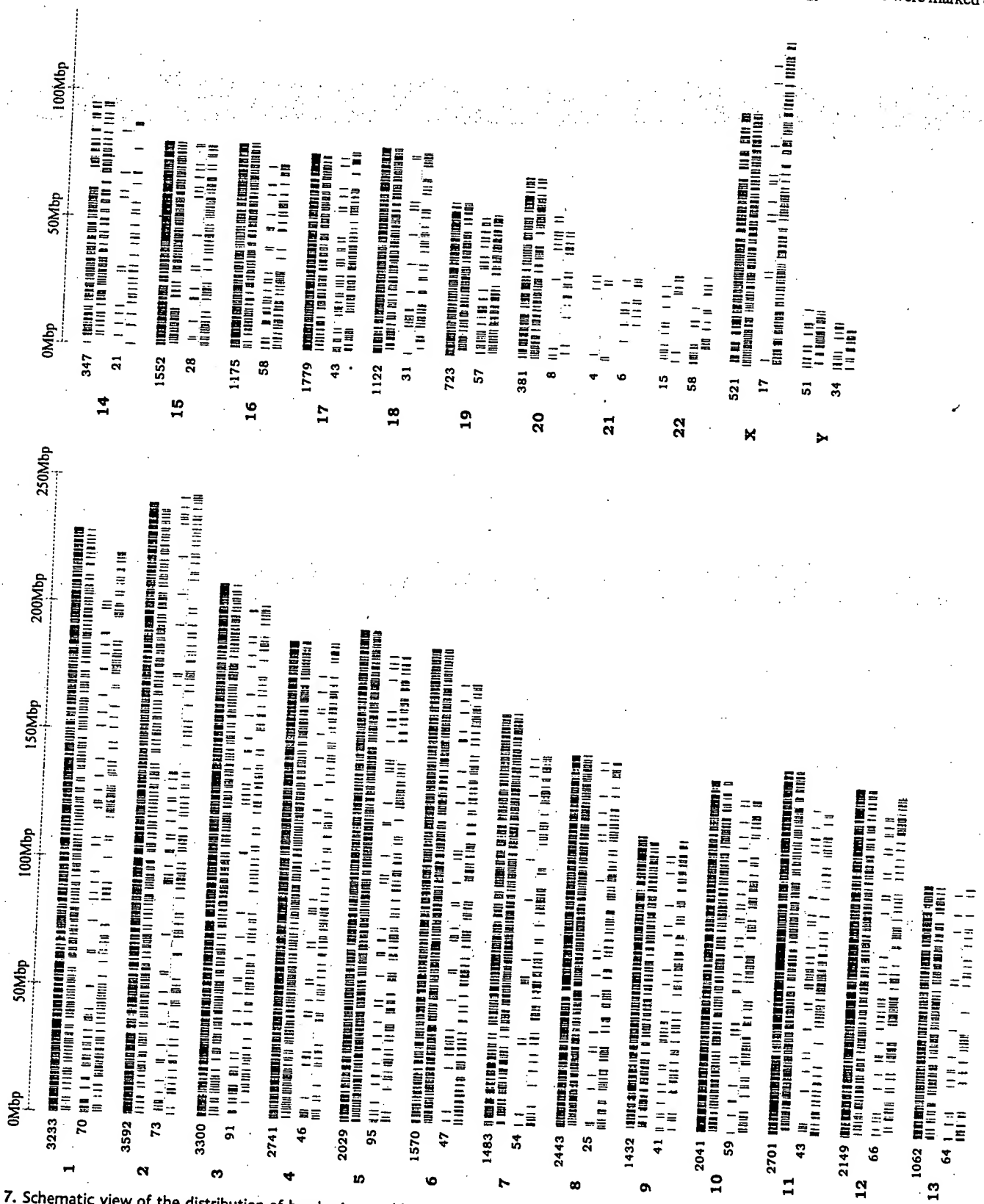

Fig. 7. Schematic view of the distribution of breakpoints and large gaps on all chromosomes. For each chromosome, the upper pair of lines represent the PFP assembly, and the lower pair of lines represent Celera's assembly. Blue tick marks represent breakpoints, whereas red tick marks represent a gap of larger than 10,000 bp. The number of breakpoints per chromosome is indicated in black, and the chromosome numbers in red.

bases flanking these regions). The other bases in the region, those not covered by any homology evidence, were replaced by N's. This sequence segment, with high confidence regions represented by the consensus genomic sequence and the remainder represented by N's, was then evaluated by Genscan to see if a consistent gene model could be generated. This procedure simplified the gene-prediction task by first establishing the boundary for the gene (not a strength of most gene-finding algorithms), and by eliminating regions with no supporting evidence. If Genscan returned a plausible gene model, it was further evaluated before being promoted to an "Otto" annotation. The final Genscan predictions were often quite different from the prediction that Genscan returned on the same region of native genomic sequence. A weakness of using Genscan to refine the gene model is the loss of valid, small exons from the final annotation.

The next step in defining gene structures based on sequence similarity was to compare each predicted transcript with the homology-based evidence that was used in previous steps to evaluate the depth of evidence for each exon in the prediction. Internal exons were considered to be supported if they were covered by homology evidence to within ±10 bases of their edges. For first and last exons, the internal edge was required to be within 10 bases, but the external edge was allowed greater latitude to allow for 5′ and 3′ untranslated regions (UTRs). To be retained, a prediction for a multi-exon gene must have evidence such that the total number of "hits," as defined above, divided by the number of exons in the prediction must be >0.66 or must correspond to a RefSeq sequence. A single-exon gene must be covered by at least three supporting hits (±10 bases on each side), and these must cover the complete predicted open reading frame. For a single-exon gene, we also required that the Genscan prediction include both a start and a stop codon. Gene models that did not meet these criteria were disregarded, and those that passed were promoted to Otto predictions. Homology-based Otto predictions do not contain 3′ and 5′ untranslated sequence. Although three de novo gene-finding programs [GRAIL, Genscan, and FgenesH (*63*)] were run as part of the computational analysis, the results of these programs were not directly used in making the Otto predictions. Otto predicted 11,226 additional genes by means of sequence similarity.

Table 7. Sensitivity and specificity of Otto and Genscan. Sensitivity and specificity were calculated by first aligning the prediction to the published RefSeq transcript, tallying the number (*N*) of uniquely aligned RefSeq bases. Sensitivity is the ratio of *N* to the length of the published RefSeq transcript. Specificity is the ratio of *N* to the length of the prediction. All differences are significant (Tukey HSD; $P < 0.001$).

Method	Sensitivity	Specificity
Otto (RefSeq only)*	0.939	0.973
Otto (homology)†	0.604	0.884
Genscan	0.501	0.633

*Refers to those annotations produced by Otto using only the Sim4-polished RefSeq alignment rather than an evidence-based Genscan prediction. †Refers to those annotations produced by supplying all available evidence to Genscan.

3.2 Otto validation

To validate the Otto homology-based process and the method that Otto uses to define the structures of known genes, we compared transcripts predicted by Otto with their corresponding (and presumably correct) transcript from a set of 4512 RefSeq transcripts for which there was a unique SIM4 alignment (Table 7). In order to evaluate the relative performance of Otto and Genscan, we made three comparisons. The first involved a determination of the accuracy of gene models predicted by Otto with only homology data other than the corresponding RefSeq sequence (Otto homology in Table 7). We measured the sensitivity (correctly predicted bases divided by the total length of the cDNA) and specificity (correctly predicted bases divided by the sum of the correctly and incorrectly predicted bases). Second, we examined the sensitivity and specificity of the Otto predictions that were made solely with the RefSeq sequence, which is the process that Otto uses to annotate known genes (Otto-RefSeq). And third, we determined the accuracy of the Genscan predictions corresponding to these RefSeq sequences. As expected, the alignment method (Otto-RefSeq) was the most accurate, and Otto-homology performed better than Genscan by both criteria. Thus, 6.1% of true RefSeq nucleotides were not represented in the Otto-refseq annotations and 2.7% of the nucleotides in the Otto-RefSeq transcripts were not contained in the original RefSeq transcripts. The discrepancies could come from legitimate differences between the Celera assembly and the RefSeq transcript due to polymorphisms, incomplete or incorrect data in the Celera assembly, errors introduced by Sim4 during the alignment process, or the presence of alternatively spliced forms in the data set used for the comparisons.

Because Otto uses an evidence-based approach to reconstruct genes, the absence of experimental evidence for intervening exons may inadvertantly result in a set of exons that cannot be spliced together to give rise to a transcript. In such cases, Otto may "split genes" when in fact all the evidence should be combined into a single transcript. We also examined the tendency of these methods to incorrectly split gene predictions. These trends are shown in Fig. 8. Both RefSeq and homology-based predictions by Otto split known genes into fewer segments than Genscan alone.

3.3 Gene number

Recognizing that the Otto system is quite conservative, we used a different gene-prediction strategy in regions where the homology evidence was less strong. Here the results of de novo gene predictions were used. For these genes, we insisted that a predicted transcript have at least two of the following types of evidence to be included in the gene set for further analysis: protein, human EST, rodent EST, or mouse genome fragment matches. This final class of predicted genes is a subset of the predictions made by the three gene-finding programs that were used in the computational pipeline. For these, there was not sufficient sequence similarity information for Otto to attempt to predict a gene structure. The three de novo gene-finding programs resulted in about 155,695 predictions, of which ~76,410 were nonredundant (nonoverlapping with one another). Of these, 57,935 did not overlap known genes or predictions made by Otto. Only 21,350 of the gene predictions that did not overlap Otto predictions were partially supported by at least one type of sequence similarity evidence, and 8619 were partially supported by two types of evidence (Table 8).

The sum of this number (21,350) and the number of Otto annotations (17,764), 39,114, is near the upper limit for the human gene complement. As seen in Table 8, if the requirement for other supporting evidence is made more stringent, this number drops rapidly so that demanding two types of evidence reduces the total gene number to 26,383 and demanding three types reduces it to ~23,000. Requiring that a prediction be supported by all four categories of evidence is too stringent because it would eliminate genes that encode novel proteins (members of currently undescribed protein families). No correction for pseudogenes has been made at this point in the analysis.

In a further attempt to identify genes that were not found by the autoannotation process or any of the de novo gene finders, we examined regions outside of gene predictions that were similar to the EST sequence, and where the EST matched the genomic sequence across a splice junction. After correcting for potential 3′ UTRs of predicted genes, about 2500 such regions remained. Addition of a requirement for at least one of the following evidence types—homology to mouse genomic sequence fragments, rodent ESTs, or cDNAs—or similarity to a known protein reduced this number to 1010. Adding this to the numbers from the previous paragraph would give us estimates of about 40,000, 27,000, and 24,000 potential genes in the human genome, depending on the stringency of evidence considered. Table 8 illustrates the number of genes and presents the degree of

confidence based on the supporting evidence. Transcripts encoded by a set of 26,383 genes were assembled for further analysis. This set includes the 6538 genes predicted by Otto on the basis of matches to known genes, 11,226 transcripts predicted by Otto based on homology evidence, and 8619 from the subset of transcripts from de novo gene-prediction programs that have two types of supporting evidence. The 26,383 genes are illustrated along chromosome diagrams in Fig. 1. These are a very preliminary set of annotations and are subject to all the limitations of an automated process. Considerable refinement is still necessary to improve the accuracy of these transcript predictions. All the predictions and descriptions of genes and the associated evidence that we present are the product of completely computational processes, not expert curation. We have attempted to enumerate the genes in the human genome in such a way that we have different levels of confidence based on the amount of supporting evidence: known genes, genes with good protein or EST homology evidence, and de novo gene predictions confirmed by modest homology evidence.

3.4 Features of human gene transcripts

We estimate the average span for a "typical" gene in the human DNA sequence to be about 27,894 bases. This is based on the average span covered by RefSeq transcripts, used because it represents our highest confidence set.

The set of transcripts promoted to gene annotations varies in a number of ways. As can be seen from Table 8 and Fig. 9, transcripts predicted by Otto tend to be longer, having on average about 7.8 exons, whereas those promoted from gene-prediction programs average about 3.7 exons. The largest number of exons that we have identified in a transcript is 234 in the titin mRNA. Table 8 compares the amounts of evidence that support the Otto and other predicted transcripts. For example, one can see that a typical Otto transcript has 6.99 of its 7.81 exons supported by protein homology evidence. As would be expected, the Otto transcripts generally have more support than do transcripts predicted by the de novo methods.

4 Genome Structure

Summary. This section describes several of the noncoding attributes of the assembled genome sequence and their correlations with the predicted gene set. These include an analysis of G+C content and gene density in the context of cytogenetic maps of the genome, an enumerative analysis of CpG islands, and a brief description of the genome-wide repetitive elements.

4.1 Cytogenetic maps

Perhaps the most obvious, and certainly the most visible, element of the structure of the genome is the banding pattern produced by Giemsa stain. Chromosomal banding studies have revealed that about 17% to 20% of the human chromosome complement consists of C-bands, or constitutive heterochromatin (*64*). Much of this heterochromatin is highly polymorphic and consists of different families of alpha satellite DNAs with various higher order repeat structures (*65*). Many chromosomes have complex inter- and intrachromosomal duplications present in pericentromeric regions (*66*). About 5% of the sequence reads were identified as alpha satellite sequences; these were not included in the assembly.

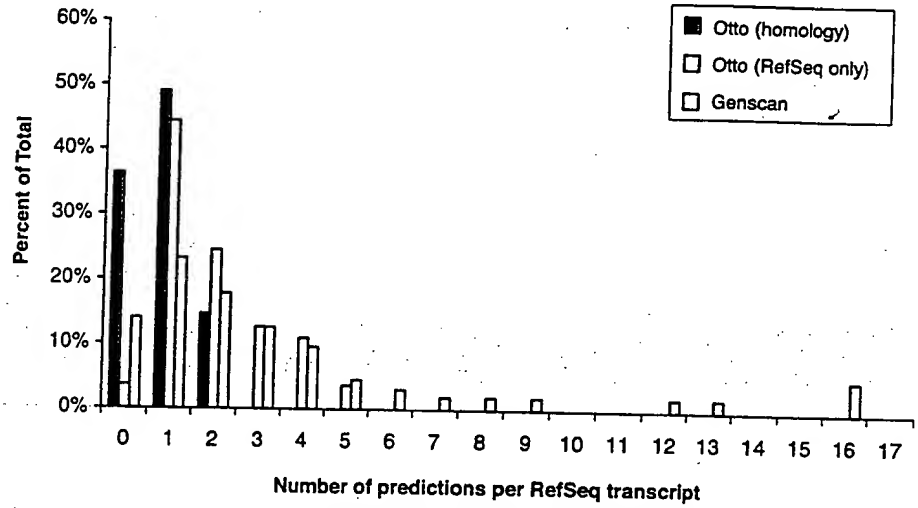

Fig. 8. Analysis of split genes resulting from different annotation methods. A set of 4512 Sim4-based alignments of RefSeq transcripts to the genomic assembly were chosen (see the text for criteria), and the numbers of overlapping Genscan, Otto (RefSeq only) annotations based solely on Sim4-polished RefSeq alignments, and Otto (homology) annotations (annotations produced by supplying all available evidence to Genscan) were tallied. These data show the degree to which multiple Genscan predictions and/or Otto annotations were associated with a single RefSeq transcript. The zero class for the Otto-homology predictions shown here indicates that the Otto-homology calls were made without recourse to the RefSeq transcript, and thus no Otto call was made because of insufficient evidence.

Table 8. Numbers of exons and transcripts supported by various types of evidence for Otto and de novo gene prediction methods. Highlighted cells indicate the gene sets analyzed in this paper (boldface, set of genes selected for protein analysis; italic, total set of accepted de novo predictions).

		Total	Types of evidence				No. of lines of evidence*			
			Mouse	Rodent	Protein	Human	≥1	≥2	≥3	≥4
Otto	Number of transcripts	17,969	17,065	14,881	15,477	16,374	**17,968**†	17,501	15,877	12,451
	Number of exons	141,218	111,174	89,569	108,431	118,869	140,710	127,955	99,574	59,804
De novo	Number of transcripts	58,032	14,463	5,094	8,043	9,220	*21,350*	**8,619**	4,947	1,904
	Number of exons	319,935	48,594	19,344	26,264	40,104	79,148	31,130	17,508	6,520
No. of exons per transcript	Otto	7.84	5.77	6.01	6.99	7.24	7.81	7.19	6.00	4.28
	De novo	5.53	3.17	3.80	3.27	4.36	3.7	3.56	3.42	3.16

*Four kinds of evidence (conservation in 3× mouse genomic DNA, similarity to human EST or cDNA, similarity to rodent EST or cDNA, and similarity to known proteins) were considered to support gene predictions from the different methods. The use of evidence is quite liberal, requiring only a partial match to a single exon of predicted transcript. †This number includes alternative splice forms of the 17,764 genes mentioned elsewhere in the text.

Examination of pericentromeric regions is ongoing.

The remaining ~80% of the genome, the euchromatic component, is divisible into G-, R-, and T-bands (*67*). These cytogenetic bands have been presumed to differ in their nucleotide composition and gene density, although we have been unable to determine precise band boundaries at the molecular level. T-bands are the most G+C- and gene-rich, and G-bands are G+C-poor (*68*). Bernardi has also offered a description of the euchromatin at the molecular level as long stretches of DNA of differing base composition, termed isochores (denoted L, H1, H2, and H3), which are >300 kbp in length (*69*). Bernardi defined the L (light) isochores as G+C-poor (<43%), whereas the H (heavy) isochores fall into three G+C-rich classes representing 24, 8, and 5% of the genome. Gene concentration has been claimed to be very low in the L isochores and 20-fold more enriched in the H2 and H3 isochores (*70*). By examining contiguous 50-kbp windows of G+C content across the assembly, we found that regions of G+C content >48% (H3 isochores) averaged 273.9 kbp in length, those with G+C content between 43 and 48% (H1+H2 isochores) averaged 202.8 kbp in length, and the average span of regions with <43% (L isochores) was 1078.6 kbp. The correlation between G+C content and gene density was also examined in 50-kbp windows along the assembled sequence (Table 9 and Figs. 10 and 11). We found that the density of genes was greater in regions of high G+C than in regions of low G+C content, as expected. However, the correlation between G+C content and gene density was not as skewed as previously predicted (*69*). A higher proportion of genes were located in the G+C-poor regions than had been expected.

Chromosomes 17, 19, and 22, which have a disproportionate number of H3-containing bands, had the highest gene density (Table 10). Conversely, of the chromosomes that we found to have the lowest gene density, X, 4, 18, 13, and Y, also have the fewest H3 bands. Chromosome 15, which also has few H3 bands, did not have a particularly low gene density in our analysis. In addition, chromosome 8, which we found to have a low gene density, does not appear to be unusual in its H3 banding.

How valid is Ohno's postulate (*71*) that mammalian genomes consist of oases of genes in otherwise essentially empty deserts? It appears that the human genome does indeed contain deserts, or large, gene-poor regions. If we define a desert as a region >500 kbp without a gene, then we see that 605 Mbp, or about 20% of the genome, is in deserts. These are not uniformly distributed over the various chromosomes. Gene-rich chromosomes 17, 19, and 22 have only about 12% of their collective 171 Mbp in deserts, whereas gene-poor chromosomes 4, 13, 18, and X have 27.5% of their 492 Mbp in deserts (Table 11). The apparent lack of predicted genes in these regions does not necessarily imply that they are devoid of biological function.

4.2 Linkage map

Linkage maps provide the basis for genetic analysis and are widely used in the study of the inheritance of traits and in the positional cloning of genes. The distance metric, centimorgans (cM), is based on the recombination rate between homologous chromosomes during meiosis. In general, the rate of recombination in females is greater than that in males, and this degree of map expansion is not uniform across the genome (*72*). One of the opportunities enabled by a nearly complete genome sequence is to produce the ultimate physical map, and to fully analyze its correspondence with two other maps that have been widely used in genome and genetic analysis: the linkage map and the cytogenetic map. This would close the loop between the mapping and sequencing phases of the genome project.

We mapped the location of the markers that constitute the Genethon linkage map to the genome. The rate of recombination, expressed as cM per Mbp, was calculated for 3-Mbp windows as shown in Table 12. Higher rates of recombination in the telomeric region of the chromosomes have been previously documented (*73*). From this mapping result, there is a difference of 4.99 between lowest rates and highest rates and the largest difference of 4.4 between males and females (4.99 to 0.47 on chromosome 16). This indicates that the variability in recombination rates among regions of the genome exceeds the differences in recombination rates between males and females. The human genome has recombination hotspots, where recombination rates vary fivefold or more over a space of 1 kbp, so the picture one gets of the magnitude of variability in recombination rate will depend on the size of the window

Table 9. Characteristics of G+C in isochores.

Isochore	G+C (%)	Fraction of genome		Fraction of genes	
		Predicted*	Observed	Predicted*	Observed
H3	>48	5	9.5	37	24.8
H1/H2	43–48	25	21.2	32	26.6
L	<43	67	69.2	31	48.5

*The predictions were based on Bernardi's definitions (*70*) of the isochore structure of the human genome.

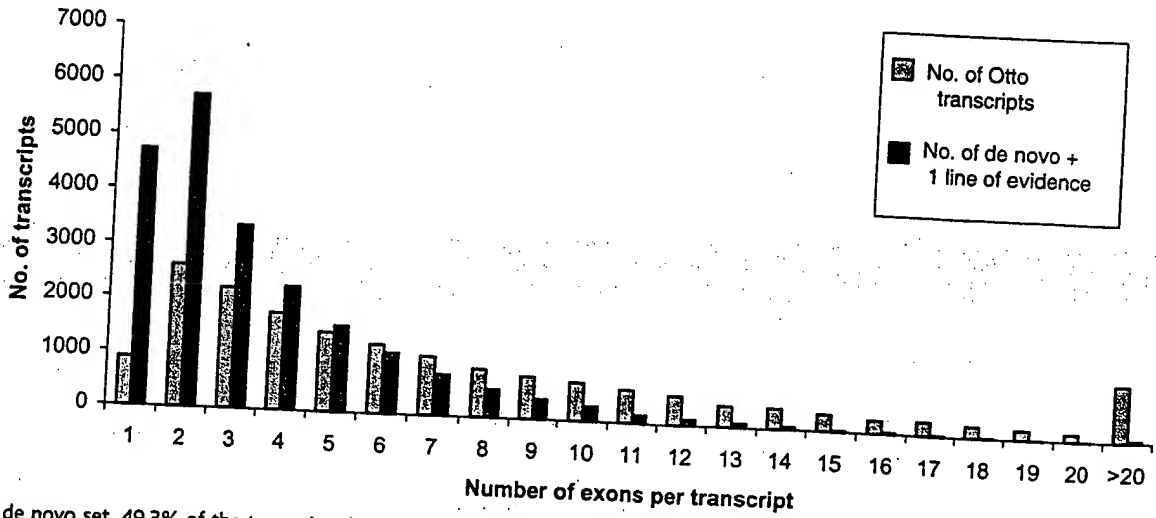

Fig. 9. Comparison of the number of exons per transcript between the 17,968 Otto transcripts and 21,350 de novo transcript predictions with at least one line of evidence that do not overlap with an Otto prediction. Both sets have the highest number of transcripts in the two-exon category, but the de novo gene predictions are skewed much more toward smaller transcripts. In the Otto set, 19.7% of the transcripts have one or two exons, and 5.7% have more than 20. In the de novo set, 49.3% of the transcripts have one or two exons, and 0.2% have more than 20.

examined. Unfortunately, too few meiotic crossovers have occurred in Centre d'Étude du Polymorphism Humain (CEPH) and other reference families to provide a resolution any finer than about 3 Mbp. The next challenge will be to determine a sequence basis of recombination at the chromosomal level. An accurate predictor for the rate for variation in recombination rates between any pair of markers would be extremely useful in designing markers to narrow a region of linkage, such as in positional cloning projects.

4.3 Correlation between CpG islands and genes

CpG islands are stretches of unmethylated DNA with a higher frequency of CpG dinucleotides when compared with the entire genome (*74*). CpG islands are believed to preferentially occur at the transcriptional start of genes, and it has been observed that most housekeeping genes have CpG islands at the 5′ end of the transcript (*75*, *76*). In addition, experimental evidence indicates that CpG island methylation is correlated with gene inactivation (*77*) and has been shown to be important during gene imprinting (*78*) and tissue-specific gene expression (*79*)

Experimental methods have been used that resulted in an estimate of 30,000 to 45,000 CpG islands in the human genome (*74*, *80*) and an estimate of 499 CpG islands on human chromosome 22 (*81*). Larsen *et al.* (*76*) and Gardiner-Garden and Frommer (*75*) used a computational method to identify CpG islands and defined them as regions of DNA of >200 bp that have a G+C content of >50% and a ratio of observed versus expected frequency of CG dinucleotide ≥0.6.

It is difficult to make a direct comparison of experimental definitions of CpG islands with computational definitions because computational methods do not consider the methylation state of cytosine and experimental methods do not directly select regions of high G+C content. However, we can determine the correlation of CpG island with gene starts, given a set of annotated genomic transcripts and the whole genome sequence. We have analyzed the publicly available annotation of chromosome 22, as well as using the entire human genome in our assembly and the computationally annotated genes. A variation of the CpG island computation was compared with Larsen *et al.* (*76*). The main differences are that we use a sliding window of 200 bp, consecutive windows are merged only if they overlap, and we recompute the CpG value upon merging, thus rejecting any potential island if it scores less than the threshold.

To compute various CpG statistics, we used two different thresholds of CG dinucleotide likelihood ratio. Besides using the original threshold of 0.6 (method 1), we used a higher threshold of CG dinucleotide likelihood ratio of 0.8 (method 2), which results in the number of CpG islands on chromosome 22 close to the number of annotated genes on this chromosome. The main results are summarized in Table 13. CpG islands computed with method 1 predicted only 2.6% of the CSA sequence as CpG, but 40% of the gene starts (start codons) are contained inside a CpG island. This is comparable to ratios reported by others (*82*). The last two rows of the table show the observed and expected average distance, respectively, of the closest CpG island from the first exon. The observed average closest CpG islands are smaller than the corresponding expected distances, confirming an association between CpG island and the first exon.

We also looked at the distribution of CpG island nucleotides among various sequence classes such as intergenic regions, introns, exons, and first exons. We computed the likelihood score for each sequence class as the ratio of the observed fraction of CpG island nucleotides in that sequence class and the expected fraction of CpG island nucleotides in that sequence class. The result of applying method 1 on CSA were scores of 0.89 for intergenic region, 1.2 for intron, 5.86 for exon, and 13.2 for first exon. The same trend was also found for chromosome 22 and after the application of a higher threshold (method 2) on both data sets. In sum, genome-wide analysis has extended earlier analysis and suggests a strong correlation between CpG islands and first coding exons.

4.4 Genome-wide repetitive elements

The proportion of the genome covered by various classes of repetitive DNA is presented in Table 14. We observed about 35% of the genome in these repeat classes, very similar to values reported previously (*83*). Repetitive sequence may be underrepresented in the Celera assembly as a result of incomplete repeat resolution, as discussed above. About 8% of the scaffold length is in gaps, and we expect that much of this is repetitive sequence. Chromosome 19 has the highest repeat density (57%), as well as the highest gene density (Table 10). Of interest, among the different classes of repeat elements, we observe a clear association of Alu elements and gene density, which was not observed between LINEs and gene density.

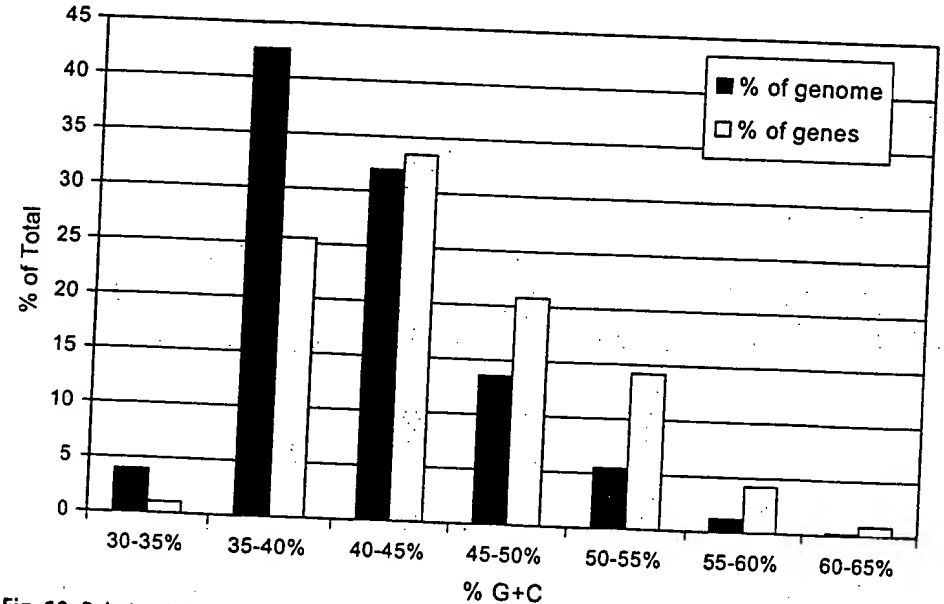

Fig. 10. Relation between G+C content and gene density. The blue bars show the percent of the genome (in 50-kbp windows) with the indicated G+C content. The percent of the total number of genes associated with each G+C bin is represented by the yellow bars. The graph shows that about 5% of the genome has a G+C content of between 50 and 55%, but that this portion contains nearly 15% of the genes.

5 Genome Evolution

Summary. The dynamic nature of genome evolution can be captured at several levels. These include gene duplications mediated by RNA intermediates (retrotransposition) and segmental genomic duplications. In this section, we document the genome-wide occurrence of retrotransposition events generating functional (intronless paralogs) or inactive genes (pseudogenes). Genes involved in translational processes and nuclear regulation account for nearly 50% of all intronless paralogs and processed pseudogenes detected in our survey. We have also cataloged the extent of segmental genomic duplication and provide evidence for 1077 duplicated blocks covering 3522 distinct genes.

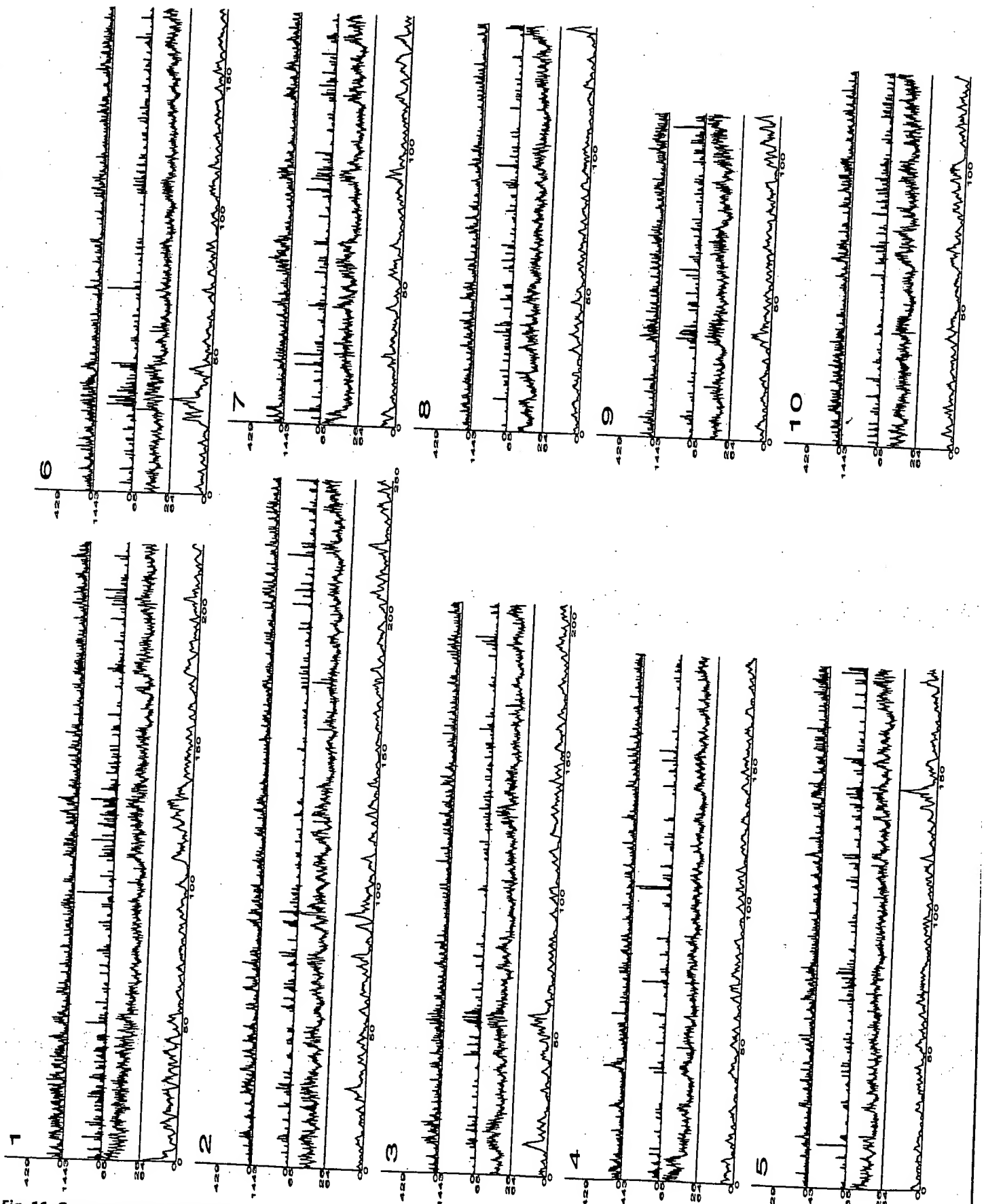

Fig. 11. Genome structural features.

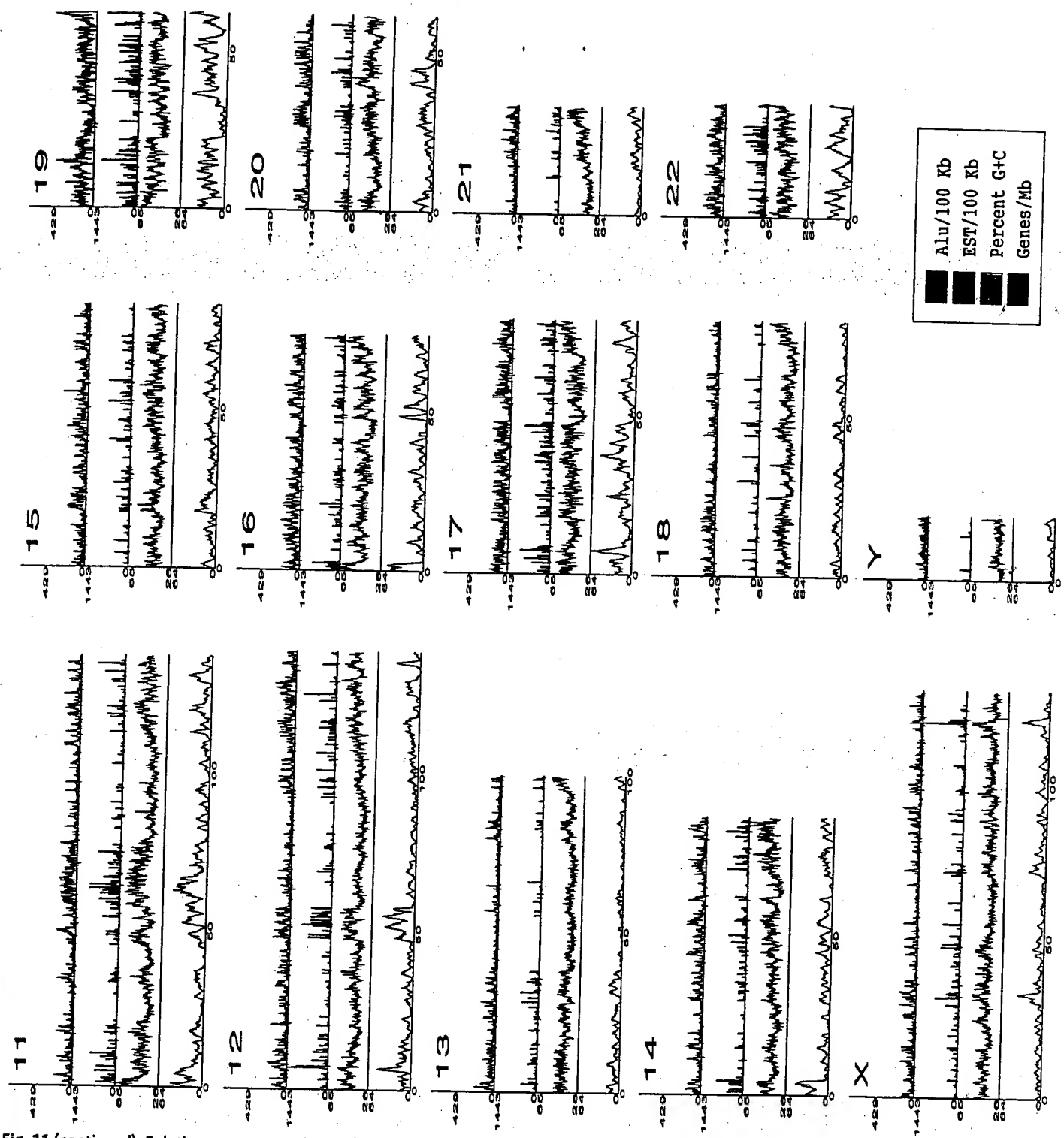

Fig. 11 (continued). Relation among gene density (orange), G+C content (green), EST density (blue), and Alu density (pink) along the lengths of each of the chromosomes. Gene density was calculated in 1-Mbp windows. The percent of G+C nucleotides was calculated in 100-kbp windows. The number of ESTs and Alu elements is shown per 100-kbp window.

5.1 Retrotransposition in the human genome

Retrotransposition of processed mRNA transcripts into the genome results in functional genes, called intronless paralogs, or inactivated genes (pseudogenes). A paralog refers to a gene that appears in more than one copy in a given organism as a result of a duplication event. The existence of both intron-containing and intronless forms of genes encoding functionally similar or identical proteins has been previously described (*84*, *85*). Cataloging these evolutionary events on the genomic landscape is of value in understanding the functional consequences of such gene-duplication events in cellular biology. Identification of conserved intronless paralogs in the mouse or other mammalian genomes should provide the basis for capturing the evolutionary chronology of these transposition events and provide insights into gene loss and accretion in the mammalian radiation.

A set of proteins corresponding to all 901

Table 10. Features of the chromosomes. De novo/any refers to the union of de novo predictions that do not overlap Otto predictions and have at least one other type of supporting evidence; de novo/2x refers to the union of de novo predictions that do not overlap Otto predictions and have at least two types of evidence. Deserts are regions of sequence with no annotated genes.

	Sequence coverage (CS assembly)						Base composition			Gene prediction*					Gene density (genes/Mbp)					
Chr.	Size (Mbp)	No. of scaffolds	Largest scaffold (Mbp)	No. of scaffolds >500 kbp	Sequence covered by scaffolds >500 kbp	% of total sequence in scaffolds >500 kbp	% repeat	% GC	No of CpG islands	Otto	De novo/any	De novo/2×	Total (Otto + de novo/any)	Total (Otto + de novo/any)	Sequence in deserts >500/kbp	Sequence in deserts >1 Mbp	Otto	De novo/any	De novo/2×	Otto + de novo/any	Otto + de novo/2×
1	220	2,549	11	82	192	88	37	42	2,335	1,743	1,710	710	3,453	2,453	29	6	8	8	3	16	11
2	240	3,263	13	78	217	91	36	40	1,703	1,183	1,771	633	2,954	1,816	55	19	5	7	2	12	7
3	200	3,532	7	78	173	87	37	40	1,271	1,013	1,414	598	2,427	1,611	50	12	5	7	3	12	8
4	186	2,180	10	70	169	91	37	38	1,081	696	1,165	449	1,861	1,145	55	18	4	6	2	10	6
5	182	3,231	11	63	163	89	37	40	1,302	892	1,244	474	2,136	1,366	46	15	5	7	2	11	7
6	172	1,713	13	58	160	93	37	40	1,384	943	1,314	524	2,257	1,467	38	9	6	7	3	13	8
7	146	1,326	14	53	130	89	38	40	1,406	759	1,072	460	1,831	1,219	26	12	5	7	3	12	8
8	146	1,772	11	54	135	92	36	40	948	583	977	357	1,560	940	33	6	4	7	2	11	6
9	113	1,616	8	40	101	89	38	41	1,315	689	848	329	1,537	1,018	22	9	6	7	3	13	8
10	130	2,005	9	55	116	89	36	42	1,087	685	968	342	1,653	1,027	21	8	5	7	2	12	7
11	132	2,814	9	44	116	88	39	42	1,461	1,051	1,134	535	2,185	1,586	27	9	8	8	4	16	12
12	134	2,614	8	51	117	87	38	41	1,131	925	936	417	1,861	1,342	24	9	7	7	3	14	10
13	99	1,038	13	34	91	91	36	38	644	341	691	241	1,032	582	31	16	4	7	2	10	5
14	87	576	11	16	83	95	40	41	913	583	700	290	1,283	873	34	20	7	8	3	14	10
15	80	1,747	8	31	70	87	37	42	722	558	640	246	1,198	804	8	1	7	8	3	15	10
16	75	1,520	8	27	62	82	40	44	1,533	748	673	247	1,421	995	13	3	10	9	3	19	12
17	78	1,683	6	40	61	78	39	45	1,489	897	648	313	1,545	1,210	15	6	12	8	4	19	15
18	79	1,333	13	18	72	92	36	40	510	283	543	189	826	472	21	10	4	7	2	10	6
19	58	2,282	3	31	38	67	57	49	2,804	1,141	534	268	1,675	1,409	3	0	20	9	4	29	23
20	61	580	14	17	58	94	41	44	997	517	469	180	986	697	7	1	8	7	3	16	11
21	33	358	10	6	32	96	38	41	519	184	265	102	449	286	15	9	6	8	3	13	8
22	36	333	11	12	32	88	44	48	1,173	494	341	147	835	641	3	0	14	9	4	23	17
X	128	1,346	4	91	93	73	46	39	726	605	860	387	1,465	992	29	8	5	6	3	11	7
Y	19	638	2	10	12	65	50	39	65	55	155	49	210	104	4	2	3	8	2	11	5
U*	75	11,542	1						479	196	278	132	474	328							
Total	2907	53,591		1,059	2,490				28,519	17,764	21,350	8,619	39,114	26,383	606	208					
Avg.	116	2,144	9	44	104	87	40	41	1,160	714	812	333	1,526	1,047	25	9	7	7	3	14	9

*Chromosomal assignment unknown.

Otto-predicted, single-exon genes were subjected to BLAST analysis against the proteins encoded by the remaining multiexon predicted transcripts. Using homology criteria of 70% sequence identity over 90% of the length, we identified 298 instances of single- to multi-exon correspondence. Of these 298 sequences, 97 were represented in the GenBank data set of experimentally validated full-length genes at the stringency specified and were verified by manual inspection.

We believe that these 97 cases may represent intronless paralogs (see Web table 1 on *Science* Online at www.sciencemag.org/cgi/content/full/291/5507/1304/DC1) of known genes. Most of these are flanked by direct repeat sequences, although the precise nature of these repeats remains to be determined. All of the cases for which we have high confidence contain polyadenylated [poly(A)] tails characteristic of retrotransposition.

Recent publications describing the phenomenon of functional intronless paralogs speculate that retrotransposition may serve as a mechanism used to escape X-chromosomal inactivation (*84*, *86*). We do not find a bias toward X chromosome origination of these retrotransposed genes; rather, the results show a random chromosome distribution of both the intron-containing and corresponding intronless paralogs. We also have found several cases of retrotransposition from a single source chromosome to multiple target chromosomes. Interesting examples include the retrotransposition of a five exon–containing ribosomal protein L21 gene on chromosome 13 onto chromosomes 1, 3, 4, 7, 10, and 14, respectively. The size of the source genes can also show variability. The largest example is the 31-exon diacylglycerol kinase zeta gene on chromosome 11 that has an intronless paralog on chromosome 13. Regardless of route, retrotransposition with subsequent gene changes in coding or noncoding regions that lead to different functions or expression patterns, represents a key route to providing an enhanced functional repertoire in mammals (*87*).

Our preliminary set of retrotransposed intronless paralogs contains a clear overrepresentation of genes involved in translational processes (40% ribosomal proteins and 10% translation elongation factors) and nuclear regulation (HMG nonhistone proteins, 4%), as well as metabolic and regulatory enzymes. EST matches specific to a subset of intronless paralogs suggest expression of these intronless paralogs. Differences in the upstream regulatory sequences between the source genes and their intronless paralogs could account for differences in tissue-specific gene expression. Defining which, if any, of these processed genes are functionally expressed and translated will require further elucidation and experimental validation.

5.2 Pseudogenes

A pseudogene is a nonfunctional copy that is very similar to a normal gene but that has been altered slightly so that it is not expressed. We developed a method for the preliminary analysis of processed pseudogenes in the human genome as a starting point in elucidating the ongoing evolutionary forces

Table 11. Genome overview.

Size of the genome (including gaps)	2.91 Gbp
Size of the genome (excluding gaps)	2.66 Gbp
Longest contig	1.99 Mbp
Longest scaffold	14.4 Mbp
Percent of A+T in the genome	54
Percent of G+C in the genome	38
Percent of undetermined bases in the genome	9
Most GC-rich 50 kb	Chr. 2 (66%)
Least GC-rich 50 kb	Chr. X (25%)
Percent of genome classified as repeats	35
Number of annotated genes	26,383
Percent of annotated genes with unknown function	42
Number of genes (hypothetical and annotated)	39,114
Percent of hypothetical and annotated genes with unknown function	59
Gene with the most exons	Titin (234 exons)
Average gene size	27 kbp
Most gene-rich chromosome	Chr. 19 (23 genes/Mb)
Least gene-rich chromosomes	Chr. 13 (5 genes/Mb), Chr. Y (5 genes/Mb)
Total size of gene deserts (>500 kb with no annotated genes)	605 Mbp
Percent of base pairs spanned by genes	25.5 to 37.8*
Percent of base pairs spanned by exons	1.1 to 1.4*
Percent of base pairs spanned by introns	24.4 to 36.4*
Percent of base pairs in intergenic DNA	74.5 to 63.6*
Chromosome with highest proportion of DNA in annotated exons	Chr. 19 (9.33)
Chromosome with lowest proportion of DNA in annotated exons	Chr. Y (0.36)
Longest intergenic region (between annotated + hypothetical genes)	Chr. 13 (3,038,416 bp)
Rate of SNP variation	1/1250 bp

*In these ranges, the percentages correspond to the annotated gene set (26, 383 genes) and the hypothetical + annotated gene set (39,114 genes), respectively.

Table 12. Rate of recombination per physical distance (cM/Mb) across the genome. Genethon markers were placed on CSA-mapped assemblies, and then relative physical distances and rates were calculated in 3-Mb windows for each chromosome. NA, not applicable.

Chrom.	Male			Sex-average			Female		
	Max.	Avg.	Min.	Max.	Avg.	Min.	Max.	Avg.	Min.
1	2.60	1.12	0.23	2.81	1.42	0.52	3.39	1.76	0.68
2	2.23	0.78	0.33	2.65	1.12	0.54	3.17	1.40	0.61
3	2.55	0.86	0.23	2.40	1.07	0.42	2.71	1.30	0.33
4	1.66	0.67	0.15	2.06	1.04	0.60	2.50	1.40	0.77
5	2.00	0.67	0.18	1.87	1.08	0.42	2.26	1.43	0.62
6	1.97	0.71	0.28	2.57	1.12	0.37	3.47	1.67	0.64
7	2.34	1.16	0.48	1.67	1.17	0.47	2.27	1.21	0.34
8	1.83	0.73	0.14	2.40	1.05	0.46	3.44	1.36	0.43
9	2.01	0.99	0.53	1.95	1.32	0.77	2.63	1.66	0.82
10	3.73	1.03	0.22	3.05	1.29	0.66	2.84	1.51	0.76
11	1.43	0.72	0.31	2.13	0.99	0.47	3.10	1.32	0.49
12	4.12	0.76	0.26	3.35	1.16	0.49	2.93	1.55	0.59
13	1.60	0.75	0.01	1.87	0.95	0.17	2.49	1.19	0.32
14	3.15	0.98	0.18	2.65	1.30	0.62	3.14	1.63	0.75
15	2.28	0.94	0.34	2.31	1.22	0.42	2.53	1.56	0.54
16	1.83	1.00	0.47	2.70	1.55	0.63	4.99	2.32	1.12
17	3.87	0.87	0.00	3.54	1.35	0.54	4.19	1.83	0.94
18	3.12	1.37	0.86	3.75	1.66	0.43	4.35	2.24	0.72
19	3.02	0.97	0.10	2.57	1.41	0.49	2.89	1.75	0.87
20	3.64	0.89	0.00	2.79	1.50	0.83	3.31	2.15	1.34
21	3.23	1.26	0.69	2.37	1.62	1.08	2.58	1.90	1.18
22	1.25	1.10	0.84	1.88	1.41	1.08	3.73	2.08	0.93
X	NA	NA	NA	NA	NA	NA	3.12	1.64	0.72
Y	NA	NA	NA	NA	NA	NA	NA	NA	NA
Genome	4.12	0.88	0.00	3.75	1.22	0.17	4.99	1.55	0.32

that account for gene inactivation. The general structural characteristics of these processed pseudogenes include the complete lack of intervening sequences found in the functional counterparts, a poly(A) tract at the 3′ end, and direct repeats flanking the pseudogene sequence. Processed pseudogenes occur as a result of retrotransposition, whereas unprocessed pseudogenes arise from segmental genome duplication.

We searched the complete set of Otto-predicted transcripts against the genomic sequence by means of BLAST. Genomic regions corresponding to all Otto-predicted transcripts were excluded from this analysis. We identified 2909 regions matching with greater than 70% identity over at least 70% of the length of the transcripts that likely represent processed pseudogenes. This number is probably an underestimate because specific methods to search for pseudogenes were not used.

We looked for correlations between structural elements and the propensity for retrotransposition in the human genome. GC content and transcript length were compared between the genes with processed pseudogenes (1177 source genes) versus the remainder of the predicted gene set. Transcripts that give rise to processed pseudogenes have shorter average transcript length (1027 bp versus 1594 bp for the Otto set) as compared with genes for which no pseudogene was detected. The overall GC content did not show any significant difference, contrary to a recent report (*88*). There is a clear trend in gene families that are present as processed pseudogenes. These include ribosomal proteins (67%), lamin receptors (10%), translation elongation factor alpha (5%), and HMG–non-histone proteins (2%). The increased occurrence of retrotransposition (both intronless paralogs and processed pseudogenes) among genes involved in translation and nuclear regulation may reflect an increased transcriptional activity of these genes.

5.3 Gene duplication in the human genome

Building on a previously published procedure (*27*), we developed a graph-theoretic algorithm, called Lek, for grouping the predicted human protein set into protein families (*89*). The complete clusters that result from the Lek clustering provide one basis for comparing the role of whole-genome or chromosomal duplication in protein family expansion as opposed to other means, such as tandem duplication. Because each complete cluster represents a closed and certain island of homology, and because Lek is capable of simultaneously clustering protein complements of several organisms, the number of proteins contributed by each organism to a complete cluster can be predicted with confidence depending on the quality of the annotation of each genome. The variance of each organism's contribution to each cluster can then be calculated, allowing an assessment of the relative importance of large-scale duplication versus smaller-scale, organism-specific expansion and contraction of protein families, presumably as a result of natural selection operating on individual protein families within an organism. As can be seen in Fig. 12, the large variance in the relative numbers of human as compared with *D. melanogaster* and *Caenorhabditis elegans* proteins in complete clusters may be explained by multiple events of relative expansions in gene families in each of the three animal genomes. Such expansions would give rise to the distribution that shows a peak at 1:1 in the ratio for human-worm or human-fly clusters with the slope spread covering both human and fly/worm predominance, as we observed (Fig. 12). Furthermore, there are nearly as many clusters where worm and fly proteins predominate despite the larger numbers of proteins in the human. At face value, this analysis suggests that natural selection acting on individual protein families has been a major force driving the expansion of at least some elements of the human protein set. However, in our analysis, the difference between an ancient whole-genome duplication followed by loss, versus piecemeal duplication, cannot be easily distinguished. In order to differentiate these scenarios, more extended analyses were performed.

Table 13. Characteristics of CpG islands identified in chromosome 22 (34-Mbp sequence length) and the whole genome (2.9-Gbp sequence length) by means of two different methods. Method 1 uses a CG likelihood ratio of ≥0.6. Method 2 uses a CG likelihood ratio of ≥0.8.

	Chromosome 22		Whole genome (CS assembly)	
	Method 1	Method 2	Method 1	Method 2
Number of CpG islands detected	5,211	522	195,706	26,876
Average length of island (bp)	390	535	395	497
Percent of sequence predicted as CpG	5.9	0.8	2.6	0.4
Percent of first exons that overlap a CpG island	44	25	42	22
Percent of first exons with first position of exon contained inside a CpG island	37	22	40	21
Average distance between first exon and closest CpG island (bp)	1,013	10,486	2,182	17,021
Expected distance between first exon and closest CpG island (bp)	3,262	32,567	7,164	55,811

Table 14. Distribution of repetitive DNA in the compartmentalized shotgun assembly sequence.

Repetitive elements	Megabases in assembled sequences	Percent of assembly	Previously predicted (%) (*83*)
Alu	288	9.9	10.0
Mammalian interspersed repeat (MIR)	66	2.3	1.7
Medium reiteration (MER)	50	1.7	1.6
Long terminal repeat (LTR)	155	5.3	5.6
Long interspersed nucleotide element (LINE)	466	16.1	16.7
Total	1025	35.3	35.6

5.4 Large-scale duplications

Using two independent methods, we searched for large-scale duplications in the human genome. First, we describe a protein family–based method that identified highly conserved blocks of duplication. We then describe our comprehensive method for identifying all interchromosomal block duplications. The latter method identified a large number of duplicated chromosomal segments covering parts of all 24 chromosomes.

The first of the methods is based on the idea of searching for blocks of highly conserved homologous proteins that occur in more than one location on the genome. For this comparison, two genes were considered equivalent if their protein products were de-

termined to be in the same family and the same complete Lek cluster (essentially paralogous genes) (*89*). Initially, each chromosome was represented as a string of genes ordered by the start codons for predicted genes along the chromosome. We considered the two strands as a single string, because local inversions are relatively common events relative to large-scale duplications. Each gene was indexed according to the protein family and Lek complete cluster (*89*). All pairs of indexed gene strings were then aligned in both the forward and reverse directions with the Smith-Waterman algorithm (*90*). A match between two proteins of the same Lek complete cluster was given a score of 10 and a mismatch −10, with gap open and extend penalties of −4 and −1. With these parameters, 19 conserved interchromosomal blocks of duplication were observed, all of which were also detected and expanded by the comprehensive method described below. The detection of only a relatively small number of block duplications was a consequence of using an intrinsically conservative method grounded in the conservative constraints of the complete Lek clusters.

In the second, more comprehensive approach, we aligned all chromosomes directly with one another using an algorithm based on the MUMmer system (*91*). This alignment method uses a suffix tree data structure and a linear-time algorithm to align long sequences very rapidly; for example, two chromosomes of 100 Mbp can be aligned in less than 20 min (on a Compaq Alpha computer) with 4 gigabytes of memory. This procedure was used recently to identify numerous large-scale segmental duplications among the five chromosomes of *A. thaliana* (*92*); in that organism, the method revealed that 60% of the genome (66 Mbp) is covered by 24 very large duplicated segments. For *Arabidopsis*, a DNA-based alignment was sufficient to reveal the segmental duplications between chromosomes; in the human genome, DNA alignments at the whole-chromosome level are insufficiently sensitive. Therefore, a modified procedure was developed and applied, as follows. First, all 26,588 proteins (9,675,713 million amino acids) were concatenated end-to-end in order as they occur along each of the 24 chromosomes, irrespective of strand location. The concatenated protein set was then aligned against each chromosome by the MUMmer algorithm. The resulting matches were clustered to extract all sets of three or more protein matches that occur in close proximity on two different chromosomes (*93*); these represent the candidate segmental duplications. A series of filters were developed and applied to remove likely false-positives from this set; for example, small blocks that were spread across many proteins were removed. To refine the filtering methods, a shuffled protein set was first created by taking the 26,588 proteins, randomizing their order, and then partitioning them into 24 shuffled chromosomes, each containing the same number of proteins as the true genome. This shuffled protein set has the identical composition to the real genome; in particular, every protein and every domain appears the same number of times. The complete algorithm was then applied to both the real and the shuffled data, with the results on the shuffled data being used to estimate the false-positive rate. The algorithm after filtering yielded 10,310 gene pairs in 1077 duplicated blocks containing 3522 distinct genes; tandemly duplicated expansions in many of the blocks explain the excess of gene pairs to distinct genes. In the shuffled data, by contrast, only 370 gene pairs were found, giving a false-positive estimate of 3.6%. The most likely explanation for the 1077 block duplications is ancient segmental duplications. In many cases, the order of the proteins has been shuffled, although proximity is preserved. Out of the 1077 blocks, 159 contain only three genes, 137 contain four genes, and 781 contain five or more genes.

To illustrate the extent of the detected duplications, Fig. 13 shows all 1077 block duplications indexed to each chromosome in 24 panels in which only duplications mapped to the indexed chromosome are displayed. The figure makes it clear that the duplications are ubiquitous in the genome. One feature that it displays is many relatively small chromosomal stretches, with one-to-many duplication relationships that are graphically striking. One such example captured by the analysis is the well-documented olfactory receptor (OR) family, which is scattered in blocks throughout the genome and which has been analyzed for genome-deployment reconstructions at several evolutionary stages (*94*). The figure also illustrates that some chromosomes, such as chromosome 2, contain many more detected large-scale duplications than others. Indeed, one of the largest duplicated segments is a large block of 33 proteins on chromosome 2, spread among eight smaller blocks in 2p, that aligns to a paralogous set on chromosome 14, with one rearrangement (see chromosomes 2 and 14 panels in Fig. 13). The proteins are not contiguous but span a region containing 97 proteins on chromosome 2 and 332 proteins on chromosome 14. The likelihood of observing this many duplicated proteins by chance, even over a span of this length, is 2.3×10^{-68} (*93*). This duplicated set spans 20 Mbp on chromosome 2 and 63 Mbp on chromosome 14, over 70% of the latter chromosome. Chromosome 2 also contains a block duplication that is nearly as large, which is shared by chromosome arm 2q and chromosome 12. This duplication incorporates two of the four known Hox gene clusters, but considerably expands the extent of the duplications proximally and distally on the pair of chromosome arms. This breadth of duplication is also seen on the two chromosomes carrying the other two Hox clusters.

An additional large duplication, between chromosomes 18 and 20, serves as a good example to illustrate some of the features common to many of the other observed large duplications (Fig. 13, inset). This duplication contains 64 detected ordered intrachromosomal pairs of homologous genes. After discounting a 40-Mb stretch of chromosome 18 free of matches to chromosome 20, which is likely to represent a large insert (between the gene assignments "Krup rel" and "collagen rel" on chromosome 18 in Fig. 13), the full duplication segment covers 36 Mb on chromosome 18 and 28 Mb on chromosome 20.

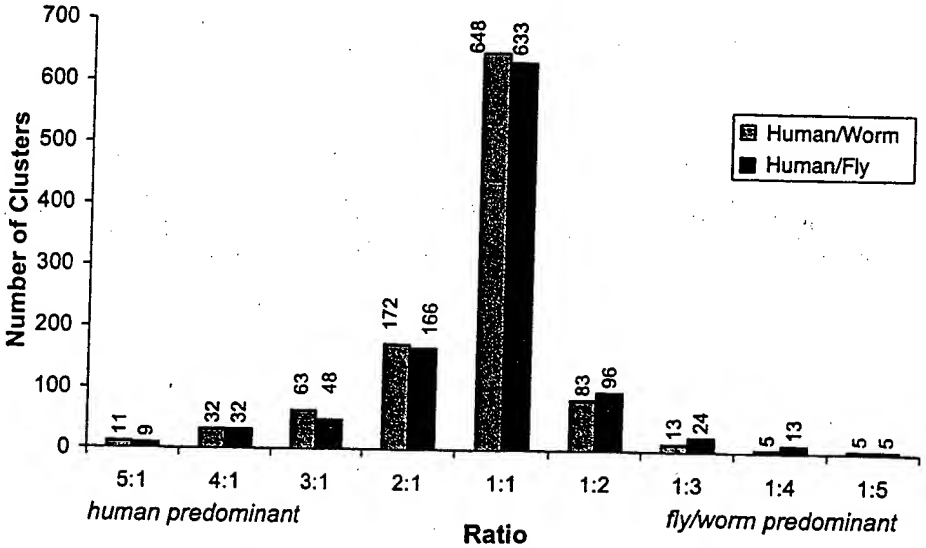

Fig. 12. Gene duplication in complete protein clusters. The predicted protein sets of human, worm, and fly were subjected to Lek clustering (*27*). The numbers of clusters with varying ratios (whole number) of human versus worm and human versus fly proteins per cluster were plotted.

By this measure, the duplication segment spans nearly half of each chromosome's net length. The most likely scenario is that the whole span of this region was duplicated as a single very large block, followed by shuffling owing to smaller scale rearrangements. As such, at least four subsequent rearrangements would need to be invoked to explain the relative insertions and inversions seen in the duplicated segment interval. The 64 protein pairs in this alignment occur among 217 protein assignments on chromosome 18, and among 322 protein assignments on chromosome 20, for a density of involved proteins of 20 to 30%. This is consistent with an ancient large-scale duplication followed by subsequent gene loss on one or both chromosomes. Loss of just one member of a gene pair subsequent to the duplication would result in a failure to score a gene pair in the block; less than 50% gene loss on the chromosomes would lead to the duplication density observed here. As an independent verification of the significance of the alignments detected, it can be seen that a substantial number of the pairs of aligning proteins in this duplication, including some of those annotated (Fig. 13), are those populating small Lek complete clusters (see above). This indicates that they are members of very small families of paralogs; their relative scarcity within the genome validates the uniqueness and robust nature of their alignments.

Two additional qualitative features were observed among many of the large-scale duplications. First, several proteins with disease associations, with OMIM (Online Mendelian Inheritance in Man) assignments, are members of duplicated segments (see web table 2 on *Science* Online at www.sciencemag.org/cgi/content/full/291/5507/1304/DC1). We have also observed a few instances where paralogs on both duplicated segments are associated with similar disease conditions. Notable among these genes are proteins involved in hemostasis (coagulation factors) that are associated with bleeding disorders, transcriptional regulators like the homeobox proteins associated with developmental disorders, and potassium channels associated with cardiovascular conduction abnormalities. For each of these disease genes, closer study of the paralogous genes in the duplicated segment may reveal new insights into disease causation, with further investigation needed to determine whether they might be involved in the same or similar genetic diseases. Second, although there is a conserved number of proteins and coding exons predicted for specific large duplicated spans within the chromosome 18 to 20 alignment, the genomic DNA of chromosome 18 in these specific spans is in some cases more than 10-fold longer than the corresponding chromosome 20 DNA. This selective accretion of noncoding DNA (or conversely, loss of noncoding DNA) on one of a pair of duplicated chromosome regions was observed in many compared regions. Hypotheses to explain which mechanisms foster these processes must be tested.

Evaluation of the alignment results gives some perspective on dating of the duplications. As noted above, large-scale ancient segmental duplication in fact best explains many of the blocks detected by this genome-wide analysis. The regions of human chromosomes involved in the large-scale duplications expanded upon above (chromosomes 2 to 14, 2 to 12, and 18 to 20) are each syntenic to a distinct mouse chromosomal region. The corresponding mouse chromosomal regions are much more similar in sequence conservation, and even in order, to their human synteny partners than the human duplication regions are to each other. Further, the corresponding mouse chromosomal regions each bear a significant proportion of genes orthologous to the human genes on which the human duplication assignments were made. On the basis of these factors, the corresponding mouse chromosomal spans, at coarse resolution, appear to be products of the same large-scale duplications observed in humans. Although further detailed analysis must be carried out once a more complete genome is assembled for mouse, the underlying large duplications appear to predate the two species' divergence. This dates the duplications, at the latest, before divergence of the primate and rodent lineages. This date can be further refined upon examination of the synteny between human chromosomes and those of chicken, pufferfish (*Fugu rubripes*), or zebrafish (*95*). The only substantial syntenic stretches mapped in these species corresponding to both pairs of human duplications are restricted to the Hox cluster regions. When the synteny of these regions (or others) to human chromosomes is extended with further mapping, the ages of the nearly chromosome-length duplications seen in humans are likely to be dated to the root of vertebrate divergence.

The MUMmer-based results demonstrate large block duplications that range in size from a few genes to segments covering most of a chromosome. The extent of segmental duplications raises the question of whether an ancient whole-genome duplication event is the underlying explanation for the numerous duplicated regions (*96*). The duplications have undergone many deletions and subsequent rearrangements; these events make it difficult to distinguish between a whole-genome duplication and multiple smaller events. Further analysis, focused especially on comparing the estimated ages of all the block duplications, derived partially from interspecies genome comparisons, will be necessary to determine which of these two hypotheses is more likely. Comparisons of genomes of different vertebrates, and even cross-phyla genome comparisons, will allow for the deconvolution of duplications to eventually reveal the stagewise history of our genome, and with it a history of the emergence of many of the key functions that distinguish us from other living things.

6 A Genome-Wide Examination of Sequence Variations

Summary. Computational methods were used to identify single-nucleotide polymorphisms (SNPs) by comparison of the Celera sequence to other SNP resources. The SNP rate between two chromosomes was ~1 per 1200 to 1500 bp. SNPs are distributed nonrandomly throughout the genome. Only a very small proportion of all SNPs (<1%) potentially impact protein function based on the functional analysis of SNPs that affect the predicted coding regions. This results in an estimate that only thousands, not millions, of genetic variations may contribute to the structural diversity of human proteins.

Having a complete genome sequence enables researchers to achieve a dramatic acceleration in the rate of gene discovery, but only through analysis of sequence variation in DNA can we discover the genetic basis for variation in health among human beings. Whole-genome shotgun sequencing is a particularly effective method for detecting sequence variation in tandem with whole-genome assembly. In addition, we compared the distribution and attributes of SNPs ascertained by three other methods: (i) alignment of the Celera consensus sequence to the PFP assembly, (ii) overlap of high-quality reads of genomic sequence (referred to as "Kwok"; 1,120,195 SNPs) (*97*), and (iii) reduced representation shotgun sequencing (referred to as "TSC"; 632,640 SNPs) (*98*). These data were consistent in showing an overall nucleotide diversity of ~8×10^{-4}, marked heterogeneity across the genome in SNP density, and an overwhelming preponderance of noncoding variation that produces no change in expressed proteins.

6.1 SNPs found by aligning the Celera consensus to the PFP assembly

Ideally, methods of SNP discovery make full use of sequence depth and quality at every site, and quantitatively control the rate of false-positive and false-negative calls with an explicit sampling model (*99*). Comparison of consensus sequences in the absence of these details necessitated a more ad hoc approach (quality scores could not readily be obtained for the PFP assembly). First, all sequence differences between the two consensus sequences were identified; these were then filtered to reduce the contribution of sequencing errors and misassembly. As a measure of the effectiveness of the filtering step, we monitored the ratio of transition and transversion substitutions, because a 2:1 ratio has been well documented as typical in mammalian evolution (*100*) and in human SNPs

(*101*, *102*). The filtering steps consisted of removing variants where the quality score in the Celera consensus was less than 30 and where the density of variants was greater than 5 in 400 bp. These filters resulted in shifting the transition-to-transversion ratio from 1.57:1 to 1.89:1. When applied to 2.3 Gbp of alignments between the Celera and PFP consensus sequences, these filters resulted in identification of 2,104,820 putative SNPs from a total of 2,778,474 substitution differences. Overlaps between this set of SNPs and those found by other methods are described below.

6.2 Comparisons to public SNP databases

Additional SNPs, including 2,536,021 from dbSNP (www.ncbi.nlm.nih.gov/SNP) and 13,150 from HGMD (Human Gene Mutation Database, from the University of Wales, UK), were mapped on the Celera consensus sequence by a sequence similarity search with the program PowerBlast (*103*). The two largest data sets in dbSNP are the Kwok and TSC sets, with 47% and 25% of the dbSNP records. Low-quality alignments with partial coverage of the dbSNP sequence and alignments that had less than 98% sequence identity between the Celera sequence and the dbSNP flanking sequence were eliminated. dbSNP sequences mapping to multiple locations on the Celera genome were discarded. A total of 2,336,935 dbSNP variants were mapped to 1,223,038 unique locations on the Celera sequence, implying considerable redundancy in dbSNP. SNPs in the TSC set mapped to 585,811 unique genomic locations, and SNPs in the Kwok set mapped to 438,032 unique locations. The combined unique SNPs counts used in this analysis, including Celera-PFP, TSC, and Kwok, is 2,737,668. Table 15 shows that a substantial fraction of SNPs identified by one of these methods was also found by another method. The very high overlap (36.2%) between the Kwok and Celera-PFP SNPs may be due in part to the use by Kwok of sequences that went into the PFP assembly. The unusually low overlap (16.4%) between the Kwok and TSC sets is due to their being the smallest two sets. In addition, 24.5% of the Celera-PFP SNPs overlap with SNPs derived from the Celera genome sequences (*46*). SNP validation in population samples is an expensive and laborious process, so confirmation on multiple data sets may provide an efficient initial validation "in silico" (by computational analysis).

One means of assessing whether the three sets of SNPs provide the same picture of human variation is to tally the frequencies of the six possible base changes in each set of SNPs (Table 16). Previous measures of nucleotide diversity were mostly derived from small-scale analysis on candidate genes (*101*), and our analysis with all three data sets validates the previous observations at the whole-genome scale. There is remarkable homogeneity between the SNPs found in the Kwok set, the TSC set, and in our whole-genome shotgun (*46*) in this substitution pattern. Compared with the rest of the data sets, Celera-PFP deviates slightly from the 2:1 transition-to-transversion ratio observed in the other SNP sets. This result is not unexpected, because some fraction of the computationally identified SNPs in the Celera-PFP comparison may in fact be sequence errors. A 2:1 transition:transversion ratio for the bona fide SNPs would be obtained if one assumed that 15% of the sequence differences in the Celera-PFP set were a result of (presumably random) sequence errors.

6.3 Estimation of nucleotide diversity from ascertained SNPs

The number of SNPs identified varied widely across chromosomes. In order to normalize these values to the chromosome size and sequence coverage, we used π, the standard statistic for nucleotide diversity (*104*). Nucleotide diversity is a measure of per-site heterozygosity, quantifying the probability that a pair of chromosomes drawn from the population will differ at a nucleotide site. In order to calculate nucleotide diversity for each chromosome, we need to know the number of nucleotide sites that were surveyed for variation, and in methods like reduced respresentation sequencing, we need to know the sequence quality and the depth of coverage at each site. These data are not readily available, so we could not estimate nucleotide diversity from the TSC effort. Estimation of nucleotide diversity from high-quality sequence overlaps should be possible, but again, more information is needed on the details of all the alignments.

Estimation of nucleotide diversity from a shotgun assembly entails calculating for each column of the multialignment, the probability that two or more distinct alleles are present, and the probability of detecting a SNP if in fact the alleles have different sequence (i.e., the probability of correct sequence calls). The greater the depth of coverage and the higher the sequence quality, the higher is the chance of successfully detecting a SNP (*105*). Even after correcting for variation in coverage, the nucleotide diversity appeared to vary across autosomes. The significance of this heterogeneity was tested by analysis of variance, with estimates of π for 100-kbp windows to estimate variability within chromosomes (for the Celera-PFP comparison, $F = 29.73$, $P < 0.0001$).

Average diversity for the autosomes estimated from the Celera-PFP comparison was 8.94×10^{-4}. Nucleotide diversity on the X chromosome was 6.54×10^{-4}. The X is expected to be less variable than autosomes, because for every four copies of autosomes in the population, there are only three X chromosomes, and this smaller effective population size means that random drift will more rapidly remove variation from the X (*106*).

Having ascertained nucleotide variation genome-wide, it appears that previous estimates of nucleotide diversity in humans based on samples of genes were reasonably accurate (*101*, *102*, *106*, *107*). Genome-wide, our estimate of nucleotide diversity was 8.98×10^{-4} for the Celera-PFP alignment, and a published estimate averaged over 10 densely resequenced human genes was 8.00×10^{-4} (*108*).

6.4 Variation in nucleotide diversity across the human genome

Such an apparently high degree of variability among chromosomes in SNP density raises the question of whether there is heterogeneity at a finer scale within chromo-

Table 15. Overlap of SNPs from genome-wide SNP databases. Table entries are SNP counts for each pair of data sets. Numbers in parentheses are the fraction of overlap, calculated as the count of overlapping SNPs divided by the number of SNPs in the smaller of the two databases compared. Total SNP counts for the databases are: Celera-PFP, 2,104,820; TSC, 585,811; and Kwok 438,032. Only unique SNPs in the TSC and Kwok data sets were included.

	TSC	Kwok
Celera-PFP	188,694 (0.322)	158,532 (0.362)
TSC		72,024 (0.164)

Table 16. Summary of nucleotide changes in different SNP data sets.

SNP data set	A/G (%)	C/T (%)	A/C (%)	A/T (%)	C/G (%)	T/G (%)	Transition: transversion
Celera-PFP	30.7	30.7	10.3	8.6	9.2	10.3	1.59:1
Kwok*	33.7	33.8	8.5	7.0	8.6	8.4	2.07:1
TSC†	33.3	33.4	8.8	7.3	8.6	8.6	1.99:1

*November 2000 release of the NCBI database dbSNP (www.ncbi.nlm.nih.gov/SNP/) with the method defined as Overlap SnpDetectionWithPolyBayes. The submitter of the data is Pui-Yan Kwok from Washington University. †November 2000 release of NCBI dbSNP (www.ncbi.nlm.nih.gov/SNP/) with the methods defined as TSC-Sanger, TSC-WICGR, and TSC-WUGSC. The submitter of the data is Lincoln Stein from Cold Spring Harbor Laboratory.

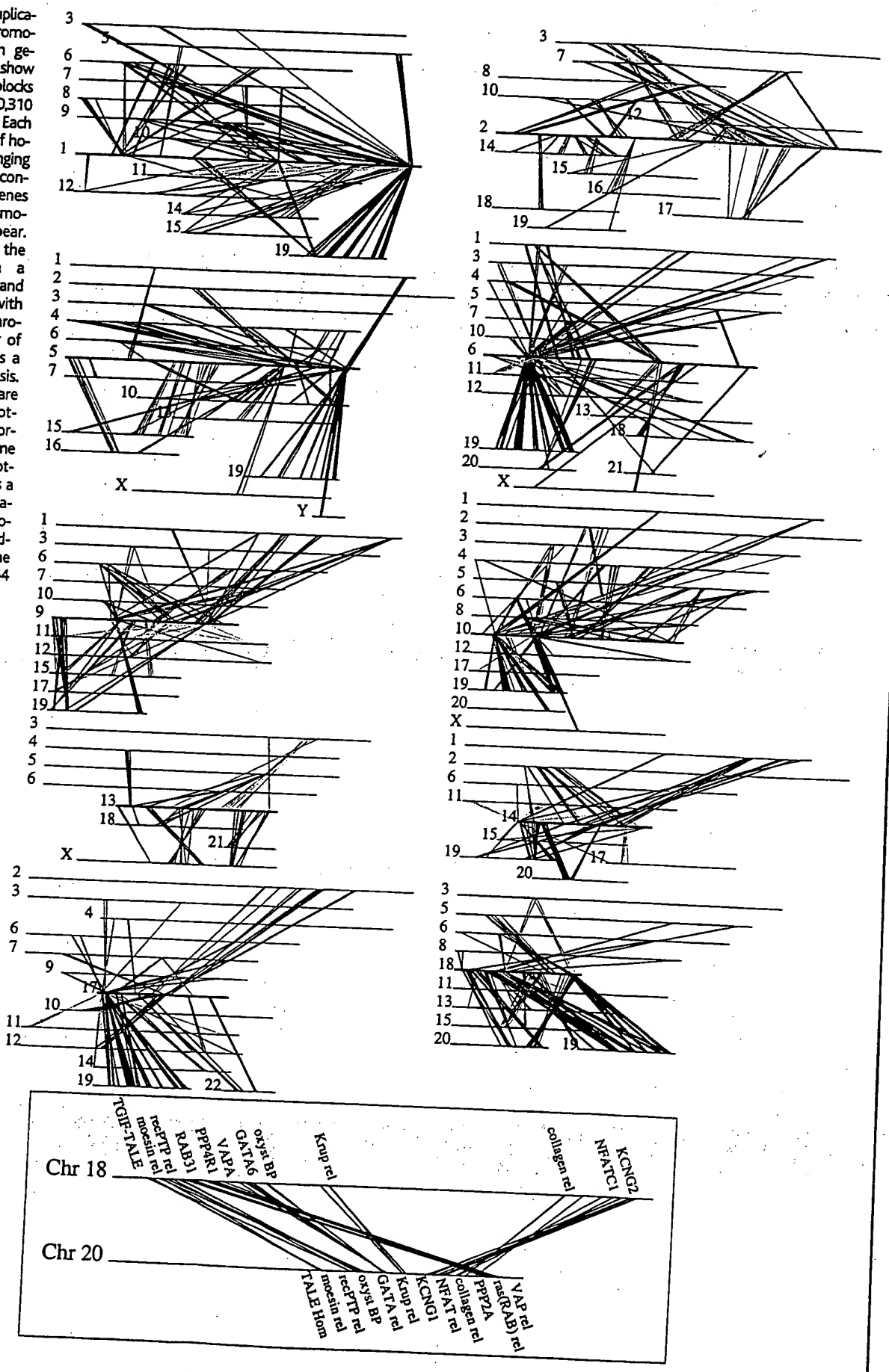

Fig. 13. Segmental duplications between chromosomes in the human genome. The 24 panels show the 1077 duplicated blocks of genes, containing 10,310 pairs of genes in total. Each line represents a pair of homologous genes belonging to a block; all blocks contain at least three genes on each of the chromosomes where they appear. Each panel shows all the duplications between a single chromosome and other chromosomes with shared blocks. The chromosome at the center of each panel is shown as a thick red line for emphasis. Other chromosomes are displayed from top to bottom within each panel ordered by chromosome number. The inset (bottom, center right) shows a close-up of one duplication between chromosomes 18 and 20, expanded to display the gene names of 12 of the 64 gene pairs shown.

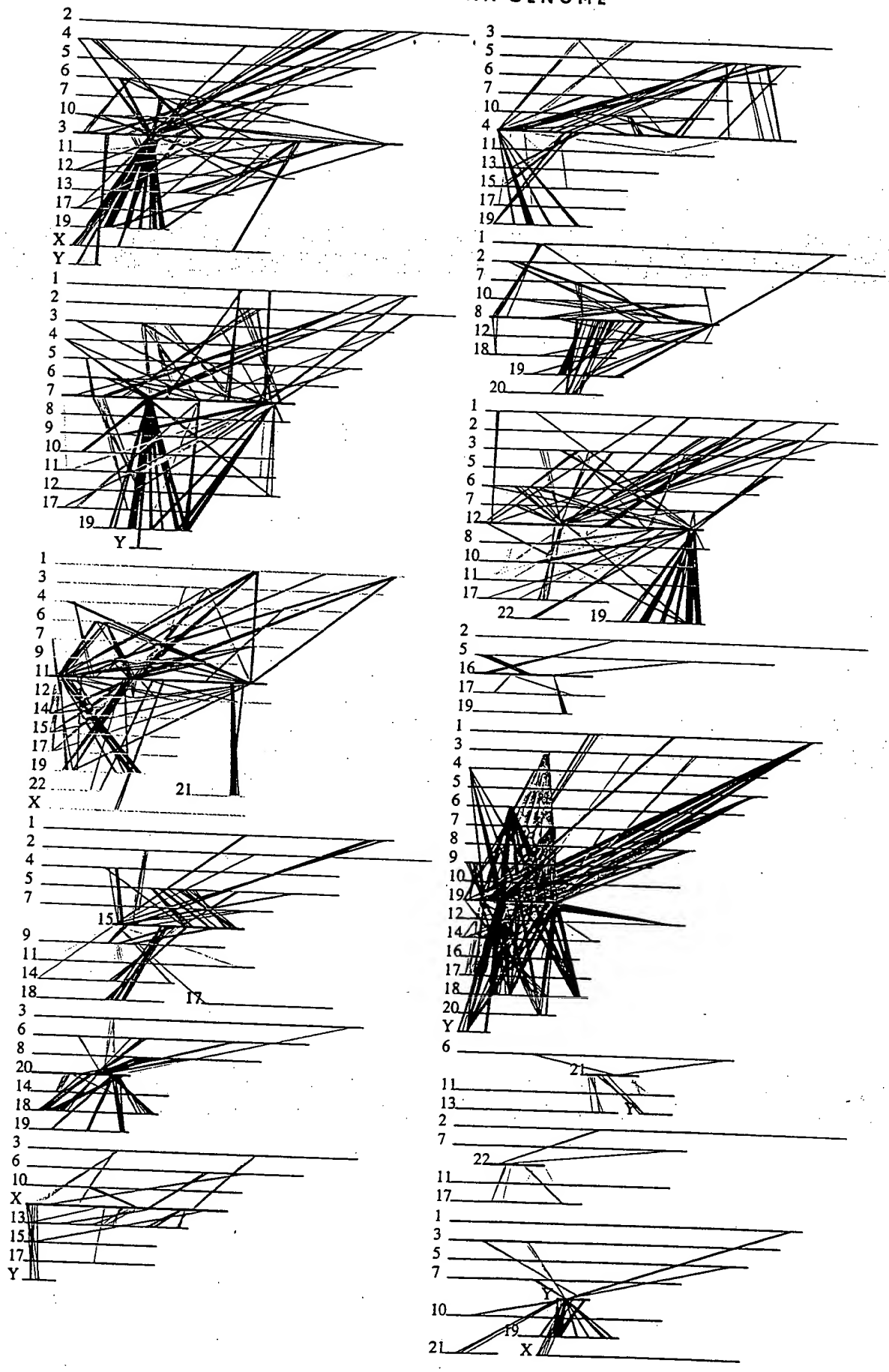

somes, and whether this heterogeneity is greater than expected by chance. If SNPs occur by random and independent mutations, then it would seem that there ought to be a Poisson distribution of numbers of SNPs in fragments of arbitrary constant size. The observed dispersion in the distribution of SNPs in 100-kbp fragments was far greater than predicted from a Poisson distribution (Fig. 14). However, this simplistic model ignores the different recombination rates and population histories that exist in different regions of the genome. Population genetics theory holds that we can account for this variation with a mathematical formulation called the neutral coalescent (*109*). Applying well-tested algorithms for simulating the neutral coalescent with recombination (*110*), and using an effective population size of 10,000 and a per-base recombination rate equal to the mutation rate (*111*), we generated a distribution of numbers of SNPs by this model as well (*112*). The observed distribution of SNPs has a much larger variance than either the Poisson model or the coalescent model, and the difference is highly significant. This implies that there is significant variability across the genome in SNP density, an observation that begs an explanation.

Several attributes of the DNA sequence may affect the local density of SNPs, including the rate at which DNA polymerase makes errors and the efficacy of mismatch repair. One key factor that is likely to be associated with SNP density is the G+C content, in part because methylated cytosines in CpG dinucleotides tend to undergo deamination to form thymine, accounting for a nearly 10-fold increase in the mutation rate of CpGs over other dinucleotides. We tallied the GC content and nucleotide diversities in 100-kbp windows across the entire genome and found that the correlation between them was positive (r = 0.21) and highly significant ($P < 0.0001$), but G+C content accounted for only a small part of the variation.

6.5 SNPs by genomic class

To test homogeneity of SNP densities across functional classes, we partitioned sites into intergenic (defined as >5 kbp from any predicted transcription unit), 5′-UTR, exonic (missense and silent), intronic, and 3′-UTR for 10,239 known genes, derived from the NCBI RefSeq database and all human genes predicted from the Celera Otto annotation. In coding regions, SNPs were categorized as either silent, for those that do not change amino acid sequence, or missense, for those that change the protein product. The ratio of missense to silent coding SNPs in Celera-PFP, TSC, and Kwok sets (1.12, 0.91, and 0.78, respectively) shows a markedly reduced frequency of missense variants compared with the neutral expectation, consistent with the elimination by natural selection of a fraction of the deleterious amino acid changes (*112*). These ratios are comparable to the missense-to-silent ratios of 0.88 and 1.17 found by Cargill *et al.* (*101*) and by Halushka *et al.* (*102*). Similar results were observed in SNPs derived from Celera shotgun sequences (*46*).

It is striking how small is the fraction of SNPs that lead to potentially dysfunctional alterations in proteins. In the 10,239 RefSeq genes, missense SNPs were only about 0.12, 0.14, and 0.17% of the total SNP counts in Celera-PFP, TSC, and Kwok SNPs, respectively. Nonconservative protein changes constitute an even smaller fraction of missense SNPs (47, 41, and 40% in Celera-PFP, Kwok, and TSC). Intergenic regions have been virtually unstudied (*113*), and we note that 75% of the SNPs we identified were intergenic (Table 17). The SNP rate was highest in introns and lowest in exons. The SNP rate was lower in intergenic regions than in introns, providing one of the first discriminators between these two classes of DNA. These SNP rates were confirmed in the Celera SNPs, which also exhibited a lower rate in exons than in introns, and in extragenic regions than in introns (*46*). Many of these intergenic SNPs will provide valuable information in the form of markers for linkage and association studies, and some fraction is likely to have a regulatory function as well.

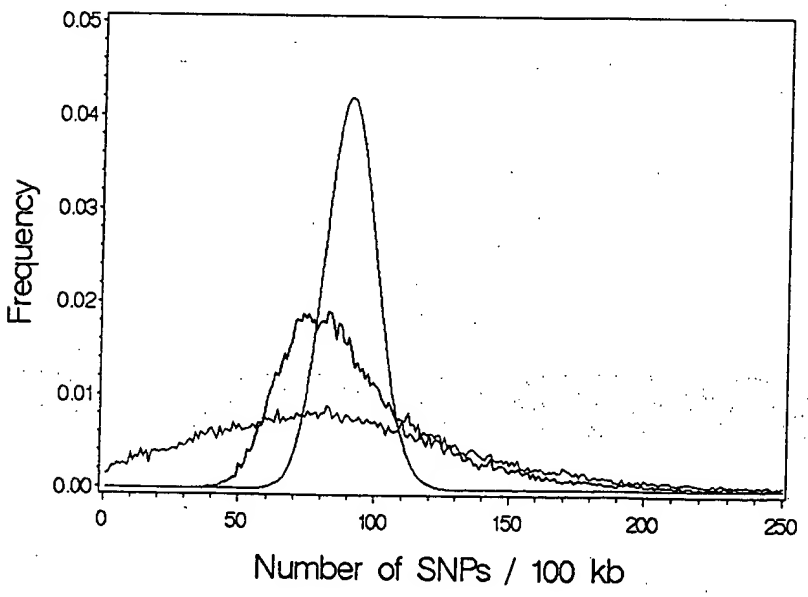

Fig. 14. SNP density in each 100-kbp interval as determined with Celera-PFP SNPs. The color codes are as follows: black, Celera-PFP SNP density; blue, coalescent model; and red, Poisson distribution. The figure shows that the distribution of SNPs along the genome is nonrandom and is not entirely accounted for by a coalescent model of regional history.

7 An Overview of the Predicted Protein-Coding Genes in the Human Genome

Summary. This section provides an initial computational analysis of the predicted protein set with the aim of cataloging prominent differences and similarities when the human genome is compared with other fully sequenced eukaryotic genomes. Over 40% of the predicted protein set in humans cannot be ascribed a molecular function by methods that assign proteins to known families. A protein domain–based analysis provides a detailed catalog of the prominent differences in the human genome when compared with the fly and worm genomes. Prominent among these are domain expansions in proteins involved in developmental regulation and in cellular processes such as neuronal function, hemostasis, acquired immune response, and cytoskeletal complexity. The final enumeration of protein families and details of protein structure will rely on additional experimental work and comprehensive manual curation.

A preliminary analysis of the predicted human protein-coding genes was conducted. Two methods were used to analyze and classify the molecular functions of 26,588 predicted proteins that represent 26,383 gene predictions with at least two lines of evidence as described above. The first method was based on an analysis at the level of protein families, with both the publicly available Pfam database (*114*, *115*) and Celera's Panther Classification (CPC) (Fig. 15) (*116*). The second method was based on an analysis at the level of protein domains, with both the Pfam and SMART databases (*115*, *117*).

The results presented here are preliminary and are subject to several limitations.

Both the gene predictions and functional assignments have been made by using computational tools, although the statistical models in Panther, Pfam, and SMART have been built, annotated, and reviewed by expert biologists. In the set of computationally predicted genes, we expect both false-positive predictions (some of these may in fact be inactive pseudogenes) and false-negative predictions (some human genes will not be computationally predicted). We also expect errors in delimiting the boundaries of exons and genes. Similarly, in the automatic functional assignments, we also expect both false-positive and false-negative predictions. The functional assignment protocol focuses on protein families that tend to be found across several organisms, or on families of known human genes. Therefore, we do not assign a function to many genes that are not in large families, even if the function is known. Unless otherwise specified, all enumeration of the genes in any given family or functional category was taken from the set of 26,588 predicted proteins, which were assigned functions by using statistical score cutoffs defined for models in Panther, Pfam, and SMART.

For this initial examination of the predicted human protein set, three broad questions were asked: (i) What are the likely molecular functions of the predicted gene products, and how are these proteins categorized with current classification methods? (ii) What are the core functions that appear to be common across the animals? (iii) How does the human protein complement differ from that of other sequenced eukaryotes?

7.1 Molecular functions of predicted human proteins

Figure 15 shows an overview of the putative molecular functions of the predicted 26,588 human proteins that have at least two lines of supporting evidence. About 41% (12,809) of the gene products could not be classified from this initial analysis and are termed proteins with unknown functions. Because our automatic classification methods treat only relatively large protein families, there are a number of "unclassified" sequences that do, in fact, have a known or predicted function. For the 60% of the protein set that have automatic functional predictions, the specific protein functions have been placed into broad classes. We focus here on molecular function (rather than higher order cellular processes) in order to classify as many proteins as possible. These functional predictions are based on similarity to sequences of known function.

In our analysis of the 12,731 additional low-confidence predicted genes (those with only one piece of supporting evidence), only 636 (5%) of these additional putative genes were assigned molecular functions by the automated methods. One-third of these 636 predicted genes represented endogenous retroviral proteins, further suggesting that the majority of these unknown-function genes are not real genes. Given that most of these additional 12,095 genes appear to be unique among the genomes sequenced to date, many may simply represent false-positive gene predictions.

The most common molecular functions are the transcription factors and those involved in nucleic acid metabolism (nucleic acid enzyme). Other functions that are highly represented in the human genome are the receptors, kinases, and hydrolases. Not surprisingly, most of the hydrolases are proteases. There are also many proteins that are members of proto-oncogene families, as well as families of "select regulatory molecules": (i) proteins involved in specific steps of signal transduction such as heterotrimeric GTP-binding proteins (G proteins) and cell cycle regulators, and (ii) proteins that modulate the activity of kinases, G proteins, and phosphatases.

Table 17. Distribution of SNPs in classes of genomic regions.

Genomic region class	Size of region examined (Mb)	Celera-PFP SNP density (SNP/Mb)
Intergenic	2185	707
Gene (intron + exon)	646	917
Intron	615	921
First intron	164	808
Exon	31	529
First exon	10	592

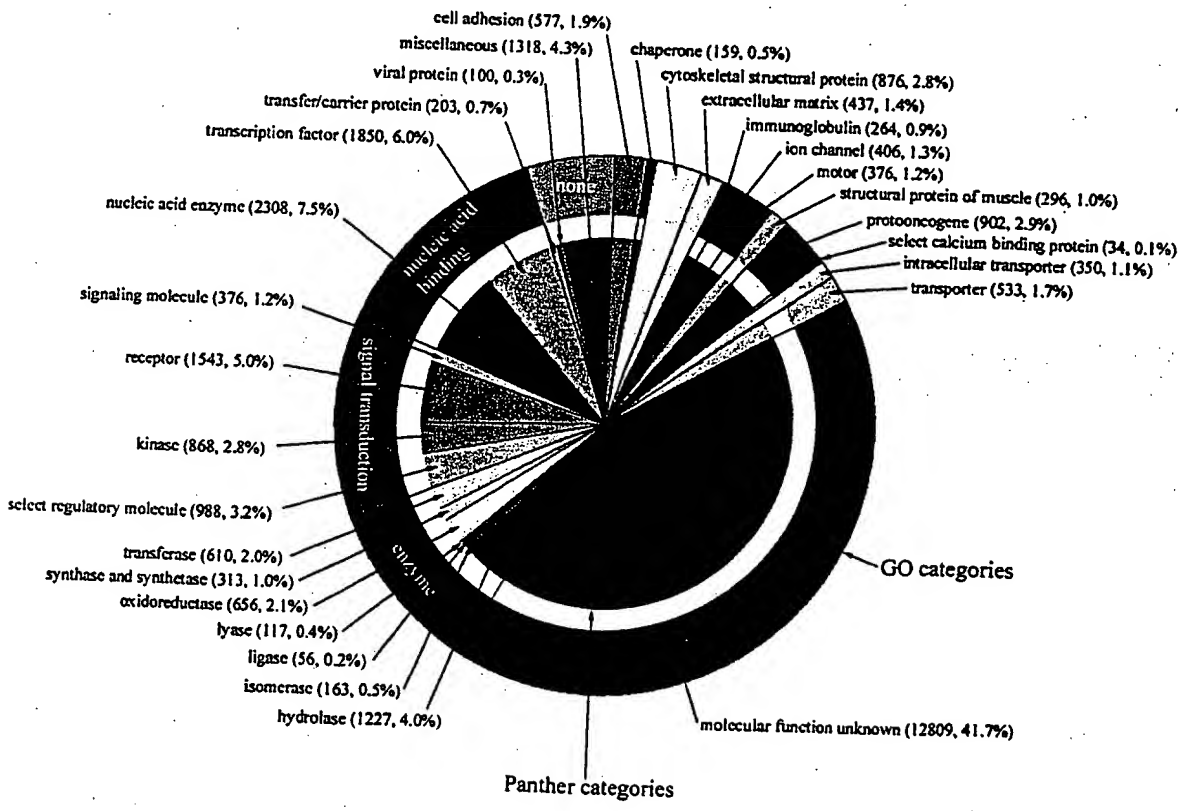

Fig. 15. Distribution of the molecular functions of 26,383 human genes. Each slice lists the numbers and percentages (in parentheses) of human gene functions assigned to a given category of molecular function. The outer circle shows the assignment to molecular function categories in the Gene Ontology (GO) (*179*), and the inner circle shows the assignment to Celera's Panther molecular function categories (*116*).

7.2 Evolutionary conservation of core processes

Because of the various "model organism" genome-sequencing projects that have already been completed, reasonable comparative information is available for beginning the analysis of the evolution of the human genome. The genomes of *S. cerevisiae* ("bakers' yeast") (*118*) and two diverse invertebrates, *C. elegans* (a nematode worm) (*119*) and *D. melanogaster* (fly) (*26*), as well as the first plant genome, *A. thaliana*, recently completed (*92*), provide a diverse background for genome comparisons.

We enumerated the "strict orthologs" conserved between human and fly, and between human and worm (Fig. 16) to address the question, What are the core functions that appear to be common across the animals? The concept of orthology is important because if two genes are orthologs, they can be traced by descent to the common ancestor of the two organisms (an "evolutionarily conserved protein set"), and therefore are likely to perform similar conserved functions in the different organisms. It is critical in this analysis to separate orthologs (a gene that appears in two organisms by descent from a common ancestor) from paralogs (a gene that appears in more than one copy in a given organism by a duplication event) because paralogs may subsequently diverge in function. Following the yeast-worm ortholog comparison in (*120*), we identified two different cases for each pairwise comparison (human-fly and human-worm). The first case was a pair of genes, one from each organism, for which there was no other close homolog in either organism. These are straightforwardly identified as orthologous, because there are no additional members of the families that complicate separating orthologs from paralogs. The second case is a family of genes with more than one member in either or both of the organisms being compared. Chervitz *et al.* (*120*) deal with this case by analyzing a phylogenetic tree that described the relationships between all of the sequences in both organisms, and then looked for pairs of genes that were nearest neighbors in the tree. If the nearest-neighbor pairs were from different organisms, those genes were presumed to be orthologs. We note that these nearest neighbors can often be confidently identified from pairwise sequence comparison without having to examine a phylogenetic tree (see legend to Fig. 16). If the nearest neighbors are not from different organisms, there has been a paralogous expansion in one or both organisms after the speciation event (and/or a gene loss by one organism). When this one-to-one correspondence is lost, defining an ortholog becomes ambiguous. For our initial computational overview of the predicted human protein set, we could not answer this question for every predicted protein. Therefore, we consider only "strict orthologs," i.e., the proteins with unambiguous one-to-one relationships (Fig. 16). By these criteria, there are 2758 strict human-fly orthologs, 2031 human-worm (1523 in common between these sets). We define the evolutionarily conserved set as those 1523 human proteins that have strict orthologs in both *D. melanogaster* and *C. elegans*.

The distribution of the functions of the conserved protein set is shown in Fig. 16. Comparison with Fig. 15 shows that, not surprisingly, the set of conserved proteins is not distributed among molecular functions in the same way as the whole human protein set. Compared with the whole human set (Fig. 15), there are several categories that are overrepresented in the conserved set by a factor of ~2 or more. The first category is nucleic acid enzymes, primarily the transcriptional machinery (notably DNA/RNA methyltransferases, DNA/RNA polymerases, helicases, DNA ligases, DNA- and RNA-processing factors, nucleases, and ribosomal proteins). The basic transcriptional and translational machinery is well known to have been conserved over evolution, from bacteria through to the most complex eukaryotes. Many ribonucleoproteins involved in RNA splicing also appear to be conserved among the animals. Other enzyme types are also overrepresented (transferases, oxidoreductases, ligases, lyases, and isomerases). Many of these en-

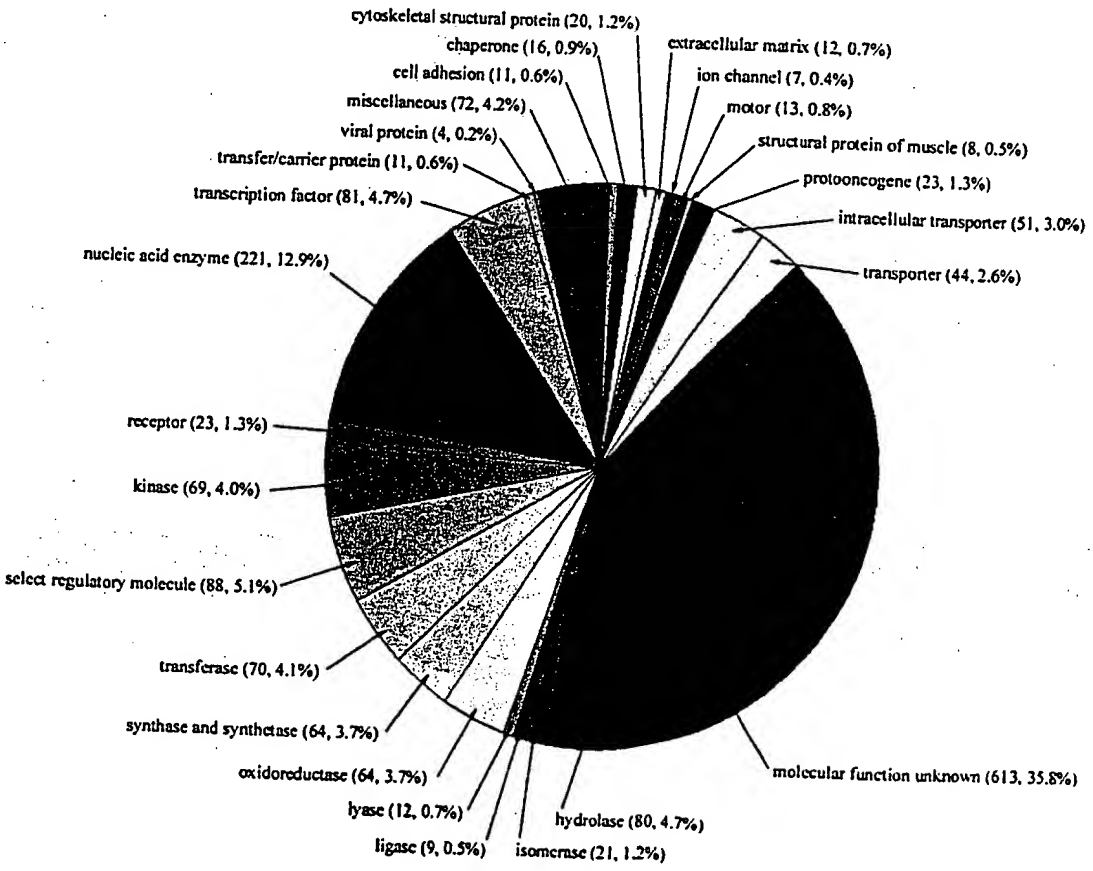

Fig. 16. Functions of putative orthologs across vertebrate and invertebrate genomes. Each slice lists the number and percentages (in parentheses) of "strict orthologs" between the human, fly, and worm genomes involved in a given category of molecular function. "Strict orthologs" are defined here as bi-directional BLAST best hits (*180*) such that each orthologous pair (i) has a BLASTP *P*-value of $\leq 10^{-10}$ (*120*), and (ii) has a more significant BLASTP score than any paralogs in either organism, i.e., there has likely been no duplication subsequent to speciation that might make the orthology ambiguous. This measure is quite strict and is a lower bound on the number of orthologs. By these criteria, there are 2758 strict human-fly orthologs, and 2031 human-worm orthologs (1523 in common between these sets).

zymes are involved in intermediary metabolism. The only exception is the hydrolase category, which is not significantly overrepresented in the shared protein set. Proteases form the largest part of this category, and several large protease families have expanded in each of these three organisms after their divergence. The category of select regulatory molecules is also overrepresented in the conserved set. The major conserved families are small guanosine triphosphatases (GTPases) (especially the Ras-related superfamily, including ADP ribosylation factor) and cell cycle regulators (particularly the cullin family, cyclin C family, and several cell division protein kinases). The last two significantly overrepresented categories are protein transport and trafficking, and chaperones. The most conserved groups in these categories are proteins involved in coated vesicle-mediated transport, and chaperones involved in protein folding and heat-shock response [particularly the DNAJ family, and heat-shock protein 60 (HSP60), HSP70, and HSP90 families]. These observations provide only a conservative estimate of the protein families in the context of specific cellular processes that were likely derived from the last common ancestor of the human, fly, and worm. As stated before, this analysis does not provide a complete estimate of conservation across the three animal genomes, as paralogous duplication makes the determination of true orthologs difficult within the members of conserved protein families.

7.3 Differences between the human genome and other sequenced eukaryotic genomes

To explore the molecular building blocks of the vertebrate taxon, we have compared the human genome with the other sequenced eukaryotic genomes at three levels: molecular functions, protein families, and protein domains.

Molecular differences can be correlated with phenotypic differences to begin to reveal the developmental and cellular processes that are unique to the vertebrates. Tables 18 and 19 display a comparison among all sequenced eukaryotic genomes, over selected protein/domain families (defined by sequence similarity, e.g., the serine-threonine protein kinases) and superfamilies (defined by shared molecular function, which may include several sequence-related families, e.g., the cytokines). In these tables we have focused on (super) families that are either very large or that differ significantly in humans compared with the other sequenced eukaryote genomes. We have found that the most prominent human expansions are in proteins involved in (i) acquired immune functions; (ii) neural development, structure, and functions; (iii) intercellular and intracellular signaling pathways in development and homeostasis; (iv) hemostasis; and (v) apoptosis.

Acquired immunity. One of the most striking differences between the human genome and the *Drosophila* or *C. elegans* genome is the appearance of genes involved in acquired immunity (Tables 18 and 19). This is expected, because the acquired immune response is a defense system that only occurs in vertebrates. We observe 22 class I and 22 class II major histocompatibility complex (MHC) antigen genes and 114 other immunoglobulin genes in the human genome. In addition, there are 59 genes in the cognate immunoglobulin receptor family. At the domain level, this is exemplified by an expansion and recruitment of the ancient immunoglobulin fold to constitute molecules such as MHC, and of the integrin fold to form several of the cell adhesion molecules that mediate interactions between immune effector cells and the extracellular matrix. Vertebrate-specific proteins include the paracrine immune regulators family of secreted 4-alpha helical bundle proteins, namely the cytokines and chemokines. Some of the cytoplasmic signal transduction components associated with cytokine receptor signal transduction are also features that are poorly represented in the fly and worm. These include protein domains found in the signal transducer and activator of transcription (STATs), the suppressors of cytokine signaling (SOCS), and protein inhibitors of activated STATs (PIAS). In contrast, many of the animal-specific protein domains that play a role in innate immune response, such as the Toll receptors, do not appear to be significantly expanded in the human genome.

Neural development, structure, and function. In the human genome, as compared with the worm and fly genomes, there is a marked increase in the number of members of protein families that are involved in neural development. Examples include neurotrophic factors such as ependymin, nerve growth factor, and signaling molecules such as semaphorins, as well as the number of proteins involved directly in neural structure and function such as myelin proteins, voltage-gated ion channels, and synaptic proteins such as synaptotagmin. These observations correlate well with the known phenotypic differences between the nervous systems of these taxa, notably (i) the increase in the number and connectivity of neurons; (ii) the increase in number of distinct neural cell types (as many as a thousand or more in human compared with a few hundred in fly and worm) (*121*); (iii) the increased length of individual axons; and (iv) the significant increase in glial cell number, especially the appearance of myelinating glial cells, which are electrically inert supporting cells differentiated from the same stem cells as neurons. A number of prominent protein expansions are involved in the processes of neural development. Of the extracellular domains that mediate cell adhesion, the connexin domain–containing proteins (*122*) exist only in humans. These proteins, which are not present in the *Drosophila* or *C. elegans* genomes, appear to provide the constitutive subunits of intercellular channels and the structural basis for electrical coupling. Pathway finding by axons and neuronal network formation is mediated through a subset of ephrins and their cognate receptor tyrosine kinases that act as positional labels to establish topographical projections (*123*). The probable biological role for the semaphorins (22 in human compared with 6 in the fly and 2 in the worm) and their receptors (neuropilins and plexins) is that of axonal guidance molecules (*124*). Signaling molecules such as neurotrophic factors and some cytokines have been shown to regulate neuronal cell survival, proliferation, and axon guidance (*125*). Notch receptors and ligands play important roles in glial cell fate determination and gliogenesis (*126*).

Other human expanded gene families play key roles directly in neural structure and function. One example is synaptotagmin (expanded more than twofold in humans relative to the invertebrates), originally found to regulate synaptic transmission by serving as a Ca^{2+} sensor (or receptor) during synaptic vesicle fusion and release (*127*). Of interest is the increased co-occurrence in humans of PDZ and the SH3 domains in neuronal-specific adaptor molecules; examples include proteins that likely modulate channel activity at synaptic junctions (*128*). We also noted expansions in several ion-channel families (Table 19), including the EAG subfamily (related to cyclic nucleotide gated channels), the voltage-gated calcium/sodium channel family, the inward-rectifier potassium channel family, and the voltage-gated potassium channel, alpha subunit family. Voltage-gated sodium and potassium channels are involved in the generation of action potentials in neurons. Together with voltage-gated calcium channels, they also play a key role in coupling action potentials to neurotransmitter release, in the development of neurites, and in short-term memory. The recent observation of a calcium-regulated association between sodium channels and synaptotagmin may have consequences for the establishment and regulation of neuronal excitability (*129*).

Myelin basic protein and myelin-associated glycoprotein are major classes of protein components in both the central and peripheral nervous system of vertebrates. Myelin P0 is a major component of peripheral myelin, and myelin proteolipid and myelin oligodendrocyte glycopotein are found in the central nervous system. Mutations in any of these

Table 18. Domain-based comparative analysis of proteins in *H. sapiens* (H), *D. melanogaster* (F), *C. elegans* (W), *S. cerevisiae* (Y), and *A. thaliana* (A). The predicted protein set of each of the above eukaryotic organisms was analyzed with Pfam version 5.5 using E value cutoffs of 0.001. The number of proteins containing the specified Pfam domains as well as the total number of domains (in parentheses) are shown in each column. Domains were categorized into cellular processes for presentation. Some domains (i.e., SH2) are listed in more than one cellular process. Results of the Pfam analysis may differ from results obtained based on human curation of protein families, owing to the limitations of large-scale automatic classifications. Representative examples of domains with reduced counts owing to the stringent E value cutoff used for this analysis are marked with a double asterisk (**). Examples include short divergent and predominantly alpha-helical domains, and certain classes of cysteine-rich zinc finger proteins.

Accession number	Domain name	Domain description	H	F	W	Y	A
		Developmental and homeostatic regulators					
PF02039	Adrenomedullin	Adrenomedullin	1	0	0	0	0
PF00212	ANP	Atrial natriuretic peptide	2	0	0	0	0
PF00028	Cadherin	Cadherin domain	100 (550)	14 (157)	16 (66)	0	0
PF00214	Calc_CGRP_IAPP	Calcitonin/CGRP/IAPP family	3	0	0	0	0
PF01110	CNTF	Ciliary neurotrophic factor	1	0	0	0	0
PF01093	Clusterin	Clusterin	3	0	0	0	0
PF00029	Connexin	Connexin	14 (16)	0	0	0	0
PF00976	ACTH_domain	Corticotropin ACTH domain	1	0	0	0	0
PF00473	CRF	Corticotropin-releasing factor family	2	1	0	0	0
PF00007	Cys_knot	Cystine-knot domain	10 (11)	2	0	0	0
PF00778	DIX	Dix domain	5	2	4	0	0
PF00322	Endothelin	Endothelin family	3	0	0	0	0
PF00812	Ephrin	Ephrin	7 (8)	2	4	0	0
PF01404	EPh_lbd	Ephrin receptor ligand binding domain	12	2	1	0	0
PF00167	FGF	Fibroblast growth factor	23	1	1	0	0
PF01534	Frizzled	Frizzled/Smoothened family membrane region	9	7	3	0	0
PF00236	Hormone6	Glycoprotein hormones	1	0	0	0	0
PF01153	Glypican	Glypican	14	2	1	0	0
PF01271	Granin	Grainin (chromogranin or secretogranin)	3	0	0	0	0
PF02058	Guanylin	Guanylin precursor	1	0	0	0	0
PF00049	Insulin	Insulin/IGF/Relaxin family	7	4	0	0	0
PF00219	IGFBP	Insulin-like growth factor binding proteins	10	0	0	0	0
PF02024	Leptin	Leptin	1	0	0	0	0
PF00193	Xlink	LINK (hyaluron binding)	13 (23)	0	1	0	0
PF00243	NGF	Nerve growth factor family	3	0	0	0	0
PF02158	Neuregulin	Neuregulin family	4	0	0	0	0
PF00184	Hormone5	Neurohypophysial hormones	1	0	0	0	0
PF02070	NMU	Neuromedin U	1	0	0	0	0
PF00066	Notch	Notch (DSL) domain	3 (5)	2 (4)	2 (6)	0	0
PF00865	Osteopontin	Osteopontin	1	0	0	0	0
PF00159	Hormone3	Pancreatic hormone peptides	3	0	0	0	0
PF01279	Parathyroid	Parathyroid hormone family	2	0	0	0	0
PF00123	Hormone2	Peptide hormone	5 (9)	0	0	0	0
PF00341	PDGF	Platelet-derived growth factor (PDGF)	5	1	0	0	0
PF01403	Sema	Sema domain	27 (29)	8 (10)	3 (4)	0	0
PF01033	Somatomedin_B	Somatomedin B domain	5 (8)	3	0	0	0
PF00103	Hormone	Somatotropin	1	0	0	0	0
PF02208	Sorb	Sorbin homologous domain	2	0	0	0	0
PF02404	SCF	Stem cell factor	2	0	0	0	0
PF01034	Syndecan	Syndecan domain	3	1	1	0	0
PF00020	TNFR_c6	TNFR/NGFR cysteine-rich region	17 (31)	1	0	0	0
PF00019	TGF-β	Transforming growth factor β-like domain	27 (28)	6	4	0	0
PF01099	Uteroglobin	Uteroglobin family	3	0	0	0	0
PF01160	Opiods_neuropep	Vertebrate endogenous opioids neuropeptide	3	0	0	0	0
PF00110	Wnt	Wnt family of developmental signaling proteins	18	7 (10)	5	0	0
		Hemostasis					
PF01821	ANATO	Anaphylotoxin-like domain	6 (14)	0	0	0	0
PF00386	C1q	C1q domain	24	0	0	0	0
PF00200	Disintegrin	Disintegrin	18	2	3	0	0
PF00754	F5_F8_type_C	F5/8 type C domain	15 (20)	5 (6)	2	0	0
PF01410	COLFI	Fibrillar collagen C-terminal domain	10	0	0	0	0
PF00039	Fn1	Fibronectin type I domain	5 (18)	0	0	0	0
PF00040	Fn2	Fibronectin type II domain	11 (16)	0	0	0	0
PF00051	Kringle	Kringle domain	15 (24)	2	2	0	0
PF01823	MACPF	MAC/Perforin domain	6	0	0	0	0
PF00354	Pentaxin	Pentaxin family	9	0	0	0	0
PF00277	SAA_proteins	Serum amyloid A protein	4	0	0	0	0
PF00084	Sushi	Sushi domain (SCR repeat)	53 (191)	11 (42)	8 (45)	0	0
PF02210	TSPN	Thrombospondin N-terminal–like domains	14	1	0	0	0
PF01108	Tissue_fac	Tissue factor	1	0	0	0	0
PF00868	Transglutamin_N	Transglutaminase family	6	1	0	0	0
PF00927	Transglutamin_C	Transglutaminase family	8	1	0	0	0

Table 18 (*Continued*)

Accession number	Domain name	Domain description	H	F	W	Y	A
PF00594	Gla	Vitamin K-dependent carboxylation/gamma-carboxyglutamic (GLA) domain	11	0	0	0	0
		Immune response					
PF00711	Defensin_beta	Beta defensin	1	0	0	0	0
PF00748	Calpain_inhib	Calpain inhibitor repeat	3 (9)	0	0	0	0
PF00666	Cathelicidins	Cathelicidins	2	0	0	0	0
PF00129	MHC_I	Class I histocompatibility antigen, domains alpha 1 and 2	18 (20)	0	0	0	0
PF00993	MHC_II_alpha**	Class II histocompatibility antigen, alpha domain	5 (6)	0	0	0	0
PF00969	MHC_II_beta**	Class II histocompatibility antigen, beta domain	7	0	0	0	0
PF00879	Defensin_propep	Defensin propeptide	3	0	0	0	0
PF01109	GM_CSF	Granulocyte-macrophage colony-stimulating factor	1	0	0	0	0
PF00047	Ig	Immunoglobulin domain	381 (930)	125 (291)	67 (323)	0	0
PF00143	Interferon	Interferon alpha/beta domain	7 (9)	0	0	0	0
PF00714	IFN-gamma	Interferon gamma	1	0	0	0	0
PF00726	IL10	Interleukin-10	1	0	0	0	0
PF02372	IL15	Interleukin-15	1	0	0	0	0
PF00715	IL2	Interleukin-2	1	0	0	0	0
PF00727	IL4	Interleukin-4	1	0	0	0	0
PF02025	IL5	Interleukin-5	1	0	0	0	0
PF01415	IL7	Interleukin-7/9 family	1	0	0	0	0
PF00340	IL1	Interleukin-1	7	0	0	0	0
PF02394	IL1_propep	Interleukin-1 propeptide	1	0	0	0	0
PF02059	IL3	Interleukin-3	1	0	0	0	0
PF00489	IL6	Interleukin-6/G-CSF/MGF family	2	0	0	0	0
PF01291	LIF_OSM	Leukemia inhibitory factor (LIF)/oncostatin (OSM) family	2	0	0	0	0
PF00323	Defensins	Mammalian defensin	2	0	0	0	0
PF01091	PTN_MK	PTN/MK heparin-binding protein	2	0	0	0	0
PF00277	SAA_proteins	Serum amyloid A protein	4	0	0	0	0
PF00048	IL8	Small cytokines (intecrine/chemokine), interleukin-8 like	32	0	0	0	0
PF01582	TIR	TIR domain	18	8	2	0	131 (143)
PF00229	TNF	TNF (tumor necrosis factor) family	12	0	0	0	0
PF00088	Trefoil	Trefoil (P-type) domain	5 (6)	0	2	0	0
		PI-PY-rho GTPase signaling					
PF00779	BTK	BTK motif	5	1	0	0	0
PF00168	C2	C2 domain	73 (101)	32 (44)	24 (35)	6 (9)	66 (90)
PF00609	DAGKa	Diacylglycerol kinase accessory domain (presumed)	9	4	7	0	6
PF00781	DAGKc	Diacylglycerol kinase catalytic domain (presumed)	10	8	8	2	11 (12)
PF00610	DEP	Domain found in Dishevelled, Egl-10, and Pleckstrin (DEP)	12 (13)	4	10	5	2
PF01363	FYVE	FYVE zinc finger	28 (30)	14	15	5	15
PF00996	GDI	GDP dissociation inhibitor	6	2	1	1	3
PF00503	G-alpha	G-protein alpha subunit	27 (30)	10	20 (23)	2	5
PF00631	G-gamma	G-protein gamma like domains	16	5	5	1	0
PF00616	RasGAP	GTPase-activator protein for Ras-like GTPase	11	5	8	3	0
PF00618	RasGEFN	Guanine nucleotide exchange factor for Ras-like GTPases; N-terminal motif	9	2	3	5	0
PF00625	Guanylate_kin	Guanylate kinase	12	8	7	1	4
PF02189	ITAM	Immunoreceptor tyrosine-based activation motif	3	0	0	0	0
PF00169	PH	PH domain	193 (212)	72 (78)	65 (68)	24	23
PF00130	DAG_PE-bind	Phorbol esters/diacylglycerol binding domain (C1 domain)	45 (56)	25 (31)	26 (40)	1 (2)	4
PF00388	PI-PLC-X	Phosphatidylinositol-specific phospholipase C, X domain	12	3	7	1	8
PF00387	PI-PLC-Y	Phosphatidylinositol-specific phospholipase C, Y domain	11	2	7	1	8
PF00640	PID	Phosphotyrosine interaction domain (PTB/PID)	24 (27)	13	11 (12)	0	0
PF02192	PI3K_p85B	PI3-kinase family, p85-binding domain	2	1	1	0	0
PF00794	PI3K_rbd	PI3-kinase family, ras-binding domain	6	3	1	0	0
PF01412	ArfGAP	Putative GTP-ase activating protein for Arf	16	9	8	6	15
PF02196	RBD	Raf-like Ras-binding domain	6 (7)	4	1	0	0
PF02145	Rap_GAP	Rap/ran-GAP	5	4	2	0	0
PF00788	RA	Ras association (RalGDS/AF-6) domain	18 (19)	7 (9)	6	1	0
PF00071	Ras	Ras family	126	56 (57)	51	23	78
PF00617	RasGEF	RasGEF domain	21	8	7	5	0
PF00615	RGS	Regulator of G protein signaling domain	27	6 (7)	12 (13)	1	0
PF02197	RIIa	Regulatory subunit of type II PKA R-subunit	4	1	2	1	0

Table 18 (*Continued*)

Accession number	Domain name	Domain description	H	F	W	Y	A
PF00620	RhoGAP	RhoGAP domain	59	19	20	9	8
PF00621	RhoGEF	RhoGEF domain	46	23 (24)	18 (19)	3	0
PF00536	SAM	SAM domain (Sterile alpha motif)	29 (31)	15	8	3	6
PF01369	Sec7	Sec7 domain	13	5	5	5	9
PF00017	SH2	Src homology 2 (SH2) domain	87 (95)	33 (39)	44 (48)	1	3
PF00018	SH3	Src homology 3 (SH3) domain	143 (182)	55 (75)	46 (61)	23 (27)	4
PF01017	STAT	STAT protein	7	1	1 (2)	0	0
PF00790	VHS	VHS domain	4	2	4	4	8
PF00568	WH1	WH1 domain	7	2	2 (3)	1	0
		Domains involved in apoptosis					
PF00452	Bcl-2	Bcl-2	9	2	1	0	0
PF02180	BH4	Bcl-2 homology region 4	3	0	1	0	0
PF00619	CARD	Caspase recruitment domain	16	0	2	0	0
PF00531	Death	Death domain	16	5	7	0	0
PF01335	DED	Death effector domain	4 (5)	0	0	0	0
PF02179	BAG	Domain present in Hsp70 regulators	5 (8)	3	2	1	5
PF00656	ICE_p20	ICE-like protease (caspase) p20 domain	11	7	3	0	0
PF00653	BIR	Inhibitor of Apoptosis domain	8 (14)	5 (9)	2 (3)	1 (2)	0
		Cytoskeletal					
PF00022	Actin	Actin	61 (64)	15 (16)	12	9 (11)	24
PF00191	Annexin	Annexin	16 (55)	4 (16)	4 (11)	0	6 (16)
PF00402	Calponin	Calponin family	13 (22)	3	7 (19)	0	0
PF00373	Band_41	FERM domain (Band 4.1 family)	29 (30)	17 (19)	11 (14)	0	0
PF00880	Nebulin_repeat	Nebulin repeat	4 (148)	1 (2)	1	0	0
PF00681	Plectin_repeat	Plectin repeat	2 (11)	0	0	0	0
PF00435	Spectrin	Spectrin repeat	31 (195)	13 (171)	10 (93)	0	0
PF00418	Tubulin-binding	Tau and MAP proteins, tubulin-binding	4 (12)	1 (4)	2 (8)	0	0
PF00992	Troponin	Troponin	4	6	8	0	0
PF02209	VHP	Villin headpiece domain	5	2	2	0	5
PF01044	Vinculin	Vinculin family	4	2	1	0	0
		ECM adhesion					
PF01391	Collagen	Collagen triple helix repeat (20 copies)	65 (279)	10 (46)	174 (384)	0	0
PF01413	C4	C-terminal tandem repeated domain in type 4 procollagen	6 (11)	2 (4)	3 (6)	0	0
PF00431	CUB	CUB domain	47 (69)	9 (47)	43 (67)	0	0
PF00008	EGF	EGF-like domain	108 (420)	45 (186)	54 (157)	0	1
PF00147	Fibrinogen_C	Fibrinogen beta and gamma chains, C-terminal globular domain	26	10 (11)	6	0	0
PF00041	Fn3	Fibronectin type III domain	106 (545)	42 (168)	34 (156)	0	1
PF00757	Furin-like	Furin-like cysteine rich region	5	2	1	0	0
PF00357	Integrin_A	Integrin alpha cytoplasmic region	3	1	2	0	0
PF00362	Integrin_B	Integrins, beta chain	8	2	2	0	0
PF00052	Laminin_B	Laminin B (Domain IV)	8 (12)	4 (7)	6 (10)	0	0
PF00053	Laminin_EGF	Laminin EGF-like (Domains III and V)	24 (126)	9 (62)	11 (65)	0	0
PF00054	Laminin_G	Laminin G domain	30 (57)	18 (42)	14 (26)	0	0
PF00055	Laminin_Nterm	Laminin N-terminal (Domain VI)	10	6	4	0	0
PF00059	Lectin_c	Lectin C-type domain	47 (76)	23 (24)	91 (132)	0	0
PF01463	LRRCT	Leucine rich repeat C-terminal domain	69 (81)	23 (30)	7 (9)	0	0
PF01462	LRRNT	Leucine rich repeat N-terminal domain	40 (44)	7 (13)	3 (6)	0	0
PF00057	Ldl_recept_a	Low-density lipoprotein receptor domain class A	35 (127)	33 (152)	27 (113)	0	0
PF00058	Ldl_recept_b	Low-density lipoprotein receptor repeat class B	15 (96)	9 (56)	7 (22)	0	0
PF00530	SRCR	Scavenger receptor cysteine-rich domain	11 (46)	4 (8)	1 (2)	0	0
PF00084	Sushi	Sushi domain (SCR repeat)	53 (191)	11 (42)	8 (45)	0	0
PF00090	Tsp_1	Thrombospondin type 1 domain	41 (66)	11 (23)	18 (47)	0	0
PF00092	Vwa	von Willebrand factor type A domain	34 (58)	0	17 (19)	0	1
PF00093	Vwc	von Willebrand factor type C domain	19 (28)	6 (11)	2 (5)	0	0
PF00094	Vwd	von Willebrand factor type D domain	15 (35)	3 (7)	9	0	0
		Protein interaction domains					
PF00244	14-3-3	14-3-3 proteins	20	3	3	2	15
PF00023	Ank	Ank repeat	145 (404)	72 (269)	75 (223)	12 (20)	66 (111)
PF00514	Armadillo_seg	Armadillo/beta-catenin-like repeats	22 (56)	11 (38)	3 (11)	2 (10)	25 (67)
PF00168	C2	C2 domain	73 (101)	32 (44)	24 (35)	6 (9)	66 (90)
PF00027	cNMP_binding	Cyclic nucleotide-binding domain	26 (31)	21 (33)	15 (20)	2 (3)	22
PF01556	DnaJ_C	DnaJ C terminal region	12	9	5	3	19
PF00226	DnaJ	DnaJ domain	44	34	33	20	93
PF00036	Efhand**	EF hand	83 (151)	64 (117)	41 (86)	4 (11)	120 (328)
PF00611	FCH	Fes/CIP4 homology domain	9	3	2	4	0
PF01846	FF	FF domain	4 (11)	4 (10)	3 (16)	2 (5)	4 (8)
PF00498	FHA	FHA domain	13	15	7	13 (14)	17

myelin proteins result in severe demyelination, which is a pathological condition in which the myelin is lost and the nerve conduction is severely impaired (*130*). Humans have at least 10 genes belonging to four different families involved in myelin production (five myelin P0, three myelin proteolipid, myelin basic protein, and myelin-oligodendrocyte glycoprotein, or MOG), and possibly more-remotely related members of the MOG family. Flies have only a single myelin proteolipid, and worms have none at all.

Intercellular and intracellular signaling pathways in development and homeostasis. Many protein families that have expanded in humans relative to the invertebrates are involved in signaling processes, particularly in response to development and differentiation

Table 18 (*Continued*)

Accession number	Domain name	Domain description	H	F	W	Y	A
PF00254	FKBP	FKBP-type peptidyl-prolyl cis-trans isomerases	15 (20)	7 (8)	7 (13)	4	24 (29)
PF01590	GAF	GAF domain	7 (8)	2 (4)	1	0	10
PF01344	Kelch	Kelch motif	54 (157)	12 (48)	13 (41)	3	102 (178)
PF00560	LRR**	Leucine Rich Repeat	25 (30)	24 (30)	7 (11)	1	15 (16)
PF00917	MATH	MATH domain	11	5	88 (161)	1	61 (74)
PF00989	PAS	PAS domain	18 (19)	9 (10)	6	1	13 (18)
PF00595	PDZ	PDZ domain (Also known as DHR or GLGF)	96 (154)	60 (87)	46 (66)	2	5
PF00169	PH	PH domain	193 (212)	72 (78)	65 (68)	24	23
PF01535	PPR**	PPR repeat	5	3 (4)	0	1	474 (2485)
PF00536	SAM	SAM domain (Sterile alpha motif)	29 (31)	15	8	3	6
PF01369	Sec7	Sec7 domain	13	5	5	5	9
PF00017	SH2	Src homology 2 (SH2) domain	87 (95)	33 (39)	44 (48)	1	3
PF00018	SH3	Src homology 3 (SH3) domain	143 (182)	55 (75)	46 (61)	23 (27)	4
PF01740	STAS	STAS domain	5	1	6	2	13
PF00515	TPR**	TPR domain	72 (131)	39 (101)	28 (54)	16 (31)	65 (124)
PF00400	WD40**	WD40 domain	136 (305)	98 (226)	72 (153)	56 (121)	167 (344)
PF00397	WW	WW domain	32 (53)	24 (39)	16 (24)	5 (8)	11 (15)
PF00569	ZZ	ZZ-Zinc finger present in dystrophin, CBP/p300	10 (11)	13	10	2	10
		Nuclear interaction domains					
PF01754	Zf-A20	A20-like zinc finger	2 (8)	2	2	0	8
PF01388	ARID	ARID DNA binding domain	11	6	4	2	7
PF01426	BAH	BAH domain	8 (10)	7 (8)	4 (5)	5	21 (25)
PF00643	Zf-B_box**	B-box zinc finger	32 (35)	1	2	0	0
PF00533	BRCT	BRCA1 C Terminus (BRCT) domain	17 (28)	10 (18)	23 (35)	10 (16)	12 (16)
PF00439	Bromodomain	Bromodomain	37 (48)	16 (22)	18 (26)	10 (15)	28
PF00651	BTB	BTB/POZ domain	97 (98)	62 (64)	86 (91)	1 (2)	30 (31)
PF00145	DNA_methylase	C-5 cytosine-specific DNA methylase	3 (4)	1	0	0	13 (15)
PF00385	Chromo	chromo' (CHRromatin Organization MOdifier) domain	24 (27)	14 (15)	17 (18)	1 (2)	12
PF00125	Histone	Core histone H2A/H2B/H3/H4	75 (81)	5	71 (73)	8	48
PF00134	Cyclin	Cyclin	19	10	10	11	35
PF00270	DEAD	DEAD/DEAH box helicase	63 (66)	48 (50)	55 (57)	50 (52)	84 (87)
PF01529	Zf-DHHC	DHHC zinc finger domain	15	20	16	7	22
PF00646	F-box**	F-box domain	16	15	309 (324)	9	165 (167)
PF00250	Fork_head	Fork head domain	35 (36)	20 (21)	15	4	0
PF00320	GATA	GATA zinc finger	11 (17)	5(6)	8 (10)	9	26
PF01585	G-patch	G-patch domain	18	16	13	4	14 (15)
PF00010	HLH**	Helix-loop-helix DNA-binding domain	60 (61)	44	24	4	39
PF00850	Hist_deacetyl	Histone deacetylase family	12	5 (6)	8 (10)	5	10
PF00046	Homeobox	Homeobox domain	160 (178)	100 (103)	82 (84)	6	66
PF01833	TIG	IPT/TIG domain	29 (53)	11 (13)	5 (7)	2	1
PF02373	JmjC	JmjC domain	10	4	6	4	7
PF02375	JmjN	JmjN domain	7	4	2	3	7
PF00013	KH-domain	KH domain	28 (67)	14 (32)	17 (46)	4 (14)	27 (61)
PF01352	KRAB	KRAB box	204 (243)	0	0	0	0
PF00104	Hormone_rec	Ligand-binding domain of nuclear hormone receptor	47	17	142 (147)	0	0
PF00412	LIM	LIM domain containing proteins	62 (129)	33 (83)	33 (79)	4 (7)	10 (16)
PF00917	MATH	MATH domain	11	5	88 (161)	1	61 (74)
PF00249	Myb_DNA-binding	Myb-like DNA-binding domain	32 (43)	18 (24)	17 (24)	15 (20)	243 (401)
PF02344	Myc-LZ	Myc leucine zipper domain	1	0	0	0	0
PF01753	Zf-MYND	MYND finger	14	14	9	1	7
PF00628	PHD	PHD-finger	68 (86)	40 (53)	32 (44)	14 (15)	96 (105)
PF00157	Pou	Pou domain—N-terminal to homeobox domain	15	5	4	0	0
PF02257	RFX_DNA_binding	RFX DNA-binding domain	7	2	1	1	0
PF00076	Rrm	RNA recognition motif (a.k.a. RRM, RBD, or RNP domain)	224 (324)	127 (199)	94 (145)	43 (73)	232 (369)
PF02037	SAP	SAP domain	15	8	5	5	6 (7)
PF00622	SPRY	SPRY domain	44 (51)	10 (12)	5 (7)	3	6
PF01852	START	START domain	10	2	6	0	23
PF00907	T-box	T-box	17 (19)	8	22	0	0

Table 18 (*Continued*)

Accession number	Domain name	Domain description	H	F	W	Y	A
PF02135	Zf-TAZ	TAZ finger	2 (3)	1 (2)	6 (7)	0	10 (15)
PF01285	TEA	TEA domain	4	1	1	1	0
PF02176	Zf-TRAF	TRAF-type zinc finger	6 (9)	1 (3)	1	0	2
PF00352	TBP	Transcription factor TFIID (or TATA-binding protein, TBP)	2 (4)	4 (8)	2 (4)	1 (2)	2 (4)
PF00567	TUDOR	TUDOR domain	9 (24)	9 (19)	4 (5)	0	2
PF00642	Zf-CCCH	Zinc finger C-x8-C-x5-C-x3-H type (and similar)	17 (22)	6 (8)	22 (42)	3 (5)	31 (46)
PF00096	Zf-C2H2**	Zinc finger, C2H2 type	564 (4500)	234 (771)	68 (155)	34 (56)	21 (24)
PF00097	Zf-C3HC4	Zinc finger, C3HC4 type (RING finger)	135 (137)	57	88 (89)	18	298 (304)
PF00098	Zf-CCHC	Zinc knuckle	9 (17)	6 (10)	17 (33)	7 (13)	68 (91)

(Tables 18 and 19). They include secreted hormones and growth factors, receptors, intracellular signaling molecules, and transcription factors.

Developmental signaling molecules that are enriched in the human genome include growth factors such as wnt, transforming growth factor–β (TGF-β), fibroblast growth factor (FGF), nerve growth factor, platelet derived growth factor (PDGF), and ephrins. These growth factors affect tissue differentiation and a wide range of cellular processes involving actin-cytoskeletal and nuclear regulation. The corresponding receptors of these developmental ligands are also expanded in humans. For example, our analysis suggests at least 8 human ephrin genes (2 in the fly, 4 in the worm) and 12 ephrin receptors (2 in the fly, 1 in the worm). In the wnt signaling pathway, we find 18 wnt family genes (6 in the fly, 5 in the worm) and 12 frizzled receptors (6 in the fly, 5 in the worm). The Groucho family of transcriptional corepressors downstream in the wnt pathway are even more markedly expanded, with 13 predicted members in humans (2 in the fly, 1 in the worm).

Extracellular adhesion molecules involved in signaling are expanded in the human genome (Tables 18 and 19). The interactions of several of these adhesion domains with extracellular matrix proteoglycans play a critical role in host defense, morphogenesis, and tissue repair (*131*). Consistent with the well-defined role of heparan sulfate proteoglycans in modulating these interactions (*132*), we observe an expansion of the heparin sulfate sulfotransferases in the human genome relative to worm and fly. These sulfotransferases modulate tissue differentiation (*133*). A similar expansion in humans is noted in structural proteins that constitute the actin-cytoskeletal architecture. Compared with the fly and worm, we observe an explosive expansion of the nebulin (35 domains per protein on average), aggrecan (12 domains per protein on average), and plectin (5 domains per protein on average) repeats in humans. These repeats are present in proteins involved in modulating the actin-cytoskeleton with predominant expression in neuronal, muscle, and vascular tissues.

Comparison across the five sequenced eukaryotic organisms revealed several expanded protein families and domains involved in cytoplasmic signal transduction (Table 18). In particular, signal transduction pathways playing roles in developmental regulation and acquired immunity were substantially enriched. There is a factor of 2 or greater expansion in humans in the Ras superfamily GTPases and the GTPase activator and GTP exchange factors associated with them. Although there are about the same number of tyrosine kinases in the human and *C. elegans* genomes, in humans there is an increase in the SH2, PTB, and ITAM domains involved in phosphotyrosine signal transduction. Further, there is a twofold expansion of phosphodiesterases in the human genome compared with either the worm or fly genomes.

The downstream effectors of the intracellular signaling molecules include the transcription factors that transduce developmental fates. Significant expansions are noted in the ligand-binding nuclear hormone receptor class of transcription factors compared with the fly genome, although not to the extent observed in the worm (Tables 18 and 19). Perhaps the most striking expansion in humans is in the C2H2 zinc finger transcription factors. Pfam detects a total of 4500 C2H2 zinc finger domains in 564 human proteins, compared with 771 in 234 fly proteins. This means that there has been a dramatic expansion not only in the number of C2H2 transcription factors, but also in the number of these DNA-binding motifs per transcription factor (8 on average in humans, 3.3 on average in the fly, and 2.3 on average in the worm). Furthermore, many of these transcription factors contain either the KRAB or SCAN domains, which are not found in the fly or worm genomes. These domains are involved in the oligomerization of transcription factors and increase the combinatorial partnering of these factors. In general, most of the transcription factor domains are shared between the three animal genomes, but the reassortment of these domains results in organism-specific transcription factor families. The domain combinations found in the human, fly, and worm include the BTB with C2H2 in the fly and humans, and homeodomains alone or in combination with Pou and LIM domains in all of the animal genomes. In plants, however, a different set of transcription factors are expanded, namely, the myb family, and a unique set that includes VP1 and AP2 domain–containing proteins (*134*). The yeast genome has a paucity of transcription factors compared with the multicellular eukaryotes, and its repertoire is limited to the expansion of the yeast-specific C6 transcription factor family involved in metabolic regulation.

While we have illustrated expansions in a subset of signal transduction molecules in the human genome compared with the other eukaryotic genomes, it should be noted that most of the protein domains are highly conserved. An interesting observation is that worms and humans have approximately the same number of both tyrosine kinases and serine/threonine kinases (Table 19). It is important to note, however, that these are merely counts of the catalytic domain; the proteins that contain these domains also display a wide repertoire of interaction domains with significant combinatorial diversity.

Hemostasis. Hemostasis is regulated primarily by plasma proteases of the coagulation pathway and by the interactions that occur between the vascular endothelium and platelets. Consistent with known anatomical and physiological differences between vertebrates and invertebrates, extracellular adhesion domains that constitute proteins integral to hemostasis are expanded in the human relative to the fly and worm (Tables 18 and 19). We note the evolution of domains such as FIMAC, FN1, FN2, and C1q that mediate surface interactions between hematopoeitic cells and the vascular matrix. In addition, there has been extensive recruitment of more-ancient animal-specific domains such as VWA, VWC, VWD, kringle, and FN3 into multidomain proteins that are involved in hemostatic regulation. Although we do not find a large expansion in the total number of serine proteases, this enzymatic domain has been specifically recruited into several of these multidomain proteins for proteolytic regulation in the vascular compartment. These are represented in plasma proteins that belong to the kinin and complement pathways. There is a

significant expansion in two families of matrix metalloproteases: ADAM (a disintegrin and metalloprotease) and MMPs (matrix metalloproteases) (Table 19). Proteolysis of extracellular matrix (ECM) proteins is critical for tissue development and for tissue degradation in diseases such as cancer, arthritis, Alzheimer's disease, and a variety of inflammatory conditions (*135*, *136*). ADAMs are a family of integral membrane proteins with a pivotal role in fibrinogenolysis and modulating interactions between hematopoietic components and the vascular matrix components. These proteins have been shown to cleave matrix proteins, and even signaling molecules: ADAM-17 converts tumor necrosis factor–α, and ADAM-10 has been implicated in the Notch signaling pathway (*135*). We have identified 19 members of the matrix metalloprotease family, and a total of 51 members of the ADAM and ADAM-TS families.

Apoptosis. Evolutionary conservation of some of the apoptotic pathway components across eukarya is consistent with its central role in developmental regulation and as a response to pathogens and stress signals. The signal transduction pathways involved in programmed cell death, or apoptosis, are mediated by interactions between well-characterized domains that include extracellular domains, adaptor (protein-protein interaction) domains, and those found in effector and regulatory enzymes (*137*). We enumerated the protein counts of central adaptor and effector enzyme domains that are found only in the apoptotic pathways to provide an estimate of divergence across eukarya and relative expansion in the human genome when compared with the fly and worm (Table 18). Adaptor domains found in proteins restricted only to apoptotic regulation such as the DED domains are vertebrate-specific, whereas others like BIR, CARD, and Bcl2 are represented in the fly and worm (although the number of Bcl2 family members in humans is significantly expanded). Although plants and yeast lack the caspases, caspase-like molecules, namely the para- and meta-caspases, have been reported in these organisms (*138*). Compared with other animal genomes, the human genome shows an expansion in the adaptor and effector domain–containing proteins involved in apoptosis, as well as in the proteases involved in the cascade such as the caspase and calpain families.

Expansions of other protein families. *Metabolic enzymes.* There are fewer cytochrome P450 genes in humans than in either the fly or worm. Lipoxygenases (six in humans), on the other hand, appear to be specific to the vertebrates and plants, whereas the lipoxygenase-activating proteins (four in humans) may be vertebrate-specific. Lipoxygenases are involved in arachidonic acid metabolism, and they and their activators have been implicated in diverse human pathology ranging from allergic responses to cancers. One of the most surprising human expansions, however, is in the number of glyceraldehyde-3-phosphate dehydrogenase (GAPDH) genes (46 in humans, 3 in the fly, and 4 in the worm). There is, however, evidence for many retrotransposed GAPDH pseudogenes (*139*), which may account for this apparent expansion. However, it is interesting that GAPDH, long known as a conserved enzyme involved in basic metabolism found across all phyla from bacteria to humans, has recently been shown to have other functions. It has a second cat-

Table 19. Number of proteins assigned to selected Panther families or subfamilies in *H. sapiens* (H), *D. melanogaster* (F), *C. elegans* (W), *S. cerevisiae* (Y), and *A. thaliana* (A).

Panther family/subfamily*	H	F	W	Y	A
Neural structure, function, development					
Ependymin	1	0	0	0	0
Ion channels	17	12	56	0	0
Acetylcholine receptor	11	24	27	0	0
Amiloride-sensitive/degenerin	22	9	9	0	30
CNG/EAG	16	3	3	0	0
IRK	10	2	4	0	0
ITP/ryanodine	61	51	59	0	19
Neurotransmitter-gated	10	0	0	0	0
P2X purinoceptor	12	12	48	1	5
TASK	15	3	3	1	0
Transient receptor	22	4	8	2	2
Voltage-gated Ca^{2+} alpha	10	3	2	0	0
Voltage-gated Ca^{2+} alpha-2	5	2	2	0	0
Voltage-gated Ca^{2+} beta	1	0	0	0	0
Voltage-gated Ca^{2+} gamma	33	5	11	0	0
Voltage-gated K^+ alpha	6	2	3	0	0
Voltage-gated KQT	11	4	4	9	1
Voltage-gated Na^+	1	0	0	0	0
Myelin basic protein	5	0	0	0	0
Myelin PO	3	1	0	0	0
Myelin proteolipid	1	0	0	0	0
Myelin-oligodendrocyte glycoprotein	2	0	0	0	0
Neuropilin	9	2	0	0	0
Plexin	22	6	2	0	0
Semaphorin	10	3	3	0	0
Synaptotagmin					
Immune response					
Defensin	3	0	0	0	0
Cytokine†	86	14	1	0	0
GCSF	1	0	0	0	0
GMCSF	1	0	0	0	0
Intercrine alpha	15	0	0	0	0
Intercrine beta	5	0	0	0	0
Inteferon	8	0	0	0	0
Interleukin	26	1	1	0	0
Leukemia inhibitory factor	1	0	0	0	0
MCSF	1	0	0	0	0
Peptidoglycan recognition protein	2	13	0	0	0
Pre-B cell enhancing factor	1	0	0	0	0
Small inducible cytokine A	14	0	0	0	0
SI cytokine	2	0	0	0	0
TNF	9	0	0	0	0
Cytokine receptor†	62	1	0	0	0
Bradykinin/C-C chemokine receptor	7	0	0	0	0
FI cytokine receptor	2	0	0	0	0
Interferon receptor	3	0	0	0	0
Interleukin receptor	32	0	0	0	0
Leukocyte tyrosine kinase receptor	3	0	0	0	0
MCSF receptor	1	0	0	0	0
TNF receptor	3	0	0	0	0
Immunoglobulin receptor†	59	0	0	0	0
T-cell receptor alpha chain	16	0	0	0	0
T-cell receptor beta chain	15	0	0	0	0
T-cell receptor gamma chain	1	0	0	0	0
T-cell receptor delta chain	1	0	0	0	0
Immunoglobulin FC receptor	8	0	0	0	0
Killer cell receptor	16	0	0	0	0
Polymeric-immunoglobulin receptor	4	0	0	0	0

alytic activity, as a uracil DNA glycosylase (*140*) and functions as a cell cycle regulator (*141*) and has even been implicated in apoptosis (*142*).

Translation. Another striking set of human expansions has occurred in certain families involved in the translational machinery. We identified 28 different ribosomal subunits that each have at least 10 copies in the genome; on average, for all ribosomal proteins there is about an 8- to 10-fold expansion in the number of genes relative to either the worm or fly. Retrotransposed pseudogenes may account for many of these expansions [see the discussion above and (*143*)]. Recent evidence suggests that a number of ribosomal proteins have secondary functions independent of their involvement in protein biosynthesis; for example, L13a and the related L7 subunits (36 copies in humans) have been shown to induce apoptosis (*144*).

There is also a four- to fivefold expansion in the elongation factor 1-alpha family (eEF1A; 56 human genes). Many of these expansions likely represent intronless paralogs that have presumably arisen from retrotransposition, and again there is evidence that many of these may be pseudogenes (*145*). However, a second form (eEF1A2) of this factor has been identied with tissue-specific expression in skeletal muscle and a complementary expression pattern to the ubiquitously expressed eEF1A (*146*).

Ribonucleoproteins. Alternative splicing results in multiple transcripts from a single gene, and can therefore generate additional diversity in an organism's protein complement. We have identified 269 genes for ribonucleoproteins. This represents over 2.5 times the number of ribonucleoprotein genes in the worm, two times that of the fly, and about the same as the 265 identified in the *Arabidopsis* genome. Whether the diversity of ribonucleoprotein genes in humans contributes to gene regulation at either the splicing or translational level is unknown.

Posttranslational modifications. In this set of processes, the most prominent expansion is the transglutaminases, calcium-dependent enzymes that catalyze the cross-linking of proteins in cellular processes such as hemostasis and apoptosis (*147*). The vitamin K–dependent gamma carboxylase gene product acts on the GLA domain (missing in the fly and worm) found in coagulation factors, osteocalcin, and matrix GLA protein (*148*). Tyrosylprotein sulfotransferases participate in the posttranslational modification of proteins involved in inflammation and hemostasis, including coagulation factors and chemokine receptors (*149*). Although there is no significant numerical increase in the counts for domains involved in nuclear protein modification, there are a number of domain arrangements in the predicted human proteins that are not found in the other currently sequenced genomes. These include the tandem association of two histone deacetylase domains in HD6 with a ubiquitin finger domain, a feature lacking in the fly genome. An additional example is the co-occurrence of important nuclear regulatory enzyme PARP (poly-ADP ribosyl transferase) domain fused to protein-interaction domains—BRCT and VWA in humans.

Concluding remarks. There are several possible explanations for the differences in phenotypic complexity observed in humans when compared to the fly and worm. Some of these relate to the prominent differences in the immune system, hemostasis, neuronal, vascular, and cytoskeletal complexity. The finding that the human genome contains fewer genes than previously predicted might be compensated for by combinatorial diversity generated at the levels of protein architecture, transcriptional and translational control, posttranslational modification of proteins, or posttranscriptional regulation. Extensive domain shuffling to increase or alter combinatorial diversity can provide an exponential

Table 19 (*Continued*)

Panther family/subfamily*	H	F	W	Y	A
MHC class I	22	0	0	0	0
MHC class II	20	0	0	0	0
Other immunoglobulin†	114	0	0	0	0
Toll receptor–related	10	6	0	0	0
Developmental and homeostatic regulators					
Signaling molecules†					
Calcitonin	3	0	0	0	0
Ephrin	8	2	4	0	0
FGF	24	1	1	0	0
Glucagon	4	0	0	0	0
Glycoprotein hormone beta chain	2	0	0	0	0
Insulin	1	0	0	0	0
Insulin-like hormone	3	0	0	0	0
Nerve growth factor	3	0	0	0	0
Neuregulin/heregulin	6	0	0	0	0
neuropeptide Y	4	0	0	0	0
PDGF	1	1	0	0	0
Relaxin	3	0	0	0	0
Stannocalcin	2	0	0	0	0
Thymopoeitin	2	0	1	0	0
Thyomosin beta	4	2	0	0	0
TGF-β	29	6	4	0	0
VEGF	4	0	0	0	0
Wnt	18	6	5	0	0
Receptors†					
Ephrin receptor	12	2	1	0	0
FGF receptor	4	4	0	0	0
Frizzled receptor	12	6	5	0	0
Parathyroid hormone receptor	2	0	0	0	0
VEGF receptor	5	0	0	0	0
BDNF/NT-3 nerve growth factor receptor	4	0	0	0	0
Kinases and phosphatases					
Dual-specificity protein phosphatase	29	8	10	4	11
S/T and dual-specificity protein kinase†	395	198	315	114	1102
S/T protein phosphatase	15	19	51	13	29
Y protein kinase†	106	47	100	5	16
Y protein phosphatase	56	22	95	5	6
Signal transduction					
ARF family	55	29	27	12	45
Cyclic nucleotide phosphodiesterase	25	8	6	1	0
G protein-coupled receptors†‡	616	146	284	0	1
G-protein alpha	27	10	22	2	5
G-protein beta	5	3	2	1	1
G-protein gamma	13	2	2	0	0
Ras superfamily	141	64	62	26	86
G-protein modulators†					
ARF GTPase-activating	20	8	9	5	15
Neurofibromin	7	2	0	2	0
Ras GTPase-activating	9	3	8	1	0
Tuberin	7	3	2	0	0
Vav proto-oncogene family	35	15	13	3	0

increase in the ability to mediate protein-protein interactions without dramatically increasing the absolute size of the protein complement (*150*). Evolution of apparently new (from the perspective of sequence analysis) protein domains and increasing regulatory complexity by domain accretion both quantitatively and qualitatively (recruitment of novel domains with preexisting ones) are two features that we observe in humans. Perhaps the best illustration of this trend is the C2H2 zinc finger–containing transcription factors, where we see expansion in the number of domains per protein, together with vertebrate-specific domains such as KRAB and SCAN. Recent reports on the prominent use of internal ribosomal entry sites in the human genome to regulate translation of specific classes of proteins suggests that this is an area that needs further research to identify the full extent of this process in the human genome (*151*). At the posttranslational level, although we provide examples of expansions of some protein families involved in these modifications, further experimental evidence is required to evaluate whether this is correlated with increased complexity in protein processing. Posttranscriptional processing and the extent of isoform generation in the human remain to be cataloged in their entirety. Given the conserved nature of the spliceosomal machinery, further analysis will be required to dissect regulation at this level.

8 Conclusions

8.1 The whole-genome sequencing approach versus BAC by BAC

Experience in applying the whole-genome shotgun sequencing approach to a diverse group of organisms with a wide range of genome sizes and repeat content allows us to assess its strengths and weaknesses. With the success of the method for a large number of microbial genomes, *Drosophila*, and now the human, there can be no doubt concerning the utility of this method. The large number of microbial genomes that have been sequenced by this method (*15*, *80*, *152*) demonstrate that megabase-sized genomes can be sequenced efficiently without any input other that the de novo mate-paired sequences. With more complex genomes like those of *Drosophila* or human, map information, in the form of well-ordered markers, has been critical for long-range ordering of scaffolds. For joining scaffolds into chromosomes, the quality of the map (in terms of the order of the markers) is more important than the number of markers per se. Although this mapping could have been performed concurrently with sequencing, the prior existence of mapping data was beneficial. During the sequencing of the *A. thaliana* genome, sequencing of individual BAC clones permitted extension of the se-

Table 19 (*Continued*)

Panther family/subfamily*	H	F	W	Y	A
Transcription factors/chromatin organization					
C2H2 zinc finger–containing†	607	232	79	28	8
COE	7	1	1	0	0
CREB	7	1	2	0	0
ETS-related	25	8	10	0	0
Forkhead-related	34	19	15	4	0
FOS	8	2	1	0	0
Groucho	13	2	1	0	0
Histone H1	5	0	1	0	0
Histone H2A	24	1	17	3	13
Histone H2B	21	1	17	2	12
Histone H3	28	2	24	2	16
Histone H4	9	1	16	1	8
Homeotic†	168	104	74	4	78
ABD-B	5	0	0	0	0
Bithoraxoid	1	8	1	0	0
Iroquois class	7	3	1	0	0
Distal-less	5	2	1	0	0
Engrailed	2	2	1	0	0
LIM-containing	17	8	3	0	0
MEIS/KNOX class	9	4	4	2	26
NK-3/NK-2 class	9	4	5	0	0
Paired box	38	28	23	0	2
Six	5	3	4	0	0
Leucine zipper	6	0	0	0	0
Nuclear hormone receptor†	59	25	183	1	4
Pou-related	15	5	4	1	0
Runt-related	3	4	2	0	0
ECM adhesion					
Cadherin	113	17	16	0	0
Claudin	20	0	0	0	0
Complement receptor-related	22	8	6	0	0
Connexin	14	0	0	0	0
Galectin	12	5	22	0	0
Glypican	13	2	1	0	0
ICAM	6	0	0	0	0
Integrin alpha	24	7	4	0	1
Integrin beta	9	2	2	0	0
LDL receptor family	26	19	20	0	2
Proteoglycans	22	9	7	0	5
Apoptosis					
Bcl-2	12	1	0	0	0
Calpain	22	4	11	1	3
Calpain inhibitor	4	0	0	0	1
Caspase	13	7	3	0	0
Hemostasis					
ADAM/ADAMTS	51	9	12	0	0
Fibronectin	3	0	0	0	0
Globin	10	2	3	0	3
Matrix metalloprotease	19	2	7	0	3
Serum amyloid A	4	0	0	0	0
Serum amyloid P (subfamily of Pentaxin)	2	0	0	0	0
Serum paraoxonase/arylesterase	4	0	3	0	0
Serum albumin	4	0	0	0	0
Transglutaminase	10	1	0	0	0
Other enzymes					
Cytochrome p450	60	89	83	3	256
GAPDH	46	3	4	3	8
Heparan sulfotransferase	11	4	2	0	0
Splicing and translation					
EF-1alpha	56	13	10	6	13
Ribonucleoproteins†	269	135	104	60	265
Ribosomal proteins†	812	111	80	117	256

*The table lists Panther families or subfamilies relevant to the text that either (i) are not specifically represented by Pfam (Table 18) or (ii) differ in counts from the corresponding Pfam models. †This class represents a number of different families in the same Panther molecular function subcategory. ‡This count includes only rhodopsin-class, secretin-class, and metabotropic glutamate-class GPCRs.

quence well into centromeric regions and allowed high-quality resolution of complex repeat regions. Likewise, in *Drosophila*, the BAC physical map was most useful in regions near the highly repetitive centromeres and telomeres. WGA has been found to deliver excellent-quality reconstructions of the unique regions of the genome. As the genome size, and more importantly the repetitive content, increases, the WGA approach delivers less of the repetitive sequence.

The cost and overall efficiency of clone-by-clone approaches makes them difficult to justify as a stand-alone strategy for future large-scale genome-sequencing projects. Specific applications of BAC-based or other clone mapping and sequencing strategies to resolve ambiguities in sequence assembly that cannot be efficiently resolved with computational approaches alone are clearly worth exploring. Hybrid approaches to whole-genome sequencing will only work if there is sufficient coverage in both the whole-genome shotgun phase and the BAC clone sequencing phase. Our experience with human genome assembly suggests that this will require at least 3× coverage of both whole-genome and BAC shotgun sequence data.

8.2 The low gene number in humans

We have sequenced and assembled ~95% of the euchromatic sequence of *H. sapiens* and used a new automated gene prediction method to produce a preliminary catalog of the human genes. This has provided a major surprise: We have found far fewer genes (26,000 to 38,000) than the earlier molecular predictions (50,000 to over 140,000). Whatever the reasons for this current disparity, only detailed annotation, comparative genomics (particularly using the *Mus musculus* genome), and careful molecular dissection of complex phenotypes will clarify this critical issue of the basic "parts list" of our genome. Certainly, the analysis is still incomplete and considerable refinement will occur in the years to come as the precise structure of each transcription unit is evaluated. A good place to start is to determine why the gene estimates derived from EST data are so discordant with our predictions. It is likely that the following contribute to an inflated gene number derived from ESTs: the variable lengths of 3′- and 5′-untranslated leaders and trailers; the little-understood vagaries of RNA processing that often leave intronic regions in an unspliced condition; the finding that nearly 40% of human genes are alternatively spliced (*153*); and finally, the unsolved technical problems in EST library construction where contamination from heterogeneous nuclear RNA and genomic DNA are not uncommon. Of course, it is possible that there are genes that remain unpredicted owing to the absence of EST or protein data to support them, although our use of mouse genome data for predicting genes should limit this number. As was true at the beginning of genome sequencing, ultimately it will be necessary to measure mRNA in specific cell types to demonstrate the presence of a gene.

J. B. S. Haldane speculated in 1937 that a population of organisms might have to pay a price for the number of genes it can possibly carry. He theorized that when the number of genes becomes too large, each zygote carries so many new deleterious mutations that the population simply cannot maintain itself. On the basis of this premise, and on the basis of available mutation rates and x-ray–induced mutations at specific loci, Muller, in 1967 (*154*), calculated that the mammalian genome would contain a maximum of not much more than 30,000 genes (*155*). An estimate of 30,000 gene loci for humans was also arrived at by Crow and Kimura (*156*). Muller's estimate for *D. melanogaster* was 10,000 genes, compared to 13,000 derived by annotation of the fly genome (*26*, *27*). These arguments for the theoretical maximum gene number were based on simplified ideas of genetic load—that all genes have a certain low rate of mutation to a deleterious state. However, it is clear that many mouse, fly, worm, and yeast knockout mutations lead to almost no discernible phenotypic perturbations.

The modest number of human genes means that we must look elsewhere for the mechanisms that generate the complexities inherent in human development and the sophisticated signaling systems that maintain homeostasis. There are a large number of ways in which the functions of individual genes and gene products are regulated. The degree of "openness" of chromatin structure and hence transcriptional activity is regulated by protein complexes that involve histone and DNA enzymatic modifications. We enumerate many of the proteins that are likely involved in nuclear regulation in Table 19. The location, timing, and quantity of transcription are intimately linked to nuclear signal transduction events as well as by the tissue-specific expression of many of these proteins. Equally important are regulatory DNA elements that include insulators, repeats, and endogenous viruses (*157*); methylation of CpG islands in imprinting (*158*); and promoter-enhancer and intronic regions that modulate transcription. The spliceosomal machinery consists of multisubunit proteins (Table 19) as well as structural and catalytic RNA elements (*159*) that regulate transcript structure through alternative start and termination sites and splicing. Hence, there is a need to study different classes of RNA molecules (*160*) such as small nucleolar RNAs, antisense riboregulator RNA, RNA involved in X-dosage compensation, and other structural RNAs to appreciate their precise role in regulating gene expression. The phenomenon of RNA editing in which coding changes occur directly at the level of mRNA is of clinical and biological relevance (*161*). Finally, examples of translational control include internal ribosomal entry sites that are found in proteins involved in cell cycle regulation and apoptosis (*162*). At the protein level, minor alterations in the nature of protein-protein interactions, protein modifications, and localization can have dramatic effects on cellular physiology (*163*). This dynamic system therefore has many ways to modulate activity, which suggests that definition of complex systems by analysis of single genes is unlikely to be entirely successful.

In situ studies have shown that the human genome is asymmetrically populated with G+C content, CpG islands, and genes (*68*). However, the genes are not distributed quite as unequally as had been predicted (Table 9) (*69*). The most G+C-rich fraction of the genome, H3 isochores, constitute more of the genome than previously thought (about 9%), and are the most gene-dense fraction, but contain only 25% of the genes, rather than the predicted ~40%. The low G+C L isochores make up 65% of the genome, and 48% of the genes. This inhomogeneity, the net result of millions of years of mammalian gene duplication, has been described as the "desertification" of the vertebrate genome (*71*). Why are there clustered regions of high and low gene density, and are these accidents of history or driven by selection and evolution? If these deserts are dispensable, it ought to be possible to find mammalian genomes that are far smaller in size than the human genome. Indeed, many species of bats have genome sizes that are much smaller than that of humans; for example, *Miniopterus*, a species of Italian bat, has a genome size that is only 50% that of humans (*164*). Similarly, *Muntiacus*, a species of Asian barking deer, has a genome size that is ~70% that of humans.

8.3 Human DNA sequence variation and its distribution across the genome

This is the first eukaryotic genome in which a nearly uniform ascertainment of polymorphism has been completed. Although we have identified and mapped more than 3 million SNPs, this by no means implies that the task of finding and cataloging SNPs is complete. These represent only a fraction of the SNPs present in the human population as a whole. Nevertheless, this first glimpse at genome-wide variation has revealed strong inhomogeneities in the distribution of SNPs across the genome. Polymorphism in DNA carries with it a snapshot of the past operation of population genetic forces, including mutation, migration, selection, and genetic drift. The availability of a dense array of SNPs will allow questions related to each of these factors to be addressed on a genome-wide basis. SNP studies can establish the range of haplo-

types present in subjects of different ethnogeographic origins, providing insights into population history and migration patterns. Although such studies have suggested that modern human lineages derive from Africa, many important questions regarding human origins remain unanswered, and more analyses using detailed SNP maps will be needed to settle these controversies. In addition to providing evidence for population expansions, migration, and admixture, SNPs can serve as markers for the extent of evolutionary constraint acting on particular genes. The correlation between patterns of intraspecies and interspecies genetic variation may prove to be especially informative to identify sites of reduced genetic diversity that may mark loci where sequence variations are not tolerated.

The remarkable heterogeneity in SNP density implies that there are a variety of forces acting on polymorphism—sparse regions may have lower SNP density because the mutation rate is lower, because most of those regions have a lower fraction of mutations that are tolerated, or because recent strong selection in favor of a newly arisen allele "swept" the linked variation out of the population (*165*). The effect of random genetic drift also varies widely across the genome. The nonrecombining portion of the Y chromosome faces the strongest pressure from random drift because there are roughly one-quarter as many Y chromosomes in the population as there are autosomal chromosomes, and the level of polymorphism on the Y is correspondingly less. Similarly, the X chromosome has a smaller effective population size than the autosomes, and its nucleotide diversity is also reduced. But even across a single autosome, the effective population size can vary because the density of deleterious mutations may vary. Regions of high density of deleterious mutations will see a greater rate of elimination by selection, and the effective population size will be smaller (*166*). As a result, the density of even completely neutral SNPs will be lower in such regions. There is a large literature on the association between SNP density and local recombination rates in *Drosophila*, and it remains an important task to assess the strength of this association in the human genome, because of its impact on the design of local SNP densities for disease-association studies. It also remains an important task to validate SNPs on a genomic scale in order to assess the degree of heterogeneity among geographic and ethnic populations.

8.4 Genome complexity

We will soon be in a position to move away from the cataloging of individual components of the system, and beyond the simplistic notions of "this binds to that, which then docks on this, and then the complex moves there. . . ." (*167*) to the exciting area of network perturbations, nonlinear responses and thresholds, and their pivotal role in human diseases.

The enumeration of other "parts lists" reveals that in organisms with complex nervous systems, neither gene number, neuron number, nor number of cell types correlates in any meaningful manner with even simplistic measures of structural or behavioral complexity. Nor would they be expected to; this is the realm of nonlinearities and epigenesis (*168*). The 520 million neurons of the common octopus exceed the neuronal number in the brain of a mouse by an order of magnitude. It is apparent from a comparison of genomic data on the mouse and human, and from comparative mammalian neuroanatomy (*169*), that the morphological and behavioral diversity found in mammals is underpinned by a similar gene repertoire and similar neuroanatomies. For example, when one compares a pygmy marmoset (which is only 4 inches tall and weighs about 6 ounces) to a chimpanzee, the brain volume of this minute primate is found to be only about 1.5 cm^3, two orders of magnitude less than that of a chimp and three orders less than that of humans. Yet the neuroanatomies of all three brains are strikingly similar, and the behavioral characteristics of the pygmy marmoset are little different from those of chimpanzees. Between humans and chimpanzees, the gene number, gene structures and functions, chromosomal and genomic organizations, and cell types and neuroanatomies are almost indistinguishable, yet the developmental modifications that predisposed human lineages to cortical expansion and development of the larynx, giving rise to language, culminated in a massive singularity that by even the simplest of criteria made humans more complex in a behavioral sense.

Simple examination of the number of neurons, cell types, or genes or of the genome size does not alone account for the differences in complexity that we observe. Rather, it is the interactions within and among these sets that result in such great variation. In addition, it is possible that there are "special cases" of regulatory gene networks that have a disproportionate effect on the overall system. We have presented several examples of "regulatory genes" that are significantly increased in the human genome compared with the fly and worm. These include extracellular ligands and their cognate receptors (e.g., wnt, frizzled, TGF-β, ephrins, and connexins), as well as nuclear regulators (e.g., the KRAB and homeodomain transcription factor families), where a few proteins control broad developmental processes. The answers to these "complexities" perhaps lie in these expanded gene families and differences in the regulatory control of ancient genes, proteins, pathways, and cells.

8.5 Beyond single components

While few would disagree with the intuitive conclusion that Einstein's brain was more complex than that of *Drosophila*, closer comparisons such as whether the set of predicted human proteins is more complex than the protein set of *Drosophila*, and if so, to what degree, are not straightforward, since protein, protein domain, or protein-protein interaction measures do not capture context-dependent interactions that underpin the dynamics underlying phenotype.

Currently, there are more than 30 different mathematical descriptions of complexity (*170*). However, we have yet to understand the mathematical dependency relating the number of genes with organism complexity. One pragmatic approach to the analysis of biological systems, which are composed of nonidentical elements (proteins, protein complexes, interacting cell types, and interacting neuronal populations), is through graph theory (*171*). The elements of the system can be represented by the vertices of complex topographies, with the edges representing the interactions between them. Examination of large networks reveals that they can self-organize, but more important, they can be particularly robust. This robustness is not due to redundancy, but is a property of inhomogeneously wired networks. The error tolerance of such networks comes with a price; they are vulnerable to the selection or removal of a few nodes that contribute disproportionately to network stability. Gene knockouts provide an illustration. Some knockouts may have minor effects, whereas others have catastrophic effects on the system. In the case of vimentin, a supposedly critical component of the cytoplasmic intermediate filament network of mammals, the knockout of the gene in mice reveals them to be reproductively normal, with no obvious phenotypic effects (*172*), and yet the usually conspicuous vimentin network is completely absent. On the other hand, ~30% of knockouts in *Drosophila* and mice correspond to critical nodes whose reduction in gene product, or total elimination, causes the network to crash most of the time, although even in some of these cases, phenotypic normalcy ensues, given the appropriate genetic background. Thus, there are no "good" genes or "bad" genes, but only networks that exist at various levels and at different connectivities, and at different states of sensitivity to perturbation. Sophisticated mathematical analysis needs to be constantly evaluated against hard biological data sets that specifically address network dynamics. Nowhere is this more critical than in attempts to come to grips with "complexity," particularly because deconvoluting and correcting complex networks that have undergone perturbation, and have resulted in human diseases, is the greatest significant challenge now facing us.

It has been predicted for the last 15 years that complete sequencing of the human ge-

nome would open up new strategies for human biological research and would have a major impact on medicine, and through medicine and public health, on society. Effects on biomedical research are already being felt. This assembly of the human genome sequence is but a first, hesitant step on a long and exciting journey toward understanding the role of the genome in human biology. It has been possible only because of innovations in instrumentation and software that have allowed automation of almost every step of the process from DNA preparation to annotation. The next steps are clear: We must define the complexity that ensues when this relatively modest set of about 30,000 genes is expressed. The sequence provides the framework upon which all the genetics, biochemistry, physiology, and ultimately phenotype depend. It provides the boundaries for scientific inquiry. The sequence is only the first level of understanding of the genome. All genes and their control elements must be identified; their functions, in concert as well as in isolation, defined; their sequence variation worldwide described; and the relation between genome variation and specific phenotypic characteristics determined. Now we know what we have to explain.

Another paramount challenge awaits: public discussion of this information and its potential for improvement of personal health. Many diverse sources of data have shown that any two individuals are more than 99.9% identical in sequence, which means that all the glorious differences among individuals in our species that can be attributed to genes falls in a mere 0.1% of the sequence. There are two fallacies to be avoided: determinism, the idea that all characteristics of the person are "hard-wired" by the genome; and reductionism, the view that with complete knowledge of the human genome sequence, it is only a matter of time before our understanding of gene functions and interactions will provide a complete causal description of human variability. The real challenge of human biology, beyond the task of finding out how genes orchestrate the construction and maintenance of the miraculous mechanism of our bodies, will lie ahead as we seek to explain how our minds have come to organize thoughts sufficiently well to investigate our own existence.

References and Notes

1. R. L. Sinsheimer, *Genomics* **5**, 954 (1989); U.S. Department of Energy, Office of Health and Environmental Research, *Sequencing the Human Genome: Summary Report of the Santa Fe Workshop*, Santa Fe, NM, 3 to 4 March 1986 (Los Alamos National Laboratory, Los Alamos, NM, 1986).
2. R. Cook-Deegan, *The Gene Wars: Science, Politics, and the Human Genome* (Norton, New York, 1996).
3. F. Sanger *et al.*, *Nature* **265**, 687 (1977).
4. P. H. Seeburg *et al.*, *Trans. Assoc. Am. Physicians* **90**, 109 (1977).
5. E. C. Strauss, J. A. Kobori, G. Siu, L. E. Hood, *Anal. Biochem.* **154**, 353 (1986).
6. J. Gocayne *et al.*, *Proc. Natl. Acad. Sci. U.S.A.* **84**, 8296 (1987).
7. A. Martin-Gallardo *et al.*, *DNA Sequence* **3**, 237 (1992); W. R. McCombie *et al.*, *Nature Genet.* **1**, 348 (1992); M. A. Jensen *et al.*, *DNA Sequence* **1**, 233 (1991).
8. M. D. Adams *et al.*, *Science* **252**, 1651 (1991).
9. M. D. Adams *et al.*, *Nature* **355**, 632 (1992); M. D. Adams, A. R. Kerlavage, C. Fields, J. C. Venter, *Nature Genet.* **4**, 256 (1993); M. D. Adams, M. B. Soares, A. R. Kerlavage, C. Fields, J. C. Venter, *Nature Genet.* **4**, 373 (1993); M. H. Polymeropoulos *et al.*, *Nature Genet.* **4**, 381 (1993); M. Marra *et al.*, *Nature Genet.* **21**, 191 (1999).
10. M. D. Adams *et al.*, *Nature* **377**, 3 (1995); O. White *et al.*, *Nucleic Acids Res.* **21**, 3829 (1993).
11. F. Sanger, A. R. Coulson, G. F. Hong, D. F. Hill, G. B. Petersen, *J. Mol. Biol.* **162**, 729 (1982).
12. B. W. J. Mahy, J. J. Esposito, J. C. Venter, *Am. Soc. Microbiol. News* **57**, 577 (1991).
13. R. D. Fleischmann *et al.*, *Science* **269**, 496 (1995).
14. C. M. Fraser *et al.*, *Science* **270**, 397 (1995).
15. C. J. Bult *et al.*, *Science* **273**, 1058 (1996); J. F. Tomb *et al.*, *Nature* **388**, 539 (1997); H. P. Klenk *et al.*, *Nature* **390**, 364 (1997).
16. J. C. Venter, H. O. Smith, L. Hood, *Nature* **381**, 364 (1996).
17. H. Schmitt *et al.*, *Genomics* **33**, 9 (1996).
18. S. Zhao *et al.*, *Genomics* **63**, 321 (2000).
19. X. Lin *et al.*, *Nature* **402**, 761 (1999).
20. J. L. Weber, E. W. Myers, *Genome Res.* **7**, 401 (1997).
21. P. Green, *Genome Res.* **7**, 410 (1997).
22. E. Pennisi, *Science* **280**, 1185 (1998).
23. J. C. Venter *et al.*, *Science* **280**, 1540 (1998).
24. M. D. Adams *et al.*, *Nature* **368**, 474 (1994).
25. E. Marshall, E. Pennisi, *Science* **280**, 994 (1998).
26. M. D. Adams *et al.*, *Science* **287**, 2185 (2000).
27. G. M. Rubin *et al.*, *Science* **287**, 2204 (2000).
28. E. W. Myers *et al.*, *Science* **287**, 2196 (2000).
29. F. S. Collins *et al.*, *Science* **282**, 682 (1998).
30. International Human Genome Sequencing Consortium (2001), *Nature* **409**, 860 (2001).
31. Institutional review board: P. Calabresi (chairman), H. P. Freeman, C. McCarthy, A. L. Caplan, G. D. Rogell, J. Karp, M. K. Evans, B. Margus, C. L. Carter, R. A. Millman, S. Broder.
32. Eligibility criteria for participation in the study were as follows: prospective donors had to be 21 years of age or older, not pregnant, and capable of giving an informed consent. Donors were asked to self-define their ethnic backgrounds. Standard blood bank screens (screening for HIV, hepatitis viruses, and so forth) were performed on all samples at the clinical laboratory prior to DNA extraction in the Celera laboratory. All samples that tested positive for transmissible viruses were ineligible and were discarded. Karyotype analysis was performed on peripheral blood lymphocytes from all samples selected for sequencing; all were normal. A two-staged consent process for prospective donors was employed. The first stage of the consent process provided information about the genome project, procedures, and risks and benefits of participating. The second stage of the consent process involved answering follow-up questions and signing consent forms, and was conducted about 48 hours after the first.
33. DNA was isolated from blood (*173*) or sperm. For sperm, a washed pellet (100 μl) was lysed in a suspension (1 ml) containing 0.1 M NaCl, 10 mM tris-Cl–20 mM EDTA (pH 8), 1% SDS, 1 mg proteinase K, and 10 mM dithiothreitol for 1 hour at 37°C. The lysate was extracted with aqueous phenol and with phenol/chloroform. The DNA was ethanol precipitated and dissolved in 1 ml TE buffer. To make genomic libraries, DNA was randomly sheared, end-polished with consecutive BAL31 nuclease and T4 DNA polymerase treatments, and size-selected by electrophoresis on 1% low-melting-point agarose. After ligation to Bst XI adapters (Invitrogen, catalog no. N408-18), DNA was purified by three rounds of gel electrophoresis to remove excess adapters, and the fragments, now with 3′-CACA overhangs, were inserted into Bst XI-linearized plasmid vector with 3′-TGTG overhangs. Libraries with three different average sizes of inserts were constructed: 2, 10, and 50 kbp. The 2-kbp fragments were cloned in a high-copy pUC18 derivative. The 10- and 50-kbp fragments were cloned in a medium-copy pBR322 derivative. The 2- and 10-kbp libraries yielded uniform-sized large colonies on plating. However, the 50-kbp libraries produced many small colonies and inserts were unstable. To remedy this, the 50-kbp libraries were digested with Bgl II, which does not cleave the vector, but generally cleaved several times within the 50-kbp insert. A 1264-bp Bam HI kanamycin resistance cassette (purified from pUCK4; Amersham Pharmacia, catalog no. 27-4958-01) was added and ligation was carried out at 37°C in the continual presence of Bgl II. As Bgl II–Bgl II ligations occurred, they were continually cleaved, whereas Bam HI–Bgl II ligations were not cleaved. A high yield of internally deleted circular library molecules was obtained in which the residual insert ends were separated by the kanamycin cassette DNA. The internally deleted libraries, when plated on agar containing ampicillin (50 μg/ml), carbenicillin (50 μg/ml), and kanamycin (15 μg/ml), produced relatively uniform large colonies. The resulting clones could be prepared for sequencing using the same procedures as clones from the 10-kbp libraries.
34. Transformed cells were plated on agar diffusion plates prepared with a fresh top layer containing no antibiotic poured on top of a previously set bottom layer containing excess antibiotic, to achieve the correct final concentration. This method of plating permitted the cells to develop antibiotic resistance before being exposed to antibiotic without the potential clone bias that can be introduced through liquid outgrowth protocols. After colonies had grown, QBot (Genetix, UK) automated colony-picking robots were used to pick colonies meeting stringent size and shape criteria and to inoculate 384-well microtiter plates containing liquid growth medium. Liquid cultures were incubated overnight, with shaking, and were scored for growth before passing to template preparation. Template DNA was extracted from liquid bacterial culture using a procedure based upon the alkaline lysis miniprep method (*173*) adapted for high throughput processing in 384-well microtiter plates. Bacterial cells were lysed; cell debris was removed by centrifugation; and plasmid DNA was recovered by isopropanol precipitation and resuspended in 10 mM tris-HCl buffer. Reagent dispensing operations were accomplished using Titertek MAP 8 liquid dispensing systems. Plate-to-plate liquid transfers were performed using Tomtec Quadra 384 Model 320 pipetting robots. All plates were tracked throughout processing by unique plate barcodes. Mated sequencing reads from opposite ends of each clone insert were obtained by preparing two 384-well cycle sequencing reaction plates from each plate of plasmid template DNA using ABI-PRISM BigDye Terminator chemistry (Applied Biosystems) and standard M13 forward and reverse primers. Sequencing reactions were prepared using the Tomtec Quadra 384-320 pipetting robot. Parent-child plate relationships and, by extension, forward-reverse sequence mate pairs were established by automated plate barcode reading by the onboard barcode reader and were recorded by direct LIMS communication. Sequencing reaction products were purified by alcohol precipitation and were dried, sealed, and stored at 4°C in the dark until needed for sequencing, at which time the reaction products were resuspended in deionized formamide and sealed immediately to prevent degradation. All sequence data were generated using a single sequencing platform, the ABI PRISM 3700 DNA Analyzer. Sample sheets were created at load time using a Java-based application that facilitates barcode scanning of the sequencing plate barcode, retrieves sample information from the central LIMS, and reserves unique trace identifiers. The application permitted a single sample sheet file in the linking directory and deleted previously created sample sheet files immediately upon scanning of a

sample plate barcode, thus enhancing sample sheet-to-plate associations.
35. F. Sanger, S. Nicklen, A. R. Coulson, *Proc. Natl. Acad. Sci. U.S.A.* **74**, 5463 (1977); J. M. Prober *et al.*, *Science* **238**, 336 (1987).
36. Celera's computing environment is based on Compaq Computer Corporation's Alpha system technology running the Tru64 Unix operating system. Celera uses these Alphas as Data Servers and as nodes in a Virtual Compute Farm, all of which are connected to a fully switched network operating at Fast Ethernet speed (for the VCF) and gigabit Ethernet speed (for data servers). Load balancing and scheduling software manages the submission and execution of jobs, based on central processing unit (CPU) speed, memory requirements, and priority. The Virtual Compute Farm is composed of 440 Alpha CPUs, which includes model EV6 running at a clock speed of 400 MHz and EV67 running at 667 MHz. Available memory on these systems ranges from 2 GB to 8 GB. The VCF is used to manage trace file processing, and annotation. Genome assembly was performed on a GS 160 running 16 EV67s (667 MHz) and 64 GB of memory, and 10 ES40s running 4 EV6s (500 MHz) and 32 GB of memory. A total of 100 terabytes of physical disk storage was included in a Storage Area Network that was available to systems across the environment. To ensure high availability, file and database servers were configured as 4-node Alpha TruClusters, so that services would fail over in the event of hardware or software failure. Data availability was further enhanced by using hardware- and software-based disk mirroring (RAID-0), disk striping (RAID-1), and disk striping with parity (RAID-5).
37. Trace processing generates quality values for base calls by means of Paracel's TraceTuner, trims sequence reads according to quality values, trims vector and adapter sequence from high-quality reads, and screens sequences for contaminants. Similar in design and algorithm to the phred program (*174*), TraceTuner reports quality values that reflect the log-odds score of each base being correct. Read quality was evaluated in 50-bp windows, each read being trimmed to include only those consecutive 50-bp segments with a minimum mean accuracy of 97%. End windows (both ends of the trace) of 1, 5, 10, 25, and 50 bases were trimmed to a minimum mean accuracy of 98%. Every read was further checked for vector and contaminant matches of 50 bp or more, and if found, the read was removed from consideration. Finally, any match to the 5′ vector splice junction in the initial part of a read was removed.
38. National Center for Biotechnology Information (NCBI); available at www.ncbi.nlm.nih.gov/.
39. NCBI; available at www.ncbi.nlm.nih.gov/HTGS/.
40. All bactigs over 3 kbp were examined for coverage by Celera mate pairs. An interval of a bactig was deemed an assembly error where there were no mate pairs spanning the interval and at least two reads that should have their mate on the other side of the interval but did not. In other words, there was no mate pair evidence supporting a join in the breakpoint interval and at least two mate pairs contradicting the join. By this criterion, we detected and broke apart bactigs at 13,037 locations, or equivalently, we found 2.13% of the bactigs to be misassembled.
41. We considered a BAC entry to be chimeric if, by the Lander-Waterman statistic (*175*), the odds were 0.99 or more that the assembly we produced was inconsistent with the sequence coming from a single source. By this criterion, 714 or 2.2% of BAC entries were deemed chimeric.
42. G. Myers, S. Selznick, Z. Zhang, W. Miller, *J. Comput. Biol.* **3**, 563 (1996).
43. E. W. Myers, J. L. Weber, in *Computational Methods in Genome Research*, S. Suhai, Ed. (Plenum, New York, 1996), pp. 73–89.
44. P. Deloukas *et al.*, *Science* **282**, 744 (1998).
45. M. A. Marra *et al.*, *Genome Res.* **7**, 1072 (1997).
46. J. Zhang *et al.*, data not shown.
47. Shredded bactigs were located on long CSA scaffolds (>500 kbp) and the distribution of these fragments on the scaffolds was analyzed. If the spread of these fragments was greater than four times the reported BAC length, the BAC was considered to be chimeric. In addition, if >20% of bactigs of a given BAC were found on a different scaffolds that were not adjacent in map position, then the BAC was also considered as chimeric. The total chimeric BACs divided by the number of BACs used for CSA gave the minimal estimate of chimerism rate.
48. M. Hattori *et al.*, *Nature* **405**, 311 (2000).
49. I. Dunham *et al.*, *Nature* **402**, 489 (1999).
50. A. B. Carvalho, B. P. Lazzaro, A. G. Clark, *Proc. Natl. Acad. Sci. U.S.A.* **97**, 13239 (2000).
51. The International RH Mapping Consortium, available at www.ncbi.nlm.nih.gov/genemap99/.
52. See http://ftp.genome.washington.edu/RM/RepeatMasker.html.
53. G. D. Schuler, *Trends Biotechnol.* **16**, 456 (1998).
54. S. F. Altschul, W. Gish, W. Miller, E. W. Myers, D. J. Lipman, *J. Mol. Biol.* **215**, 403 (1990).
55a. M. Olivier *et al.*, *Science* **291**, 1298 (2001).
55b. See http://genome.ucsc.edu/.
56. N. Chaudhari, W. E. Hahn, *Science* **220**, 924 (1983); R. J. Milner, J. G. Sutcliffe, *Nucleic Acids Res.* **11**, 5497 (1983).
57. D. Dickson, *Nature* **401**, 311 (1999).
58. B. Ewing, P. Green, *Nature Genet.* **25**, 232 (2000).
59. H. Roest Crollius *et al.*, *Nature Genet.* **25**, 235 (2000).
60. M. Yandell, in preparation.
61. K. D. Pruitt, K. S. Katz, H. Sicotte, D. R. Maglott, *Trends Genet.* **16**, 44 (2000).
62. Scaffolds containing greater than 10 kbp of sequence were analyzed for features of biological importance through a series of computational steps, and the results were stored in a relational database. For scaffolds greater than one megabase, the sequence was cut into single megabase pieces before computational analysis. All sequence was masked for complex repeats using Repeatmasker (*52*) before gene finding or homology-based analysis. The computational pipeline required ~7 hours of CPU time per megabase, including repeat masking, or a total compute time of about 20,000 CPU hours. Protein searches were performed against the nonredundant protein database available at the NCBI. Nucleotide searches were performed against human, mouse, and rat Celera Gene Indices (assemblies of cDNA and EST sequences), mouse genomic DNA reads generated at Celera (3×), the Ensembl gene database available at the European Bioinformatics Institute (EBI), human and rodent (mouse and rat) EST data sets parsed from the dbEST database (NCBI), and a curated subset of the RefSeq experimental mRNA database (NCBI). Initial searches were performed on repeat-masked sequence with BLAST 2.0 (*54*) optimized for the Compaq Alpha computeserver and an effective database size of 3×10^9 for BLASTN searches and 1×10^9 for BLASTX searches. Additional processing of each query-subject pair was performed to improve the alignments. All protein BLAST results having an expectation score of $<1 \times 10^{-4}$, human nucleotide BLAST results having an expectation score of $<1 \times 10^{-8}$ with >94% identity, and rodent nucleotide BLAST results having an expectation score of $<1 \times 10^{-8}$ with >80% identity were then examined on the basis of their high-scoring pair (HSP) coordinates on the scaffold to remove redundant hits, retaining hits that supported possible alternative splicing. For BLASTX searches, analysis was performed separately for selected model organisms (yeast, mouse, human, *C. elegans*, and *D. melanogaster*) so as not to exclude HSPs from these organisms that support the same gene structure. Sequences producing BLAST hits judged to be informative, nonredundant, and sufficiently similar to the scaffold sequence were then realigned to the genomic sequence with Sim4 for ESTs, and with Lap for proteins. Because both of these algorithms take splicing into account, the resulting alignments usually give a better representation of intron-exon boundaries than standard BLAST analyses and thus facilitate further annotation (both machine and human). In addition to the homology-based analysis described above, three ab initio gene prediction programs were used (*63*).
63. E. C. Uberbacher, Y. Xu, R. J. Mural, *Methods Enzymol.* **266**, 259 (1996); C. Burge, S. Karlin, *J. Mol. Biol.* **268**, 78 (1997); R. J. Mural, *Methods Enzymol.* **303**, 77 (1999); A. A. Salamov, V. V. Solovyev, *Genome Res.* **10**, 516 (2000); Floreal *et al.*, *Genome Res.* **8**, 967 (1998).
64. G. L. Miklos, B. John, *Am. J. Hum. Genet.* **31**, 264 (1979); U. Francke, *Cytogenet. Cell Genet.* **65**, 206 (1994).
65. P. E. Warburton, H. F. Willard, in *Human Genome Evolution*, M. S. Jackson, T. Strachan, G. Dover, Eds. (BIOS Scientific, Oxford, 1996), pp. 121–145.
66. J. E. Horvath, S. Schwartz, E. E. Eichler, *Genome Res.* **10**, 839 (2000).
67. W. A. Bickmore, A. T. Sumner, *Trends Genet.* **5**, 144 (1989).
68. G. P. Holmquist, *Am. J. Hum. Genet.* **51**, 17 (1992).
69. G. Bernardi, *Gene* **241**, 3 (2000).
70. S. Zoubak, O. Clay, G. Bernardi, *Gene* **174**, 95 (1996).
71. S. Ohno, *Trends Genet.* **1**, 160 (1985).
72. K. W. Broman, J. C. Murray, V. C. Sheffield, R. L. White, J. L. Weber, *Am. J. Hum. Genet.* **63**, 861 (1998).
73. M. J. McEachern, A. Krauskopf, E. H. Blackburn, *Annu. Rev. Genet.* **34**, 331 (2000).
74. A. Bird, *Trends Genet.* **3**, 342 (1987).
75. M. Gardiner-Garden, M. Frommer, *J. Mol. Biol.* **196**, 261 (1987).
76. F. Larsen, G. Gundersen, R. Lopez, H. Prydz, *Genomics* **13**, 1095 (1992).
77. S. H. Cross, A. Bird, *Curr. Opin. Genet. Dev.* **5**, 309 (1995).
78. J. Peters, *Genome Biol.* **1**, reviews1028.1 (2000) (http://genomebiology.com/2000/1/5/reviews/1028).
79. C. Grunau, W. Hindermann, A. Rosenthal, *Hum. Mol. Genet.* **9**, 2651 (2000).
80. F. Antequera, A. Bird, *Proc. Natl. Acad. Sci. U.S.A.* **90**, 11995 (1993).
81. S. H. Cross *et al.*, *Mamm. Genome* **11**, 373 (2000).
82. D. Slavov *et al.*, *Gene* **247**, 215 (2000).
83. A. F. Smit, A. D. Riggs, *Nucleic Acids Res.* **23**, 98 (1995).
84. D. J. Elliott *et al.*, *Hum. Mol. Genet.* **9**, 2117 (2000).
85. A. V. Makeyev, A. N. Chkheidze, S. A. Lievhaber, *J. Biol. Chem.* **274**, 24849 (1999).
86. Y. Pan, W. K. Decker, A. H. H. M. Huq, W. J. Craigen, *Genomics* **59**, 282 (1999).
87. P. Nouvel, *Genetica* **93**, 191 (1994).
88. I. Goncalves, L. Duret, D. Mouchiroud, *Genome Res.* **10**, 672 (2000).
89. Lek first compares all proteins in the proteome to one another. Next, the resulting BLAST reports are parsed, and a graph is created wherein each protein constitutes a node; any hit between two proteins with an expectation beneath a user-specified threshold constitutes an edge. Lek then uses this graph to compute a similarity between each protein pair *ij* in the context of the graph as a whole by simply dividing the number of BLAST hits shared in common between the two proteins by the total number of proteins hit by *i* and *j*. This simple metric has several interesting properties. First, because the similarity metric takes into account both the similarity and the differences between the two sequences at the level of BLAST hits, the metric respects the multidomain nature of protein space. Two multidomain proteins, for instance, each containing domains A and B, will have a greater pairwise similarity to each other than either one will have to a protein containing only A or B domains, so long as A-B–containing multidomain proteins are less frequent in the proteome than are single-domain proteins containing A or B domains. A second interesting property of this similarity metric is that it can be used to produce a similarity matrix for the proteome as a whole without having to first produce a multiple alignment for each protein family, an error-prone and very time-consuming process. Finally, the metric does not require that either sequence have significant homology to the other in order to have a defined similarity to each other, only that they

share at least one significant BLAST hit in common. This is an especially interesting property of the metric, because it allows the rapid recovery of protein families from the proteome for which no multiple alignment is possible, thus providing a computational basis for the extension of protein homology searches beyond those of current HMM- and profile-based search methods. Once the whole-proteome similarity matrix has been calculated, Lek first partitions the proteome into single-linkage clusters (*27*) on the basis of one or more shared BLAST hits between two sequences. Next, these single-linkage clusters are further partitioned into subclusters, each member of which shares a user-specified pairwise similarity with the other members of the cluster, as described above. For the purposes of this publication, we have focused on the analysis of single-linkage clusters and what we have termed "complete clusters," e.g., those subclusters for which every member has a similarity metric of 1 to every other member of the subcluster. We believe that the single-linkage and complete clusters are of special interest, in part, because they allow us to estimate and to compare sizes of core protein sets in a rigorous manner. The rationale for this is as follows: If one imagines for a moment a perfect clustering algorithm capable of perfectly partitioning one or more perfectly annotated protein sets into protein families, it is reasonable to assume that the number of clusters will always be greater than, or equal to, the number of single-linkage clusters, because single-linkage clustering is a maximally agglomerative clustering method. Thus, if there exists a single protein in the predicted protein set containing domains A and B, then it will be clustered by single linkage together with all single-domain proteins containing domains A or B. Likewise, for a predicted protein set containing a single multidomain protein, the number of real clusters must always be less than or equal to the number of complete clusters, because it is impossible to place a unique multidomain protein into a complete cluster. Thus, the single-linkage and complete clusters plus singletons should comprise a lower and upper bound of sizes of core protein sets, respectively, allowing us to compare the relative size and complexity of different organisms' predicted protein set.

90. T. F. Smith, M. S. Waterman, *J. Mol. Biol.* **147**, 195 (1981).
91. A. L. Delcher *et al.*, *Nucleic Acids Res.* **27**, 2369 (1999).
92. *Arabidopsis* Genome Initiative, *Nature* **408**, 796 (2000).

93. The probability that a contiguous set of proteins is the result of a segmental duplication can be estimated approximately as follows. Given that protein A and B occur on one chromosome, and that A′ and B′ (paralogs of A and B) also exist in the genome, the probability that B′ occurs immediately after A′ is 1/*N*, where *N* is the number of proteins in the set (for this analysis, $N = 26{,}588$). Allowing for B′ to occur as any of the next *J*-1 proteins [leaving a gap between A′ and B′ increases the probability to $(J - 1)/N$; allowing B′A′ or A′B′ gives a probability of $2(J - 1)/N$]. Considering three genes ABC, the probability of observing A′B′C′ elsewhere in the genome, given that the paralogs exist, is $1/N^2$. Three proteins can occur across a spread of five positions in six ways; more generally, we compute the number of ways that *K* proteins can be spread across *J* positions by counting all possible arrangements of $K - 2$ proteins in the $J - 2$ positions between the first and last protein. Allowing for a spread to vary from *K* positions (no gaps) to *J* gives

$$L = \sum_{X=K-2}^{J-2} \binom{X}{K-2}$$

arrangements. Thus, the probability of chance occurrence is L/N^{K-1}. Allowing for both sets of genes (e.g., ABC and A′B′C′) to be spread across *J* positions increases this to L^2/N^{K-1}. The duplicated segment might be rearranged by the operations of reversal or translocation; allowing for *M* such rearrangements gives us a probability $P = L^2M/N^{K-1}$. For example, the probability of observing a duplicated set of three genes in two different locations, where the three genes occur across a spread of five positions in both locations, is $36/N^2$; the expected number of such matched sets in the predicted protein set is approximately $(N)36/N^2 = 36/N$, a value $\ll 1$. Therefore, any such duplications of three genes are unlikely to result from random rearrangements of the genome. If any of the genes occur in more than two copies, the probability that the apparent duplication has occurred by chance increases. The algorithm for selecting candidate duplications only generates matched protein sets with $P \ll 1$.

94. B. J. Trask *et al.*, *Hum. Mol. Genet.* **7**, 13 (1998); D. Sharon *et al.*, *Genomics* **61**, 24 (1999).
95. W. B. Barbazuk *et al.*, *Genome Res.* **10**, 1351 (2000); A. McLysaght, A. J. Enright, L. Skrabanek, K. H. Wolfe, *Yeast* **17**, 22 (2000); D. W. Burt *et al.*, *Nature* **402**, 411 (1999).
96. Reviewed in L. Skrabanek, K. H. Wolfe, *Curr. Opin. Genet. Dev.* **8**, 694 (1998).
97. P. Taillon-Miller, Z. Gu, Q. Li, L. Hillier, P. Y. Kwok, *Genome Res.* **8**, 748 (1998); P. Taillon-Miller, E. E. Piernot, P. Y. Kwok, *Genome Res.* **9**, 499 (1999).
98. D. Altshuler *et al.*, *Nature* **407**, 513 (2000).
99. G. T. Marth *et al.*, *Nature Genet.* **23**, 452 (1999).
100. W.-H. Li, *Molecular Evolution* (Sinauer, Sunderland, MA, 1997).
101. M. Cargill *et al.*, *Nature Genet.* **22**, 231 (1999).
102. M. K. Halushka *et al.*, *Nature Genet.* **22**, 239 (1999).
103. J. Zhang, T. L. Madden, *Genome Res.* **7**, 649 (1997).
104. M. Nei, *Molecular Evolutionary Genetics* (Columbia Univ. Press, New York, 1987).

105. From the observed coverage of the sequences at each site for each individual, we calculated the probability that a SNP would be detected at the site if it were present. For each level of coverage, there is a binomial sampling of the two homologs for each individual, and a heterozygous site could only be ascertained if both homologs are present, or if two alleles from different individuals are present. With coverage *x* from a given individual, both homologs are present in the assembly with probability $1 - (1/2)x^{-1}$. Even if both homologs are present, the probability that a SNP is detected is <1 because a fraction of sites failed the quality criteria. Integrating over coverage levels, the binomial sampling, and the quality distribution, we derived an expected number of sites in the genome that were ascertained for polymorphism for each individual. The nucleotide diversity was then the observed number of variable sites divided by the expected number of sites ascertained.

106. M. W. Nachman, V. L. Bauer, S. L. Crowell, C. F. Aquadro, *Genetics* **150**, 1133 (1998).
107. D. A. Nickerson *et al.*, *Nature Genet.* **19**, 233 (1998); D. A. Nickerson *et al.*, *Genomic Res.* **10**, 1532 (2000); L. Jorde *et al.*, *Am. J. Hum. Genet.* **66**, 979 (2000); D. G. Wang *et al.*, *Science* **280**, 1077 (1998).
108. M. Przeworski, R. R. Hudson, A. Di Rienzo, *Trends Genet.* **16**, 296 (2000).
109. S. Tavare, *Theor. Popul. Biol.* **26**, 119 (1984).
110. R. R. Hudson, in *Oxford Surveys in Evolutionary Biology*, D. J. Futuyma, J. D. Antonovics, Eds. (Oxford Univ. Press, Oxford, 1990), vol. 7, pp. 1–44.
111. A. G. Clark *et al.*, *Am. J. Hum. Genet.* **63**, 595 (1998).
112. M. Kimura, *The Neutral Theory of Molecular Evolution* (Cambridge Univ. Press, Cambridge, 1983).
113. H. Kaessmann, F. Heissig, A. von Haeseler, S. Paabo, *Nature Genet.* **22**, 78 (1999).
114. E. L. Sonnhammer, S. R. Eddy, R. Durbin, *Proteins* **28**, 405 (1997).
115. A. Bateman *et al.*, *Nucleic Acids Res.* **28**, 263 (2000).

116. Brief description of the methods used to build the Panther classification. First, the June 2000 release of the GenBank NR protein database (excluding sequences annotated as fragments or mutants) was partitioned into clusters using BLASTP. For the clustering, a seed sequence was randomly chosen, and the cluster was defined as all sequences matching the seed to statistical significance (E-value $< 10^{-5}$) and "globally" alignable (the length of the match region must be >70% and <130% of the length of the seed). If the cluster had more than five members, and at least one from a multicellular eukaryote, the cluster was extended. For the extension step, a hidden Markov Model (HMM) was trained for the cluster, using the SAM software package, version 2. The HMM was then scored against GenBank NR (excluding mutants but including fragments for this step), and all sequences scoring better than a specific (NLL-NULL) score were added to the cluster. The HMM was then retrained (with fixed model length) and all sequences in the cluster were aligned to the HMM to produce a multiple sequence alignment. This alignment was assessed by a number of quality measures. If the alignment failed the quality check, the initial cluster was rebuilt around the seed using a more restrictive E-value, followed by extension, alignment, and reassessment. This process was repeated until the alignment quality was good. The multiple alignment and "general" (i.e., describing the entire cluster, or "family") HMM (*176*) were then used as input into the BETE program (*177*). BETE calculates a phylogenetic tree for the sequences in the alignment. Functional information about the sequences in each cluster were parsed from SwissProt (*178*) and GenBank records. "Tree-attribute viewer" software was used by biologist curators to correlate the phylogenetic tree with protein function. Subfamilies were manually defined on the basis of shared function across subtrees, and were named accordingly. HMMs were then built for each subfamily, using information from both the subfamily and family (K. Sjölander, in preparation). Families were also manually named according to the functions contained within them. Finally, all of the families and subfamilies were classified into categories and subcategories based on their molecular functions. The categorization was done by manual review of the family and subfamily names, by examining SwissProt and GenBank records, and by review of the literature as well as resources on the World Wide Web. The current version (2.0) of the Panther molecular function schema has four levels: category, subcategory, family, and subfamily. Protein sequences for whole eukaryotic genomes (for the predicted human proteins and annotated proteins for fly, worm, yeast, and *Arabidopsis*) were scored against the Panther library of family and subfamily HMMs. If the score was significant (the NLL-NULL score cutoff depends on the protein family), the protein was assigned to the family or subfamily function with the most significant score.

117. C. P. Ponting, J. Schultz, F. Milpetz, P. Bork, *Nucleic Acids Res.* **27**, 229 (1999).
118. A. Goffeau *et al.*, *Science* **274**, 546, 563 (1996).
119. *C. elegans* Sequencing Consortium, *Science* **282**, 2012 (1998).
120. S. A. Chervitz *et al.*, *Science* **282**, 2022 (1998).
121. E. R. Kandel, J. H. Schwartz, T. Jessell, *Principles of Neural Science* (McGraw-Hill, New York, ed. 4, 2000).
122. D. A. Goodenough, J. A. Goliger, D. L. Paul, *Annu. Rev. Biochem.* **65**, 475 (1996).
123. D. G. Wilkinson, *Int. Rev. Cytol.* **196**, 177 (2000).
124. F. Nakamura, R. G. Kalb, S. M. Strittmatter, *J. Neurobiol.* **44**, 219 (2000).
125. P. J. Horner, F. H. Gage, *Nature* **407**, 963 (2000); P. Casaccia-Bonnefil, C. Gu, M. V. Chao, *Adv. Exp. Med. Biol.* **468**, 275 (1999).
126. S. Wang, B. A. Barres, *Neuron* **27**, 197 (2000).
127. M. Geppert, T. C. Sudhof, *Annu. Rev. Neurosci.* **21**, 75 (1998); J. T. Littleton, H. J. Bellen, *Trends Neurosci.* **18**, 177 (1995).
128. A. Maximov, T. C. Sudhof, I. Bezprozvanny, *J. Biol. Chem.* **274**, 24453 (1999).
129. B. Sampo *et al.*, *Proc. Natl. Acad. Sci. U.S.A.* **97**, 3666 (2000).
130. G. Lemke, *Glia* **7**, 263 (1993).
131. M. Bernfield *et al.*, *Annu. Rev. Biochem.* **68**, 729 (1999).
132. N. Perrimon, M. Bernfield, *Nature* **404**, 725 (2000).
133. U. Lindahl, M. Kusche-Gullberg, L. Kjellen, *J. Biol. Chem.* **273**, 24979 (1998).
134. J. L. Riechmann *et al.*, *Science* **290**, 2105 (2000).
135. T. L. Hurskainen, S. Hirohata, M. F. Seldin, S. S. Apte, *J. Biol. Chem.* **274**, 25555 (1999).

136. R. A. Black, J. M. White, *Curr. Opin. Cell Biol.* **10**, 654 (1998).
137. L. Aravind, V. M. Dixit, E. V. Koonin, *Trends Biochem. Sci.* **24**, 47 (1999).
138. A. G. Uren *et al.*, *Mol. Cell* **6**, 961 (2000).
139. P. Garcia-Meunier, M. Etienne-Julan, P. Fort, M. Piechaczyk, F. Bonhomme, *Mamm. Genome* **4**, 695 (1993).
140. K. Meyer-Siegler *et al.*, *Proc. Natl. Acad. Sci. U.S.A.* **88**, 8460 (1991).
141. N. R. Mansur, K. Meyer-Siegler, J. C. Wurzer, M. A. Sirover, *Nucleic Acids Res.* **21**, 993 (1993).
142. N. A. Tatton, *Exp. Neurol.* **166**, 29 (2000).
143. N. Kenmochi *et al.*, *Genome Res.* **8**, 509 (1998).
144. F. W. Chen, Y. A. Ioannou, *Int. Rev. Immunol.* **18**, 429 (1999).
145. H. O. Madsen, K. Poulsen, O. Dahl, B. F. Clark, J. P. Hjorth, *Nucleic Acids Res.* **18**, 1513 (1990).
146. D. M. Chambers, J. Peters, C. M. Abbott, *Proc. Natl. Acad. Sci. U.S.A.* **95**, 4463 (1998); A. Khalyfa, B. M. Carlson, J. A. Carlson, E. Wang, *Dev. Dyn.* **216**, 267 (1999).
147. D. Aeschlimann, V. Thomazy, *Connect. Tissue Res.* **41**, 1 (2000).
148. P. Munroe *et al.*, *Nature Genet.* **21**, 142 (1999); S. M. Wu, W. F. Cheung, D. Frazier, D. W. Stafford, *Science* **254**, 1634 (1991); B. Furie *et al.*, *Blood* **93**, 1798 (1999).
149. J. W. Kehoe, C. R. Bertozzi, *Chem. Biol.* **7**, R57 (2000).
150. T. Pawson, P. Nash, *Genes Dev.* **14**, 1027 (2000).
151. A. W. van der Velden, A. A. Thomas, *Int. J. Biochem. Cell Biol.* **31**, 87 (1999).
152. C. M. Fraser *et al.*, *Science* **281**, 375 (1998); H. Tettelin *et al.*, *Science* **287**, 1809 (2000).
153. D. Brett *et al.*, *FEBS Lett.* **474**, 83 (2000).
154. H. J. Muller, H. Kern, Z. *Naturforsch. B* **22**, 1330 (1967).
155. H. J. Muller, in *Heritage from Mendel*, R. A. Brink, Ed. (Univ. of Wisconsin Press, Madison, WI, 1967), p. 419.
156. J. F. Crow, M. Kimura, *Introduction to Population Genetics Theory* (Harper & Row, New York, 1970).
157. K. Kobayashi *et al.*, *Nature* **394**, 388 (1998).
158. A. P. Feinberg, *Curr. Top. Microbiol. Immunol.* **249**, 87 (2000).
159. C. A. Collins, C. Guthrie, *Nature Struct. Biol.* **7**, 850 (2000).
160. S. R. Eddy, *Curr. Opin. Genet. Dev.* **9**, 695 (1999).
161. Q. Wang, J. Khillan, P. Gadue, K. Nishikura, *Science* **290**, 1765 (2000).
162. M. Holcik, N. Sonenberg, R. G. Korneluk, *Trends Genet.* **16**, 469 (2000).
163. T. A. McKinsey, C. L. Zhang, J. Lu, E. N. Olson, *Nature* **408**, 106 (2000).
164. E. Capanna, M. G. M. Romanini, *Caryologia* **24**, 471 (1971).
165. J. Maynard Smith, *J. Theor. Biol.* **128**, 247 (1987).
166. D. Charlesworth, B. Charlesworth, M. T. Morgan, *Genetics* **141**, 1619 (1995).
167. J. E. Bailey, *Nature Biotechnol.* **17**, 616 (1999).
168. R. Maleszka, H. G. de Couet, G. L. Miklos, *Proc. Natl. Acad. Sci. U.S.A.* **95**, 3731 (1998).
169. G. L. Miklos, *J. Neurobiol.* **24**, 842 (1993).
170. J. P. Crutchfield, K. Young, *Phys. Rev. Lett.* **63**, 105 (1989); M. Gell-Mann, S. Lloyd, *Complexity* **2**, 44 (1996).
171. A. L. Barabasi, R. Albert, *Science* **286**, 509 (1999).
172. E. Colucci-Guyon *et al.*, *Cell* **79**, 679 (1994).
173. J. Sambrook, E. F. Fritch, T. Maniatis, *Molecular Cloning: A Laboratory Manual* (Cold Spring Harbor Laboratory Press, Cold Spring Harbor, NY, ed. 2, 1989).
174. B. Ewing, P. Green, *Genome Res.* **8**, 186 (1998); B. Ewing, L. Hillier, M. C. Wendl, P. Green, *Genome Res.* **8**, 175 (1998).
175. E. S. Lander, M. S. Waterman, *Genomics* **2**, 231 (1988).
176. A. Krogh, K. Sjölander, *J. Mol. Biol.* **235**, 1501 (1994).
177. K. Sjölander, *Proc. Int. Soc. Mol. Biol.* **6**, 165 (1998).
178. A. Bairoch, R. Apweiler, *Nucleic Acids Res.* **28**, 45 (2000).
179. GO, available at www.geneontology.org/.
180. R. L. Tatusov, M. Y. Galperin, D. A. Natale, E. V. Koonin, *Nucleic Acids Res.* **28**, 33 (2000).

181. We thank E. Eichler and J. L. Goldstein for many helpful discussions and critical reading of the manuscript, and A. Caplan for advice and encouragement. We also thank T. Hein, D. Lucas, G. Edwards, and the Celera IT staff for outstanding computational support. The cost of this project was underwritten by the Celera Genomics Group of the Applera Corporation. We thank the Board of Directors of Applera Corporation: J. F. Abely Jr. (retired), R. H. Ayers, J.-L. Bélingard, R. H. Hayes, A. J. Levine, T. E. Martin, C. W. Slayman, O. R. Smith, G. C. St. Laurent Jr., and J. R. Tobin for their vision, enthusiasm, and unwavering support and T. L. White for leadership and advice. Data availability: The genome sequence and additional supporting information are available to academic scientists at the Web site (www.celera.com). Instructions for obtaining a DVD of the genome sequence can be obtained through the Web site. For commercial scientists wishing to verify the results presented here, the genome data are available upon signing a Material Transfer Agreement, which can also be found on the Web site.

5 December 2000; accepted 19 January 2001

EXHIBIT M

THE HUMAN GENOME

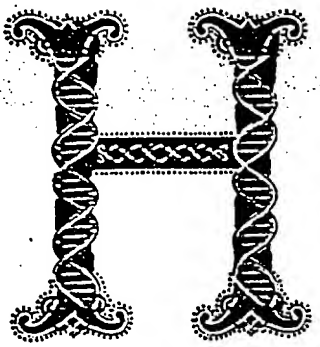

Humanity has been given a great gift. With the completion of the human genome sequence, we have received a powerful tool for unlocking the secrets of our genetic heritage and for finding our place among the other participants in the adventure of life.

This week's issue of *Science* contains the report of the sequencing of the human genome from a group of authors led by Craig Venter of Celera Genomics. The report of the sequencing of the human genome from the publicly funded consortium of laboratories led by Francis Collins appears in this week's *Nature*. This stunning achievement has been portrayed—often unfairly—as a competition between two ventures, one public and one private. That characterization detracts from the awesome accomplishment jointly unveiled this week. In truth, each project contributed to the other. The inspired vision that launched the publicly funded project roughly 10 years ago reflected, and now rewards, the confidence of those who believe that the pursuit of large-scale fundamental problems in the life sciences is in the national interest. The technical innovation and drive of Craig Venter and his colleagues made it possible to celebrate this accomplishment far sooner than was believed possible. Thus, we can salute what has become, in the end, not a contest but a marriage (perhaps encouraged by shotgun) between public funding and private entrepreneurship.

A historic moment for the scientific endeavor.

There are excellent scientific reasons for applauding an outcome that has given us two winners. Two sequences are better than one; the opportunity for comparison and convergence is invaluable. Indeed, a real-world proof of the importance of access to both sets of data can be found in the pages of this issue of *Science*, in the comparative analysis by Olivier *et al.* (p. 1298).

Although we have made the point before, it is worth repeating that the sequencing of the human genome represents, not an ending, but the beginning of a new approach to biology. As Galas says in his Viewpoint (p. 1257), the knowledge that all of the genetic components of any process can be identified will give extraordinary new power to scientists. Because of this breakthrough, research can evolve from analyzing the effects of individual genes to a more integrated view that examines whole ensembles of genes as they interact to form a living human being. Several articles in this issue highlight how this approach is already beginning to revolutionize the way we look at human disease.

This has been a massive project, on a scale unparalleled in the history of biology, but of course it has built on the scientific insights of centuries of investigators. By coincidence, this landmark announcement falls during the week of the anniversary of the birth of Charles Darwin. Darwin's message that the survival of a species can depend on its ability to evolve in the face of change is peculiarly pertinent to discussions that have gone on in the past year over access to the Celera data. (Full information regarding the agreements that were reached to make the data available can be found at www.sciencemag.org/feature/data/announcement/gsp.shl.) We are willing to be flexible in allowing data repositories other than the traditional GenBank, while insisting on access to all the data needed to verify conclusions. In this domain, change is everywhere: Commercial researchers are producing more and more potentially valuable sequences, yet (at least in the United States) laws governing databases provide scant protection against piracy. Had the Celera data been kept secret, it would have been a serious loss to the scientific community. We hope that our adaptability in the face of change will enable other proprietary data to be published after peer review, in a way that satisfies our continuing commitment to full access.

It should be no surprise that an achievement so stunning, and so carefully watched, has created new challenges for the scientific venture. *Science* is proud to have played a role in bringing this discovery onto the public stage. It is literally true that this is a historic moment for the scientific endeavor. The human genome has been called the Book of Life. Rather, it is a library, in which, with rules that encourage exploration and reward creativity, we can find many of the books that will help define us and our place in the great tapestry of life.

Barbara R. Jasny and Donald Kennedy

EXHIBIT N

BLAST of SEQ ID NO:23 versus Human genome

```
MEGABLAST 1.2.3-Paracel [2001-11-20]
Reference:
Zheng Zhang, Scott Schwartz, Lukas Wagner, and Webb Miller (2000),
"A greedy algorithm for aligning DNA sequences",
J Comput Biol 2000; 7(1-2):203-14.
Database: Homo_sapiens.latestgp.masked.fa
           44,521 sequences; 200,768,834,160 total letters
Query= seqid23
         (3660 letters)
```

Sequences producing significant alignments:	Score (bits)	E Value
AC007600.5.1.183083	505	e-140
AC096996.1.1.194627	454	e-124

```
>AC007600.5.1.183083
          Length = 183083

 Score =  505 bits (255), Expect = e-140
 Identities = 255/255 (100%)
 Strand = Plus / Plus


Query: 1355  agaagtttttcctccaggagagccctgttttctatgtccagacattacaagaccccagca 1414
              ||||||||||||||||||||||||||||||||||||||||||||||||||||||||||||
Sbjct: 46566 agaagtttttcctccaggagagccctgttttctatgtccagacattacaagaccccagca 46625


Query: 1415  aagctctggtctttgaggaggccaccttgtcatggcaacagacctgtcccgggatcgtca 1474
              ||||||||||||||||||||||||||||||||||||||||||||||||||||||||||||
Sbjct: 46626 aagctctggtctttgaggaggccaccttgtcatggcaacagacctgtcccgggatcgtca 46685


Query: 1475  atggggcactggagctggagaggaacgggcatgcttctgaggggatgaccaggcctagag 1534
              ||||||||||||||||||||||||||||||||||||||||||||||||||||||||||||
Sbjct: 46686 atggggcactggagctggagaggaacgggcatgcttctgaggggatgaccaggcctagag 46745


Query: 1535  atgccctcgggccagaggaagaagggaacagcctgggcccagagttgcacaagatcaacc 1594
              ||||||||||||||||||||||||||||||||||||||||||||||||||||||||||||
Sbjct: 46746 atgccctcgggccagaggaagaagggaacagcctgggcccagagttgcacaagatcaacc 46805


Query: 1595  tggtggtgtccaagg 1609
              |||||||||||||||
Sbjct: 46806 tggtggtgtccaagg 46820


 Score =  458 bits (231), Expect = e-125
 Identities = 234/235 (99%)
 Strand = Plus / Plus


Query: 544   atattgattataccaaagatcctggaatattcagaagagcagttggggaatgttgtccat 603
              ||||||||||||||||||||||||||||||||||||||||||||||||||||||||||||
Sbjct: 34936 atattgattataccaaagatcctggaatattcagaagagcagttggggaatgttgtccat 34995


Query: 604   ggagtgggactctgctttgccctttttctctccgaatgtgtgaagtctctgagtttctcc 663
              ||||||||||||||||||||||||||||||||||||||||||||||||||||||||||||
```

```
Sbjct: 34996 ggagtgggactctgctttgccctttttctctccgaatgtgtgaagtctctgagtttctcc 35055


Query: 664   tccagttggatcatcaaccaacgcacagccatcaggttccaagcagctgtttcctccttt 723
              ||||||||||||||||||||||||||||||||||||||| ||||||||||||||||||
Sbjct: 35056 tccagttggatcatcaaccaacgcacagccatcaggttccgagcagctgtttcctccttt 35115


Query: 724   gcctttgagaagctcatccaatttaagtctgtaatacacatcacctcaggagagg 778
              ||||||||||||||||||||||||||||||||||||||||||||||||||||||||||
Sbjct: 35116 gcctttgagaagctcatccaatttaagtctgtaatacacatcacctcaggagagg 35170


 Score =  454 bits (229), Expect = e-124
 Identities = 229/229 (100%)
 Strand = Plus / Plus


Query: 2217  ggttttccgctgccccatgagtttctttgacaccatcccaataggccggcttttgaactg 2276
              ||||||||||||||||||||||||||||||||||||||||||||||||||||||||||||
Sbjct: 70337 ggttttccgctgccccatgagtttctttgacaccatcccaataggccggcttttgaactg 70396


Query: 2277  cttcgcaggggacttggaacagctggaccagctcttgcccatcttttcagagcagttcct 2336
              ||||||||||||||||||||||||||||||||||||||||||||||||||||||||||||
Sbjct: 70397 cttcgcaggggacttggaacagctggaccagctcttgcccatcttttcagagcagttcct 70456


Query: 2337  ggtcctgtccttaatggtgatcgccgtcctgttgattgtcagtgtgctgtctccatatat 2396
              ||||||||||||||||||||||||||||||||||||||||||||||||||||||||||||
Sbjct: 70457 ggtcctgtccttaatggtgatcgccgtcctgttgattgtcagtgtgctgtctccatatat 70516


Query: 2397  cctgttaatgggagccataatcatggttatttgcttcatttattatatg 2445
              ||||||||||||||||||||||||||||||||||||||||||||||||||
Sbjct: 70517 cctgttaatgggagccataatcatggttatttgcttcatttattatatg 70565


 Score =  408 bits (206), Expect = e-110
 Identities = 206/206 (100%)
 Strand = Plus / Plus


Query: 1877  agattggagagcggggcctcaacctctctgggggcagaaacagaggatcagcctggccc 1936
              ||||||||||||||||||||||||||||||||||||||||||||||||||||||||||||
Sbjct: 57285 agattggagagcggggcctcaacctctctgggggcagaaacagaggatcagcctggccc 57344


Query: 1937  gcgccgtctattccgaccgtcagatctacctgctggacgacccccctgtctgctgtggacg 1996
              ||||||||||||||||||||||||||||||||||||||||||||||||||||||||||||
Sbjct: 57345 gcgccgtctattccgaccgtcagatctacctgctggacgacccccctgtctgctgtggacg 57404


Query: 1997  cccacgtggggaagcacatttttgaggagtgcattaagaagacactcagggggaagacgg 2056
              ||||||||||||||||||||||||||||||||||||||||||||||||||||||||||||
Sbjct: 57405 cccacgtggggaagcacatttttgaggagtgcattaagaagacactcagggggaagacgg 57464


Query: 2057  tcgtcctggtgacccaccagctgcag 2082
              |||||||||||||||||||||||||
Sbjct: 57465 tcgtcctggtgacccaccagctgcag 57490


 Score =  385 bits (194), Expect = e-103
 Identities = 194/194 (100%)
```

Strand = Plus / Plus

```
Query: 2857  aagatgtgtgtctcggaagctcctttacacatggaaggcacaagttgtccccaggggtgg 2916
             ||||||||||||||||||||||||||||||||||||||||||||||||||||||||||||
Sbjct: 80649 aagatgtgtgtctcggaagctcctttacacatggaaggcacaagttgtccccaggggtgg 80708


Query: 2917  ccacagcatggggaaatcatatttcaggattatcacatgaaatacagagacaacacaccc 2976
             ||||||||||||||||||||||||||||||||||||||||||||||||||||||||||||
Sbjct: 80709 ccacagcatggggaaatcatatttcaggattatcacatgaaatacagagacaacacaccc 80768


Query: 2977  accgtgcttcacggcatcaacctgaccatccgcggccacgaagtggtgggcatcgtggga 3036
             ||||||||||||||||||||||||||||||||||||||||||||||||||||||||||||
Sbjct: 80769 accgtgcttcacggcatcaacctgaccatccgcggccacgaagtggtgggcatcgtggga 80828


Query: 3037  aggacgggctctgg 3050
             ||||||||||||||
Sbjct: 80829 aggacgggctctgg 80842
```

Score = 371 bits (187), Expect = 2e-99
Identities = 187/187 (100%)
Strand = Plus / Plus

```
Query: 2583  gtttaagaggctgactgatgcgcagaataactacctgctgttgtttctatcttccacacg 2642
             ||||||||||||||||||||||||||||||||||||||||||||||||||||||||||||
Sbjct: 73139 gtttaagaggctgactgatgcgcagaataactacctgctgttgtttctatcttccacacg 73198


Query: 2643  atggatggcattgaggctggagatcatgaccaaccttgtgaccttggctgttgccctgtt 2702
             ||||||||||||||||||||||||||||||||||||||||||||||||||||||||||||
Sbjct: 73199 atggatggcattgaggctggagatcatgaccaaccttgtgaccttggctgttgccctgtt 73258


Query: 2703  cgtggcttttggcatttcctccacccccctactcctttaaagtcatggctgtcaacatcgt 2762
             ||||||||||||||||||||||||||||||||||||||||||||||||||||||||||||
Sbjct: 73259 cgtggcttttggcatttcctccacccccctactcctttaaagtcatggctgtcaacatcgt 73318


Query: 2763  gctgcag 2769
             |||||||
Sbjct: 73319 gctgcag 73325
```

Score = 347 bits (175), Expect = 3e-92
Identities = 178/179 (99%)
Strand = Plus / Plus

```
Query: 776   aggccatcagcttcttcaccggtgatgtaaactacctgtttgaaggggtgtgctatggac 835
             ||||||||||||||||||||||||||||||||||||||||||||||||||||||||||||
Sbjct: 41478 aggccatcagcttcttcaccggtgatgtaaactacctgtttgaaggggtgtgctatggac 41537


Query: 836   ccctagtactgatcacctgcgcatcgctggtcatctgcagcatttcttcctacttcatta 895
             ||||||||||||||||||||||||||||||||||||||||||||||||||||||||||||
Sbjct: 41538 ccctagtactgatcacctgcgcatcgctggtcatctgcagcatttcttcctacttcatta 41597


Query: 896   ttggatacactgcatttattgccatcttatgctatctcctggttttcccactggaggta 954
             |||||||||||||||||||||||||||||||||||||||||||||||||||| ||||
Sbjct: 41598 ttggatacactgcatttattgccatcttatgctatctcctggttttcccactggcggta 41656
```

```
 Score =  337 bits (170), Expect = 3e-89
 Identities = 170/170 (100%)
 Strand = Plus / Plus


Query: 3401  agatcatccttatcgatgaagccacagcctccattgacatggagacagacaccctgatcc 3460
              ||||||||||||||||||||||||||||||||||||||||||||||||||||||||||||
Sbjct: 90103 agatcatccttatcgatgaagccacagcctccattgacatggagacagacaccctgatcc 90162


Query: 3461  agcgcacaatccgtgaagccttccagggctgcaccgtgctcgtcattgcccaccgtgtca 3520
              ||||||||||||||||||||||||||||||||||||||||||||||||||||||||||||
Sbjct: 90163 agcgcacaatccgtgaagccttccagggctgcaccgtgctcgtcattgcccaccgtgtca 90222


Query: 3521  ccactgtgctgaactgtgaccacatcctggttatgggcaatgggaaggtg 3570
              ||||||||||||||||||||||||||||||||||||||||||||||||||
Sbjct: 90223 ccactgtgctgaactgtgaccacatcctggttatgggcaatgggaaggtg 90272


 Score =  321 bits (162), Expect = 2e-84
 Identities = 162/162 (100%)
 Strand = Plus / Plus


Query: 235   aggtttcctgccccccagcccctggacaatgctggcctgttctcctacctcaccgtgtca 294
              ||||||||||||||||||||||||||||||||||||||||||||||||||||||||||||
Sbjct: 29801 aggtttcctgccccccagcccctggacaatgctggcctgttctcctacctcaccgtgtca 29860


Query: 295   tggctcaccccgctcatgatccaaagcttacggagtcgcttagatgagaacaccatccct 354
              ||||||||||||||||||||||||||||||||||||||||||||||||||||||||||||
Sbjct: 29861 tggctcaccccgctcatgatccaaagcttacggagtcgcttagatgagaacaccatccct 29920


Query: 355   ccactgtcagtccatgatgcctcagacaaaaatgtccaaagg 396
              |||||||||||||||||||||||||||||||||||||||||
Sbjct: 29921 ccactgtcagtccatgatgcctcagacaaaaatgtccaaagg 29962


 Score =  319 bits (161), Expect = 7e-84
 Identities = 161/161 (100%)
 Strand = Plus / Plus


Query: 3049  gggaagtcctccttgggcatggctctcttccgcctggtggagcccatggcaggccggatt 3108
              |||||||||||||||||||||||||||||||||||||||||||||||||||||||||||||
Sbjct: 82347 gggaagtcctccttgggcatggctctcttccgcctggtggagcccatggcaggccggatt 82406


Query: 3109  ctcattgacggcgtggacatttgcagcatcggcctggaggacttgcggtccaagctctca 3168
              |||||||||||||||||||||||||||||||||||||||||||||||||||||||||||||
Sbjct: 82407 ctcattgacggcgtggacatttgcagcatcggcctggaggacttgcggtccaagctctca 82466


Query: 3169  gtgatccctcaagatccagtgctgctctcaggaaccatcag 3209
              |||||||||||||||||||||||||||||||||||||||
Sbjct: 82467 gtgatccctcaagatccagtgctgctctcaggaaccatcag 82507


 Score =  299 bits (151), Expect = 6e-78
 Identities = 151/151 (100%)
```

Strand = Plus / Plus

```
Query: 393   aaggcttcaccgcctttgggaagaagaagtctcaaggcgagggattgaaaaagcttcagt 452
             ||||||||||||||||||||||||||||||||||||||||||||||||||||||||||||
Sbjct: 33335 aaggcttcaccgcctttgggaagaagaagtctcaaggcgagggattgaaaaagcttcagt 33394


Query: 453   gcttctggtgatgctgaggttccagagaacaaggttgattttcgatgcacttctgggcat 512
             ||||||||||||||||||||||||||||||||||||||||||||||||||||||||||||
Sbjct: 33395 gcttctggtgatgctgaggttccagagaacaaggttgattttcgatgcacttctgggcat 33454


Query: 513   ctgcttctgcattgccagtgtactcgggcca 543
             |||||||||||||||||||||||||||||||
Sbjct: 33455 ctgcttctgcattgccagtgtactcgggcca 33485
```

Score = 297 bits (150), Expect = 3e-77
Identities = 150/150 (100%)
Strand = Plus / Plus

```
Query: 950   aggtattcatgacaagaatggctgtgaaggctcagcatcacacatctgaggtcagcgacc 1009
             ||||||||||||||||||||||||||||||||||||||||||||||||||||||||||||
Sbjct: 42421 aggtattcatgacaagaatggctgtgaaggctcagcatcacacatctgaggtcagcgacc 42480


Query: 1010  agcgcatccgtgtgaccagtgaagttctcacttgcattaagctgattaaaatgtacacat 1069
             ||||||||||||||||||||||||||||||||||||||||||||||||||||||||||||
Sbjct: 42481 agcgcatccgtgtgaccagtgaagttctcacttgcattaagctgattaaaatgtacacat 42540


Query: 1070  gggagaaaccatttgcaaaaatcattgaag 1099
             |||||||||||||||||||||||||||||
Sbjct: 42541 gggagaaaccatttgcaaaaatcattgaag 42570
```

Score = 293 bits (148), Expect = 4e-76
Identities = 151/152 (99%)
Strand = Plus / Plus

```
Query: 1098  agacctaagaaggaaggaaaggaagctattggagaagtgcgggcttgtccagagcctgac 1157
             |||||||||||||||||||||||| ||||||||||||||||||||||||||||||||||||
Sbjct: 42736 agacctaagaaggaaggaaaggaaactattggagaagtgcgggcttgtccagagcctgac 42795


Query: 1158  aagtataaccttgttcatcatccccacagtggccacagcggtctgggttctcatccacac 1217
             ||||||||||||||||||||||||||||||||||||||||||||||||||||||||||||
Sbjct: 42796 aagtataaccttgttcatcatccccacagtggccacagcggtctgggttctcatccacac 42855


Query: 1218  atccttaaagctgaaactcacagcgtcaatgg 1249
             |||||||||||||||||||||||||||||||
Sbjct: 42856 atccttaaagctgaaactcacagcgtcaatgg 42887
```

Score = 289 bits (146), Expect = 6e-75
Identities = 188/202 (93%)
Strand = Plus / Plus

```
Query: 1877  agattggagagcggggcctcaacctctctgggggcagaaacagaggatcagcctggccc 1936
             ||||||| ||||||||||||||||||||||||||||||  |||||||| ||||||||||
```

```
Sbjct: 142145 agattggggagcggggcctcaacctctctgggggggcagaggcagaggattagcctggccc 142204


Query: 1937   gcgccgtctattccgaccgtcagatctacctgctggacgacccccctgtctgctgtggacg 1996
              |||| ||||| |||||||||||| |||||||||||||||||||||||||| || |||||||
Sbjct: 142205 gcgctgtctactccgaccgtcagctctacctgctggacgacccccctgtcggccgtggacg 142264


Query: 1997   cccacgtggggaagcacatttttgaggagtgcattaagaagacactcaggggaagacgg 2056
              |||||||||||||||| | |||||||||||||||||||||| |||||||| ||||| |
Sbjct: 142265 cccacgtggggaagcacgtctttgaggagtgcattaagaagacgctcaggggaaagacag 142324


Query: 2057   tcgtcctggtgacccaccagct 2078
              |||||||||||||||||||||
Sbjct: 142325 tcgtcctggtgacccaccagct 142346


 Score =  278 bits (140), Expect = 2e-71
 Identities = 140/140 (100%)
 Strand = Plus / Plus


Query: 2445  gatgttcaagaaggccatcggtgtgttcaagagactggagaactatagccggtctccttt 2504
              ||||||||||||||||||||||||||||||||||||||||||||||||||||||||||||
Sbjct: 70675 gatgttcaagaaggccatcggtgtgttcaagagactggagaactatagccggtctccttt 70734


Query: 2505  attctcccacatcctcaattctctgcaaggcctgagctccatccatgtctatggaaaaac 2564
              ||||||||||||||||||||||||||||||||||||||||||||||||||||||||||||
Sbjct: 70735 attctcccacatcctcaattctctgcaaggcctgagctccatccatgtctatggaaaaac 70794


Query: 2565  tgaagacttcatcagccagt 2584
              ||||||||||||||||||||
Sbjct: 70795 tgaagacttcatcagccagt 70814


 Score =  278 bits (140), Expect = 2e-71
 Identities = 140/140 (100%)
 Strand = Plus / Plus


Query: 2080  cagtacttagaattttgtggccagatcattttgttggaaaatgggaaaatctgtgaaaat 2139
              ||||||||||||||||||||||||||||||||||||||||||||||||||||||||||||
Sbjct: 59486 cagtacttagaattttgtggccagatcattttgttggaaaatgggaaaatctgtgaaaat 59545


Query: 2140  ggaactcacagtgagttaatgcagaaaaaggggaaatatgcccaacttatccagaagatg 2199
              ||||||||||||||||||||||||||||||||||||||||||||||||||||||||||||
Sbjct: 59546 ggaactcacagtgagttaatgcagaaaaaggggaaatatgcccaacttatccagaagatg 59605


Query: 2200  cacaaggaagccacttcggt 2219
              ||||||||||||||||||||
Sbjct: 59606 cacaaggaagccacttcggt 59625


 Score =  276 bits (139), Expect = 9e-71
 Identities = 139/139 (100%)
 Strand = Plus / Plus


Query: 100   aaaacctatactctccaagatggcccctggagtcagcaagagagaaatcctgaggctcca 159
              |||||||||||||||||||||||||||||||||||||||||||||||||||||||||||||
```

```
Sbjct: 27194 aaaacctatactctccaagatggcccctggagtcagcaagagagaaatcctgaggctcca 27253


Query: 160   gggagggcagctgtcccaccgtgggggaagtatgatgctgccttgagaaccatgattccc 219
              ||||||||||||||||||||||||||||||||||||||||||||||||||||||||||||
Sbjct: 27254 gggagggcagctgtcccaccgtgggggaagtatgatgctgccttgagaaccatgattccc 27313


Query: 220   ttccgtcccaagccgaggt 238
              ||||||||||||||||||
Sbjct: 27314 ttccgtcccaagccgaggt 27332


 Score =  252 bits (127), Expect = 1e-63
 Identities = 127/127 (100%)
 Strand = Plus / Plus


Query: 1679  agatgcacttgctcgagggctcggtgggggtgcagggaagcctggcctatgtcccccagc 1738
              ||||||||||||||||||||||||||||||||||||||||||||||||||||||||||||
Sbjct: 52228 agatgcacttgctcgagggctcggtgggggtgcagggaagcctggcctatgtcccccagc 52287


Query: 1739  aggcctggatcgtcagcgggaacatcagggagaacatcctcatgggaggcgcatatgaca 1798
              ||||||||||||||||||||||||||||||||||||||||||||||||||||||||||||
Sbjct: 52288 aggcctggatcgtcagcgggaacatcagggagaacatcctcatgggaggcgcatatgaca 52347


Query: 1799  aggcccg 1805
              |||||||
Sbjct: 52348 aggcccg 52354


 Score =  226 bits (114), Expect = 8e-56
 Identities = 114/114 (100%)
 Strand = Plus / Plus


Query: 3289  atctcaaagttccccaaaaagctgcatacagatgtggtggaaaacggtggaaacttctct 3348
              ||||||||||||||||||||||||||||||||||||||||||||||||||||||||||||
Sbjct: 87547 atctcaaagttccccaaaaagctgcatacagatgtggtggaaaacggtggaaacttctct 87606


Query: 3349  gtgggggagaggcagctgctctgcattgccagggctgtgcttcgcaactccaag 3402
              ||||||||||||||||||||||||||||||||||||||||||||||||||||
Sbjct: 87607 gtgggggagaggcagctgctctgcattgccagggctgtgcttcgcaactccaag 87660


 Score =  216 bits (109), Expect = 7e-53
 Identities = 109/109 (100%)
 Strand = Plus / Plus


Query: 1248  ggccttcagcatgctggcctccttgaatctccttcggctgtcagtgttctttgtgcctat 1307
              ||||||||||||||||||||||||||||||||||||||||||||||||||||||||||||
Sbjct: 44216 ggccttcagcatgctggcctccttgaatctccttcggctgtcagtgttctttgtgcctat 44275


Query: 1308  tgcagtcaaaggtctcacgaattccaagtctgcagtgatgaggttcaag 1356
              |||||||||||||||||||||||||||||||||||||||||||||||||||||||||||
Sbjct: 44276 tgcagtcaaaggtctcacgaattccaagtctgcagtgatgaggttcaag 44324


 Score =  196 bits (99), Expect = 7e-47
```

```
 Identities = 99/99 (100%)
 Strand = Plus / Plus


Query: 1     atgactaggaagaggacatactgggtgcccaactcttctggtggcctcgtgaatcgtggc 60
              ||||||||||||||||||||||||||||||||||||||||||||||||||||||||||||
Sbjct: 25846 atgactaggaagaggacatactgggtgcccaactcttctggtggcctcgtgaatcgtggc 25905


Query: 61    atcgacataggcgatgacatggtttcaggacttatttat 99
              |||||||||||||||||||||||||||||||||||||
Sbjct: 25906 atcgacataggcgatgacatggtttcaggacttatttat 25944


 Score =  188 bits (95), Expect = 2e-44
 Identities = 95/95 (100%)
 Strand = Plus / Plus


Query: 3566  aggtggtagaatttgatcggccggaggtactgcggaagaagcctgggtcattgttcgcag 3625
              |||||||||||||||||||||||||||||||||||||||||||||||||||||||||||||
Sbjct: 90397 aggtggtagaatttgatcggccggaggtactgcggaagaagcctgggtcattgttcgcag 90456


Query: 3626  ccctcatggccacagccacttcttcactgagataa 3660
              |||||||||||||||||||||||||||||||||||
Sbjct: 90457 ccctcatggccacagccacttcttcactgagataa 90491


 Score =  182 bits (92), Expect = 1e-42
 Identities = 92/92 (100%)
 Strand = Plus / Plus


Query: 2768  agctggcgtccagcttccaggccactgcccggattggcttggagacagaggcacagttca 2827
              ||||||||||||||||||||||||||||||||||||||||||||||||||||||||||||||
Sbjct: 79077 agctggcgtccagcttccaggccactgcccggattggcttggagacagaggcacagttca 79136


Query: 2828  cggctgtagagaggatactgcagtacatgaag 2859
              |||||||||||||||||||||||||||||||
Sbjct: 79137 cggctgtagagaggatactgcagtacatgaag 79168


 Score =  161 bits (81), Expect = 4e-36
 Identities = 81/81 (100%)
 Strand = Plus / Plus


Query: 3208  agattcaacctagatccctttgaccgtcacactgaccagcagatctgggatgccttggag 3267
              |||||||||||||||||||||||||||||||||||||||||||||||||||||||||||||
Sbjct: 86796 agattcaacctagatccctttgaccgtcacactgaccagcagatctgggatgccttggag 86855


Query: 3268  aggacattcctgaccaaggcc 3288
              |||||||||||||||||||||
Sbjct: 86856 aggacattcctgaccaaggcc 86876


 Score =  147 bits (74), Expect = 6e-32
 Identities = 74/74 (100%)
 Strand = Plus / Plus
```

```
Query: 1805  gatacctccaggtgctccactgctgctccctgaatcgggacctggaacttctgccctttg 1864
              ||||||||||||||||||||||||||||||||||||||||||||||||||||||||||||
Sbjct: 54466 gatacctccaggtgctccactgctgctccctgaatcgggacctggaacttctgccctttg 54525


Query: 1865  gagacatgacagag 1878
              ||||||||||||||
Sbjct: 54526 gagacatgacagag 54539


 Score =  147 bits (74), Expect = 6e-32
 Identities = 74/74 (100%)
 Strand = Plus / Plus


Query: 1607  aggggatgatgttaggggtctgcggcaacacggggagtggtaagagcagcctgttgtcag 1666
              ||||||||||||||||||||||||||||||||||||||||||||||||||||||||||||
Sbjct: 49269 aggggatgatgttaggggtctgcggcaacacggggagtggtaagagcagcctgttgtcag 49328


Query: 1667  ccatcctggaggag 1680
              ||||||||||||||
Sbjct: 49329 ccatcctggaggag 49342


>AC096996.1.1.194627
          Length = 194627

 Score =  454 bits (229), Expect = e-124
 Identities = 229/229 (100%)
 Strand = Plus / Minus


Query: 2217  ggttttccgctgccccatgagtttctttgacaccatcccaataggccggcttttgaactg 2276
              ||||||||||||||||||||||||||||||||||||||||||||||||||||||||||||
Sbjct: 173330 ggttttccgctgccccatgagtttctttgacaccatcccaataggccggcttttgaactg 173271


Query: 2277  cttcgcaggggacttggaacagctggaccagctcttgcccatcttttcagagcagttcct 2336
              ||||||||||||||||||||||||||||||||||||||||||||||||||||||||||||
Sbjct: 173270 cttcgcaggggacttggaacagctggaccagctcttgcccatcttttcagagcagttcct 173211


Query: 2337  ggtcctgtccttaatggtgatcgccgtcctgttgattgtcagtgtgctgtctccatatat 2396
              ||||||||||||||||||||||||||||||||||||||||||||||||||||||||||||
Sbjct: 173210 ggtcctgtccttaatggtgatcgccgtcctgttgattgtcagtgtgctgtctccatatat 173151


Query: 2397  cctgttaatgggagccataatcatggttatttgcttcatttattatatg 2445
              |||||||||||||||||||||||||||||||||||||||||||||||
Sbjct: 173150 cctgttaatgggagccataatcatggttatttgcttcatttattatatg 173102


 Score =  408 bits (206), Expect = e-110
 Identities = 206/206 (100%)
 Strand = Plus / Minus


Query: 1877  agattggagagcggggcctcaacctctctgggggggcagaaacagaggatcagcctggccc 1936
              ||||||||||||||||||||||||||||||||||||||||||||||||||||||||||||
Sbjct: 186382 agattggagagcggggcctcaacctctctgggggggcagaaacagaggatcagcctggccc 186323


Query: 1937  gcgccgtctattccgaccgtcagatctacctgctggacgacccccctgtctgctgtggacg 1996
              ||||||||||||||||||||||||||||||||||||||||||||||||||||||||||||
```

```
Sbjct: 186322 gcgccgtctattccgaccgtcagatctacctgctggacgacccccctgtctgctgtggacg 186263


Query: 1997   cccacgtggggaagcacatttttgaggagtgcattaagaagacactcaggggaagacgg 2056
              ||||||||||||||||||||||||||||||||||||||||||||||||||||||||||||
Sbjct: 186262 cccacgtggggaagcacatttttgaggagtgcattaagaagacactcaggggaagacgg 186203


Query: 2057   tcgtcctggtgacccaccagctgcag 2082
              |||||||||||||||||||||||||
Sbjct: 186202 tcgtcctggtgacccaccagctgcag 186177


 Score =  385 bits (194), Expect = e-103
 Identities = 194/194 (100%)
 Strand = Plus / Minus


Query: 2857   aagatgtgtgtctcggaagctcctttacacatggaaggcacaagttgtccccaggggtgg 2916
              ||||||||||||||||||||||||||||||||||||||||||||||||||||||||||||
Sbjct: 163018 aagatgtgtgtctcggaagctcctttacacatggaaggcacaagttgtccccaggggtgg 162959


Query: 2917   ccacagcatggggaaatcatatttcaggattatcacatgaaatacagagacaacacaccc 2976
              ||||||||||||||||||||||||||||||||||||||||||||||||||||||||||||
Sbjct: 162958 ccacagcatggggaaatcatatttcaggattatcacatgaaatacagagacaacacaccc 162899


Query: 2977   accgtgcttcacggcatcaacctgaccatccgcggccacgaagtggtgggcatcgtggga 3036
              ||||||||||||||||||||||||||||||||||||||||||||||||||||||||||||
Sbjct: 162898 accgtgcttcacggcatcaacctgaccatccgcggccacgaagtggtgggcatcgtggga 162839


Query: 3037   aggacgggctctgg 3050
              ||||||||||||||
Sbjct: 162838 aggacgggctctgg 162825


 Score =  371 bits (187), Expect = 2e-99
 Identities = 187/187 (100%)
 Strand = Plus / Minus


Query: 2583   gtttaagaggctgactgatgcgcagaataactacctgctgttgtttctatcttccacacg 2642
              ||||||||||||||||||||||||||||||||||||||||||||||||||||||||||||
Sbjct: 170528 gtttaagaggctgactgatgcgcagaataactacctgctgttgtttctatcttccacacg 170469


Query: 2643   atggatggcattgaggctggagatcatgaccaaccttgtgaccttggctgttgccctgtt 2702
              ||||||||||||||||||||||||||||||||||||||||||||||||||||||||||||
Sbjct: 170468 atggatggcattgaggctggagatcatgaccaaccttgtgaccttggctgttgccctgtt 170409


Query: 2703   cgtggcttttggcatttcctccacccccctactcctttaaagtcatggctgtcaacatcgt 2762
              ||||||||||||||||||||||||||||||||||||||||||||||||||||||||||||
Sbjct: 170408 cgtggcttttggcatttcctccacccccctactcctttaaagtcatggctgtcaacatcgt 170349


Query: 2763   gctgcag 2769
              |||||||
Sbjct: 170348 gctgcag 170342


 Score =  337 bits (170), Expect = 3e-89
 Identities = 170/170 (100%)
```

Strand = Plus / Minus

```
Query: 3401   agatcatccttatcgatgaagccacagcctccattgacatggagacagacaccctgatcc 3460
              ||||||||||||||||||||||||||||||||||||||||||||||||||||||||||||
Sbjct: 153564 agatcatccttatcgatgaagccacagcctccattgacatggagacagacaccctgatcc 153505


Query: 3461   agcgcacaatccgtgaagccttccagggctgcaccgtgctcgtcattgcccaccgtgtca 3520
              ||||||||||||||||||||||||||||||||||||||||||||||||||||||||||||
Sbjct: 153504 agcgcacaatccgtgaagccttccagggctgcaccgtgctcgtcattgcccaccgtgtca 153445


Query: 3521   ccactgtgctgaactgtgaccacatcctggttatgggcaatgggaaggtg 3570
              ||||||||||||||||||||||||||||||||||||||||||||||||||
Sbjct: 153444 ccactgtgctgaactgtgaccacatcctggttatgggcaatgggaaggtg 153395
```

Score = 319 bits (161), Expect = 7e-84
Identities = 161/161 (100%)
Strand = Plus / Minus

```
Query: 3049   gggaagtcctccttgggcatggctctcttccgcctggtggagcccatggcaggccggatt 3108
              ||||||||||||||||||||||||||||||||||||||||||||||||||||||||||||
Sbjct: 161320 gggaagtcctccttgggcatggctctcttccgcctggtggagcccatggcaggccggatt 161261


Query: 3109   ctcattgacggcgtggacatttgcagcatcggcctggaggacttgcggtccaagctctca 3168
              ||||||||||||||||||||||||||||||||||||||||||||||||||||||||||||
Sbjct: 161260 ctcattgacggcgtggacatttgcagcatcggcctggaggacttgcggtccaagctctca 161201


Query: 3169   gtgatccctcaagatccagtgctgctctcaggaaccatcag 3209
              |||||||||||||||||||||||||||||||||||||||
Sbjct: 161200 gtgatccctcaagatccagtgctgctctcaggaaccatcag 161160
```

Score = 289 bits (146), Expect = 6e-75
Identities = 188/202 (93%)
Strand = Plus / Minus

```
Query: 1877   agattggagagcggggcctcaacctctctgggggcagaaacagaggatcagcctggccc 1936
              ||||||| ||||||||||||||||||||||||||||  |||||||| ||||||||||
Sbjct: 101522 agattggggagcggggcctcaacctctctgggggcagaggcagaggattagcctggccc 101463


Query: 1937   gcgccgtctattccgaccgtcagatctacctgctggacgacccccctgtctgctgtggacg 1996
              |||| ||||| |||||||||||| ||||||||||||||||||||||| || |||||||
Sbjct: 101462 gcgctgtctactccgaccgtcagctctacctgctggacgacccccctgtcggccgtggacg 101403


Query: 1997   cccacgtggggaagcacatttttgaggagtgcattaagaagacactcaggggaagacgg 2056
              |||||||||||||||| | |||||||||||||||||||||| |||||||| ||||| |
Sbjct: 101402 cccacgtggggaagcacgtctttgaggagtgcattaagaagacgctcaggggaaagacag 101343


Query: 2057   tcgtcctggtgacccaccagct 2078
              |||||||||||||||||||||
Sbjct: 101342 tcgtcctggtgacccaccagct 101321
```

Score = 278 bits (140), Expect = 2e-71
Identities = 140/140 (100%)

Strand = Plus / Minus

```
Query: 2080   cagtacttagaattttgtggccagatcattttgttggaaaatgggaaaatctgtgaaaat 2139
              ||||||||||||||||||||||||||||||||||||||||||||||||||||||||||||
Sbjct: 184181 cagtacttagaattttgtggccagatcattttgttggaaaatgggaaaatctgtgaaaat 184122


Query: 2140   ggaactcacagtgagttaatgcagaaaaaggggaaatatgcccaacttatccagaagatg 2199
              ||||||||||||||||||||||||||||||||||||||||||||||||||||||||||||
Sbjct: 184121 ggaactcacagtgagttaatgcagaaaaaggggaaatatgcccaacttatccagaagatg 184062


Query: 2200   cacaaggaagccacttcggt 2219
              ||||||||||||||||||||
Sbjct: 184061 cacaaggaagccacttcggt 184042
```

Score = 278 bits (140), Expect = 2e-71
Identities = 140/140 (100%)
Strand = Plus / Minus

```
Query: 2445   gatgttcaagaaggccatcggtgtgttcaagagactggagaactatagccggtctccttt 2504
              ||||||||||||||||||||||||||||||||||||||||||||||||||||||||||||
Sbjct: 172992 gatgttcaagaaggccatcggtgtgttcaagagactggagaactatagccggtctccttt 172933


Query: 2505   attctcccacatcctcaattctctgcaaggcctgagctccatccatgtctatggaaaaac 2564
              ||||||||||||||||||||||||||||||||||||||||||||||||||||||||||||
Sbjct: 172932 attctcccacatcctcaattctctgcaaggcctgagctccatccatgtctatggaaaaac 172873


Query: 2565   tgaagacttcatcagccagt 2584
              ||||||||||||||||||||
Sbjct: 172872 tgaagacttcatcagccagt 172853
```

Score = 252 bits (127), Expect = 1e-63
Identities = 127/127 (100%)
Strand = Plus / Minus

```
Query: 1679   agatgcacttgctcgagggctcggtgggggtgcagggaagcctggcctatgtcccccagc 1738
              ||||||||||||||||||||||||||||||||||||||||||||||||||||||||||||
Sbjct: 191439 agatgcacttgctcgagggctcggtgggggtgcagggaagcctggcctatgtcccccagc 191380


Query: 1739   aggcctggatcgtcagcgggaacatcagggagaacatcctcatgggaggcgcatatgaca 1798
              ||||||||||||||||||||||||||||||||||||||||||||||||||||||||||||
Sbjct: 191379 aggcctggatcgtcagcgggaacatcagggagaacatcctcatgggaggcgcatatgaca 191320


Query: 1799   aggcccg 1805
              |||||||
Sbjct: 191319 aggcccg 191313
```

Score = 226 bits (114), Expect = 8e-56
Identities = 114/114 (100%)
Strand = Plus / Minus

```
Query: 3289   atctcaaagttccccaaaaagctgcatacagatgtggtggaaaacggtggaaacttctct 3348
              ||||||||||||||||||||||||||||||||||||||||||||||||||||||||||||
```

```
Sbjct: 156120 atctcaaagttccccaaaaagctgcatacagatgtggtggaaaacggtggaaacttctct 156061


Query: 3349   gtgggggagaggcagctgctctgcattgccagggctgtgcttcgcaactccaag 3402
              ||||||||||||||||||||||||||||||||||||||||||||||||||||
Sbjct: 156060 gtgggggagaggcagctgctctgcattgccagggctgtgcttcgcaactccaag 156007


 Score =  188 bits (95), Expect = 2e-44
 Identities = 95/95 (100%)
 Strand = Plus / Minus


Query: 3566   aggtggtagaatttgatcggccggaggtactgcggaagaagcctgggtcattgttcgcag 3625
              ||||||||||||||||||||||||||||||||||||||||||||||||||||||||||
Sbjct: 153270 aggtggtagaatttgatcggccggaggtactgcggaagaagcctgggtcattgttcgcag 153211


Query: 3626   ccctcatggccacagccacttcttcactgagataa 3660
              |||||||||||||||||||||||||||||||||||
Sbjct: 153210 ccctcatggccacagccacttcttcactgagataa 153176


 Score =  182 bits (92), Expect = 1e-42
 Identities = 92/92 (100%)
 Strand = Plus / Minus


Query: 2768   agctggcgtccagcttccaggccactgcccggattggcttggagacagaggcacagttca 2827
              ||||||||||||||||||||||||||||||||||||||||||||||||||||||||||||
Sbjct: 164590 agctggcgtccagcttccaggccactgcccggattggcttggagacagaggcacagttca 164531


Query: 2828   cggctgtagagaggatactgcagtacatgaag 2859
              ||||||||||||||||||||||||||||||
Sbjct: 164530 cggctgtagagaggatactgcagtacatgaag 164499


 Score =  161 bits (81), Expect = 4e-36
 Identities = 81/81 (100%)
 Strand = Plus / Minus


Query: 3208   agattcaacctagatccctttgaccgtcacactgaccagcagatctgggatgccttggag 3267
              |||||||||||||||||||||||||||||||||||||||||||||||||||||||||||
Sbjct: 156871 agattcaacctagatccctttgaccgtcacactgaccagcagatctgggatgccttggag 156812


Query: 3268   aggacattcctgaccaaggcc 3288
              |||||||||||||||||||||
Sbjct: 156811 aggacattcctgaccaaggcc 156791


 Score =  147 bits (74), Expect = 6e-32
 Identities = 74/74 (100%)
 Strand = Plus / Minus


Query: 1805   gatacctccaggtgctccactgctgctccctgaatcgggacctggaacttctgcccctttg 1864
              ||||||||||||||||||||||||||||||||||||||||||||||||||||||||||||
Sbjct: 189201 gatacctccaggtgctccactgctgctccctgaatcgggacctggaacttctgcccctttg 189142


Query: 1865   gagacatgacagag 1878
```

```
                ||||||||||||||
Sbjct: 189141 gagacatgacagag 189128


 Score =  147 bits (74), Expect = 6e-32
 Identities = 74/74 (100%)
 Strand = Plus / Minus

Query: 1607   aggggatgatgttaggggtctgcggcaacacggggagtggtaagagcagcctgttgtcag 1666
               ||||||||||||||||||||||||||||||||||||||||||||||||||||||||||
Sbjct: 194398 aggggatgatgttaggggtctgcggcaacacggggagtggtaagagcagcctgttgtcag 194339


Query: 1667   ccatcctggaggag 1680
               ||||||||||||||
Sbjct: 194338 ccatcctggaggag 194325
```